

Geochemical and Isotopic Studies of rivers draining Deccan basalts

A THESIS

Submitted for the Award of Ph. D degree of

Mohan Lal Sukhadia University, Udaipur, India

In the

Faculty of Science

BY

Anirban Das



Under the Supervision of

Prof. S. Krishnaswami

Planetary & Geosciences Division

**Physical Research Laboratory, Navrangpura, Ahmedabad,
India-380 009.**

Mohan Lal Sukhadia University, Udaipur

Year of submission: 2005

DECLARATION

I hereby declare that the work incorporated in the present thesis entitled “Geochemical and Isotopic Studies of rivers draining Deccan basalts” is my own work and is original. This work (in part or in full) has not been submitted to any University for the award of a degree or a Diploma.

Anirban Das

CERTIFICATE

I feel great pleasure in certifying that the thesis entitled “Geochemical and Isotopic Studies of rivers draining Deccan basalts” embodies a record of the results of investigations carried out by Anirban Das under my guidance.

I am satisfied with the analysis of data, interpretation of results and the conclusions drawn.

He has completed the residential requirement as per rules.

I recommend the submission of thesis.

16th March, 2005

**S. Krishnaswami,
Sr. Professor
Physical Research Laboratory**

dedicated to my mother,
and
to the fond memory of my father

Acknowledgements

The last five-six years have been an enjoyable stage in the learning process. This has been made possible with sincere guidance, help and wishes from many individuals. I, sincerely, would like to express my gratitude to all of them.

Working under the guidance of Prof. S. Krishnaswami (Swami) has always been pleasurable. There was ample freedom to pursue my own plans— starting with field campaigns to the final data acquisitions. Suggestions and discussions during experiments were always fruitful. Regarding the most important phase of the Ph. D. — the interpretations of the data, was a real learning stage. Interpretation and analytical appreciation of data from all possible ways was really enjoyable. I always tried to learn (however small) from his in-depth knowledge— through every discussion we had.

Sincere guidance, involvement and concerns from Profs. M. M. Sarin and B. L. K. Somayajulu throughout the tenure are worth mentioning. Positive criticism at stages helped me towards correct ways of doing things. Learning Sr chemistry with Sunil (Dr. Sunil K. Singh) and discussions on numerous topics in geochemistry was always pleasurable. I am thankful to Profs. S. K. Bhattacharya and Kanchan Pande for their guidance and involvement in significant portions of the thesis.

I thank Profs. N. Bhandari, J. N. Goswami, A. K. Singhvi, R. Ramesh, S. V. S. Murthy; Drs. S. K. Gupta, P.N. Shukla and J. R. Trivedi, for their interests in the work, and for their interactions at times—especially during the area seminars. I am also thankful to Drs. J. S. Ray and D. Banerjee for their help during several stages. The sincere criticism and interests of Academic committee members, which helped me in shaping many critical aspects of the thesis, is acknowledged. I am thankful to Prof. Harish chandra and Dr. S. Ramachandran for their concern towards my work. I am also thankful to Drs. AnilKumar (NGRI), R. R. Navalgund (NRSA), N. J. Pawar (Pune) for their help.

I am extremely thankful to four seniors; Bhavsar Bhai, Ravi, Renga and Viswanathan for their support through out the tenure. I also thank Renga for critically (and painfully too) going through the final draft of the thesis.

Life at chemistry laboratory was really pleasant—courtesy the companies of Tarun, Pauline, Sudheer, Neeraj and Santosh. Spending time with the companies of Rajesh, Koushik and Vinai Rai for late night tea, was always fun— and I still cherish it.

I have honest friendship with Prasanta and Tarak, which extends well beyond our professional (however small) careers. Relationship with Soumen da, Subrata and Saikrishna since the early days of Ahmedabad was always enjoyable.

Life at PRL in the company of Sudeshna, Jayesh, Lokesh, Manoj, Jayendra, Harish, Dilip, Sreyas, Yogesh, Mortekai, Vinay, Rudra, Sanath, Satya, Subimal, Parimal, Sasadhar, Pradyumna, Manish, Murali, Charan, Panda kept me rejuvenated. Suggestions at times from senior colleagues—Anil, Navin, Jani, Deshpande, Rao, Madhusudhan also helped me in various ways.

I am thankful to Sanjeev and Harsha for their support, care, concerns and company. I spent some memorable times, in the company of some ex-PRLites— Nandu, Rajneesh, Jitti, Alok, Mittu, Aninda, Maibam, Prosenjit, Ashish_da, and I thank them all.

It is worth mentioning the association of Supriyo da-Prakritidi, Soumen da-Jhuma di, Dipu-Rumi di, for their selfless and moral support. I am extremely fortunate to have friends in Sujay-Sambita, Sujoy-Krishna and Arindam since the early B.Sc. days. Spending time with the next generation smart kids—Shailee, Ayushi, Monu, Markandeya and Tanishi was always fun.

I sincerely thank staffs of library, computer centre, workshop, liquid nitrogen and glass blowing for their help.

No words, perhaps can express acknowledgement and gratitude to parents, and family members, and many would not disagree that it is not easy to fulfil such a long-term goal without their moral support and patience.

CONTENTS

List of Tables

List of Figures

Chapter 1	Introduction	1-10
1.1	Introduction	2
1.2	Objective of the thesis	8
1.3	Structure of the thesis	9
Chapter 2	Materials and Methods	11-37
I	Materials	11-24
2.1	General characteristics of the Deccan Traps and drainage basin	12
2.1.1	Climate of the region	14
2.1.2	Characteristics of rivers studied	20
II	Sampling and analytical methods	25-37
2.2	Sampling	25
2.2.1	River water	26
2.2.2	Bank sediments	26
2.3	Analytical techniques	26
Chapter 3	Major ion chemistry	38-77
3.1	Introduction	39
3.2	Results	41
3.2.1	Major ion chemistry	41
3.2.2	Dissolved silica	46
3.2.3	Total dissolved silica and its spatial variability	49
3.2.4	Inter-annual variability of major ions	50
	Discussion	51
3.3.1	Mineral weathering	51
3.3.2	Sources of major ions to rivers of Deccan	53
3.3.2.1	Atmospheric supply	53
3.3.2.2	Other sources of Na, Cl and SO ₄	55
3.3.3	Chemical weathering rates	59
3.3.4	Variability in CWRs among different Deccan Trap regions	63
3.3.5	Silicate weathering rates	64
3.3.5.1	Role of carbonates in Ca budget	68
3.3.5.2	Comparison of silicate weathering rates	71
3.3.6	Temperature dependence on weathering	73
3.3.7	CO ₂ consumption rates	74
3.4	Summary and conclusions	76
Chapter 4	Carbon isotopes in DIC	78-100
4.1	Introduction	79
4.2	Results	81
4.3	Discussion	83
4.3.1	Sources of DIC and their $\delta^{13}\text{C}$	83

4.3.1.1	Dissolution of atmospheric CO ₂	85
4.3.1.2	Weathering of silicates	86
4.3.1.3	Carbonate weathering	88
4.3.2	δ ¹³ C in DIC of Deccan rivers: silicate/carbonate weathering	88
4.3.3	δ ¹³ C of carbonates and bed sediments	96
4.3.4	pCO ₂ of Deccan rivers	97
4.4	Conclusions	99
Chapter 5	Geochemistry of river sediments	101-126
5.1	Introduction	102
5.2	Results and discussion	106
5.2.1	Sodium, Magnesium, Calcium and Strontium	106
5.2.2	Potassium and Barium	112
5.2.3	Iron and Titanium	114
5.3	Measure of depletion/enrichment in sediments	116
5.4	Chemical index of alteration (CIA)	117
5.5	Sediment composition and physical erosion	120
5.6	Minor elements	123
5.7.1	Manganese and Phosphorous	123
5.7.2	V, Cr, Ni, Cu and Zn	123
5.7	Conclusions	125
Chapter 6	Sr concentration and ⁸⁷Sr/⁸⁶Sr in river waters	127-145
6.1	Introduction	128
6.2	Results and discussions	130
6.2.1	Sources of dissolved Sr	132
6.2.2	Sr in Deccan basalts	133
6.2.3	Sr co-variation with other elements	134
6.2.4	Role of Deccan in Sr isotopic excursions of oceans at ~66 Ma	137
6.3	Conclusions	144
Chapter 7	Synthesis and scope of future research	146-152
7.1	Major ion chemistry	147
7.2	Carbon isotopes	148
7.3	Sr isotopes	149
7.4	Major and trace elements in sediments	150
7.5	Scope of future research	150
	References	153-167
	List of publication	168

List of Tables

Tables	Content	Page
2.1	Comparison of dissolved silica in acidified and unacidified samples	29
2.2	Accuracy check for Sr and Ba in Merck and G-2 standards (by ultrasonic nebulizer)	29
2.3	Repeat analysis of $^{87}\text{Sr}/^{86}\text{Sr}$ in river waters	31
3.1	Major ion concentration, total dissolved solids, cations, anions and the normalized inorganic charge balance in rivers draining the Deccan Traps.	42-44
3.2	Dissolved silica and TDS in Deccan and other world rivers	48
3.3	Average abundances of major element oxides and major minerals in Deccan basalts	52
3.4	Major ions and silica released from weathering of minerals present in Deccan	53
3.5	Major ion composition of rainwater from Deccan region	54
3.6	Atmospheric composition of rainwater to the rivers in Deccan	56
3.7	Measured and expected major ion ratios in rivers	67
3.8	Silicate cations, TDS-silicate, carbonate-Ca, chemical weathering, silicate weathering and CO_2 consumption rates	69
3.9	Comparison of silicate weathering rates in Deccan and the Himalaya	72
4.1	$\delta^{13}\text{C}$, Si, HCO_3 and CSI in rivers, and $\delta^{13}\text{C}$ in basalts and sediments	83
4.2	Fractionation due to conversion of CO_2 to other carbonate species	86
4.3	Expected $\delta^{13}\text{C}$ in rivers from different weathering conditions	87
4.4	Weathering reactions of silicate minerals of Deccan	92
4.5	pCO_2 in rivers and flux out of rivers	98
5.1	Major and trace element concentrations in river sediments	102
5.2	Average major element concentrations, and Sr and Ba in sediments from different groups of rivers	108
5.3	Regression analysis of Mg and Ca_{sil} , Na and Sr abundances in sediments	112
5.4	Percentage depletion/enrichment in Deccan Trap sediments	118
5.5	Abundances of trace elements in Deccan	124
6.1	Ca, Mg, Na, HCO_3 , Si, Sr, and $^{87}\text{Sr}/^{86}\text{Sr}$ in rivers	131
6.2	Mg, Ca, Sr and $^{87}\text{Sr}/^{86}\text{Sr}$ in different Formations of Deccan Trap	133
6.3	Statistical analysis of dissolved Sr-major ion data	136
6.4	Sr concentration of large rivers flowing through Deccan	141
6.5	Expected change in $^{87}\text{Sr}/^{86}\text{Sr}$ of oceans at K/T due to Sr supplied from Deccan	142

List of figures

Figures	Content	Page
1.1	Map of India with many of the major rivers	7
2.1	Areal extent of the Deccan Traps with major rivers flowing through it and (b) Rainfall contours and the exposures of saline soils within the basin	13,15
2.2	Mean monthly rainfall of (a) Konkan and Goa, and Madhyamaharashtra region; (b) mean monthly rainfall of Pune and Mahabaleshwar; discharge of rivers (c) Krishna at Alamatti and (d) Bhima at Takli	16
2.3	Monthly variation of maximum and minimum temperatures of (a) west-central India, (b) Pune and (c) Mahabaleshwar	17
2.4	Distribution of laterites in western Deccan region	18
2.5	Sampling locations of rivers, rainfall monitoring stations and major cities	22
2.6	Sketch of CO ₂ extraction line	30
2.7	Reproducibility of (a) major, (b) minor and trace element analysis in sediments	32
2.8	Accuracy check of (a) major element, (b) minor and trace element analysis in W-1 and W-2	32
3.1	Scatter plot of total inorganic cations and anions	45
3.2	Ternary plots of (a) anions and (b) cations; (c) relative proportion of Na, Ca and Mg to the total cation budget	45,47
3.3	Scatter plots of Si and HCO ₃	49
3.4	Frequency distribution of total dissolved solids	50
3.5	Inter-annual variability in major ion abundances	51
3.6	Scatter plot of (a) Cl and SO ₄ and (b) Na versus (Cl + SO ₄)	58
3.7	Frequency distribution of chemical weathering rates	61
3.8	Distribution of calcite saturation index	62
3.9	Scatter plots of (a) Ca* vs. Mg*, and (b) Na* vs. Mg*	66
3.10	Frequency distribution of silicate weathering rates	70
3.11	Distribution of CO ₂ consumption rates	75
4.1	Sampling locations for river waters analysed for δ ¹³ C	82
4.2	Frequency distribution of δ ¹³ C values in DIC	84
4.3	Fraction of carbon species as a function of pH	84
4.4	Variation of δ ¹³ C with 1/[HCO ₃]	89
4.5	Mg* vs. HCO ₃ for five selected samples	90
4.6	Plot of δ ¹³ C vs. Si/HCO ₃	91
4.7	Comparison of measured and expected δ ¹³ C of DIC in rivers	96
4.8	pCO ₂ in the rivers measured for δ ¹³ C analyses	99
5.1	Ternary plot of (a) Al ₂ O ₃ , (Ca*O+Na ₂ O) and K ₂ O and (b) Al ₂ O ₃ , (Ca*O+Na ₂ O+K ₂ O), and (FeO+MgO) in sediments	105
5.2	Frequency distribution of (a) Na, (b) Mg, (c) Ca _{sil} and (d) Sr abundances in sediments	107
5.3	Scatter plots of (a) Na, (b) Mg, (c) Ca _{sil} and (d) Sr abundances relative to Al in sediments	109
5.4	Scatter plots of (a) Ca _{sil} and (b) Na vs. Mg in sediments	111

5.5	Plots of (a) Sr and (b) Ca_{sil} with Mg in sediments	111
5.6	Scatter plot of Ba vs. K in sediments	114
5.7	Variation of Ti abundances with Fe in sediments	115
5.8	Chemical index of alteration (CIA) of river sediments	119
5.9	Frequency distribution of CIA in river sediments	120
5.10	Scatter plot of predicted and suspended sediment yield	121
5.11	Variation of Mn/Al vs. Fe/Al in sediments	124
6.1	Variation of Sr with (a) Ca^* , (b) Mg^* , (c) Na^* and (d) HCO_3 in waters	135
6.2	Scatter plot of (a) Sr vs. Si and (b) Sr vs. Si/ HCO_3 in rivers	137
6.3	Sr isotope excursions in oceans before KTB	139
6.4	Required Sr flux from Deccan at round K/T to explain $^{87}Sr/^{86}Sr$ dip at around K/T	144

Chapter One

Introduction

1.1 INTRODUCTION

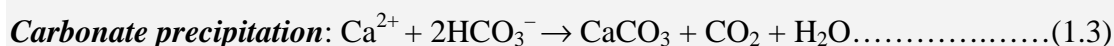
Weathering is the process of chemical and physical breakdown of minerals contained in rocks. Water, air and glaciers are the primary weathering agents, which also carry the breakdown products from continents to the oceans. Weathering and erosion are important processes in earth system, as they control, to a great extent, the landscape evolution of the earth and geochemical cycles of elements. Rivers serve as one of the links between the continents and the oceans; they transport the products of chemical and physical weathering occurring on the continents. These products are transported as dissolved solids and particulate matter to the oceans. Apart from determining the geomorphic (or landscape) evolution of the continents, and the geochemical cycles of elements, weathering processes also regulate the abundance of CO₂ in atmosphere. CO₂ is a green house gas, which is consumed during chemical weathering. Changes in chemical weathering rates can alter the budget of CO₂ in the atmosphere and therefore the temperature on continents. Enhanced chemical weathering consumes more CO₂ and thus decreases the temperature on continents. Chemical weathering, therefore, serves as a negative feedback to global temperature rise on longer (Ma) time scales (Walker et al., 1981).

Chemical weathering is a chemical reaction; therefore it requires a “substrate” and “reacting agents” for it to occur. The substrates on the earth surface are the minerals in rocks and the reacting agents are acids such as carbonic acid (H₂CO₃; from dissolution of CO₂); sulfuric acid (H₂SO₄; derived from pyrite oxidative weathering and a number of organic acids (oxalic, acetic and humic) which liberate protons to weather the minerals. In addition to these acids, H₂O also acts an agent in dissolving evaporite minerals. Among the various acids, H₂CO₃ is the dominant source of protons for chemical weathering reactions. The carbonic acid that takes part in these weathering reactions, though is formed from the dissolution of atmospheric CO₂, the main reaction takes place in the soil zone where the pCO₂ levels are much higher than that of the atmosphere (Dever, 1983). In addition to H₂CO₃, weathering through organic acids (e.g. in Cameroon rivers; Viers et al., 2000) and weathering due to H₂SO₄ may also be important on local and regional scales (Galy and France-Lanord, 1999).

Various factors control the rate and intensity of chemical weathering. These include lithology, runoff, temperature, tectonic-relief, and biogenic activity-vegetation

cover (Garrels and Mackenzie, 1971; Stallard and Edmond, 1983; Meybeck, 1986; Volk, 1987; Brady, 1991; Berner, 1992; Raymo and Rudimann, 1992; Velbel, 1993; Bluth and Kump, 1994; Brady and Carroll, 1994; Drever, 1994; Amiotte-Suchet and Probst, 1995; Edmond et al., 1995; White and Blum, 1995; Dalai et al., 2002). The relative dominance of these parameters in controlling chemical weathering continues to be a topic of debate (Berner and Berner, 1997; Edmond and Huh, 1997). It is, however, generally accepted that basin lithology is the dominant factor regulating chemical weathering (Meybeck, 1986; Amiotte-Suchet and Probst, 1995), though physical parameters such as temperature and runoff also have been shown to influence chemical weathering significantly (Berner, 1983; Kump et al., 2000). Huh et al. (1998 a and b) studied in detail the fluvial geochemistry of the eastern Siberian rivers, which have arctic/sub-arctic climate. They observed that the overall dissolved fluxes are comparable to that of rivers of tropical and temperate regions. This led them to conclude that physical erosion and resulting exposure of fresh rocks overcome large temperature effects, and that they play important role in determining the chemical weathering and erosion rates.

Among the rock types, e.g., silicates, carbonates, shales and evaporites present on continents, weathering of silicates is the only net sink for atmospheric CO₂ on long time scale (Berner, 1983). Carbonates rocks, though consume CO₂ during their weathering returns the CO₂ to the atmosphere during CaCO₃ precipitation in the oceans. In contrast, evaporite weathering does not consume CO₂ during their weathering. The weathering reaction of silicate, carbonates and precipitation of CaCO₃ can be expressed by the following reactions:



Combining equations (1.1) and (1.3) which describe the weathering cycle of Ca and HCO₃, show how CO₂ from the atmosphere gets consumed during silicate weathering. The reactions (2) and (3) are carbonate weathering/precipitation reactions and are the reverse of each other. Thus, in carbonate weathering there is no net uptake of CO₂. It

must, however, be mentioned that the precipitation of CaCO_3 in oceans occurs on million year time scale, which is roughly the residence time of HCO_3^- in oceans.

Thus, in general, the study of river geochemistry provides details to understand the contemporary exogenic cycles of elements, their sources to and sinks from rivers, their fluxes to the oceans, the chemical denudation rates of the basin, and most importantly, the present day atmospheric CO_2 drawdown. Further, with additional data on physical weathering and climate parameters, it is also possible to obtain better insight into the factors influencing chemical weathering and erosion, particularly, the coupling between chemical-physical weathering and erosion.

A key factor, regulating chemical weathering is the lithology of the drainage basin (Bluth and Kump, 1994). Therefore, to determine average global riverine fluxes of elements to oceans and CO_2 consumption rates, it is necessary to know chemical weathering and associated erosion rates of various lithologies and factors regulating it. During the past decade, a major emphasis has been in this direction, i.e., to determine the contemporary chemical erosion and CO_2 consumption rates of various basins with different lithologies. In this context, in addition to broad division of lithologies into silicates, carbonates and evaporites, many studies have further subdivided silicates into basalts, granites and shales (Amiotte-Suchet et al., 1995). Among these studies, those on basalts have gained more attention in recent years (Louvat and Allegre, 1997; Dessert et al., 2001; Steffansson and Gislason, 2001) mainly to assess the weathering rates relative to those of granites and gneisses and their overall role in the CO_2 consumption rates. The present day exposure area of basalts on land is $\sim 7 \times 10^6$ km^2 , about $\sim 5.2\%$ of total continental area of 135×10^6 km^2 (Amiotte-Suchet et al., 2003). The major exposures of basalts on the continents are the Siberian Traps, Deccan, Columbia river basalts, Ethiopia, Iceland and the Parana. Thus, basalts are a significant component of continental surface exposure and their weathering can influence surficial geochemical cycles of elements. Further, as basalts differ from other igneous rocks (granites/ gneisses), in the abundance of silica and in the presence of Ca, Mg and Fe rich minerals, the study of their weathering provides a measure of relative weatherability of these minerals and activation energy under natural conditions.

Studies on basalts have drawn attention in the last decade or so, following the work on Iceland basalts (Gislason and Eugster, 1987; Gislason et al., 1996; Steffansson and Gislason, 2001). These studies were primarily motivated by the quest

to determine basalt weathering rates, their dependence on various physical/climatological parameters and their comparison with other silicate lithologies (Meybeck, 1986; Amiotte-Suchet and Probst, 1995).

The pioneering study of Gislason and Eugster (1987) on rivers from north eastern Iceland set the stage for more detailed studies of basalt weathering. These include those from the Hawaii, Reunion, and the Deccan Traps (Bluth and Kump, 1994; Louvat and Allegre, 1997; Dessert et al., 2001). These regions experience a relatively wide range of rainfall, temperature and relief parameters and hence have provided a means to characterize their effect on basalt weathering. The studies by Gislason et al. (1996) and Steffansson and Gislason (2001) on rivers draining Iceland basalts show that runoff, age of basalts and vegetation/glacial cover are the key factors regulating their chemical weathering. The average annual temperature of Iceland is ~ 5 °C and average runoff in rivers draining them is 1200 mm y^{-1} . The chemical weathering and erosion rates reported for these basins are $\sim 41 \text{ t km}^{-2} \text{ y}^{-1}$ (Gislason et al., 1996) and $\sim 55 \text{ t km}^{-2} \text{ y}^{-1}$ (Louvat, 1997). The higher chemical weathering rates are typical of regions with high runoff and in those basins which have glasses in their basalts. The runoff dependence on chemical weathering rate is lower in older rocks than in the younger ones. The vegetation cover of Iceland is not a primary variable determining overall chemical denudation rate. In contrast to Iceland, the Reunion Island is a tectonically active region experiencing a tropical and oceanic climate characterized by high rainfall and relief. The major source of solutes in the rivers draining the Reunion is the weathering of basalts, however, some of the rivers also receive dominant input from oceans (sea salts) and thermal springs (Louvat and Allegre, 1997). The Reunion Island is characterized by high chemical weathering rates (CWR), ~ 63 to $\sim 170 \text{ t km}^{-2} \text{ y}^{-1}$, and a much higher mechanical weathering rate of 1100 to $2850 \text{ t km}^{-2} \text{ y}^{-1}$. All these are some of the highest among the world and bring out the importance of runoff, relief and active-tectonics on chemical weathering.

In India, Deccan Traps in the central-western region and the Himalayas in the north, are two major landforms. Between them, it is known that the Himalaya plays a significance role in controlling many earth system processes on a global scale (Raymo and Rudimann, 1992; Berner and Berner, 1996). Deccan Traps is located in the west/south-west part of India and at present covers an area of $\sim 5 \times 10^5 \text{ km}^2$ and volume of $\sim 10^6 \text{ km}^3$ (Dessert at al., 2001); roughly $\sim 8\%$ of the total basalt area on continents. It is estimated that about two-thirds of the volume of Deccan Traps have been eroded

since its eruption. Controversy still surrounds the age and duration of their emplacement, however, it is accepted that the major pulse of the volcanic eruptions took place during 67-65 Ma (Courtillet et al., 1986; Venkatesan et al., 1993; Allegre et al., 1999; Pande, 2002). There exist reports of even younger (62 Ma) basalts from the Gilbert Hill basalts near Mumbai (Sheth et al., 2001). It has also been estimated that during their eruption, $\sim 10^{18}$ moles of CO_2 was released (Javoy and Michard, 1989), which might have played a crucial role in the mass extinctions around ~ 65 Ma, commonly known as the K-T extinctions (Courtillet et al., 1986), which itself is a topic of research among many geochemists.

Deccan Traps are tholeiitic basalts. The Traps provide an opportunity to determine quantitatively chemical weathering and erosion rates of a large basaltic province. The major rivers that flow through the Deccan Traps are the Krishna, Godavari, Narmada-Tapti-Wainganga (NTW) and the Bhima. Of these, the Wainganga and the Bhima are tributaries of the Godavari and the Krishna respectively. The Godavari and the Krishna flows into the Bay of Bengal whereas the Narmada and the Tapti drains into the Arabian sea. In addition, there are a number of smaller streams draining the Deccan Traps and flowing into the Arabian sea. All these rivers account for a total annual discharge of $\sim 250 \text{ km}^3$ (Subramanian, 2000). Among these rivers, the Godavari is the third largest in India, after the Ganga and the Brahmaputra, and is placed 40th in terms of discharge on a global scale. The NTW rivers flowing through the northern part of the Deccan Traps and the Godavari draining the central Deccan have been studied earlier to some extent by Dessert et al. (2001), and Biksham and Subramanian (1988) respectively. Many of these rivers have part of their drainage through lithologies other than the Deccan Traps, for example, the NTW, and some of its tributaries flow through Vindhyan carbonates and alluvial deposits. Deccan basalts dominate the upstream Godavari river basin whereas granites, gneisses and sedimentary rocks (sandstone, quartzite and shales) are predominant in its lower catchment (Sarin et al., 2002). Similarly, the Krishna river system, studied as a part of this thesis, drains Deccan basalts in its upper reaches and Archean crystallines downstream. The Krishna system includes the Krishna river, its larger tributaries and sub-tributaries and a number of medium/small size rivers flowing in the western ghats. The lithology of the upper Krishna and the Bhima basins is almost entirely basalts, however, minor amounts of saline/alkaline soils (Bhattacharjee and Bhargava, 1982), laterite soils (Widdowson and Cox, 1996) and

calcareous deposits such as calc-tufas are also known to be dispersed in the basins (Pawar, 1988). The major rivers of India are shown in Fig. 1.1.

Prior to this work, Ramesh and Subramanian (1988) have reported the chemistry of a few Krishna water samples collected during 1981-1984. These results yield a chemical weathering rate of $\sim 41 \text{ t km}^{-2} \text{ y}^{-1}$ for the entire basin, based on measurements at the mouth of the Krishna river at Vijaywada. This weathering rate includes basalts in the upper reaches and Archean crystalline rocks in the lower reaches. Therefore, the data by Ramesh and Subramanian (1988) gives a composite weathering rate for the Deccan Traps and the Archean shield and not only for the weathering of basalts. A more detailed study on weathering of Deccan basalts is by Dessert et al. (2001) on the northern Deccan Traps, based on the major ion chemistry and Sr isotope composition of the Narmada-Tapti-Wainganga rivers.

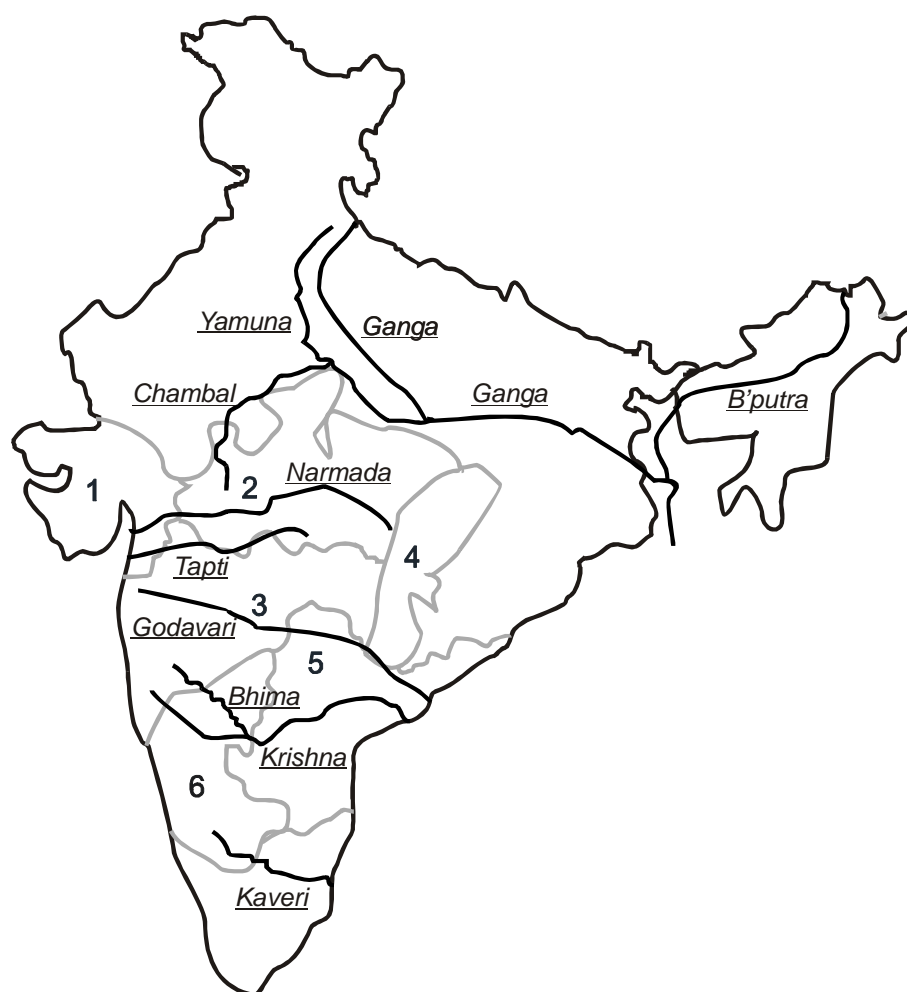


Figure 1.1 Map of India with the major rivers. The boundaries of states are also shown in gray colour. States: 1.Gujarat, 2. Madhya Pradesh, 3. Maharashtra, 4. Chhattishgarh, 5. Andhra Pradesh, 6. Karnataka.

The results led to the conclusions that the Deccan Traps weather faster than the world average silicate rocks, with chemical weathering rates varying between 21-63 t km⁻² y⁻¹. Further, “average” activation energy of ~42 kJ mole⁻¹ was estimated for the global basaltic provinces, based on HCO₃ as a proxy of silicate (basalt) weathering. The use of HCO₃ as a proxy of basalt weathering requires that all of it be derived from basalt weathering, a requirement that needs to be validated. For example, in the NTW basin there are reports of presence of Vindhayan carbonates. These issues will be discussed in detail in the chapters to follow.

The determination of chemical weathering and erosion rates of the Deccan Traps has to be based on chemistry of rivers, which drain almost entirely basalts. The Krishna river system in the upper reaches and the minor rivers draining the coastal tracts and draining into the Arabian sea seem to satisfy this requirement quite satisfactorily. This study is, therefore, based on these “selected” rivers and follows a multi-tracer approach, which includes major ion chemistry and Sr isotope composition of rivers, $\delta^{13}\text{C}$ of dissolved inorganic carbon, and major and minor elements in river sediments.

1.2 OBJECTIVES OF THE THESIS

The thesis aims to study the various facets on contemporary weathering and erosion of the Deccan Traps, India. The objectives of the thesis are:

1. To obtain baseline data on the major ion and isotopic composition (Sr and C) in the Krishna system in its upper reaches, which drain almost entirely the Deccan Traps—apportion the abundances to various sources (atmospheric, chemical weathering of the basin, anthropogenic and agricultural inputs), and to derive total dissolved fluxes transported out of the Deccan Traps.
2. To derive the chemical, silicate weathering and associated CO₂ consumption rates in the basin, assess the factors influencing the weathering rates and CO₂ consumption, and their contributions to the global budget.
3. To compare the rates of weathering and erosion within the various regions of the Deccan, and also with other “basaltic” provinces of world and the major river basins of India, especially, those in the Himalaya. The aim is to understand better the different factors contributing to the weathering and erosion rates.

4. To study the mobility of various elements during weathering and transport as reflected through their abundances in dissolved phase and bed sediments.
5. To assess the potential of C isotopes in dissolved inorganic carbon as a proxy of silicate-carbonate weathering.
6. To evaluate the role of Deccan Trap weathering on the Sr isotope excursions in oceans around Cretaceous/Tertiary boundary.

The objectives have been achieved based on a comprehensive study of (i) dissolved major ions, Sr and Ba, and isotopes of Sr and C in river water and (ii) a suite of major (Ca, Na, Mg, K, Fe, Al, Fe, Ti, Mn and P), minor (Zn, Cu, Sr, Ba and Ni) elements, carbonate content and Sr isotopes in bed sediments. The sampling comprises a set of 63 samples from 23 different rivers collected during two monsoon seasons (August-September of 2001 and 2002). The rivers include the Krishna, Bhima, Ghod, the Nira, and a number of medium and small rivers draining the western ghats.

1.3 STRUCTURE OF THE THESIS

The thesis is divided into seven chapters.

Chapter 1 provides an overall introduction to chemical weathering with emphasis on current understanding of weathering of basalts, the importance to study them in terms of their role to overall riverine chemical fluxes and global CO₂ consumption. The chapter also discusses the present knowledge on weathering of Deccan basalts, and the motivation to initiate the work described in this thesis.

Chapter 2 gives a detailed description of the study areas, sampling and the analytical procedures. The description of the study area includes information on their general geology, major and minor lithologies of the drainage basin, vegetation, rainfall and temperature in the region. The sampling and analytical procedures discuss the techniques of sample preparation and chemical treatment (for sediment samples, C and Sr isotopes), measurement procedures, precision and accuracy.

Chapter 3 focuses on the major ion composition of the rivers sampled in this study, chemical and silicate weathering in the Deccan Traps, their fluxes transported out, CO₂ consumption rates and the role of minor lithologies (such as alkaline and saline soils, carbonates) in modifying their chemistry. This chapter also provides a comparison of the rates of chemical weathering and CO₂ consumption in various

regions of the Deccan Traps, with those reported for the northern Deccan Traps, and also with the rivers draining the Himalaya. This comparison has yielded a better understanding of the factors regulating chemical weathering in the Deccan and the role of basalts on exogenic cycles of elements and atmospheric CO₂ drawdown.

Chapter 4 discusses the carbon isotope composition of dissolved inorganic carbon and its potential to use it as a proxy of silicate weathering. The results show that, in the rivers analysed, the $\delta^{13}\text{C-Si/HCO}_3$ coupled system can serve as a proxy to delineate silicate/carbonate contribution to DIC.

Chapter 5 brings out the detailed geochemical study of the major and minor elements in the bed sediments. These include the relative mobility of elements (mainly Na, Ca, Sr and Mg) w.r.t to the host rock (basalts) and corroborate with the major ion composition in the dissolved phase.

Chapter 6 provides results of Sr concentration and isotope ratio ($^{87}\text{Sr}/^{86}\text{Sr}$) in river waters, the relative mobility of Sr w.r.t. other elements (such as Mg). This chapter also discusses the role of Deccan Traps in the Sr isotope excursions at K/T boundary.

Chapter 7 presents synthesis of results obtained in this study on chemical weathering and erosion of Deccan Traps, based on a multi-proxy approach, and future directions.

Chapter Two
Materials and methods

I. MATERIALS

2.1 General characteristics of the Deccan Traps and drainage basin

To achieve the objectives set out in Chapter one, viz., to evaluate the significance of various sources contributing to major elements to rivers draining the Deccan, understand the behaviour of elements during basalt weathering and their subsequent transport, and to determine chemical and silicate weathering rates of the Deccan basin and associated CO₂ consumption rates— knowledge about the geohydrological characteristics of the drainage basin is needed. These include data on (i) the chemical and mineralogical composition of major rocks (basalt), and abundance and composition of minor lithologies scattered in the basin, (ii) climate factors such as rainfall, temperature, and their spatial and temporal variations, and (iii) soils and vegetation types of the region. In addition information on anthropogenic activities, which can modify the natural weathering signals would also be very useful. Information on some of the above properties of the basin are available in literature and this chapter discusses these, particularly the physical characteristics of the river basins.

The ‘Deccan Traps’ which rests on an Archean crust of the Indian Shield (Krishnan, 1982) is the major lithology of the drainage basins of headwaters of the Krishna, Bhima river system and those of the west flowing western ghat rivers. The word “Trap” originates from the Swedish word “Trappa” and indicates a stair-like or step-like topography, prevalent in many of the basalt exposures from the Deccan. The Deccan Traps are considered to be the second most extensive geological formation of the peninsular India, next only to the Archean igneous-metamorphic province in the southern India. Presently, the Deccan Traps cover an area of $\sim 5 \times 10^5$ km², however, its area at the time of emplacement might have three times of the present (Krishnan, 1982). The initial volume of the lava is estimated to be $\sim 1 \times 10^6$ km³, with an associated CO₂ release of 10^{18} moles (Javoy and Michard, 1989). The Traps stretch from Kutchch in the west to Jabalpur in the east, and from Sagar in the north to Belgaum in the south, covering parts of the states of the Gujarat, Madhya Pradesh, Maharashtra and the Karnataka, however, two-thirds of the Deccan Traps are located in the state of Maharashtra (Deshpande, 1998). The extent of the Deccan Traps is shown on an Indian map (Fig. 2.1a). The thickness of the lava pile varies from ~ 200 m to as high as ~ 2000 m in the western ghat range. The age of the Deccan Traps is

still a matter of debate and a wide range of ages from 69 to 60 Ma have been reported based on K-Ar, Ar-Ar and Re-Os methods (Courtillot, 1986; Venkatesan et al., 1993; Allegre et al., 1999; Sheth et al., 2001; Pande, 2002). However, there is a general accord among the gathered data that major emplacement of Deccan Traps took place within the time interval of 67–65 Ma ago.

The Deccan Traps are mainly tholeiitic lavas. The lava pile has been subdivided into various Subgroups and Formations based on mineralogy and chemistry. The lava flows of the south-western region (most of the rivers sampled in this study drain this region) have been divided into three Subgroups consisting of ten Formations. The Kalsubhai subgroup includes lower most Formations, the Jawahar, Igatpuri, Neral, Thakurwadi and the Bhimashanker—composed mainly of compound flows containing olivine, clinopyroxene and plagioclase phenocrysts. The Khandala and the Bushe Formations comprise the Lonavala subgroup. The Khandala formation is made of simple flows with a wide range of chemical composition in contrast to the coarse grain, compound flows of the Bushe formation that exhibits remarkably narrow

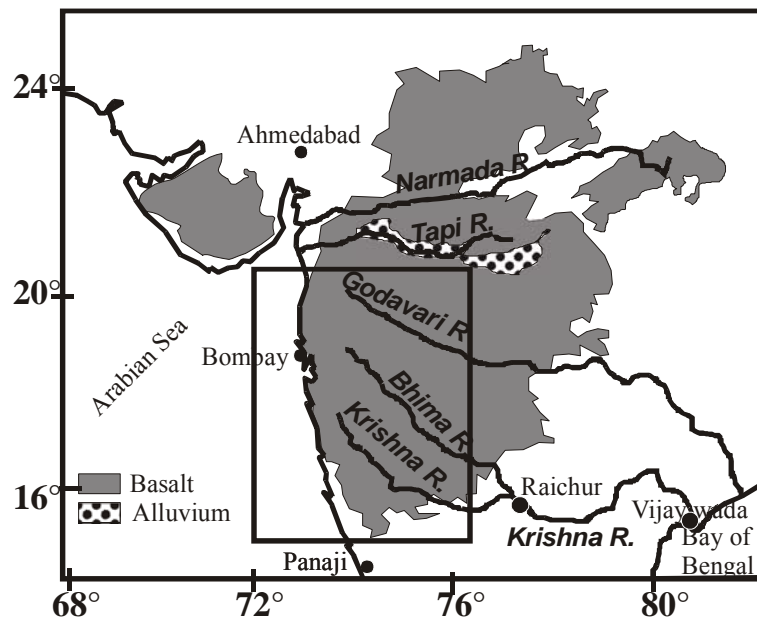


Figure 2.1a. Map of western India showing the Deccan Trap region. Major rivers and cities are also shown.

range of chemical composition. The Wai subgroup, forming the upper succession, includes five Formations—the Desur, Panhala, Mahabaleshwar, Ambenali and the Poladpur. The lavas of this subgroup are simple flows, fine groundmass with

plagioclase phenocrysts and minor amounts of olivine and clinopyroxene. The Deccan Traps have been studied extensively for their mineralogy and geochemistry and the data have been summarized in a number of review articles (Mahoney, 1988; Subbarao et al., 2000; Sen, 2001). Mineralogical studies of some of the tholeiites suggest that olivine in them have fosterite between Fo₇₇ to Fo₈₈ (Sen, 1980, 1986; Beane, 1988). Plagioclase phenocrysts have anorthite in the range of 61% to 82% whereas megacryst are more sodic (Sen, 1986). Augite and pigeonite are more common among pyroxenes (Sethna and Sethna, 1988) with rare occurrence of orthopyroxenes (Chandrasekharam et al., 2000). Titanomagnetite, ilmenite and sulfides are the common opaques (De, 1974; Sen, 2001). Occurrences of calcite amygdaloidal are also reported in some of the flows (Subbarao et al., 2000).

The rivers that are sampled as a part of this study are the headwaters of the Krishna and the Bhima, their tributaries and the west flowing western ghat (WFWG) rivers. All these samples were collected in the state of Maharashtra, and flow almost entirely through the Deccan Traps, more specifically through the Thakurwadi and the Bhimashanker Formations of the Kalsubhai subgroup and all the Formations of the Wai subgroup.

2.1.1 CLIMATE OF THE REGION

The climate of the region is influenced significantly by its physiographic features and are divided into three types: the tropical wet type in the windward side of the western ghats, i.e., the coastal districts of Maharashtra; the semi-arid or steppe type in south-central parts of the state which comes under the rain shadow zone of the mountain range of the western ghats, and the rest of the region which has tropical (Savannah) type climate (CPCB, 90).

(i) Rainfall and temperature

The rainfall over a region essentially controls the hydrologic cycle and therefore, weathering of the basin. Most (~85%) of the rainfall in the region occurs in the months of July, August, September and October, i.e., during the south-west monsoon. The rest (~15%) of the rainfall occurs in winter months during November to February (Naik et al., 2001). The average annual rainfall, ~2000-2500 mm y⁻¹,

(Fig. 2.1b) in the coastal district (Sindhudurg, Ratnagiri, Raigarh and Thane) is among the highest observed in the region. The highest rainfall of 6200 mm y^{-1} is observed at

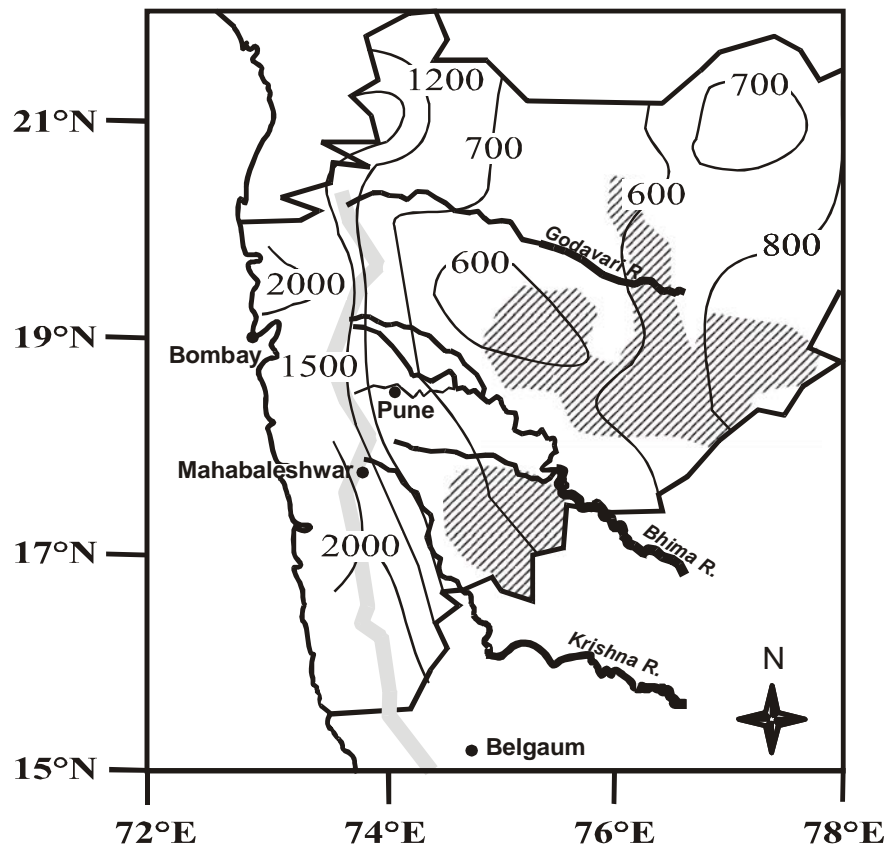


Figure 2.1b. Map showing rainfall contours (values on the contour lines are annual rainfall in mm), and the distribution of saline soils (shaded) in the Deccan region. The rainfall map from (IITM, Pune) and the saline soil map modified from CSSRI (Karnal), India. The western ghats are shown as a band parallel to the west-coast.

Mahabaleshwar in the western ghats and the rainfall decreases to $\sim 700 \text{ mm y}^{-1}$ at Pune and in interior parts of the region (Naik et al, 2001; <http://www.tropmet.res.in>). The monthly average rainfall for two regions on either sides of the western ghat mountain divide (the Konkan and Goa and the Madhya Maharashtra) is shown in Fig. 2.2a. The mean monthly rainfall during the last decade for Pune and Mahabaleshwar is shown in the Figs. 2.2b. The eastern region off the high altitude western ghats falls in the rain shadow zone and hence the rainfall in these areas is scanty ($\sim 600\text{--}700 \text{ mm y}^{-1}$; Fig. 2.1b) and these regions are prone to draught. The rainfall pattern is reflected in the monthly discharge data for the rivers (Fig. 2.2 c and d; UNESCO, 1993).

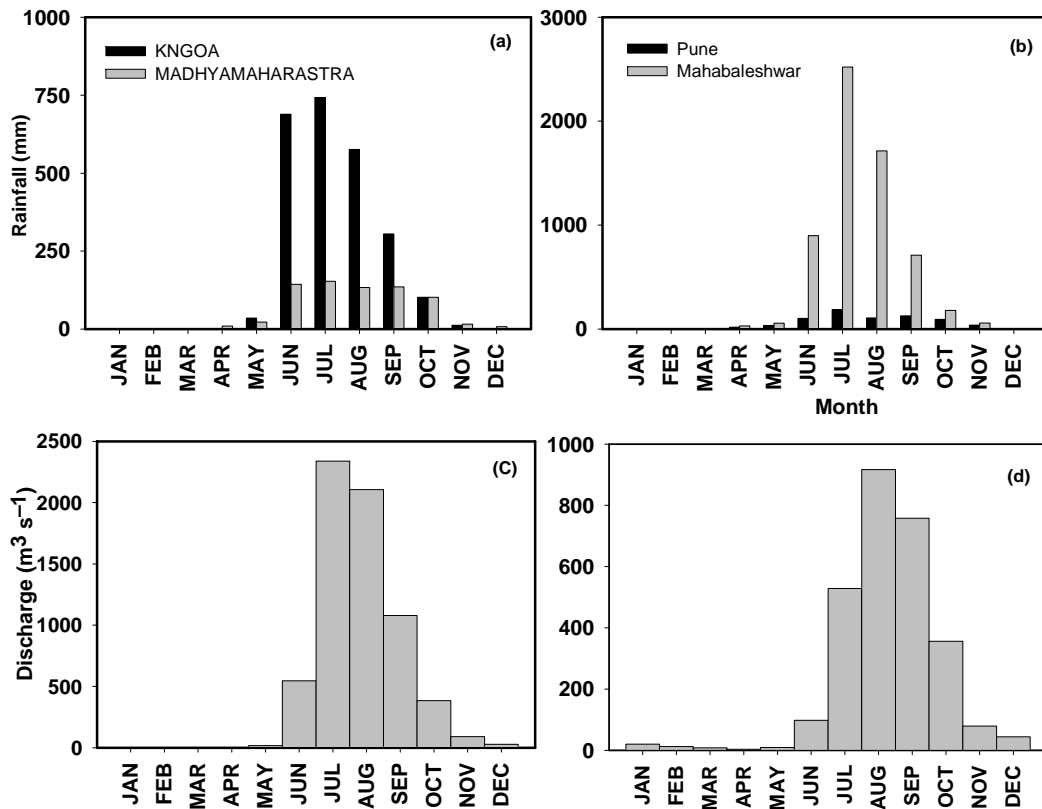


Figure 2.2 (a) Mean monthly rainfall of Konkan and Goa (KNGOA), and Madhyamaharashtra (MM). It is evident from the figure that KG, comprising the coastal districts of Maharashtra, receives much more rainfall than MM. It is also seen that ~85% of rainfall occurs during June-September (b) mean monthly rainfall at Mahabaleshwar and the Pune city (c) mean monthly discharge of the Krishna at Alamatti. Most of river discharge is during the months of June-September (d) mean monthly discharge of Bhima at Takli, most of the discharge occurs during the monsoon. Discharge of Bhima is ~50% of that of Krishna at Alamatti (Data from UNESCO, 1993).

Figures 2.2c and 2.2d show mean monthly variation of discharge ($\text{m}^3 \text{s}^{-1}$) observed for the Krishna at Alamatti, and the Bhima at Takli. The obvious feature discernable from this figure is that ~85% of the annual discharge occurs during the months of June to September, coinciding with south-west monsoon periods of high rainfall. The average maximum temperature of the region (the west-central Indian region as per “Meteorological divisions”) varies between 30°C to 34°C, and the minimum between 16°C to 24°C (<http://www.tropmet.res.in>; Fig. 2.3a). For Pune and Mahabaleshwar, the monthly variations of average maximum and minimum are shown in Fig. 2.3b and Fig. 2.3c, respectively.

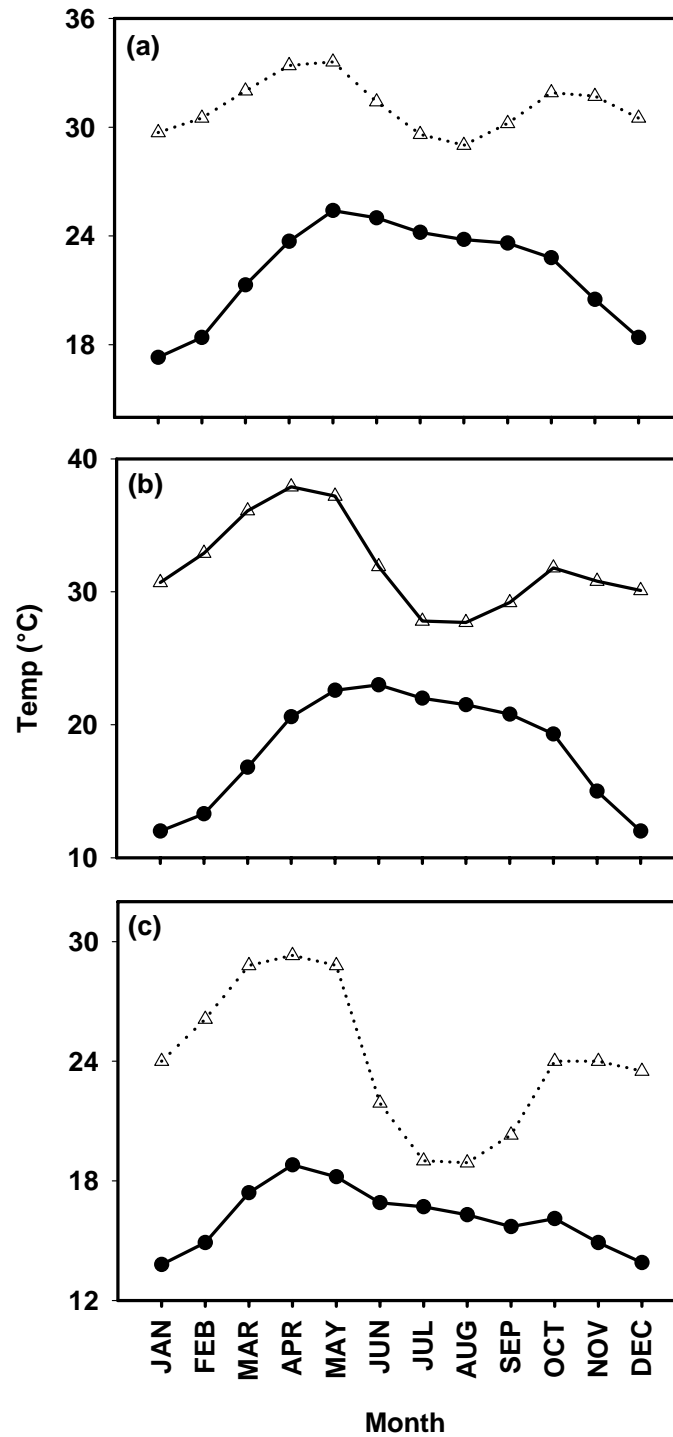


Figure 2.3a. Monthly variation of maximum (open triangle) and minimum temperature (filled circle) of westcentral India. Similar variations for (b) Pune and (c) Mahabaleshwar (Data from www.tropmet.res.in; CPCB, 90).

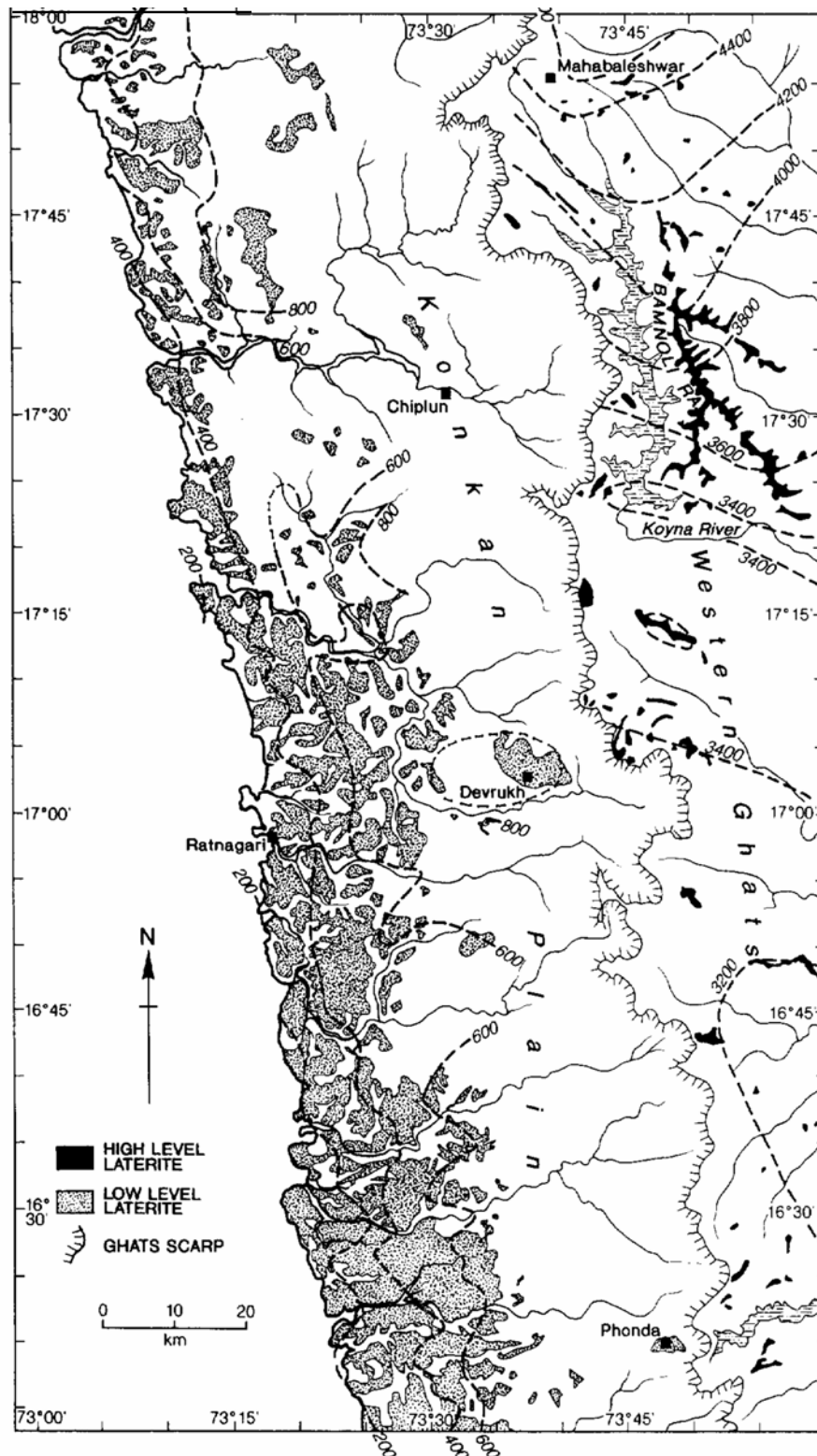


Figure 2.4. Distribution of laterite soils in the western Deccan Traps (Fig. taken from Widdowson and Cox, 1996).

(ii) Soils of the region

The soils in the basin can be grouped into two major categories; the black soil and the red soil (CPCB, 90; Deshpande, 1998). However, based on the extent of weathering these can be subdivided into several categories such as deep black, medium black, shallow black, mixed red and black, laterite, red sandy, skeletal and alluvial soils (CPCB 90).

Most of the Krishna basin in the western region is dominated by black soil. These soils, derived from the weathering of basalts are abundant in smectite/montmorillonite group of clay minerals (CPCB, 90; Kessarkar et al., 2003). Subsequent weathering and leaching of black soils results in red loamy and laterite soils. Red soils have kaolinite as the predominant clay mineral and occur in the eastern and southern parts of the basin. Laterite soils are common in regions of high rainfall such as the regions around Mahabaleshwar and coastal districts of Maharashtra. In some areas, the basalt has been extensively weathered and covered with laterites. The distribution of the laterites in the Deccan Traps is shown in [Fig. 2.5](#) (taken from Widdowson and Cox, 1996).

There are also reports of alkaline and saline soils dispersed in the upland Bhima and the Krishna basins (Bhargava and Bhattacharjee, 1982; [Fig. 2.1b](#)). Remote sensing studies (NRSA maps, 1998) also have documented the presence of salt affected soils in Maharashtra, especially in the basins of the Bhima, Krishna, Nira, Mutha rivers and also along the coastal tracts of the Arabian sea. The soils are mostly Na- sulfates and chlorides with minor abundances of the carbonates and bicarbonates. These might have formed by evaporation of the ground water locked in the soil zone in summer season.

(iii) Vegetation

The natural vegetation, which influences the intensity of weathering, depends on various climate factors such as rainfall, temperature and soil moisture in the region, in addition to physiographic locations and environmental factors. Information on the vegetation and ecology are available in Puri et al. (1989). The Deccan is characterized by a distinct mountain range, the western ghats, which acts as a 'geographical divider' of the region. The coastal districts of Maharashtra, on the western side of the divide has an areal coverage of ~6%, whereas the Deccan interior, on the eastern side of the divide cover ~94% of the Trap area. The high altitude regions of the western ghats

receive more rainfall and have “tropical evergreen forests”, the plant species are tall, mature and thickly wooded. The tropical evergreen forest is dominated by teak type trees (e.g. *Tectonica grandis*, *Terminilia tomentosa*, *Adinia*, *Laennea* and *Cleistantus collinus*). Other vegetation consists of mixed type (*Hardwickia bintxa*, *Chloroxylon swientenia*, *Bosewillia serrata*) and bamboo type (*Dendrocalamus strictus*; CPCB, 90). The eastern part, with lesser and gradual decrease in rainfall is characterized by “dry deciduous forest”. The “western preplain”, which experiences semi-arid to arid climate have a stunted growth of forest cover varying from “South Indian Tropical dry deciduous mixed forest” (includes varieties of bamboo type, fuel type such as *Albizza lebbeck*, *Acacia sundra*, *Premna tomentosa* and Teak type) to the dry thorny type (e.g. *Acacia latronum* and *Acacia kurpica*).

Agriculture, and fertilizer use

Agriculture is the dominant land use of the Krishna basin and accounts for ~50% of the cultivatable land in Maharashtra. The major crops grown depend on the rainfall, climate and the topography of the basin. The main crops in Maharashtra are sugarcane, cotton, millets, wheat, rice and groundnut. The fertilizers that are generally used are urea (N=46.6%), superphosphates and Murate of potash (95% KCl). Pawar and Shaikh (1995) reported contamination of ground water due to fertilizers use, with most of them being easily soluble in water. Their effects in modifying the stream water chemistry are discussed in chapter four.

2.1.2 Characteristics of rivers studied

The rivers in the present study include the headwaters of the Krishna, its tributaries and sub-tributaries that drain through the Deccan Traps. These rivers flow east, and the Krishna finally drains into the Bay of Bengal (Fig. 2.1b). In addition to the Krishna system, six rivers that flow west into the Arabian sea are also studied as a part of this work. The two groups of rivers are on either side of the western ghats, the Krishna system on the eastern side draining into the Bay of Bengal and the WFWG rivers on the west side flowing into the Arabian sea. The climate of the basins of two groups especially rainfall is dictated by the western ghats; the western side receiving a factor of ~3-4 more rainfall. The characteristics of all these are listed briefly in the following sections.

The Krishna

The Krishna is one of the major rivers of peninsular India along with the Godavari and the Kaveri (Cauvery). The Krishna originates as a small stream in the western ghats, near Mahabaleshwar (13°N, 73.5°E) at an elevation of ~1340 m (a.s.l). It traverses eastward ~25 km through the rocky terrains of the Deccan Traps, from Mahabaleshwar to the town of Wai. It then flows eastward (covering a stretch of ~440 kms) and finally drains into the Bay of Bengal covering a length of ~720 kms. The Krishna river has two dams at Srisaïlam and Nagarjunasagar, however, both are downstream of the present study area. The average annual discharges of the Krishna at Alamatti (out of Deccan Traps) and at Vijaywada (at the mouth) are $1.73 \times 10^{13} \ell \text{ y}^{-1}$ and $6.8 \times 10^{13} \ell \text{ y}^{-1}$.

The Krishna drains through the state of Maharashtra (69347 km²), Karnataka (113965 km²) and Andhra Pradesh (85474 km²). The lithology of the river basin in Maharashtra is almost entirely tholeiite basalts, with scattered alkaline/saline soils (Bhargava and Bhattacharjee, 1982), laterites (Widdowson and Cox, 1996) and calcareous tufas (Pawar, 1988). Downstream of Maharashtra, in the states of Karnataka and Andhra Pradesh, the Krishna basin includes granites, granitoids, green stones, schists, amphibolites and gneisses. Its first tributary, the Koyna meets the Krishna near Karad. Subsequently, the Varna and the Panchganga joins the Krishna at Sangli and Kurundwad respectively (Fig.2.6). Dudhganga joins the Krishna mainstream at a distance of ~310 km from its origin. About 201 km from the confluence of the Dudhganga-Krishna, Ghataprabha joins the river. The largest of the tributaries, the Bhima, mixes with Krishna near Raichur (in Karnataka).

The Bhima

The Bhima originates in the hills of Bhimashanker near a temple, a little north of Pune. The river traverses in a south-easterly direction (Pawar, 1988) and joins the Krishna at a distance of ~860 km from its origin. This is the largest tributary of the Krishna, with a drainage area of 76614 km² (Rao, 1975). The discharge of the Bhima at Takli (in the Deccan Traps) is $7.2 \times 10^{12} \ell \text{ y}^{-1}$.

The lithology of the Bhima basin in Maharashtra is also almost entirely Deccan Traps, however, there are reports of calcareous tufas in the upland of the Bhima basin and

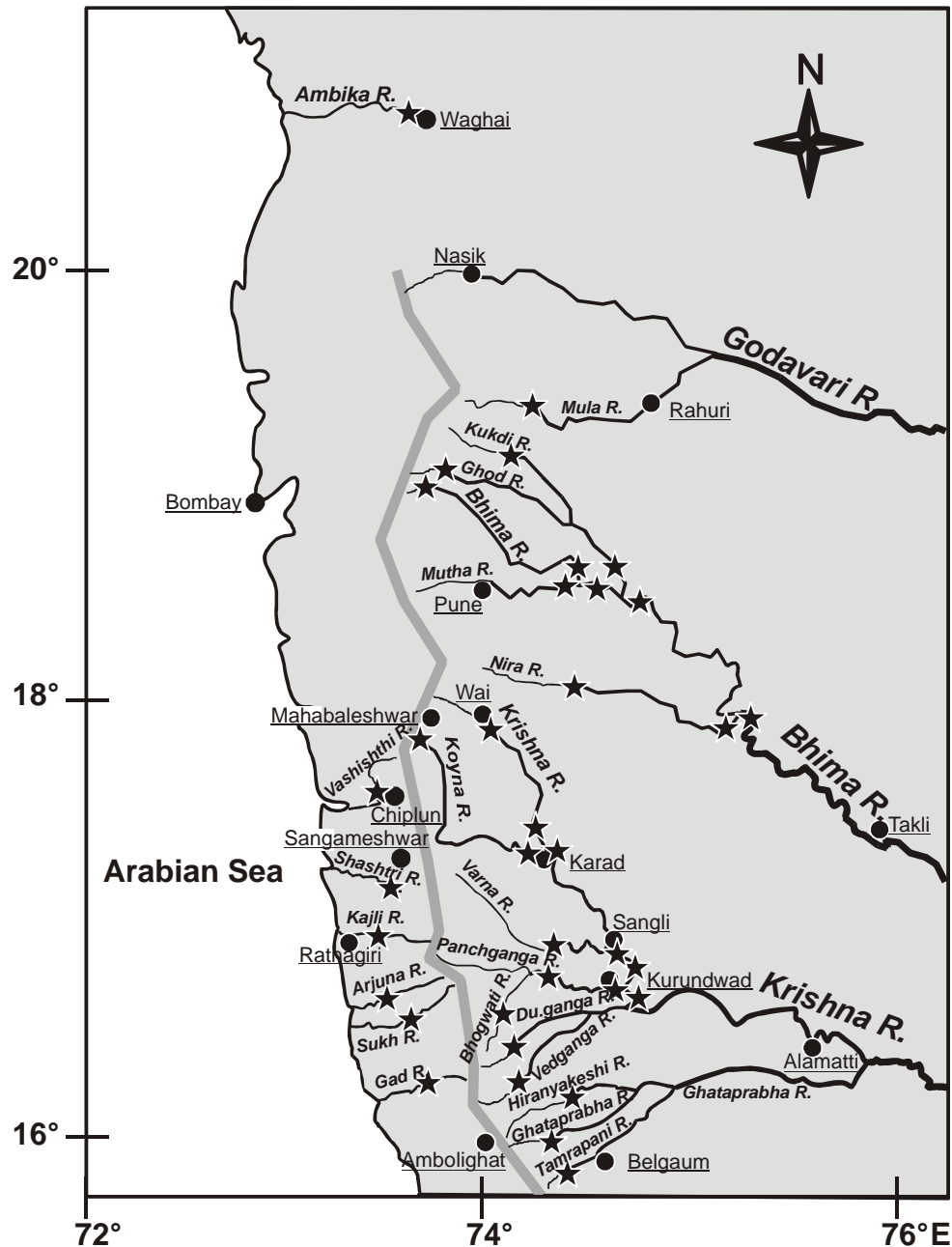


Figure 2.5. Sample locations, rainfall monitoring stations and major cities. The rivers sampled in this study are from the Krishna system in the Deccan Traps and the west flowing western ghat rivers. The western ghats is shown as a shaded band running nearly parallel to the west coast.

of alkaline/saline soils are also reported in the region (Bhargava and Bhattacharjee, 1982). The tufas are finely laminated calcium carbonate deposits formed during the

Holocene (Pawar, 1988). The thickness of these tufas varies from few cms to tens of meters.

The tributaries of the Bhima are the Ghod, Nira and the Mutha rivers. The Bhima meets the Ghod near Daund, the Nira at Narsinghpur and the Mutha near Pargaon (Fig. 2.6). There are several check dams along the course of the Bhima and its tributaries and, hence, the discharge of the rivers are regulated by water released from these dams.

The Koyna

The Koyna merges with the Krishna, near Karad. It has a drainage area of 2036 km². The river flows entirely in Maharashtra and has an elevation range of ~550-1460 m. The river flows a distance of ~650 km south-ward before it is dammed near Koyna nagar. The climate of the Koyna basin is sub-tropical, with highest rainfall at Mahabaleshwar (~6200 mm y⁻¹) and the lowest of ~750 mm y⁻¹ at Karad (Naik et al., 2001).

The lithology of the Koyna basin is almost entirely Deccan Traps of the Mahabaleshwar and the Ambenali Formations (Kaila et al., 1981; Mahoney, 1988). A characteristic red coloured layer “red bole” are usually found between two consecutive lava flows of this basin. Secondary minerals such as zeolites, quartz and calcite are also reported in these lava flows (Naik et al., 2001). Laterite soils also occur in the basin as caps over basalts at elevation ranging from 975–1400 m (a.s.l) with annual rainfall >2000 mm (Naik et al., 2001). They are reddish-brown in colour with thickness ranging from 2–30 m. They are highly ferruginous and sometimes as thin lenses of bauxite (Thorat and Ravi Kumar, 1987).

The Ghod

The Ghod also originates near the Bhimashanker hill range and traverses a length of ~140 km before merging with the Bhima near Daund. The Ghod river, being in close proximity of the Bhima basin, also forms a part of the Bhima basin and drains a similar lithology with the Traps accounting for almost all of the drainage basin. Saline/alkaline soils are reported in the Ghod basin (Bhargava and Bhattcharjee, 1982). River Kukdi is a tributary of the Ghod river.

The Mutha and the Nira

The Mutha is another tributary of the Bhima. It originates near Kharakwasla lake and joins the Bhima at Pargaon; its drainage basin includes industrial areas of Pune and Pimpri. The Deccan basalts are the primary lithology of the basin, however, anthropogenic inputs can be a potential source of major ions to these waters. The river Nira originates near Bhatghar lake and joins the Bhima near Narsinghpur. The water flow in this river is generally lean to moderate, even in the monsoon season (when sampling was done in 2001 and 2002). This is due to several check dams built in its upstream that manage water for agricultural needs.

The Varna, Panchganga, Dudhganga and the Vedganga

The Varna originates in the western ghats, has a drainage area of $\sim 2000 \text{ km}^2$. It covers a length of $\sim 110 \text{ km}$ before its confluence with the Krishna near Sangli (CPCB, 90). The Panchganga originates near western ghats, has a drainage area of $\sim 2600 \text{ km}^2$, confluences with the Krishna near Kurundwad (CPCB, 90). The river Bhogwati is a tributary of the Panchganga. The river Dudhganga has a drainage area of $\sim 2550 \text{ km}^2$ (CPCB, 90) joins the Krishna near Dhankali, the state boundary of Maharashtra and Karnataka. The Vedganga is a tributary of the Dudhganga. All these rivers, almost entirely, drain the Deccan Traps.

The Ghataprabha

The Ghataprabha river originates in south of the Deccan Traps in Maharashtra near the high mountains at Ambolighat. It has a drainage area of $\sim 8330 \text{ km}^2$. It has two tributaries—the Hiranyakeshi and the Tambrapani (CPCB, 90).

The Vashishthi, Shastri, Kajli, Arjuna, Sukh and the Gad

These are a set of six rivers from north to south (Fig. 2.6), draining into the Arabian sea, unlike the rivers of the Krishna river system that flow eastward and drain into the Bay of Bengal. These six rivers are small streams and all of them originate in the west part of the western ghats. The region, which the rivers drain have a thick vegetation cover, with high rainfall ($\sim 2000\text{-}2500 \text{ mm y}^{-1}$). In addition to the Deccan basalts, which make up most of the drainage basin, there are reports of low-lying coastal lateritic soils in some parts of region (Widdowson and Cox, 1996). Physical erosion of these laterite soils were evident during sampling, the waters were often red coloured due to fine suspended matter dispersed in them.

II. SAMPLING AND ANALYTICAL METHODS

This section of the chapter describes the sampling methods and analytical techniques that are employed in this study.

2.2. SAMPLING

The sampling for the present work was done in the monsoon season of the years 2001 and 2002, during the months of August–September, corresponding to high flow stages. About eighty-five percent of the annual rainfall occurs in the months of June to September, which represent the south-west monsoon season in India and high flow stages of Indian rivers (Fig. 2.3a,b). The choice of monsoon season for sampling is two fold: (i) the main goal of this study is to understand different aspects of weathering of basalts. Monsoon season, with high discharge, would be ideal to address this objective, as the river water chemistry during this season would be dominated by chemical weathering of basalt and rainwater. Impact of input from groundwater and anthropogenic sources would be minimum (ii) the Bhima and the Krishna are large and perennial rivers, whereas many others are seasonal, they are either dry or have lean flow during non-monsoon seasons. This makes their sampling during monsoon the ideal period to characterize weathering in their basins. Sampling was done during two consecutive years (2001 and 2002) to get substantial database as well as to assess the inter-annual variability. The details of the sampling locations are listed in Appendix 2.1. The sampling which includes river waters, suspended particulate matter and bed sediments are discussed below:

2.2.1. River water

The parameters measured in the dissolved phase of river water are major ions, $^{87}\text{Sr}/^{86}\text{Sr}$, $\delta^{13}\text{C}$ of dissolved inorganic carbon, Sr and Ba. The water sampling was done, as far as possible, from mid-stream of the river with the help of boats or from bridges to avoid local heterogeneity and possible human influences near the river banks. For major ions, Sr isotopes and trace elements, one litre samples were collected in pre-cleaned high-density polyethylene (HDPE) bottles, which were copiously rinsed with the ambient river water. The water is filtered (within 6 to 10 hours) through 0.4 μm Nucleopore filters and split into two aliquots. One aliquot (~200 mL) was kept un-acidified and used for the analyses of Na and K, and anions (Cl , NO_3 and SO_4). The second aliquot (~500 mL) was acidified with high purity HNO_3 to pH ~2 and was used for the analysis of Ca, Mg, Sr, Ba and Sr isotopes. Samples for alkalinity measurements were collected directly into ~125 mL bottles wherever waters appeared clear. For samples that were turbid, samples were

first collected in one litre bottles and after a few hours, the clear supernatant was decanted to ~125 ml bottles. These decanted samples were used for the alkalinity measurements. For $\delta^{13}\text{C}$ measurements, samples were collected in ~125 ml glass bottles. Soon after collection, the samples were poisoned with saturated HgCl_2 , sealed with rubber septum-aluminum cap, and wrapped with a thick black paper (to avoid photosynthetic activity) and brought to the laboratory and kept refrigerated until analysis. The sampling for $\delta^{13}\text{C}$ measurement was done only during the campaign of 2001.

Along with the samples, the procedural blanks were also processed by using double distilled water.

2.2.2. Bank sediments

Bank sediments were collected far away from cities and towns to minimize the influence of domestic and industrial contributions. The sampling was done with the help of a pre-cleaned plastic scoop from distances less than a few meters from the waterfront of rivers. The sediments were stored in plastic bags, and brought to the laboratory. In the laboratory, part of the sediments were transferred to glass beakers and dried at $\sim 90^\circ\text{C}$. Subsequently, it was powdered to $<100\text{-}\mu\text{m}$ size using an agate mortar and nylon sieves and stored in plastic containers. Care was taken to avoid metal contact during powdering and sieving.

In addition, some samples of basalts were also powdered using Spex ball mill with stainless steel balls to very fine powder. These were used exclusively for the analysis of carbonates and carbon isotopes in them.

2.3. ANALYTICAL TECHNIQUES

(a) Locations: The sampling location (latitude and longitude) measurements were done using global positioning system (Model: Magellan GPS310). The accuracy of measurements was checked by measuring the geographical location of Pune city, the location from where sampling campaign was started.

(b) Altitude: The measurement of altitude of the sampling sites was carried out in the 2001 field campaign through altimeter (Pretel: Model ALTIplus K2) as well as GPS (Model: Magellan GPS310). Both the techniques yielded agreeable results ($\sim \pm 5\%$). In both cases, the instruments were calibrated with a “reference point- the Wilson point” in the Mahabaleshwar plateau, for which the altitude is a-priori known to be 1492 m. In the field campaign of 2002, only the GPS was used. Since the locations in most of the cases were the same, the independent measurements in two years give the reproducibility of

measurements. The precision of measurements based on repeat measurements of altitude is better than 2%.

(b) pH, temperature and electrical conductivity: The pH and the electrical conductivity (EC) of the river waters were measured at site using a multi-purpose kit (Model: Multiline 7000). Prior to measurements, the pH probe was calibrated with freshly prepared buffer solutions of pH 4.0 and 9.2, and the EC probe with 0.01 M KCl solution. The precision of pH measurements is better than 0.1 units and that of EC measurement is better than $10 \mu\text{S cm}^{-1}$. Temperature of river waters was measured by a portable thermometer (MA line), with precision better than $0.1 \text{ }^\circ\text{C}$. In all the measurements mentioned above, readings were taken only after they attained stable values. Temperature and EC values attained stability generally within a minute, whereas pH usually needed 2-3 minutes to stabilize.

(d) Major ions: Alkalinity measurements in the samples were done on unfiltered but decanted samples by acid titration using dilute HCl ($\sim 0.01 \text{ M}$) using an Auto-titrator (Metrohm 702 SM Titrino) fitted with glass electrode. The measurements were generally done within a few days after the samples were brought to the laboratory. The measurement was based on fixed end point method corresponding to two end points at pH values of 8.3 and 4.3 for the CO_3^{2-} and the total carbonate species (HCO_3^- and CO_3^{2-}). Analysis carried out on one sample, both in the filtered and unfiltered split yielded nearly identical alkalinity. Based on repeat measurements ($n=8$) the precision of the measurements is calculated to be 0.25%.

Cl, NO_3 and SO_4 were determined by Ion chromatography (Dionex series 2000i/SP) in filtered un-acidified samples. F peak was not detectable in a few randomly selected samples; hence no attempts were made to measure F in other samples. The system was calibrated using standards prepared from analytical grade reagents. The separation of the ions as per their retention time was done on AS4A column using a mixture of 1.8 mM Na_2CO_3 and 1.7 mM NaHCO_3 as the eluent. Samples with low concentrations were measured at a more sensitive conductivity scale. In a few cases, as and when needed the samples were suitably diluted with de-ionized distilled water to fit into the scale of measurements. Internal check standards of different concentrations were run during analyses to check the accuracy of the measurement. Based on replicate analyses of different samples, the precision of measurement for Cl was found to be 1%, for NO_3 and SO_4 , these were 3.9% and 3.3% respectively.

Among the cations, Na and K measurements were carried out in the filtered un-acidified samples using flame-AAS (Perkin Elmer Model 4000) using acetylene-air mixture as fuel, at wavelengths of 589 nm (Na) and 776.5 nm (K). The accuracy of measurement was checked by measuring Merck[®] and Calmix-7[®] standards of known concentrations. The precisions based on repeat measurements for Na (n=6) and K (n=11) are 1.8% and 4.1% respectively.

Ca and Mg measurements were done in the filtered, acidified splits by inductively coupled plasma-atomic emission spectrometry (ICP-AES; Jobin Yvon, Model 38S). The measurements were done by sequential scanning of the emission wavelengths at 279.806 nm (Mg) and 422.673 nm (for Ca). Ca and Mg standards were made by dissolving pure anhydrous CaCO₃ and Mg metal in acids. The accuracy of measurements is checked by analysis of known strengths of Merck standards and through laboratory check standards. The precisions of the Ca and Mg measurements are 4.8 % respectively.

Si analysis was done by spectrophotometer (Model Beckman 26) using the Mo-blue method (Strickland and Parson, 1972) at a wavelength of 810 nm. The working Si-standard was prepared by dissolving Na₂SiF₆ salt in double distilled water. The analyses were done in filtered, un-acidified aliquots. In some samples, Si measurements were checked in both the acidified and un-acidified splits; they show similar Si concentration within analytical uncertainties (Table 2.1). The precision for Si measurement is 1.4%.

(e) Strontium and Barium

Sr and Ba were measured in the acidified samples using ICP-AES coupled to an ultrasonic nebulizer (USN) following Dalai (2001). Calibration of the instrument was done with standard solutions made from analytical grade Sr(NO₃)₂ and Ba(NO₃)₂. NaCl was added to the standards to match the TDS concentration with those of the samples. It also serves to increase the ionic strength of the solution, thereby, preventing potential adsorption of elements on the tubing walls of USN.

The accuracy of measurements were checked by analysing commercial standards (Merck) and also with dissolved USGS standards (G-2), the results are listed in Table 2.2. Based on replicate analyses, the precision for Sr and Ba measurements are calculated to be 3.7% and 2.6% respectively.

Table. 2.1. Dissolved silica concentration in acidified and un-acidified samples in seven samples collected (in 2001).

Rivers	Dissolved Silica	
	Acidified ($\mu\text{g ml}^{-1}$)	Unacidified ($\mu\text{g ml}^{-1}$)
BHM-1	8.45	8.42
BHM-2	8.15	8.23
BHM-4	10.50	10.56
NIRA-2	8.68	8.71
MTH-1	12.06	12.01
VRN-1	8.45	8.79
SHT-1	9.90	9.65

Table 2.2 Analysis of Sr and Ba in standards (Merck and G-2) for accuracy check.

Sr ($\mu\text{g l}^{-1}$)			Ba ($\mu\text{g l}^{-1}$)		
Merck					
Expected	Mean	Range	Expected	Mean	Range
4	3.9±0.2	3.7-4.1	4	3.82±0.05	3.7-3.9
10	10.2±0.2	9.96-10.4	5	4.9±0.1	4.7-5.0
50	48.5±1.4	47.5-49.5	25	23.7±0.03	23.6-23.7
100	96.2±2.2	95-99	50	49.2±2.0	48.5-52.2
G-2[#]					
Expected	Mean	Range	Expected	Mean	Range
478	486	475, 496	1880	1876	1825, 1927

[#] in $\mu\text{g g}^{-1}$;

(f) $\delta^{13}\text{C}$ measurements

Carbon isotope ratios ($^{13}\text{C}/^{12}\text{C}$) were measured in purified CO_2 extracted from the water samples, using a stable isotope mass spectrometer (Geo 20-20 PDZ Europa). The extraction line is shown in Fig. 2.6. The volume of water required for analysis was generally 10-50 ml, depending on their HCO_3^- content, so as to yield $\sim 20 \mu\text{mol}$ of CO_2 . The water is injected into an evacuated glass bottle containing $\sim 2 \text{ ml}$ of 100% H_3PO_4 . The evolved gases were passed through a silica gel Trap (at -90°C) into a spiral trap maintained at liquid N_2 temperature. Water vapour gets trapped in the silica gel trap whereas the CO_2 in the spiral trap. In the next step, the CO_2 from spiral trap was pumped into trap T1, by replacing the LN_2 in spiral trap with slush (-90°C) and placing LN_2 trap under T1. The CO_2 in T1 was purified sequentially by trapping-thawing-retrapping between traps T2 and T3. The final purified CO_2 is collected in Trap T4 for isotope analysis. Based on four experiments using natural seawater, the extraction yield and the

precision of measurements are determined to be $\sim 90\%$ and $\pm 0.2\%$ (seawater $\delta^{13}\text{C} = -2.79 \pm 0.2\%$).

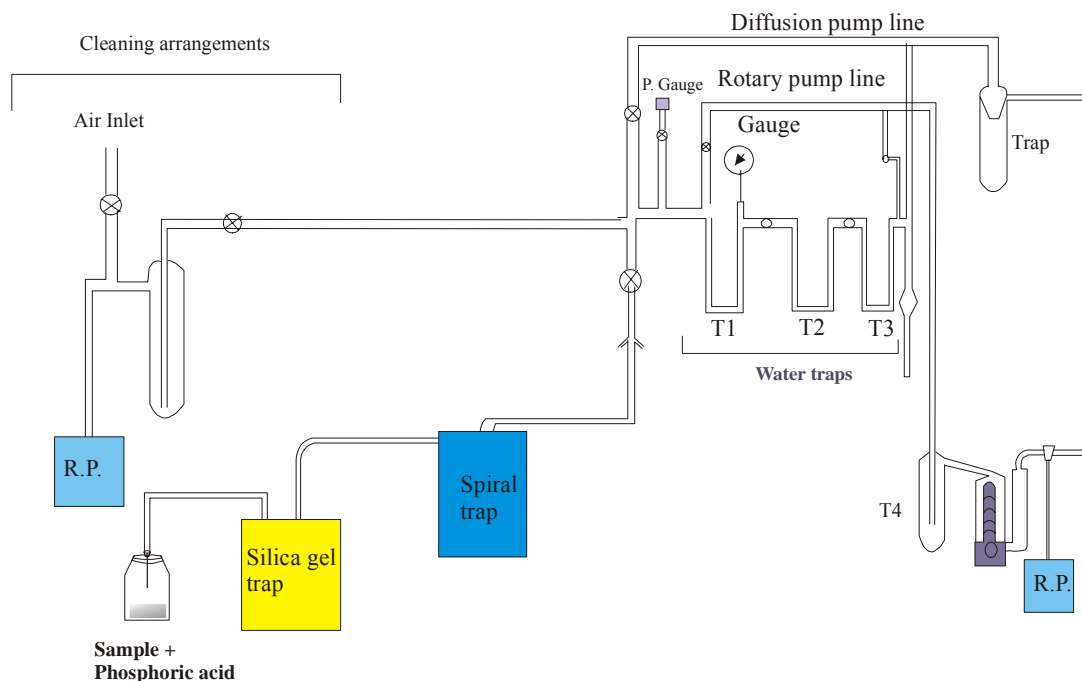


Fig. 2.6. Extraction line for CO_2 from dissolved inorganic carbon from water samples. The necessary vacuum required during the extractions is obtained by the rotary pump (RP in Fig.) and the diffusion pumps.

(g) Sr isotopes

Sr isotopes were measured in water samples using a solid source mass spectrometer (VG 354) in a single collection mode, at the National Geophysical Research Institute, Hyderabad. Sr was separated from the other interfering elements and Rb by ion exchange chromatography. Separation was done in quartz columns containing Dowex 50X8 (200-400 mesh). The columns were conditioned with 2N HCl and samples were adjusted to this acid strength. About 50 to 150 ml of filtered, acidified river water was taken in thoroughly cleaned FEP beakers and evaporated to near dryness. The volume of water used for Sr isotope analysis was decided based on Sr concentration in water such that the final amount of Sr is a few \sim micrograms. To the residue, about ~ 1 ml of HNO_3 acid (Seastar baseline) was added to oxidize organic matter and dried completely. The residue was converted to chloride-form with HCl and dissolved in 1.25 ml of 2N HCl. The solution was centrifuged in 1.5 ml tubes and the clear supernatant was loaded on the resin column and Sr was separated following conventional procedures (Dalai, 2001)

The pure Sr fraction was dried, dissolved in a few μl volume of 0.5N HNO_3 , and loaded with H_3PO_4 on degassed high purity Ta filaments. The Sr isotope measurements were carried out in single collector mode. During the period of measurements, the Sr standard (SRM 987) was run repeatedly to check for accuracy and reproducibility. The results yielded a value of 0.710226 ± 0.000043 (1σ , $n=6$). A few samples were run twice; the results are reported in Table 2.3.

Table 2.3 Repeat runs of three samples.

Sample	Run I	Run II	Run III
KRS-5	0.706831 ± 21	0.706835 ± 16	0.708192 ± 17
KJL-1	0.706138 ± 20	0.706157 ± 74	-
HRN-1	0.708192 ± 17	0.708192 ± 49	-

For determination of procedural and Sr blanks, the treatments, as done for samples, were repeated with 100 ml Milli Q water. Based on five runs, the blank for the overall measurements is determined to be 0.5 to 3 ng. $^{87}\text{Sr}/^{86}\text{Sr}$ in the blanks were not measured and the samples were not corrected for blanks, as it was estimated that its effect would be within errors of measurements.

(h) Sediments

(i) Dissolution

A known weight of finely powdered ($<100 \mu\text{m}$) sediments were taken in quartz crucibles and combusted at $\sim 450^\circ\text{C}$ to remove organic matter in them. The samples were completely transferred to PTFE dishes and treated ($3 \times 5 \text{ ml}$) with HF to remove the silica. The samples were then digested with HCl-HNO_3 mixture (2-3 times). The samples were generally brought to solution through these acid digestions. In a few samples, there was visible residue after HCl-HNO_3 treatment. These samples were centrifuged, the residue was quantitatively transferred to dish and HF and other digestion procedures were repeated until the residue was brought to solution completely. The solution were mixed and made to 50 ml in 1N HCl . Five samples were digested in duplicate to check the overall precision of analyses (Fig. 2.7a,b). Similarly, the USGS standards W-1 and W-2 were dissolved and suitably diluted to check the accuracy of analyses (Fig. 2.8a,b).

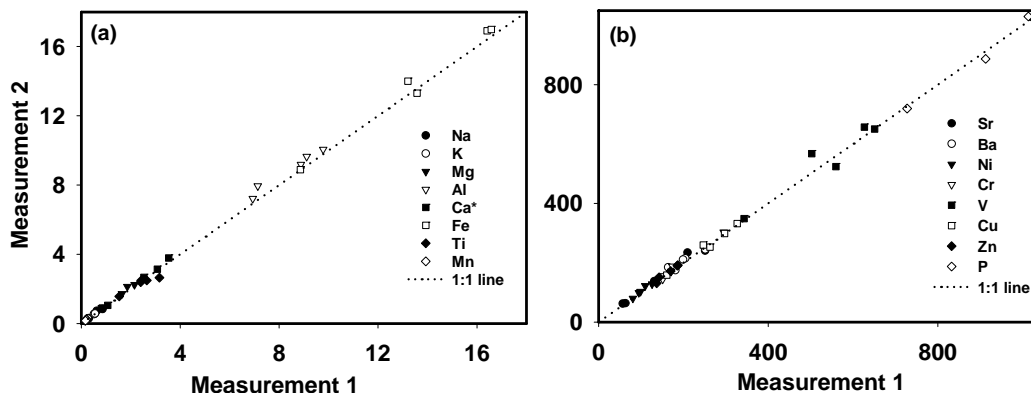


Figure 2.7a. Reproducibility in overall elemental (major elements) analysis from repeat measurements of five sediment samples (b) similar exercise for trace elements (also includes P). The repeat measurements show a very good agreement between them.

Major elements

Na, K, Fe and Mn were measured by Flame-AAS. Single element standards were used for calibration of the instrument for respective measurements. For the measurements in AAS, all the samples were suitably diluted to bring them into the linear range of absorbance-concentration relation. Other major elements (Ca, Mg, Al and Ti) were measured using ICP-AES. The wavelengths for the absorption and emission lines used for these measurements are reported in [Appendix 2.2](#). The precision of measurements based on the five repeat measurements for various elements are also reported in [Appendix 2.2](#).

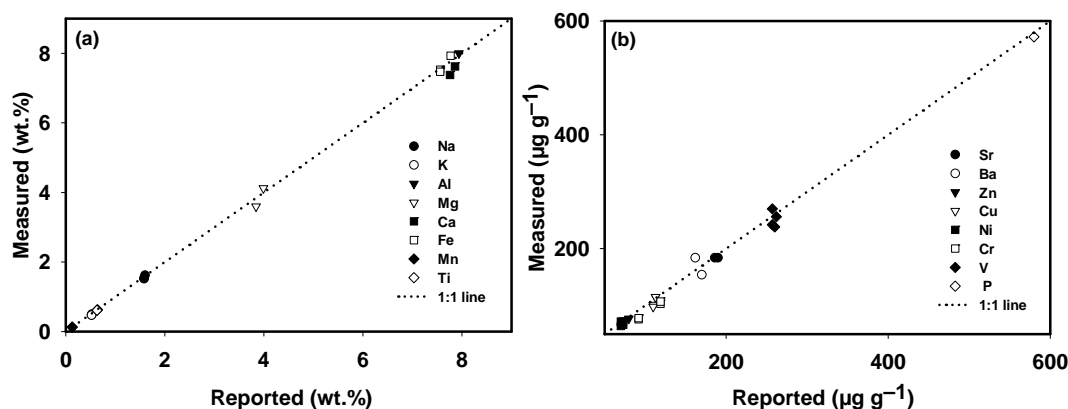


Figure 2.8a. Comparison of measured and reported major elemental concentrations (in wt.%) in W-1 and W-2 (b) similar comparison for minor elements concentrations (includes P). These results, as evident, show very good agreement between measured and reported values, attesting to the overall accuracy of measurements.

Trace elements

Cu and Zn were measured by AAS following conventional procedures. The accuracy of measurements was checked by measuring concentration of W-1 and W-2 and comparing with their reported values (Fig.2.8 a,b). Measurements of Sr, Ba, V, Cr and Ni were done using ICP-AES, the instrument was calibrated with available standards, such as 23 elements Merck. Phosphorous was measured by measuring the absorption of its complex with ammonium molybdate at wavelength 885 nm using a spectrophotometer. The accuracy of P measurement was checked with W-1 standards. The coefficient of variation for all the elements is discussed in Appendix 2.2.

Carbonate in sediments and basalts

The carbonate content in sediments and basalts were measured with a coulometer (UIC Coulometer; Model 5012). The instrument was calibrated with Na_2CO_3 solution prepared from analytical grade salt. Prior to preparation of standards, it was dried overnight to eliminate any moisture. CO_2 was liberated from solution/sediments by treating samples with 40% H_3PO_4 at 70 °C for 10 minutes in an extraction cell. About 100 mg of sediment was taken for the analyses. The liberated CO_2 was purified with CO_2 free from air, by passing through a column with silica gel and anhydrous MgClO_4 and measured in the coulometer titration cell. To check the accuracy, known weight of pure CaCO_3 was analysed for the amount of CO_2 liberated. Based on repeat analysis, the precision of measurement is determined to be 2.4%.

Appendix 2.1 Location, altitude, temperature, pH and electrical conductivity (EC) of Deccan Trap rivers sampled.

Code	River	Year	Lat. (°N)	Long. (°E)	Sampling locations and remarks	Altitude (m)	Temp. (°C)	pH	EC ($\mu\text{S cm}^{-1}$)
<u>Krishna mainstream</u>									
KRS-1	Krishna	2002	16.79	74.63	Krishna before confluence with Panchganga	534	24.4	7.58	184
		2001				545	24.8	7.64	197
KRS-2	"	2002	16.65	74.64	After confluence with Panchganga	614	24.9	7.17	122
		2001				540	23.8	7.52	114
KRS-3	"	2002	17.30	74.19	Krishna after confluence with Koyna, near Karad	564	25.5	7.76	189
		2001				572	-	7.63	96
KRS-4	"	2002	17.40	74.11	Krishna near Umbraj before confluence with Koyna	583	36.4	8.08	242
		2001				575	24	8.01	187
KRS-5	"	2002	16.80	74.57	Krishna after confluence with Varna	569	24.9	7.42	176
		2001				-	24.5	7.62	182
KRS-6	"	2002	17.94	73.90	Krishna at Wai twon, affected by anthropogenic activity.	-	25.1	8.38	324
		2001				696	24.3	8.11	395
<u>Bhima mainstream</u>									
BHM-1	Bhima	2002	19.03	73.63	River Bhima near origin.	642	21.9	7.38	79
		2001				624	22.9	7.74	76
BHM-2	"	2001	18.57	74.34	Bhima before confluence with MTH-1	517	25.3	8.39	538
BHM-3		"				2002	18.57	74.38	Bhima after confluence with MTH-1
	2001		523	25.3	7.74	510			
BHM-4	"	2002	18.40	74.57	Bhima after confluence with Ghod river (almost dry)	501	24.4	7.7	418
		2001				512	24.8	7.82	607
BHM-5	"	2001	17.97	75.14	Bhima after confluence with Nira (NIRA-2)	462	27.2	8.36	702

Code	River	Year	Lat. (°N)	Long. (°E)	Sampling locations and remarks	Altitude (m)	Temp. (°C)	pH	EC ($\mu\text{S cm}^{-1}$)
<u>Tributaries of Bhima</u>									
GHOD-1	Ghod	2002	19.08	73.77	River Ghod near origin.	677	22.8	7.99	213
		2001				664	24.2	8	179
GHOD-2	Ghod	2002			Ghod river before mixing Bhima (BHM-4)	517	27.2	8.36	812
MTH-1	Mutha	2002	18.57	74.34	Mutha before confluence with Bhima (BHM-2)	559	24.7	7.66	362
		2001				-	25.5	7.54	490
NIRA-1	Nira	2002	17.94	74.94	Nira river at Baramati	547	29.6	8.61	824
		2001				475	25.5	9.13	509
NIRA-2	Nira	2002	17.97	75.14	Nira before confluence with Bhima (BHM-5)	474	27.8	8.54	345
		2001				451	28.6	9.2	373
KUK-1	Kukdi	2002	-	-	Kukadi river, a tributary of Ghod	-	25	8.69	481
Western Ghats and other rivers									
<u>Tributaries of Krishna</u>									
KYN-1	Koyna	2002	17.27	74.18	Koyna before confluence with Krishna	568	26.1	7.35	126
		2001				570	23.7	7.38	85
KYN-2	Koyna	2002	17.93	73.61	Koyna at origin, near Mahabaleshwar	-	21.1	6.99	41
		2001				726	20.2	7.25	42
VRN-1	Varna	2002	16.87	74.36	Varna river before mixing Krishna	550	24.3	7.13	124
		2001				556	23.4	7.56	129
PGN-1	Panchganga	2002	16.69	74.60	Panchganga before confluence with Krishna (KRS-1)	541	24.4	7.12	95
		2001				543	23.5	7.38	81
PGN-2	Panchganga	2002	16.76	74.26	Panchganga near shepathe village	562	24.7	7.17	93

Code	River	Year	Lat. (°N)	Long. (°E)	Sampling locations and remarks	Altitude (m)	Temp. (°C)	pH	EC ($\mu\text{S cm}^{-1}$)
GTP-1	Ghataprabha	2002	16.01	74.27	River Ghataprabha near Adkur village	710	23.5	7.03	40
		2001				687	22	7.76	32
HRN-1	Hiranyakeshi	2002	16.36	74.35	Hiranyakeshi river, Chandkhand-Gadinglaj road	679	25.2	7.04	41
		2001				633	22.8	7.14	53
TPN-1	Tambrapani	2002	15.92	74.29	Tambrapani river, Chandkhand-Belgaum road	747	23.4	7.12	55
		2001				688	22	7.1	41
DDG-1	Dudhganga	2002	16.43	74.14	River Doodhganga, near Gargoti	546	24.7	7.03	109
		2001				558	23.4	7.35	144
VDG-1	Vedganga	2002	16.36	74.15	River Vedganga, near Gargoti	611	27.4	7.06	76
		2001				562	23.1	7.05	69
BGW-1	Bhogwati	2002	16.50	74.05	River Bhogwati, near Amjai village	632	23.8	7.06	85
		2001				561	22.8	7.1	57
<u>West flowing rivers</u>									
ARJ-1	Arjuna	2002	16.65	74.02	River Arjuna near Rajapur	28	26.2	6.92	76
GAD-1	Gad	2002	16.26	73.72	River Gad near Kasal	34	24.9	7	73
SUKH-1	Sukh	2002	16.56	73.63	Sukh river near Khare patan village	15	25.7	6.97	73
		2001				19	26.2	7.39	76
KJL-1	Kajli	2002	16.93	73.51	Kajli river near Lanjha	-	26.1	7.01	94
		2001				23	26.5	7.18	85
SHT-1	Shashtri	2002	17.18	73.55	Shashtri river near Sangameshwar	-	25.1	6.92	78
		2001				8	25.2	7.22	73
VAT-1	Vashishthi	2002	17.53	73.54	Vashishti river near Chiplun	-	25.8	6.99	83
		2001				12	25.5	7.16	81
<u>Others</u>									
AMB-1	Ambika	2002	-	-	Ambika river near Waghai	-	24.8	7.7	188
MULA-1	Mula	2002	19.32	74.18	River Mula, a tributary of Godavari river	616	23.5	7.45	165

Appendix 2.2. Atomic absorption and emission wavelengths (λ) used for various elemental analyses (in sediments) by AAS and ICP-AES, and Spectrophotometry (S'metry), and the precision of analyses.

Element	Tech.	λ (nm)	CV(%)	Element	Tech.	λ (nm)	CV(%)
Na	AAS	589	2.5	Sr	ICP-AES	421.552	2.4
K	AAS	768.4	1.9	Ba	ICP-AES	455.403	2.3
Mg	ICP-AES	279.806	2.6	Ni	do	231.604	1.9
Ca	ICP-AES	422.673	1.8	Cr	do	267.716	1.6
Al	ICP-AES	396.673	2.1	V	do	311.071	2.3
Fe	AAS	271.9	1.1	Cu	AAS	327.4	1.1
Ti	ICP-AES	338.376	3.0	P	S'metry	885	2.2
Mn	AAS	280.1	1.9	Zn	AAS	213.9	1.3

Based on a number of repeat measurements, the precision of measurement is given by the coefficient of variation (CV) as:

$$CV(\%) = [\{\Sigma(d_i/x_m)^2\}/2n]^{1/2}$$

where d_i is difference between the repeats, x_m is the mean of the repeats and n is the no. of repeats measured.

Chapter Three
Major ion chemistry

3.1 INTRODUCTION

Rivers carry the imprints of erosion on the continents in the form of dissolved and particulate materials. The dominant fraction of dissolved constituents (solutes) in rivers is derived from chemical weathering of minerals contained in the rocks and soils of the drainage basin. The proportion of various elements in the dissolved phase is a complex function of their relative abundances in minerals and of the mode and rate of their weathering. Chemical weathering of rocks involves consumption of CO₂, a greenhouse gas, which exerts strong influence on climate; however, among the various rock types present on the earth's surface, weathering of silicate rocks is only responsible for net CO₂ consumption (Berner et al., 1983, Kump et al., 2000; Amiotte-Suchet et al., 2003; Dessert et al., 2003). Several parameters regulate the rate and intensity of chemical weathering and associated CO₂ consumption rates. These include lithology of the drainage basin, runoff, temperature, rainfall, vegetation and relief. The coupling between temperature and silicate weathering is considered a key factor in long-term climate stability (Berner et al., 1983; Velbel, 1993). More recently, Edmond and Huh (1997) suggested that 'lithology is the dominant variable determining the chemical yields from orogenic belts'. Some of the earlier studies (Meybeck, 1986; Bluth and Kump, 1994; Amiotte-Suchet and Probst, 1995; Amiotte-Suchet et al., 2003) have demonstrated that granites and gneisses are more resistant to weathering than basalts. Some recent works on basaltic provinces have confirmed that they weather rapidly and that their weathering exerts important control on marine geochemical balances and global change (Louvart and Allegre, 1997; Dessert et al., 2001; Amiotte-Suchet et al., 2003; Dessert et al., 2003).

The work presented in this chapter is also on the chemical weathering of Deccan basalts, carried out as a part of ongoing investigations on weathering of major lithological basins of India, based on chemical and isotopic composition (discussed in later chapters) of rivers. These studies, in a broader sense, have been motivated by the quest to determine the role of major land forms in India, such as the Himalaya and the Deccan Traps in contributing to dissolved fluxes of elements and isotopes to oceans and to CO₂ drawdown from the atmosphere (Sarin et al., 1989; 1992; Krishnaswami et al., 1999; Dalai et al., 2002). More specifically, the goals of this study are to (i) get baseline data on the major ion composition of rivers draining the Deccan Traps—identify the sources and processes contributing to them, (ii) derive chemical weathering rates and CO₂ consumption for the region studied, (iii) compare the

present results with those available for the northern Deccan and other major basins of India such as the headwaters of the Ganga in the Himalaya, and (iv) determine the contribution of Deccan basalts to global riverine flux of major ions and atmospheric CO₂ drawdown.

In this study, two approaches were followed to achieve these goals. One is based on the study of small rivers, to understand chemical weathering of basalt and to use them as end member values for assessing mixing proportions. The second approach is the study of larger rivers, which integrate contribution from various tributaries. These studies yield data on chemical weathering of large river basins, which are important to derive dissolved fluxes transported to the oceans.

The earlier study on weathering and erosion of Deccan Traps (Dessert et al., 2001) was based on the three watersheds, the Narmada, the Tapti, and the Wainganga–Wardha (Godavari tributaries) in the northern region. Major ion composition of rivers draining this region (Dessert et al., 2001) suggests that the chemical erosion rates of basalts are higher than those for other silicate rocks. This work also provided estimates of activation energy for basalt weathering, ~42 KJ/mol, based on a global data base, marginally lower than that derived for granites, ~55–80 kJ/mol (White and Blum, 1995; White et al., 1999b; Dalai et al., 2002) indicating that basalts may be weathered more easily from energy considerations.

As already discussed in chapter two, the work described in this thesis is based on the Krishna river system (the headwaters of the river Krishna and its tributaries all draining the southern Deccan Traps) and a number of small/medium rivers in the western ghats, many of which drain into the Arabian Sea. Among the rivers of the Deccan Traps, the headwaters of the Krishna and the Godavari are better suited for determining weathering rates of basalts as they flow almost entirely through them. The Narmada–Tapti–Wainganga (NTW) rivers which have been studied (Dessert et al., 2001) though drain predominantly through Deccan basalts, part of their basins are in the Indian shield, Vindhyan carbonates, sediments and alluvial deposits. Further, the Narmada and Tapti rivers flow through areas severely affected by tectonics, and therefore more prone to inputs from ground water and hydrothermal waters. A number of hydrothermal springs have been reported along the Narmada–Tapti lineament (Chandrasekhar and Prasad, 1998; Minissale et al., 2000).

Much earlier to these studies, Ramesh and Subramanian (1988) had reported major ion composition of the Krishna river and a few of its major tributaries as a part of their work to determine fluxes of various elements transported by this river system to the Bay of Bengal. Their sampling was focused more on the larger tributaries and along the lower stretches of the Krishna, which predominantly drain Precambrian granites and metasediments, unlike this work, which is on the headwaters of the Krishna and its tributaries draining the Deccan basalts.

3.2 RESULTS

3.2.1 Major ion chemistry

The major ion concentrations, total dissolved solids (TDS) of the rivers sampled are reported in Table 3.1. Also reported are the calculated normalized inorganic charge balance of the samples. As reported in chapter 2 (Table 2.1), the pH of the samples varies from near neutral to mildly alkaline (6.9 to 9.2) with most of them in the range of 7.0–8.0. The range in electrical conductivity (EC) of the samples is from 32 to 824 $\mu\text{S cm}^{-1}$. The lower EC values are observed in samples collected near the origin of rivers and/or due to dilution resulting from high rainfall events. The water temperature variations are from about 22 °C to 30 °C.

The cationic charge (TZ^+) varies from ~290 to 8380 μE , similar to the range reported for the NTW rivers (Dessert et al., 2001). The TZ^+ and TZ^- are reasonably well balanced, with $\text{TZ}^+ = (0.96 \pm 0.003)\text{TZ}^- + 24$ ($r^2 = 0.999$, $n = 63$; Fig. 3.1). The slope of 0.96 is an indication of a minor cation deficiency. The extent of $(\text{TZ}^+ - \text{TZ}^-)$ charge imbalance is characterized in terms of normalized inorganic charge balance ($\text{NICB} = |(\text{TZ}^+ - \text{TZ}^-)|/\text{TZ}^+$). The NICB values in the samples are generally <5% (Table 3.1) with the average for all 63 samples being 3.1%. The NICB values are within the cumulative uncertainties in major ion measurements. It is also borne out from the NICB estimates that contribution of organic ligands such as oxalates, acetates and humates is not significant to the charge balance as has been reported for some of the tropical rivers (Viers et al., 2000).

HCO_3^- dominates the anion charge (38–91% of TZ^-), as evident from the ternary plot for anions (Fig. 3.2a), which show clustering of points near the HCO_3^- apex. It is also seen from Fig. 3.2a that many points lie along the mixing line of HCO_3^-

Table 3.1 Major ion compositions of rivers flowing through the Deccan Traps.

Code	River	Ca (μM)	Mg (μM)	Na (μM)	K (μM)	HCO ₃ (μM)	Cl (μM)	SO ₄ (μM)	NO ₃ (μM)	TZ ⁺ (μE)	TZ ⁻ (μE)	Si (μM)	TDS (mg/l)	NICB (%)
Krishna mainstream														
KRS-1	Krishna	454	270	484	20	1468	287	90	39	1952	1974	334	168	-1.1
		434	294	549	24	1418	337	125	29	2029	2034	313	169	-0.2
KRS-2	"	329	206	363	17	862	262	69	20	1450	1282	291	114	11.6
		232	151	288	15	776	230	58	24	1069	1146	228	96	-7.2
KRS-3	"	490	295	410	19	1653	221	46	21	1999	1987	350	172	0.6
		206	141	219	11	802	150	18	8	924	996	274	90	-7.8
KRS-4	"	645	375	503	22	2226	268	55	29	2565	2633	419	225	-2.7
		460	311	415	18	1672	225	56	21	1975	2030	341	173	-2.8
KRS-5	"	390	247	468	17	1326	279	86	27	1759	1804	327	153	-2.6
		397	271	489	19	1290	326	116	35	1844	1883	302	156	-2.1
KRS-6	"	903	578	587	26	3252	283	43	81	3575	3702	520	314	-3.6
		1162	717	568	35	3995	335	70	92	4361	4562	639	385	-4.6
Bhima mainstream														
BHM-1	Bhima	182	110	174	10	585	133	19	5	768	761	309	75	0.9
		170	121	171	10	609	140	20	6	763	795	300	76	-4.2
BHM-2	"	795	628	2260	42	2162	1313	886	58	5148	5305	293	385	-3.0
BHM-3	"	768	479	1229	49	2464	627	342	89	3772	3864	396	307	-2.4
		932	618	1839	77	2815	1094	598	127	5016	5232	379	396	-4.3
BHM-4	"	822	547	1494	38	2499	779	490	65	4270	4323	390	337	-1.2
		1004	713	2444	73	2972	1364	881	13	5951	6111	377	454	-2.7
BHM-5	"	999	921	2950	77	2934	2183	1054	15	6867	7240	323	511	-5.4

Code	River	Ca (μM)	Mg (μM)	Na (μM)	K (μM)	HCO ₃ (μM)	Cl (μM)	SO ₄ (μM)	NO ₃ (μM)	TZ ⁺ (μE)	TZ ⁻ (μE)	Si (μM)	TDS (mg/l)	NICB (%)
Tributaries of Bhima														
GHOD-1	Ghod	610	340	327	17	1999	193	40	61	2244	2333	418	202	-4.0
		493	278	291	18	1644	212	38	20	1851	1952	390	170	-5.5
GHOD-2	Ghod	973	1206	3960	65	4624	2333	752	114	8383	8575	563	640	-2.3
MTH-1	Mutha	771	464	1137	48	2501	593	256	95	3655	3701	398	298	-1.3
		990	593	1569	97	3125	1003	370	213	4832	5081	429	395	-5.2
NIRA-1	Nira	672	641	5630	27	3631	1397	1566	62	8283	8222	396	622	0.7
		468	448	2867	35	1934	1068	1058	0	4734	5118	335	375	-8.1
NIRA-2	Nira	584	395	1498	39	2123	654	423	27	3495	3650	336	284	-4.4
		459	416	1742	49	1856	884	579	0	3541	3898	310	289	-10.1
KUK-1	Kukdi	784	965	1685	32	4161	886	129	83	5215	5388	506	428	-3.3
Western ghat and other rivers														
Tributaries of Krishna														
KYN-1	Koyna	309	201	276	10	1111	176	18	14	1306	1337	353	122	-2.4
		205	133	194	8	713	139	13	13	878	891	272	83	-1.5
KYN-2	Koyna	81	59	103	5	300	75	10	0	388	395	179	40	-1.8
		92	60	100	5	301	86	10	5	409	412	165	40	-0.7
VRN-1	Varna	297	185	273	31	990	195	37	24	1268	1283	292	114	-1.2
		290	192	288	12	1045	202	34	29	1264	1344	313	118	-6.3
PGN-1	Panchganga	208	125	239	15	611	208	40	12	920	911	238	81	1.0
		175	115	190	12	585	165	26	11	782	813	200	71	-4.0
PGN-2	Panchganga	212	138	210	11	680	179	21	27	921	928	257	84	-0.8
GTP-1	Ghataprabha	74	52	127	6	212	116	10	16	385	364	126	34	5.5
		57	36	101	5	170	100	9	12	292	300	91	27	-2.7

Code	River	Ca (μM)	Mg (μM)	Na (μM)	K (μM)	HCO ₃ (μM)	Cl (μM)	SO ₄ (μM)	NO ₃ (μM)	TZ ⁺ (μE)	TZ ⁻ (μE)	Si (μM)	TDS (mg/l)	NICB (%)
HRN-1	Hiranyakeshi	71	54	131	5	216	120	11	10	386	368	128	34	4.7
		107	71	132	10	337	133	15	11	498	511	129	45	-2.6
TPN-1	Tambrapani	107	74	150	9	319	146	14	27	521	520	166	48	0.2
		75	56	115	12	234	119	11	13	389	388	117	35	0.3
DDG-1	Dudhganga	289	168	223	10	835	177	33	35	1147	1113	268	100	3.0
		373	232	264	19	1226	215	33	41	1493	1548	344	136	-3.7
VDG-1	Vedganga	172	110	178	7	562	148	13	25	749	761	247	71	-1.6
		148	108	163	7	530	136	12	18	682	708	241	66	-3.8
BGW-1	Bhogwati	193	128	192	9	603	159	17	46	843	842	271	79	0.1
		124	80	144	8	395	130	14	19	560	572	176	52	-2.1
West flowing rivers														
GAD-1	Gad	153	114	179	9	604	108	12	0	722	736	323	75	-1.9
SUKH-1	Sukh	163	130	165	7	624	102	12	4	758	754	332	77	0.5
		158	132	167	6	656	115	12	6	753	801	341	80	-6.4
KJL-1	Kajli	162	128	168	6	633	101	11	4	754	760	353	78	-0.8
		196	151	180	5	755	117	12	2	879	898	396	91	-2.2
SHT-1	Shastri	181	127	178	6	678	111	12	3	800	816	386	84	-2.0
		163	126	160	5	623	110	12	3	743	760	344	77	-2.3
VAT-1	Vashishthi	197	142	176	6	725	104	12	3	860	856	391	88	0.5
		173	137	167	6	716	114	14	5	793	863	364	86	-8.8
Others														
AMB-1	Ambika	539	349	265	15	1876	130	28	1	2056	2063	685	200	-1.8
MULA-1	Mula	391	310	304	8	1446	199	42	36	1714	1765	334	152	-3.0

and (Cl+SO₄) apices, with 9–62% contribution from (Cl+SO₄). Cl is next in

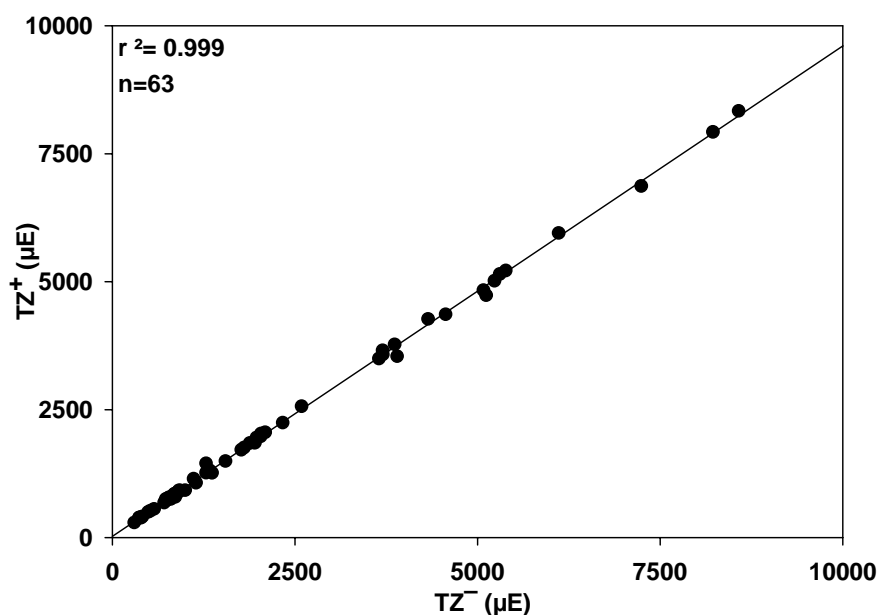


Fig.3.1. Plot of the inorganic cations and anions in the waters sampled. They show a good charge balance between them.

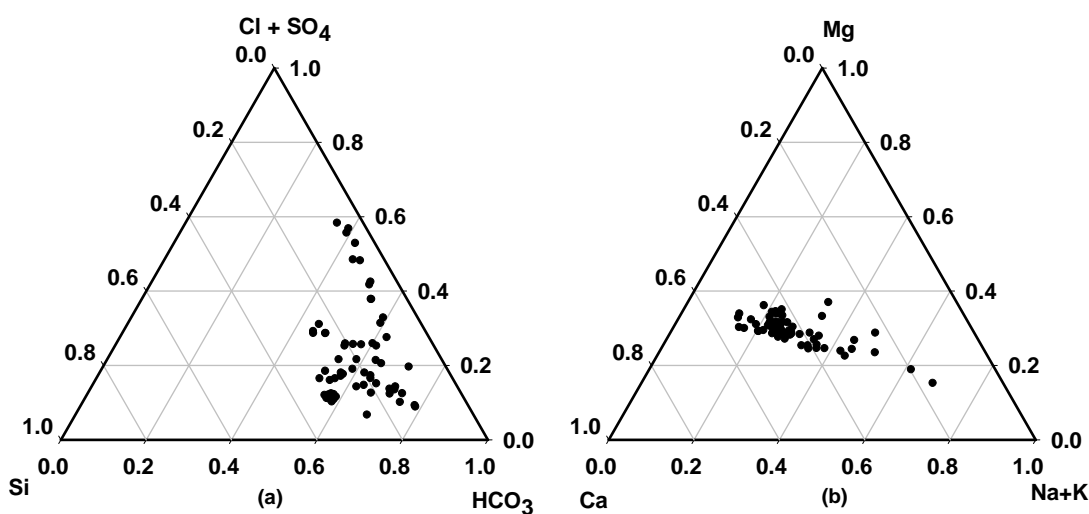


Figure 3.2 Ternary plots for anions (3.2a) and cations (3.2b). The anions are dominated by HCO₃, with a mixing trend with (Cl+SO₄). The cations lean towards Ca, with most samples in Ca–(Na+K) region.

abundance to HCO₃ with concentration ranging from 75–2333 μE and accounting for ~6 to 33% of anion charge. However, in five samples from the Bhima river and four from the Nira, SO₄ contribution to the total anion charge is more than that of Cl (Table 3.1). The Bhima samples are from its lower reaches, BHM-2, 3 and 4 (Table 3.1). The sample from near the origin of the Bhima (BHM-1) has much higher Cl

than SO_4 with Cl/SO_4 equivalent ratio of 3.5. In samples BHM-2, 3 and 4, both Cl and SO_4 abundances are factors of 5–50 over BHM-1 with Cl/SO_4 equivalent ratio <1 . This requires supply of both Cl and SO_4 to the river along its traverse with relatively more input of SO_4 compared to Cl . The NO_3 levels in the samples are generally less than $<50 \mu\text{E}$ except in samples from the lower reaches of the Bhima, Nira and the Ghod that also have higher Cl and SO_4 . The implications of these results are discussed in subsequent sections. The general trend in the anion abundances follow those reported for the northern Deccan Trap rivers (Dessert et al., 2001).

Ca is the dominant cation, with contribution ranging from 17% to 53% of TZ^+ . Mg follows Ca with concentration in the range of 72 to 2412 μE , and accounting for 16% to 36% of cation charge. The contribution of alkali metal ions (Na+K) to TZ^+ is between 14 to 68% with Na making up most of it. Ternary diagram for cations (Fig 3.2b) shows that most of the samples lie in the zone that is dominated by Ca & Mg with remaining in the Ca and (Na+K) zone. A better assessment to the total charge contribution by the individual cations was done by plotting Z vs. TZ^+ ($Z = \text{Ca, Mg and Na}$; Fig. 3.2c). The different lines in the plots show the Z/TZ^+ ratios corresponding to 1.0, 0.6 and 0.4. In case of Na, most of the sample points (55 out of 63) are below the 0.4 ratio line; for Ca, most of the points (40 out of 63) fall in between 0.6–0.4 lines. For Mg, except three, all the samples have ratios less than 0.35.

3.2.2 Dissolved Silica

The dissolved silica content in the rivers is in the range of 91 to 685 μM (Table 3.1; mean 323 μM) and accounts for 4–28% of the TDS. The Si abundances are between those expected based on solubility of quartz ($\sim 100 \mu\text{M}$) and amorphous silica ($\sim 2000 \mu\text{M}$) at 25 °C. The silica concentrations are similar to those in the NTW rivers (Dessert et al., 2001) and others draining basalts such as those from the Reunion Island (Louvat and Allegre, 1997) and Iceland (Steffansson and Gislason, 2001). However, compared to the Congo (Gaillardet et al., 1995; Dupre et al., 1996), the Amazon (Gaillardet et al., 1997), the Ganges-Brahmaputra and the Yamuna river systems (Sarin et al., 1989; Galy and France Lanord, 1999; Dalai et al., 2002) dissolved silica in Deccan rivers is generally higher (Table. 3.2).

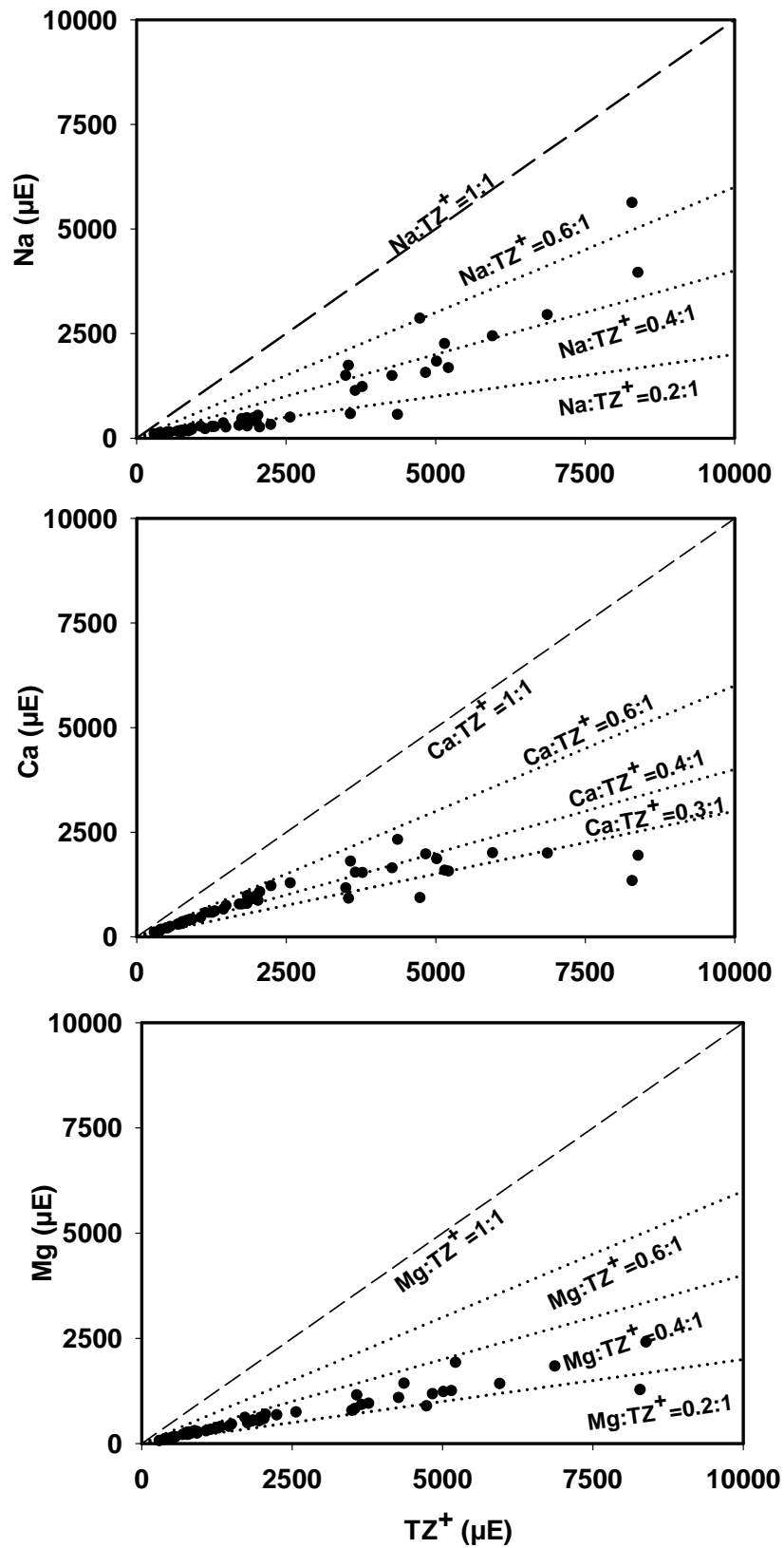


Fig. 3.2c Relative proportions of Na, Ca and Mg to the total cation charge budget. In most samples Na and Mg contributions are less than 40%, while Ca accounts for 40%–60%.

Table 3.2 Dissolved Silica and total dissolved solids (TDS) in Deccan and other world river basins.

River basin	Dissolved silica (μM)	TDS ($\text{mg } \ell^{-1}$)	Reference
Southern Deccan	91—685	27—640	This study
Northern Deccan	187—836	17—717	Dessert et al., 2001
Reunion	182—1064	24—580	Louvat and Allegre, 1997
Iceland	-	36—84	Steffansson and Gislason, 2001
Congo	150—225	26—36	Dupre et. al., 1996
Amazon	60—160	6—55	Gaillardet et al., 1995
Ganga-Brahmaputra	71—296	91—461	Sarin et al., 1989
Ganga-Brahmaputra	2—320	6—880	Galy and France-Lanord, 1999
Yamuna	67—378	32—622	Dalai et al., 2002

Silica shows an overall increasing trend with HCO_3^- with distinctly different $\text{SiO}_2/\text{HCO}_3^-$ ratios for the western ghat rivers relative to others (Fig. 3.3). The western ghat rivers, both flowing into the Arabian sea and those belonging to the Krishna system and draining into the Bay of Bengal, have $\text{SiO}_2/\text{HCO}_3^-$ molar ratios of ~ 0.33 – 0.5 , significantly higher than the ratios of ~ 0.1 – 0.2 in the other rivers analysed. This $\text{SiO}_2/\text{HCO}_3^-$ ratio depends on the substrate available for chemical weathering in the basins and on the end product of the weathering reactions. Based on the chemical and mineralogical composition of the Deccan basalts, the weathering of basalt to kaolinite and smectite would release Si and HCO_3^- with ratios of ~ 0.33 – 0.5 (discussed later). The low ratios of 0.1 – 0.2 , in the Bhima system and some of the Krishna rivers can be due to the supply of alkalinity from other sources such as carbonates, salt affected soils and anthropogenic inputs.

The silica concentrations are similar to those in the NTW rivers (Dessert et al., 2001) and others draining basalts such as those from the Reunion Island (Louvat and Allegre, 1997) and Iceland (Steffansson and Gislason, 2001). However, compared to the Congo (Gaillardet et al., 1995; Dupre et al., 1996), the Amazon (Gaillardet et al., 1997), the Ganges-Brahmaputra and the Yamuna river systems (Sarin et al., 1989;

Galy and France Lanord, 1999; Dalai et al., 2002) dissolved silica in Deccan rivers is generally higher (Table. 3.2).

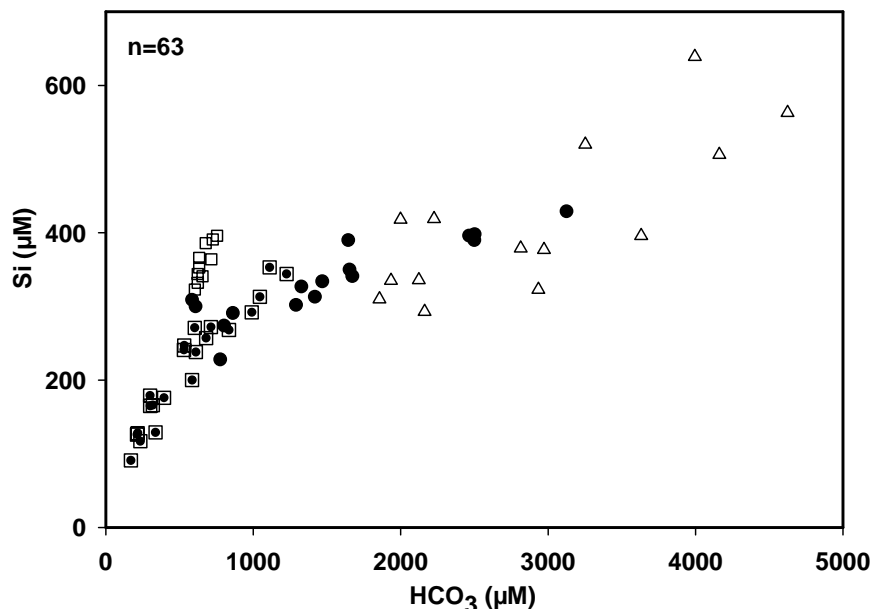


Fig.3.3 Scatter plot of Si—HCO₃ abundances. Si increases as a function of HCO₃ with two different slopes. Samples shown in open and dotted squares are from the east flowing smaller tributaries of the Krishna and the west flowing western ghat rivers, and have a slope 0.33–0.5. The samples from the larger tributaries of the Krishna, the Bhima and its tributaries (shown in circles) have a lesser slope of 0.1–0.2, most likely due to contributions of HCO₃ from other sources such as carbonates. The open triangles are samples with CSI>0.

3.2.3 Total dissolved solids and its spatial variability

The total dissolved solids (TDS) in rivers include input of elements from all sources— chemical weathering, atmospheric and the anthropogenic components. TDS in the waters (Table 3.1) vary over a wide range, 27–640 mg ℓ^{-1} (n=63; Fig. 3.4), with a mean of 176 mg ℓ^{-1} . This is similar to the range of ~17 to ~717 mg ℓ^{-1} for NTW rivers (Dessert et al., 2001), ~24 to ~580 mg ℓ^{-1} for rivers from the Reunion (Louvart and Allegre, 1997) and higher than the range of ~36 to ~84 mg ℓ^{-1} for rivers from the Iceland (Steffansson and Gislason, 2001). However, compared to major world rivers, such as the Congo (Gaillardet et al., 1995; Dupre et al., 1996) and the Amazon (Stallard and Edmond, 1983; Probst et al., 1994), the TDS levels in the rivers of the Krishna system are higher; whereas they are comparable to those of the Ganges-Brahmaputra system (Sarin et al., 1989; Galy and France-Lanord, 1999; Dalai et al., 2002). The TDS-data in some major river basins of the world are listed in Table 3.2.

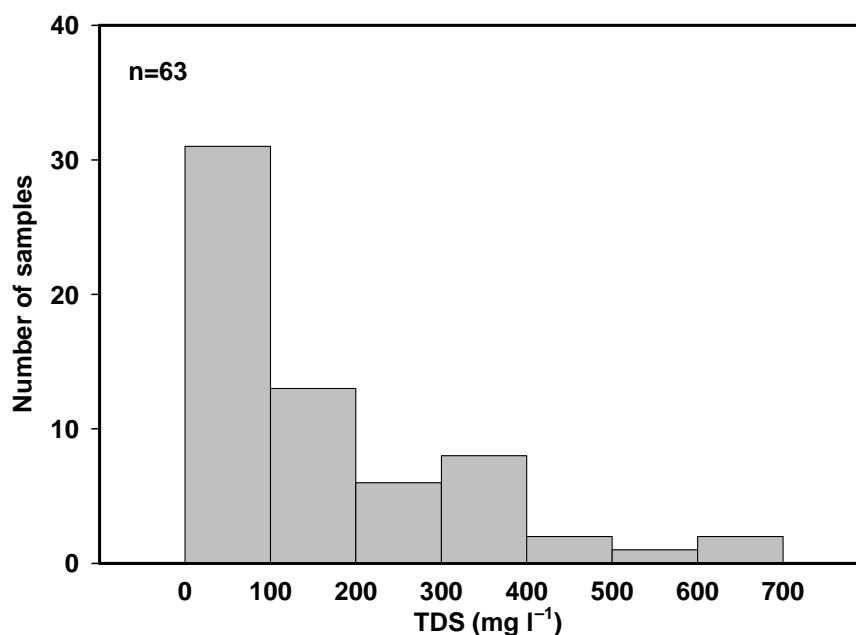


Fig.3.4. Frequency distribution of total dissolved solids (TDS). The range in TDS though is wide (~27 to ~640 mg ℓ⁻¹), about half of the samples have TDS < 100 mg ℓ⁻¹. The high TDS samples are from the lower reaches of the Bhima, Ghod, Nira and the Kukdi, all of which have high Cl, SO₄ and HCO₃.

Variations in TDS among the water sheds of the Krishna River System have been assessed by comparing the two year average TDS in the various sub-basins: The average TDS (mg ℓ⁻¹) in the various sub-basins decrease as: Ghod (337±261, n=3) ≈ Bhima mainstream (318±162, n=8) > Krishna mainstream (185±87, n=12) > west flowing western ghat rivers (82±5, n=10) > east flowing tributaries of Krishna (70±33, n=21). One obvious feature is the higher TDS in the Bhima and the Ghod rivers as compared to the others; a possible contributor being the high concentration of SO₄ in the Bhima (Table 3.1).

3.2.4 Inter Annual variability in major ions

The analyses of samples collected during two successive monsoon seasons provide an opportunity to assess the extent of inter annual variability in the major ion concentrations. Based on average major ion abundances in the rivers, it is seen that the mean concentrations in 2002 samples (n=29) are generally within ±20% of the 2001 (n=34) mean (Fig. 3.5), for Cl (-20%), SiO₂ (+14%), HCO₃ (+9%), NO₃ (+11%), Na (-4%), Mg (+1.7%) and Ca (-1.5%).

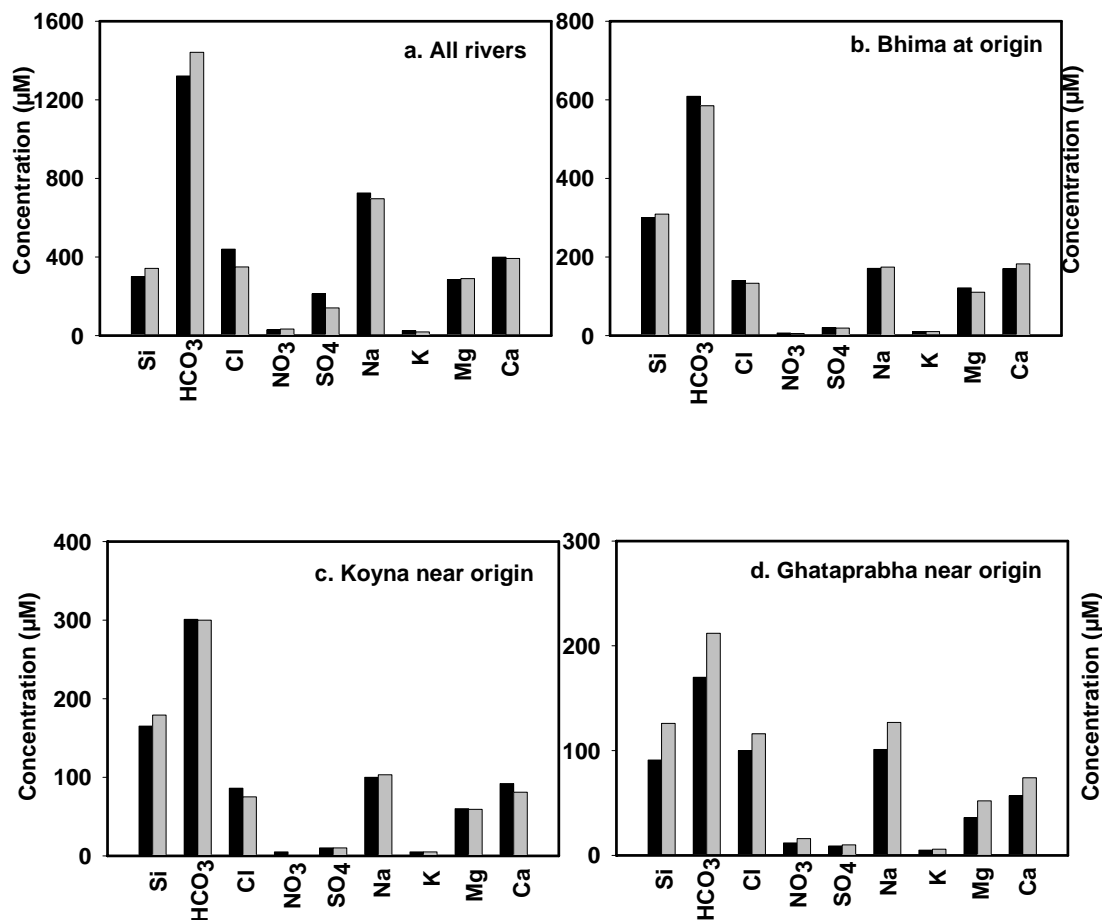


Fig.3.5 Inter annual variability in major ion abundances ■ 2001, ■ 2002 (a) average of all samples ($n=63$) (b) Bhima river at its origin (c) Koyna and (d) Ghataprabha. The average inter-annual variability in major ion abundance is within $\pm 30\%$, most likely indicating the natural variations.

The inter-annual variability for SO_4 and K are $\sim -35\%$ and 28% respectively. The variability in SO_4 most likely results from its high and varying concentration in the Bhima river. This river has average SO_4 concentration of $688 \mu\text{M}$ during 2001 ($n=5$), a factor of about 2.4 higher than the 2002 average ($n=3$) of $284 \mu\text{M}$. This compares with the average SO_4 values of $69 \mu\text{M}$ and $17 \mu\text{M}$ for the Krishna ($n=12$) and WG rivers ($n=31$) respectively. The results of three other rivers, the Bhima at its origin, the Koyna and the Ghataprabha (Fig. 3.5) show that inter annual variability of major ions in these three rivers is generally $<30\%$.

3.3 Discussion

3.3.1 Mineral weathering: The dissolved constituents in river water are primarily derived from the weathering of the minerals present in the basin. The abundances of ions in water depend on the abundances of minerals in the rock and their relative rate

of weathering. The molar ratio in waters, relative to that in rocks, provides a measure of the relative mobility of elements during chemical weathering (discussed in later sections, and in chapter 4). The molar ratios (e.g., Mg/Ca, Ca/Na and Si/HCO₃) released to waters are calculated from the constituent mineral abundances, which in turn are derived from the abundances of oxides in the basalts (Subbarao et al., 2000, see Table 3.3) and CIPW norm calculations (MINPET, 90).

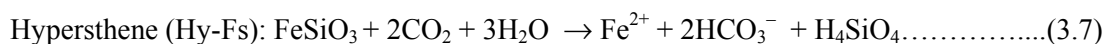
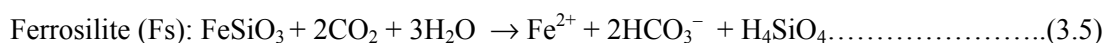
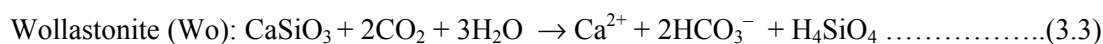
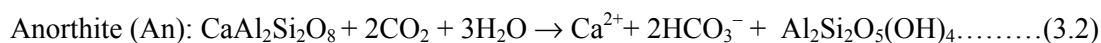
Table 3.3 Average abundances^s (wt%) of major element oxides and major minerals and in the Deccan basalts.

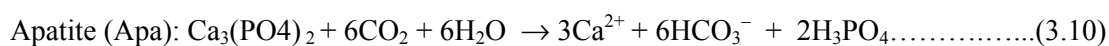
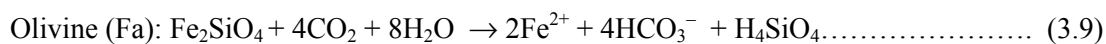
Formation	SiO ₂	CaO	MgO	K ₂ O	Na ₂ O	[#] Ca/Na	[#] Ca/Mg	[#] Na/Mg	Major Minerals [@]
Poladpur (n=4)	Av. 49.8 (σ) 0.4	10.7 0.5	6.16 0.81	0.20 0.05	2.40 0.27	2.50 0.36	1.26 0.13	0.52 0.13	Ol+Pl
Ambenali (n=3)	Av. 48.1 (σ) 0.5	11.1 0.6	6.08 0.71	0.23 0.10	2.48 0.16	2.49 0.26	1.32 0.13	0.54 0.10	Ol+Pl
Maha' war* (n=3)	Av. 48.7 (σ) 0.9	10.7 1.1	5.56 0.22	0.35 0.13	2.64 0.26	2.25 0.17	1.39 0.21	0.62 0.08	Ol+Pl
Bushe (n=3)	Av. 53.2 (σ) 1.0	10.0 0.6	6.33 1.58	0.82 0.32	2.69 0.26	2.07 0.3	1.17 0.22	0.58 0.16	Ol+Pl+Aug
Thakurwadi (n=9)	Av. 51.5 (σ) 1.5	9.7 1.6	6.49 1.42	0.53 0.35	2.19 0.27	2.58 0.52	1.07 0.1	0.43 0.12	Ol+Pl+Aug
Bhimashanker (n=3)	Av. 50.3 (σ) 0.6	9.8 0.4	5.95 0.08	0.66 0.12	3.18 0.15	1.70 0.13	1.18 0.04	0.70 0.03	Ol
Overall average (σ)	50.5 1.8	10.2 1.2	6.2 1.1	0.47 0.31	2.5 0.4	2.34 0.46	1.19 0.17	0.53 0.13	

[#] Molar ratio; Ol (olivine), Pl (Plagioclase) and Aug (Augite): (*Mahabaleshwar)

^s Subbarao et al., 2000; @ Sen, 2001

The balanced equations for chemical weathering of the minerals that commonly occur in basalts can be written as:





The moles of various ions released per mole of the reacting minerals mentioned above are given in Table 3.4.

Table 3.4 Moles of ions (Na, K, Mg, HCO₃) and silica released per mole of mineral weathered.

Mineral	Na	K	Mg	Ca	HCO ₃	H ₄ SiO ₄	Mineral	Na	K	Mg	Ca	HCO ₃	H ₄ SiO ₄
Q						1	Fs					2	1
Or		2			2	4	Hy-Ens			1		2	1
Ab	2				2	4	Hy-Fs					2	1
An				1	2		Ol-Fo			2		4	1
Wo				1	2	1	Ol-Fa					4	1
Ens			1		2	1	Apa				3	6	

3.3.2 Sources of major ions to rivers of Deccan

Determination of chemical and silicate weathering rates from the major ion composition of rivers requires data on their contributions from various sources to rivers. The chemical weathering of rocks and minerals present in the basin, dry and wet atmospheric depositions and anthropogenic inputs are the primary sources of major ions to rivers. It is necessary to constrain the contributions from these sources to the major ion budgets to derive chemical weathering rates of the basin and associated CO₂ drawdown. The sources and their relative contributions to the major ions chemistry are discussed below.

3.3.2.1 Atmospheric supply: Contribution from atmospheric deposition can be determined from knowledge of regional rainwater composition. Table 3.5 lists the major ion composition of rainwater from five locations of the Deccan region (Fig. 2.2). Of these, three are from the monitoring stations of the Indian Institute of Tropical Meteorology (IITM), Pune (Parashar et al., 1996), and the other two are single samples collected as a part of this study during August 2002. Among the three IITM stations, one is located at Dona Paula (near Panaji, Fig. 2.1), Goa, a coastal station. The rainwater chemistry at this station therefore should reflect the oceanic end member composition. The two other sites are, Pune (18°32' N, 73°51' E, 559 m asl;

Fig. 2.2), an inland urban station situated ~100 km off the west coast of India and Sinhagad (18°21' N, 73°45' E, 1400 m asl), a hill station in the western ghats, located ~18 km southwest of Pune. The two samples collected as a part of this study are from Ambolighat, a high altitude site (16°36' N, 74°35' E, 690 m asl; Fig. 2.2) near the origin of the Hiranyakeshi river and from Sangameshwar (17°11' N, 73°32' E, 7 m asl; Fig. 2.2) on the bank of the Shastri river.

Table 3.5 Major ion composition of rainwater (μM) from the Deccan region.

Location	N	Na	K	Mg	Ca	Cl	NO₃	SO₄	NH₄
<u>Inland Stations</u>									
Pune#	12	41	2	9	27	50	8	11	11
Sinhagad#	17	46	2	9	18	51	6	12	13
Ambolighat*	1	17	8	-	9	11	0	3	47
Samgameshwar*	1	26	4	-	10	28	6	8	0
Weighted mean		42	2	9	21	48	7	11	13
<u>Coastal station</u> [#]									
Goa	6	115	3	15	23	135	6	16	7

[#]Parashar et al., 1996, * Present study

Cl in rainwater from Goa is ~135 μM whereas it is 50 μM and 51 μM for the Pune and Sinhagad samples respectively. The Ambolighat and Sangameshwar samples have 11 and 28 μM of Cl (Table 3.5). Chloride concentration in rains from Bombay, another coastal station is ~138 μM , (Sequeria and Kelkar 1978; Sarin et al., 1989) nearly identical to that measured at Goa. The decrease in Cl as a function of distance inland from sea is because of rain out. The Cl/Na molar ratios are same within errors for the three IITM sites, with a value of ~1.17, typical of marine end member. This suggests that there is no discernible contribution of Na from other sources such as silicates to these rain samples. Cl/Na ratios at Ambolighat and Sangameshwar are 0.64 & 1.07 respectively, indicating supply of dust derived Na to rain, particularly, in the sample from Ambolighat. In all these discussions, it is assumed that there is no significant loss of Cl from sea salt.

In the six west flowing rivers collected within 10–20 km of the west coast, Cl concentration is in the range of 101 to 117 μM (Table 3.1). These values are marginally lower than Cl in rains off Goa and Bombay, and suggest that in these streams Cl can be entirely from precipitation. Cl in the smaller tributaries of the

Krishna, in the interior Deccan province, ranges from ~75 to 215 μM (Table 3.1). This compares with average Cl of rains, ~48 μM , from this region (Table 3.5) and suggests that in many of these rivers there can be a significant contribution of rainwater Cl . The effect of evapo-transpiration (ratio of discharge over precipitation) in enhancing the major ion abundances in rain is calculated from the precipitation and the runoff values of the regions. Based on the precipitation for the Deccan interior (~770 mm y^{-1}) and corresponding runoff of ~463 mm y^{-1} , the evaporative enrichment is calculated to be ~40%. Therefore, the rainwater contribution of Cl to the east flowing rivers is ~80 μM , 48 μM being the rainwater Cl concentration. The atmospheric contribution of Cl to the Deccan Trap rivers, varies from as low as ~3% to as high as ~100% (average: 20%). The contribution to specific streams, however, can be quite different from the mean values given above, as it would depend on the Cl content of local rain. The contribution of rain to the major ion budget of X (=Na, Ca, Mg and SO_4) is calculated from the relation:

$$X_{rr} = (X/\text{Cl})_{\text{rain}} \times \text{Cl}_{\text{rain}} / f_{et} \dots \dots \dots (3.11)$$

where X_{rr} is the contribution of rain (μM) to rivers; (X/Cl) is the molar abundance ratio in rains; f_{et} is the correction factor for evapo-transpiration. For the west flowing western ghat rivers, in which all Cl and SO_4 can be from rain, $f_{et} \approx 1$, for the interior Deccan, $f_{et} \approx 0.6$ has been used.

Table 3.6 lists the average rainwater contribution to the major ions (Na, Ca, Mg, Cl and SO_4) for the various groups of rivers such as the Krishna, Bhima, east flowing rivers and the westflowing rivers. These estimates (Table 3.6) show that the west flowing western ghat rivers, all SO_4 and most of Na can be accounted for from rains. For Ca and Mg, the rainwater supply can account for a maximum of 15% (average 13%) and 13% (average 11%) respectively. Further, these calculations suggest that for many of the interior river samples, rainwater contribution of major ions, particularly Mg and Ca, forms only a minor component.

3.3.2.2 Other sources of Na, Cl and SO_4

Many of the Krishna and Bhima tributaries have Cl and SO_4 in excess of that can be supported by rain. Potential sources are dissolution of halites, supply from saline soils/alkaline soil, discharge from springs or groundwater and anthropogenic inputs. For SO_4 , pyrite oxidation can be an additional source. There are no reports of halite

exposures in these river basins; hence, they are unlikely sources for Na and Cl. The other potential sources of these ions and their significance are discussed below.

Table 3.6 Atmospheric contributions of major ions.

River		C_r	C_{rain}	C^*_{rain}	C^*_{rain}/C_r (%)
West flowing (n=10)	Cl	110	135	135	~100
	SO ₄	12	16	16	~100
	Na	172	115	115	67
	Ca	171	23	23	13
	Mg	132	15	15	11
Krishna and Bhima tributaries (East flowing; n=31)	Cl	398	48	80	20
	SO ₄	181	11	18	10
	Na	790	42	70	9
	Ca	338	21	35	10
	Mg	262	9	15	6
Krishna Mainstream (n=12)	Cl	267	48	80	30
	SO ₄	69	11	18	26
	Na	445	42	70	16
	Ca	509	21	35	7
	Mg	321	9	15	5
Bhima mainstream (n=8)	Cl	954	48	80	8
	SO ₄	536	11	18	3
	Na	1570	42	70	4
	Ca	709	21	35	5
	Mg	517	9	15	3

C: average concentration (μM), subscript *r* and *rain* refer to river and rain, C^*_{rain} : rain water concentration corrected for evapotranspiration.

(i) Spring and groundwater: Recently, Naik et al. (2001) have reported the major ion composition of several springs in the basin of the Koyna river, one of the tributaries of Krishna, these have average Cl of $\sim 310 \mu\text{M}$ (range: 197–394 μM) and SO₄ of 38 μM (range: 0–560 μM). From the distribution of springs in this basin, Naik et al. (2002), estimate that on an average that there is one spring per km² of drainage area with an average flow of $\sim 1.3 \times 10^7 \ell \text{ y}^{-1}$. This would contribute to a runoff $\sim 13 \text{ mm y}^{-1}$, $\sim 3\%$ of average river runoff for the region. Considering this estimate for the Koyna basin to be representative of the rivers of the region, it would lead to infer that maximum contribution of springs to Cl (minimum Cl: KYN-2 with 75 μM) and SO₄ (minimum SO₄: for GTP-1 with 9 μM) budget of rivers is only $\sim 10\%$. The effect of groundwater on the riverine major ion budget can be derived independently by the following approach. The discharge of the river Krishna during the summer months is $\sim 10 \text{ m}^3 \text{ s}^{-1}$, $\sim 2\%$ of the annual discharge of $\sim 551 \text{ m}^3 \text{ s}^{-1}$. If this supply is taken to be

the ground water input to these rivers, with the available major ion composition of groundwater, it is seen that the contribution from groundwater to the river is very negligible.

(ii) Saline/Alkaline soils: Occurrences of saline and alkaline soils containing NaCl and Na₂SO₄ scattered in the Deccan Plateau have been reported (Bhargava and Bhattacharjee, 1982). The source(s) of sodium salts (NaCl, Na₂SO₄ and carbonates) in these saline soils can be evaporative enrichment of precipitation. Remote sensing studies by the National Remote Sensing Agency (NRSA), Hyderabad, also have documented (through maps) the presence of salt affected soils in Maharashtra, especially in the basins of the Bhima, Krishna, Nira, Mutha rivers and also along the coastal trails of the Arabian sea (NRSA, 1998). In the present study, as will be discussed later; high Cl seems to be a result of weathering of saline soils and/or anthropogenic inputs. Dessert et al. (2001) attributed the very high Cl in Kalimachak and Panjkra of the Narmada–Tapti system to anthropogenic sources.

(iii) Anthropogenic sources: The main contributors to anthropogenic materials in the drainage basin are fertilizers from agricultural practices and sewage. Part of the Krishna basin in Maharashtra is subject to intense agricultural activities, the main crops being sugarcane and cereals. Pawar et al. (1997), based on spatial and temporal variations of major ion chemistry of shallow groundwaters near a sugarmill in Deccan show that the mill effluents can be a significant source of Cl and NO₃ to surface and groundwater. They also inferred that urea and muriate of potash used as fertilizers can be source for these ions. In some of the rivers, such as the Bhima in its lower reaches (BHM-2, 3, 4 and 5), the Ghod, Mutha, Nira, and the Kukdi, all of which have high NO₃ with high Cl (and SO₄), there is an indication that anthropogenic activities may be influencing their composition, the likely source for all these ions being fertilizers and sewage. This inference is also attested by the strong correlation among SO₄–Cl, and (Cl +SO₄)–Na (Figs. 3.6 a and 3.6b). Analysis of the data of Dessert et al. (2001) for the NTW rivers also show similar Cl–SO₄ and Na–(Cl +SO₄) trends. Dessert et al. (2001) attributed the high Cl in Kalimachak and Panjkra rivers of the Narmada–Tapti system to anthropogenic sources. It is tempting to interpret these observations in terms of a common source for Cl, SO₄ and Na such as anthropogenic inputs and saline soils.

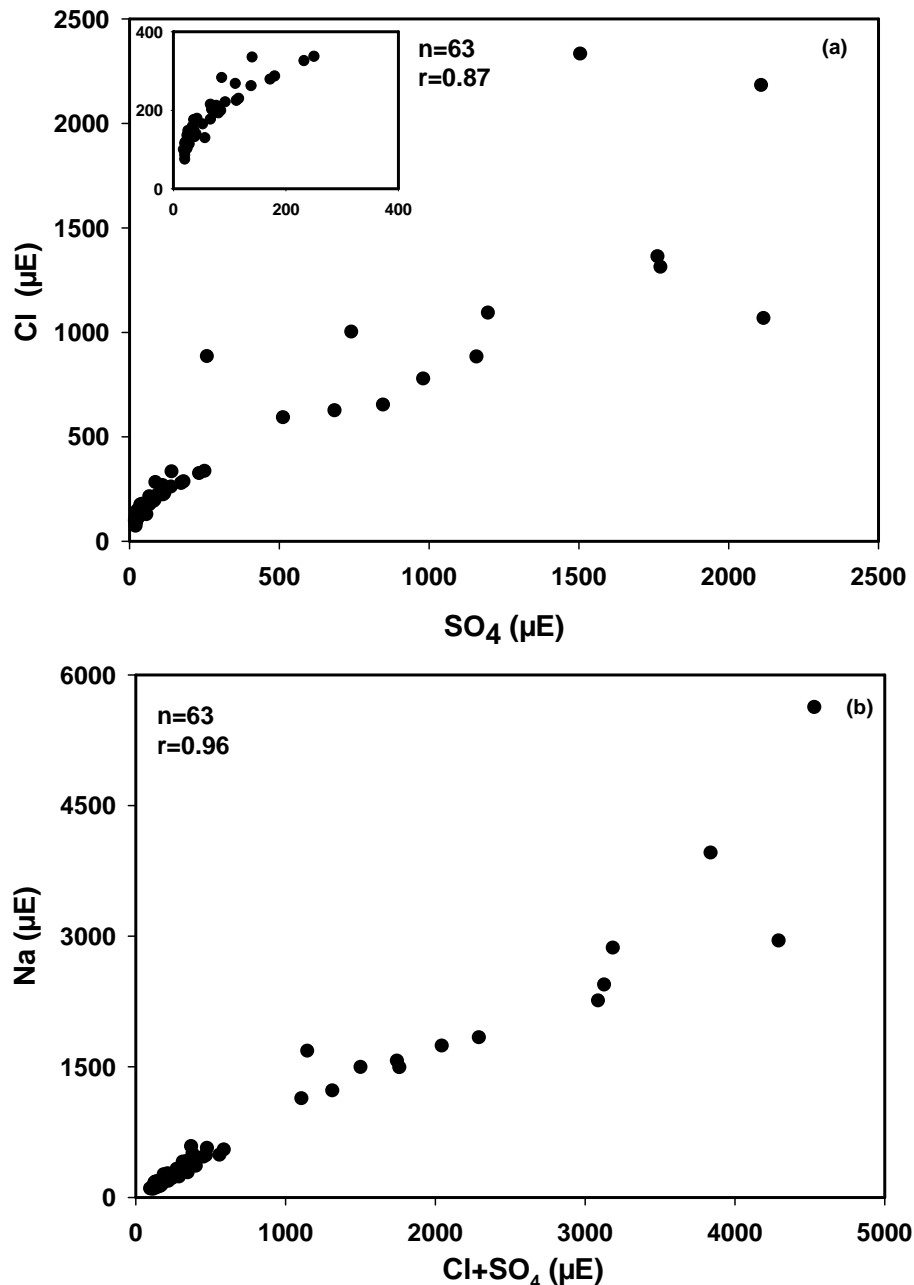


Fig.3.6 (a) Scatter plot of Cl vs. SO_4 , the data shows an increasing trend with a good positive correlation, (b) Na vs. $(\text{Cl}+\text{SO}_4)$. These also show a strong correlation with a slope of 0.89 ± 0.03 . The dominant sources contributing to these ions are anthropogenic inputs and/or saline/alkaline soils dispersed in parts of the Bhima and the Krishna basin.

Estimation of individual contributions from salt affected soils and anthropogenic sources to Cl, SO_4 and Na budgets of rivers draining into the Bay of Bengal remains elusive. It is, however, possible to derive the total contribution from these two sources by assuming that all Cl in rivers, in excess of that can be supplied from rains, is from them. The contribution of Cl and Na from anthropogenic and salt affected soils (μM) to rivers of Deccan interior can be derived from

$$Cl_s = Cl_r - Cl_{rain}/0.6 \dots \dots \dots (3.12a)$$

$$Na_s = Cl_s \dots \dots \dots (3.12b)$$

where subscripts *s* and *r* refer to salt affected plus anthropogenic sources and rivers, and 0.6 is the correction for evapo-transpiration factor.

Such an approach would suggest that in the west flowing western ghat rivers, there is no discernible contribution of Cl and Na from these sources, whereas in the Krishna and the Bhima tributaries (n=31) and in the Krishna main stream, they can contribute ~80% and ~70% of Cl and ~40% of Na. In all these calculations it is assumed that Cl derived from basalts is insignificant and that NaCl is the only source of Na from saline soils and anthropogenic sources.

3.3.3 Chemical weathering rates

Determination of chemical weathering rates (CWR) requires information on the quantum of various elements supplied to the dissolved phase of rivers from weathering of their basins. In the preceding section, atmospheric contribution of Cl and other major ions to rivers was derived based on rainwater composition. The amount of dissolved elements supplied to rivers via chemical weathering of the basin ($X^* = Na, K, Ca, Mg$ and SO_4) is calculated by subtracting the contributions from rainwater, saline soils and anthropogenic sources from the river water concentration. Two approaches are used to correct for the atmospheric contribution, one for the group of western ghat rivers that drain into the Arabian sea (Table 3.1, n=10), and the other for those which belong to the Krishna system (n=53; includes Ambika) and drain into the Bay of Bengal. The dissolved major ion concentrations in rivers (μM) resulting from chemical weathering of the basin (X^*) are calculated as:

Case 1: For rivers flowing into the Arabian Sea, all Cl can be accounted for from rain. In these samples:

$$X^* = X_r - X_{rr} \dots \dots \dots (3.13)$$

where $X = Na, K, Ca, Mg$ and SO_4 , *r* refers to river, X_{rr} is calculated based on equation (3.11) and $f_{et} \approx 1$.

Case 2: For the rivers draining into the Bay of Bengal (Deccan interior)

X^* for K, Ca, Mg and SO_4 can also be calculated based on the above relation (3.11) and $f_{et} = 0.6$.

For Na, additional correction is needed because of its input from saline soils/anthropogenic sources. Na^* is given by:

$$\text{Na}^* = \text{Na}_r - (\text{Na}_{rr} + \text{Na}_s) \dots \dots \dots (3.14a)$$

$$\text{Na}^* = \text{Na}_r - \text{Cl}_r + \{1 - (\text{Na}/\text{Cl})\} \times \text{Cl}_{rain}/f_{et} \dots \dots \dots (3.14b)$$

where Na_r and Cl_r are the concentrations in rivers, the second term on RHS of equation (3.14b) is a result of $(\text{Na}/\text{Cl})_{rain}$ being $\neq 1$.

The total dissolved solids corrected for atmospheric, saline soils and anthropogenic inputs, TDS^* ($=\Sigma\text{X}^* + \text{SiO}_2$) is the amount of dissolved species in rivers derived from chemical weathering of the basin. TDS^* varies from $\sim 7 \text{ mg } \ell^{-1}$ to $\sim 312 \text{ mg } \ell^{-1}$, the high values ($>80 \text{ mg } \ell^{-1}$) are in samples from the Bhima and its tributaries. This estimate assumes that all alkalinity in the rivers is derived from atmospheric/soil CO_2 (silicate weathering) and therefore, there is no contribution of HCO_3 to TDS^* . Conversion of TDS^* to chemical weathering rates of the basin requires knowledge of runoff of individual rivers. The runoff data for individual rivers is sparse, the weathering rate calculations are based on average runoff of the major rivers of the region, $\sim 463 \text{ mm } \text{y}^{-1}$ for the Krishna system and $\sim 1690 \text{ mm } \text{y}^{-1}$ for rivers flowing into the Arabian sea. This is consistent with the average runoff values of $\sim 476 \text{ mm } \text{y}^{-1}$ estimated based on annual discharge ($1.73 \times 10^{13} \ell$) and catchment area (36286 km^2) of the Krishna at Alamatti (UNESCO, 1993) and the value of $452 \text{ mm } \text{y}^{-1}$, used for the Narmada basin (Borole et al., 1982). The above runoff corresponds to about 60% of the average annual precipitation (770 mm) for this region during the last decade (<http://www.tropmet.res.in>). For the west flowing rivers there is no data on runoff, however, a value of $1685 \text{ mm } \text{y}^{-1}$ is used which is the runoff of the river Mandvi at Ganjem, Goa (Shankar et al., 2004). This is about 67% of the annual precipitation ($\sim 2500 \text{ mm}$) for this region (<http://www.tropmet.res.in>).

The chemical weathering rates in the individual river basins over the two years of sampling vary from ~ 3 to $\sim 144 \text{ t km}^{-2} \text{ y}^{-1}$ (Fig. 3.7) with an average of $\sim 36 \text{ t km}^{-2} \text{ y}^{-1}$. There is no significant inter-annual variability in 2001 and 2002. The value of $\sim 36 \text{ t km}^{-2} \text{ y}^{-1}$ is identical to that reported by Dessert et al. (2001) for the NTW rivers draining the northern region of the Deccan Traps, however, in those basins the range in CWR is much narrower, $21\text{--}63 \text{ t km}^{-2} \text{ y}^{-1}$. Closer look at the distribution of CWR in the Krishna system shows two main groups, one at $\sim 15 \text{ t km}^{-2} \text{ y}^{-1}$ (belonging to the east flowing smaller tributaries of the Krishna), and the other at $\sim 55 \text{ t km}^{-2} \text{ y}^{-1}$, comprised mainly of the west flowing western ghat rivers. About 10% of the samples have values in excess of $\sim 60 \text{ t km}^{-2} \text{ y}^{-1}$; these are the Bhima and its tributaries. The

average CWR derived is based on data of all rivers analysed and does not consider the influence, if any, of anthropogenic supply and/or calcite precipitation in measured major ion abundance. The sources of uncertainty in these CWR estimates are:

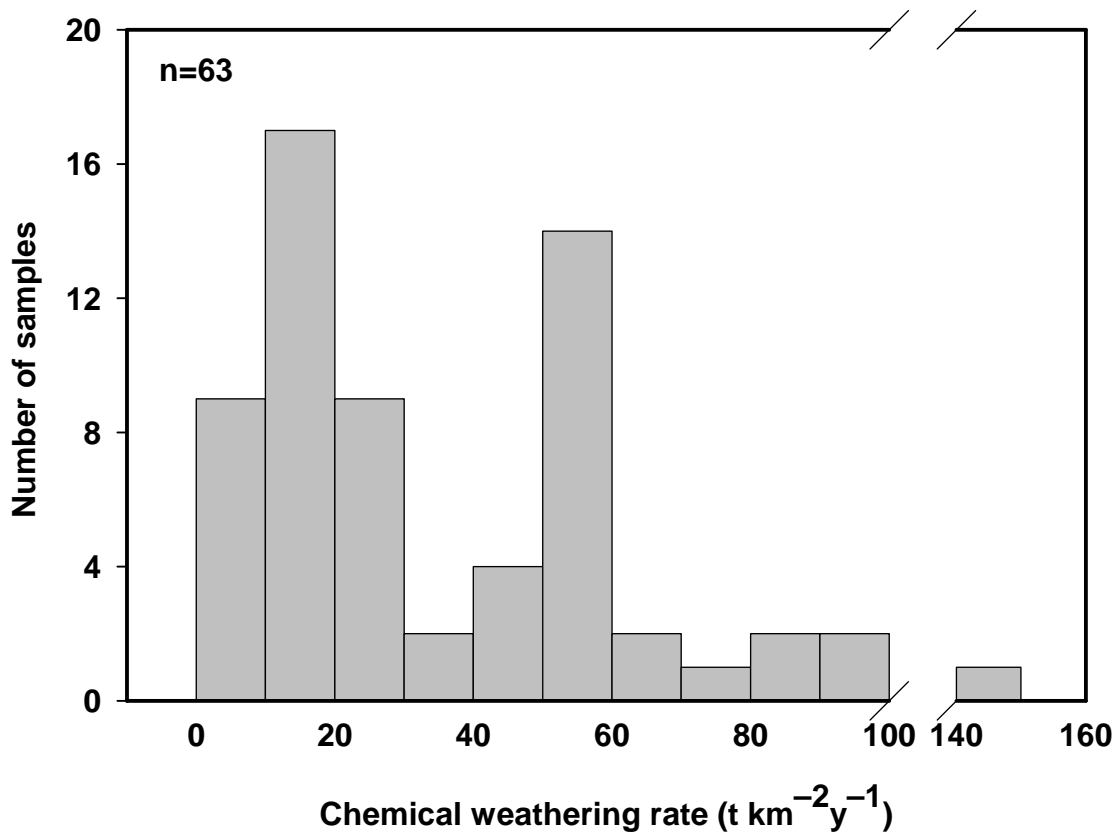


Fig.3.7. Frequency distribution of chemical weathering rates (CWR). The data show two peaks. The peak between 50–60 t km⁻² y⁻¹ represents samples from the west flowing western ghat rivers, which have a factor of ~4 higher runoff compared to the smaller (east) flowing tributaries of the Krishna river (first peak, 10-20 t km⁻² y⁻¹). Rivers with >70 t km⁻² y⁻¹ CWR have very high Cl, SO₄ and NO₃ and belong to the Bhima (lower reaches), Nira, Ghod and the Kukdi.

(i) **supply of Ca from carbonates.** Carbonates in the form of calcite have been reported in some of the Deccan flows (Sukeshwala et al., 1972; Jeffery et al., 1988). To check on this further, carbonate content of sixteen samples of Deccan basalts from Mahabaleshwar, Igatpuri and Ambenali were measured by coulometry. The results show that many of the samples have measurable carbonate in them, with concentration between 0 to 0.92 wt.% (mean 0.2 wt.%). The abundance of carbonates though low, they could be an additional source of Ca to selected rivers, as they weather more rapidly than silicates. If carbonates are important in Ca budget of rivers analysed then a part of the alkalinity has to be derived from their weathering making

the CWRs calculated above lower limits. This is discussed in more detail in the next section.

(ii) calcite precipitation: The removal of Ca from dissolved phase via calcite precipitation can also underestimate the CWRs. Calcite saturation indices (CSI; Langmuir, 1971) at 25°C were calculated using the approach of Drever (1997), to check on the possibility of removal of Ca by calcite precipitation. The results show that 49 out of 63 samples are undersaturated in calcite (CSI: <0; Fig. 3.8), while

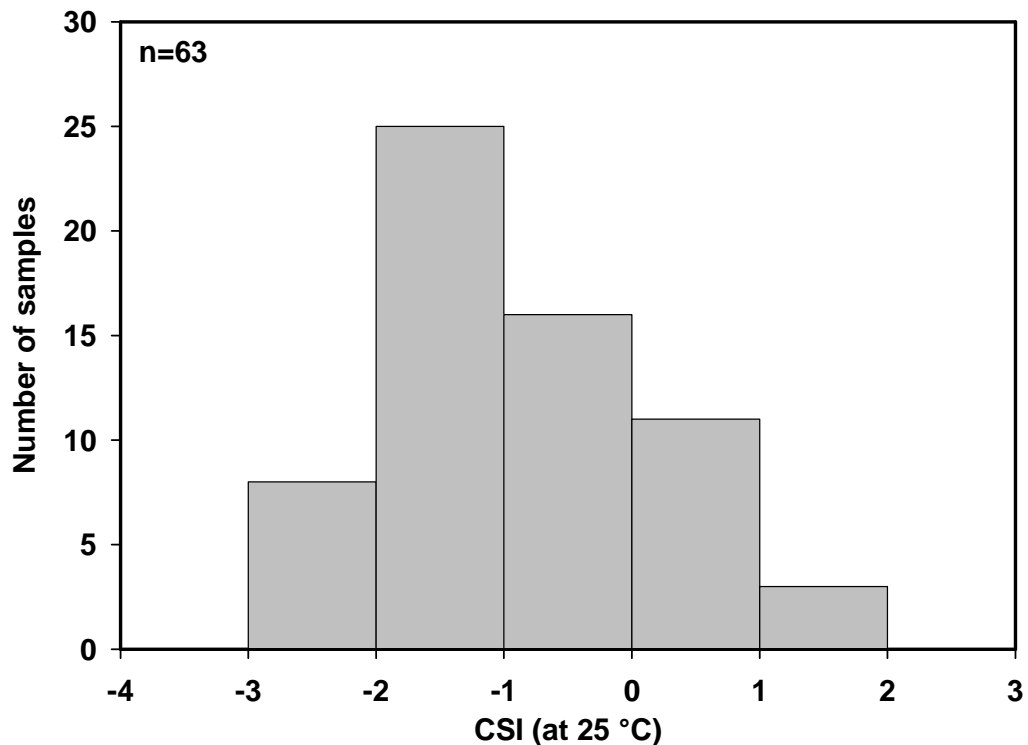


Fig.3.8. Distribution of calcite saturation index (CSI) of samples analysed. 49 of the samples are under-saturate w.r.t. calcite, while 14 samples (mostly the Bhima at lower reaches, and its tributaries) are supersaturated.

the remaining 14 show slight to moderate supersaturation. It is unclear if supersaturation would lead to calcite precipitation, as it may also depend upon other physico-chemical conditions of rivers (Dalai et al., 2002). The Ca/Mg ratios of these “calcite supersaturated” rivers (as discussed in the next section), however, seem to indicate removal of Ca. The source(s) of these carbonates, though, is (are) not established, a part of it could be its precipitation from rivers. It is interesting to mention that a similar calculation for streams from the NTW system (using data of Dessert et al., 2001) show that a number of them are also supersaturated in calcite.

(iii) anthropogenic supply: The impact of this source on Na and Cl abundances has already been considered. There could be other ions such as SO₄, which could also be derived from this source. The role of this in major ion abundances and hence CWRs of the basins is difficult to quantify.

Therefore, to avoid uncertainties in CWRs arising from this source and also in Ca budget due to calcite precipitation, CWRs were recalculated by excluding the data of the samples with high SO₄ (>100 μM) and Cl (>300 μM) that are affected by anthropogenic supply or calcite supersaturation. These include the Bhima in its lower reaches (BHM-2, 3, 4 and 5), its tributaries (the Ghod, Mutha, Nira and the Kukdi) and some of the Krishna samples (KRS-1, 4 and 5). This recalculation brings down the maximum CWR for the Krishna system rivers (n=33; includes Ambika, Table 3.1) to ~34 t km⁻² y⁻¹ (mean: 14 t km⁻² y⁻¹). The six west flowing western ghat rivers have higher and similar CWRs (48–60 t km⁻² y⁻¹), compared to the east flowing western ghat rivers, GTP-1, KYN-2, HRN-1 and TPN-1, that have CWR, <10 t km⁻² y⁻¹. These results suggest that there is considerable variability in chemical weathering rates even among adjacent basins of the Deccan Traps.

Assuming that the average CWR for the Krishna system, ~14 t km⁻² y⁻¹, as typical of the Deccan interior and ~54 t km⁻² y⁻¹ for the west of the western ghats (~6% of the total Deccan Trap area), the area weighted CWR for the Deccan Trap is calculated to be ~16 t km⁻² y⁻¹. This translates to a chemical erosion flux (CEF) of ~0.8×10⁷ tons y⁻¹ and an erosion rate of 5.8 mm ky⁻¹ for the Deccan basalts. If this rate has been operative since the emplacement of the Deccan basalts about 65 Ma ago, about 400 m thick basalt rock would have been chemically eroded. The present day CEF, however, could be lower than in the past, because of decrease in both the aerial coverage of Deccan Traps and its chemical weathering. Further, the CWR may have decreased over time due to development of soil cover (Bluth and Kump, 1994).

3.3.4 Variability in CWRs among different Deccan Trap regions

The CWR for the Krishna system in the southern Deccan averages ~14 t km⁻² y⁻¹, about four times lower than that for the west flowing rivers, ~54 t km⁻² y⁻¹, though their average TDS* overlap. The major difference between these two regions is runoff; the western region has four times the runoff of the Krishna system. This coupled with the observations that (i) river water temperatures of the two regions are roughly similar and (ii) physical weathering in these basins as indicated from their suspended matter concentrations do not show any discernible

trend, suggests that runoff determines the CWR in these basins. Similar inference on the coupling between CWR and runoff has been reported earlier (Bluth and Kump, 1994).

The CWR in the northern Deccan, as deduced from the chemistry of NTW rivers (Dessert et al., 2001) is 2–3 times that for the Krishna system determined in this study. This difference seems to result from higher intensity of chemical weathering of the NTW basins, their rivers have 2–3 times more TDS* than the Krishna system rivers.

Possible explanations for the difference in TDS* and hence CWR between the north and the south Deccan are (i) natural variability in intensity chemical weathering in the different regions of the Deccan Traps, (ii) underestimation of the weathering rates in this study because of sample selection criteria used in calculation (rejection of high Cl, SO₄ and calcite supersaturated samples), and (iii) contributions from sources in addition to basalts which results in higher TDS* in NTW rivers. In this context, the role of easily weatherable Vindhayan carbonates/sediments of the basin, and groundwater/anthropogenic inputs in supplying major ions to these rivers require further scrutiny. The high NO₃ (>50 μM), SO₄ (>100 μM) levels and higher Na*/Mg* and Na*/Ca* (in the NTW waters) relative to basalts are pointers to input from such sources.

3.3.5 Silicate weathering rates

The determination of silicate weathering rates (SWR) is an important goal of river water studies as it is a major sink for atmospheric CO₂ on long time (Ma) scales (Garrels and Mackenzie, 1971; Berner et al., 1983; Kump et al., 2000; Amiotte-Suchet et al., 2003; Dessert et al., 2003). The rivers analysed in this study flow entirely through the Deccan basalts. It is, therefore, expected that the major ion abundances of these rivers (corrected for rain input) is from silicate weathering. If this is valid then the CWR derived in the earlier section would be the same as their silicate weathering rate (SWR). This presumption can be in error if minor phases such as carbonates present in basalts and in river sediments act as a significant source of Ca and alkalinity to rivers and if other sources (saline soils, anthropogenic supply) influence river water chemistry. It has been shown earlier that inputs from such sources can be important for some of the rivers analysed. Therefore, an independent estimate of silicate weathering rates has been made based on various elemental ratios

in rivers and in basalts. The silicate weathering rates are generally calculated using a suitable proxy (e.g. Na^* concentration in rivers, Na^* is Na corrected for Cl) and assumptions regarding the release of various elements relative to Na from rocks to water (Singh et al., 1998; Galy and France-Lanord, 1999; Dalai et al., 2002, Jacobson et al., 2002). For some of the rivers sampled in this study, Na^* may not be a suitable proxy for silicate weathering, as they may also be receiving Na from saline soils and anthropogenic sources. Ca may not also be a proper proxy for silicates as part of its abundance in rivers can be from carbonates. Further, its behaviour in rivers can be non-conservative leading to its removal through precipitation. Dessert et al. (2001) have used HCO_3^- as an index of basalt weathering to derive CO_2 consumption rates. This requires bicarbonate to be supplied entirely from silicate weathering; a requirement that needs to be verified considering that carbonates are present in basalts, in river sediments and in the basin, and their weathering can also supply alkalinity to rivers. Alkaline soils can be another source of alkalinity to some of these rivers, the significance of this source, however, needs to be assessed.

Because of the uncertainties associated with the commonly used surrogates of silicate weathering, in this work, dissolved Mg has been used as an index for its calculation. In the rivers studied, Mg is supplied almost entirely through weathering of Deccan basalts. Dolomite weathering can be another source of Mg but there are no reports of its occurrence in the basin. Further, the involvement of Mg in the riverine nutrient cycles, if any, is assumed to be insignificant. Figs. 3.9 a,b are scatter diagrams of Ca^* and Na^* vs. Mg^* in rivers with, $\text{CSI} < 0$, $\text{Cl} < 300 \mu\text{M}$ and $\text{SO}_4 < 100 \mu\text{M}$ (these rivers have been selected as they avoid ambiguities arising from calcite supersaturation, major anthropogenic and saline soil inputs). The plots show strong positive correlation between these elements, consistent with that expected if basalt weathering is the dominant source for them.

The silicate component of major cations in rivers are calculated using Mg as a proxy as follows:

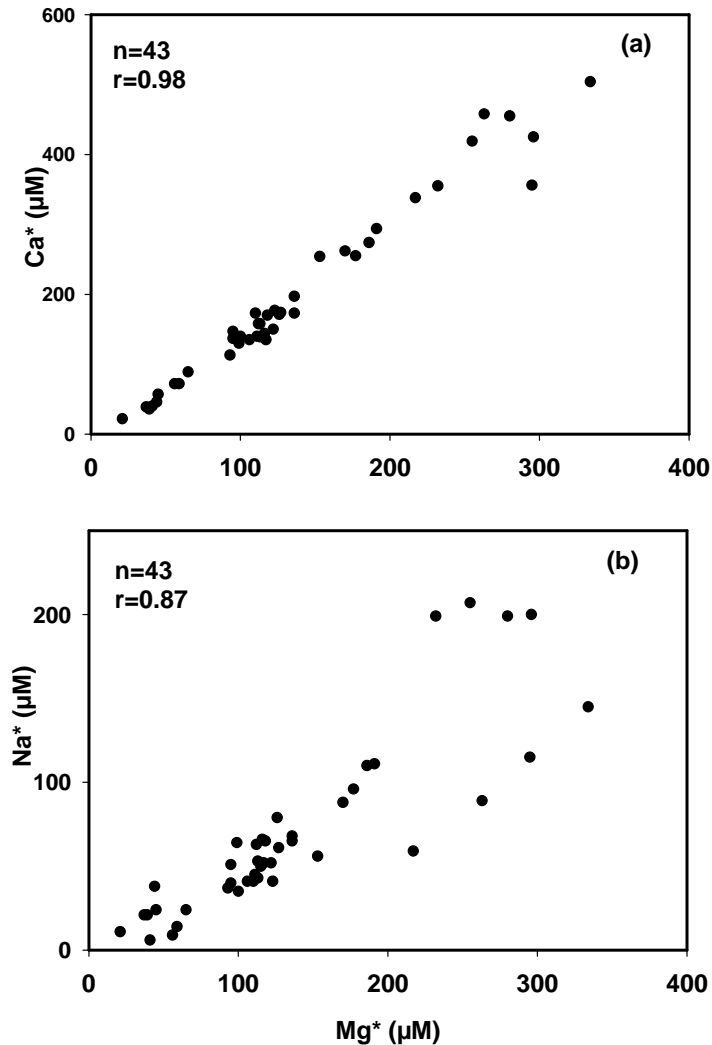
$$\text{i). } \text{Mg}_{\text{sil}} = \text{Mg}_r - \text{Mg}_{\text{rr}} \dots \dots \dots (3.15)$$

$$\text{ii). } \text{K}_{\text{sil}} \approx \text{K}_r - \text{K}_{\text{rr}} \dots \dots \dots (3.16)$$

$$\text{iii). } \text{Ca}_{\text{sil}} = \text{Mg}_{\text{sil}} \times (\text{Ca/Mg})_{\text{sol}} \dots \dots \dots (3.17)$$

$$\text{iv). } \text{Na}_{\text{sil}} = \text{Mg}_{\text{sil}} \times (\text{Na/Mg})_{\text{sol}} \dots \dots \dots (3.18)$$

where the subscripts *sil*, *r* and *sol* are silicates, river and solution respectively. Mg_{rr} (K_{rr}) is the contribution of Mg (K) from rain to rivers.



Figs.3.9 (a) Scatter plot of Ca^* vs. Mg^* , the data show very high correlation (b) plot of Na^* vs. Mg^* , these elements also show a good correlation. These significant correlations coupled with elemental ratios overlapping with those in basalts suggest that Mg, Ca and Na are released to rivers from basalts without major fractionation.

$(Ca/Mg)_{sol}$ and $(Na/Mg)_{sol}$ are the ratios with which Ca and Na are released relative to Mg, from basalts to rivers. These are calculated assuming that these elements are released to rivers in the same ratio as their abundance in basalts, $Ca/Mg = 1.19$ and $Na/Mg = 0.51$ (Table 3.3). The accuracy of estimation of various silicate derived cations in rivers depends critically on how well $(Ca/Mg)_{sol}$ and $(Na/Mg)_{sol}$ can be constrained. Independent estimates of these ratios are also made from Ca^* , Mg^* and Na^* data of the small west flowing rivers (VAT-1, SUKH-1, SHT-1, KJL-1, GAD-1 and ARJ-1; Fig. 2.2, Table 3.1).

These rivers were selected as only two sources; rain and silicate weathering determine their major ion chemistry. In these rivers, Cl and SO_4 can be accounted entirely by rain, their $[HCO_3/(Cl+SO_4)]$ molar ratio is in excess of 5 and $SiO_2 > 300 \mu M$,

indicating the dominance of silicate weathering contribution to their cation budget. Sr isotopes have also been analysed in many of these samples, the $^{87}\text{Sr}/^{86}\text{Sr}$ ratios of most of them lie in the range of 0.705—0.707 (see chapter 6). These ratios overlap with the range of $^{87}\text{Sr}/^{86}\text{Sr}$ of basalts (Subbarao et al., 2000) and further supports the dominant role of silicate weathering in contributing Sr and other major ions. The Ca^*/Mg^* and Na^*/Mg^* ratios derived from the six west flowing western ghat rivers are 1.27 ± 0.08 and 0.49 ± 0.08 respectively; these ratios overlap with the corresponding ratios in basalts.

Table 3.7 presents a comparison of Ca^*/Mg^* and Na^*/Mg^* ratios measured in the Krishna tributaries (n=33) and western flowing rivers (n=10); samples with $\text{CSI} < 0$, and $\text{Cl} < 300 \mu\text{M}$ and $\text{SO}_4 < 100 \mu\text{M}$) with those expected based on chemical and mineralogical composition of the basalts. Among these, in some of the rivers, Na^* concentrations are quite low (Fig. 3.9b), and hence are subject to larger uncertainties.

Table 3.7. Measured and expected major ion ratios.

Ratio	Measured	Expected
(1)	(2)	
Ca^*/Mg^*	1.38 ± 0.21	1.27 ± 0.08
Na^*/Mg^*	0.48 ± 0.18	0.49 ± 0.08
HCO_3/Mg^*	5.85 ± 0.59	5.70 ± 0.23
Ca^*/Na^*	3.34 ± 1.5	2.62 ± 0.33

(1) Krishna system (n=33), (2) west flowing rivers (n=10)

These results show that the measured average Ca^*/Mg^* ratios in the Krishna (and its tributaries) are marginally higher than that expected from basalts. This can be ascribed either to the presence of other source(s) of Ca to rivers or to a slight preferential mobility of Ca over Mg from basalts to water. Ca rich minor phases in the basalts (such as carbonates and apatites) that are easily weatherable can be the other sources for Ca. The close similarity of these ratios, between basalts and river water, however, indicates near stoichiometric release of Ca, Mg and Na to rivers from basalt. This is in contrast to the results from the Reunion where fractionation among Ca, Mg and Na during weathering has been suggested, with preferential release of Na over Ca and Mg (Louvat and Allegre, 1997). In samples analysed in this work, such major fractionation is not evident.

Extension of this calculation to all rivers analysed brings out two other important observations: (i) the rivers that are supersaturated with calcite (e.g. NIRA-1, NIRA-2, GHOD-2, KUK-1, BHM-5) show deficiency of Ca relative to its estimated

supply from basalts. This finding is an indication that in these rivers, calcite precipitation may have influenced their Ca concentration. (ii) Na* in the Bhima in its lower reaches; Ghod, Mutha, Nira and the Kukdi (Table 3.1) are quite in excess of Na_{sil}. These rivers also have high Cl, SO₄ and attests to the inference made earlier that Na contribution from saline/alkaline soils and anthropogenic sources might be important.

The total silicate cations [$\Sigma(\text{Ca}_{sil} + \text{Mg}_{sil} + \text{Na}_{sil} + \text{K}_{sil})$] in the above selected rivers (Cl < 300 μM , SO₄ < 100 μM and CSI < 0) range from 105 to 1652 μE (Table 3.8). This corresponds to ~36 and ~85% of TZ⁺ (average: 66%), the balance being contributed by rain and other sources. The silicate fraction of cations in the Deccan rivers are much higher than those determined for the Ganga–Brahmaputra river system (Galy and France–Lanord, 1999; Krishnaswami et al, 1999; Dalai et al., 2002; Jacobson et al., 2002). This is expected as the basins of the Deccan rivers are covered almost entirely with basalts, whereas silicates, carbonates and other sedimentaries all occur in the drainage basins of the head waters of the Ganga–Yamuna in the Himalaya.

The silicate weathering rates for the “selected rivers” are calculated using the relation:

$$\text{SWR} = \text{TDS}_{sil} \times \text{runoff}$$

where $\text{TDS}_{sil} = [\Sigma(\text{Ca}_{sil} + \text{Mg}_{sil} + \text{Na}_{sil} + \text{K}_{sil})] + \text{SiO}_2$ (all in units of mg ℓ^{-1})

The SWRs in these rivers vary from ~3 to ~60 t km⁻² y⁻¹ with an area weighted average of 15 t km⁻² y⁻¹ (Table 3.8). The frequency distribution of the SWRs is shown in Fig.3.10.

3.3.5.1 Role of carbonates in Ca budget

Ca rich minor phases such as calcites, apatites and bytownite present in rocks can be a major source of Ca to rivers draining them as shown in some of the earlier studies on granite watersheds (Blum et al., 1998; White et al., 1999a; Jacobson et al., 2002; Oliva et al., 2004). The role of such phases in contributing to Ca budget of Deccan rivers is evaluated below. In most of the rivers analysed, Ca* is equal to or in excess of Ca_{sil}. If this excess results from the supply of Ca from carbonates in basalts (or in the basin) to rivers, a limit on their contribution can be estimated as:

Table 3.8 Silicate cations and carbonate-Ca concentration, chemical, silicate weathering rates and CO₂ consumption rates (CO₂ CR) of selected rivers (n=43).

River	$\Sigma(\text{Cat})_{\text{sil}}$ (μE)	TDS _{sil} (mg l^{-1})	Ca _c (μM)	CWR ($\text{t km}^{-2} \text{y}^{-1}$)	SWR ($\text{t km}^{-2} \text{y}^{-1}$)	CO ₂ CR ($10^5 \text{ km}^{-2} \text{y}^{-1}$)
KRS-1	1269	42.1	116	26	20	5.9
KRS-2	951	34.0	67	19	16	4.4
	679	25.6	35	14	12	3.1
KRS-3	1390	45.2	122	25	21	6.4
	626	27.3	21	13	13	2.9
KRS-4	1468	46.0	73	25	21	6.8
KRS-5	1153	39.7	79	24	18	5.3
BHM-1	473	26.8	34	13	12	2.2
	527	27.2	9	13	13	2.4
GHOD-1	1306	46.1	145	24	21	6.0
KYN-1	920	37.1	53	18	17	4.3
	584	26.4	30	13	12	2.7
KYN-2	218	14.5	-	7	7	1.0
	223	13.7	3	6	6	1.0
VRN-1	862	32.9	60	17	15	4.0
	878	34.0	44	17	16	4.1
PGN-1	552	24.0	42	13	11	2.6
	500	20.8	21	10	10	2.3
PGN-2	612	26.1	31	13	12	2.8
GTP-1	184	10.8	-	5	5	0.9
	105	7.3	-	3	3	0.5
HRN-1	193	11.0	-	5	5	0.9
	282	12.7	5	6	6	1.3
TPN-1	295	15.1	2	7	7	1.4
	210	10.8	-	5	5	1.0
DDG-1	758	29.2	72	15	14	3.5
	1081	39.5	80	20	18	5.0
VDG-1	470	23.0	24	11	11	2.2
	460	22.4	2	10	10	2.1
BGW-1	560	26.0	24	12	12	2.6
	324	16.2	12	8	8	1.5
ARJ-1	574	319	6	54	54	9.7
GAD-1	492	27.9	12	48	47	8.3
SUKH-1	569	29.8	3	50	50	9.6
	577	30.4	-	51	51	9.7
KJL-1	558	30.8	5	52	52	9.4
	670	35.3	11	60	59	11.3
SHT-1	553	32.7	25	57	55	9.3
	547	30.1	8	51	51	9.2
VAT-1	627	34.2	23	59	58	10.6
	602	32.2	5	54	54	10.1
AMB-1	1652	69.7	107	34	32	7.6
MULA-1	1453	45.1	5	22	21	6.7

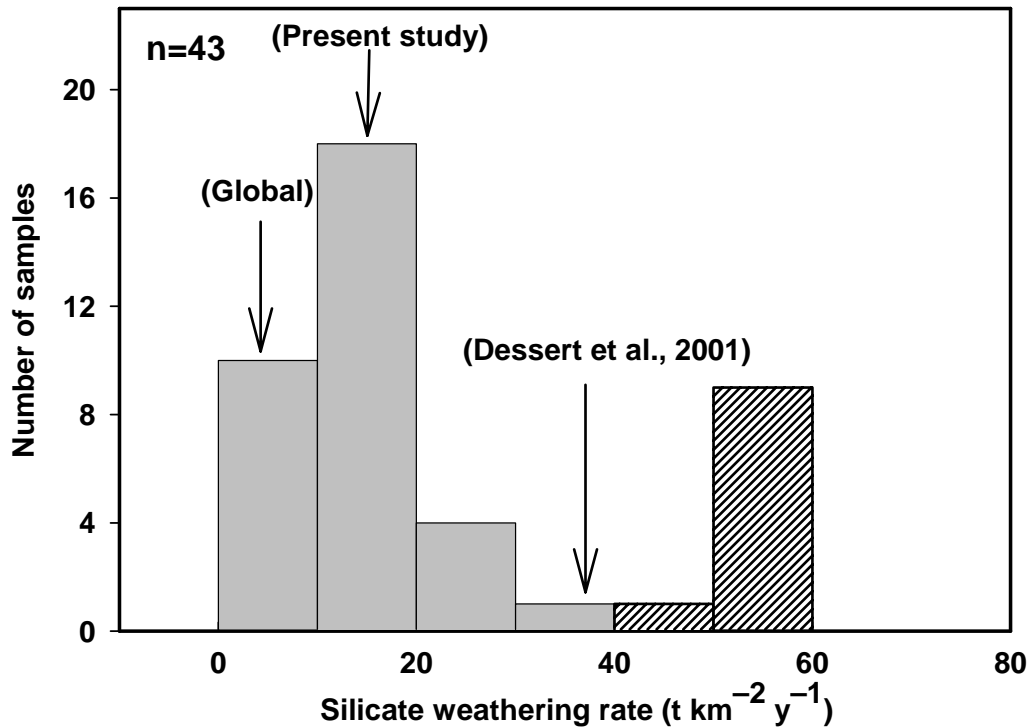


Fig.3.10. Distribution of silicate weathering rates in selected samples of the Krishna system and the west flowing western ghat rivers (hatched lines). The SWR in the WFWR are much higher than that of the Krishna system and is a result of higher runoff in the region. The chemical weathering rate based on the results of northern Deccan (Dessert et al., 2001), the area-weighted average SWR for the Deccan basin in the present study and the global silicate weathering rate are also shown for comparison.

$$\text{Ca}_c = \text{Ca}_r - (\text{Ca}_{rr} + \text{Ca}_{sil}) \dots \dots \dots (3.19a)$$

$$= \text{Ca}_r - \{ \text{Ca}_{rr} + (\text{Ca}/\text{Mg})_{sol} \times \text{Mg}_{sil} \} \dots \dots (3.19b)$$

where subscript *c* refer to carbonate contribution (μM), and other subscripts are defined in appendix.

Ca_c ranges from ~ 0 to $\sim 145 \mu\text{M}$ with a mean of $38 \mu\text{M}$, in the selected samples (Table 3.8). This corresponds to ~ 0 and $\sim 29\%$ of measured Ca in these rivers. Measurement of $\delta^{13}\text{C}$ of dissolved inorganic carbon (DIC) in these waters also attest to the contribution of carbonate derived DIC in them. $\delta^{13}\text{C}$ values in these waters show range from $\sim -20\text{‰}$ to -8‰ (see chapter 4). These are interpreted in terms of mixing of two DIC end members, generated from silicate and carbonate weathering with CO_2 from C_3 vegetation. This model requires that samples enriched in ^{13}C , -13‰ to -8‰ , have high carbonate component of DIC. The carbonates in these samples enriched in ^{13}C are at or above calcite supersaturation or have signatures of anthropogenic inputs (high Cl and SO_4).

In the rivers used in calculation, the maximum average Ca contribution from carbonates is ~29%. This is unlike in some watersheds draining granites/gneiss where Ca supply from such minor phases is reported to be more significant (Blum et al., 1998; White et al., 1999b; Oliva et al., 2004). This difference is attributable to high Ca in basalts, relative ease of their weathering and their relatively low carbonate content. Further, though carbonates may weather orders of magnitude more rapidly than basalts, in natural environment the weathering of calcites contained in silicate rocks would be limited by the rate of their exposure.

3.3.5.2 Comparison of silicate weathering rates

The silicate weathering rates in the Krishna system and the west flowing western ghat rivers derived from major ion chemistry are summarized in Table 3.9 (also Fig. 3.9). The SWR of the Krishna (KRS-2, at Alamatti) is $\sim 14 \text{ t km}^2 \text{ y}^{-1}$. The average SWR for rivers of the Krishna system in the Deccan interior is $\sim 13 \text{ t km}^2 \text{ y}^{-1}$ and that of the west flowing western ghat rivers is $\sim 53 \text{ t km}^2 \text{ y}^{-1}$, marginally lower than the average CWR. The area weighted SWR for the above rivers is $\sim 15 \text{ t km}^2 \text{ y}^{-1}$. The west flowing western ghat rivers, though have TDS_{sil} ($\text{SiO}_2 + \Sigma(\text{Cat})_{\text{sil}}$, in unit of mg l^{-1}) nearly identical to those of the east flowing western ghat rivers of the Krishna system, their SWRs are a factor of ~ 4 higher, caused mainly by increased runoff of similar proportion (Table 3.9). This re-emphasizes the importance of runoff in determining weathering rates (Bluth and Kump, 1994; Amiotte-Suchet and Probst, 1995; Louvat and Allegre, 1997; Kump et al., 2000). Further, this study also has shown that in some basins of the Deccan Trap, the SWR can be low ($< 10 \text{ t km}^2 \text{ y}^{-1}$) possibly due to soil cover and hence “transport limited” (Stallard, 1995)

Comparison of SWRs of the south and western regions of the Deccan Traps based on this study with the reported results from northern region (Dessert et al., 2001) is strictly not possible as only CWR data are available for the latter. The use of CWR for SWR for the northern Deccan region needs better understanding on the roles of sources such as Vindhayan carbonates/sediments and anthropogenic/saline soils and supersaturation of calcite in contributing to the major ion budget of the rivers draining this region.

Table 3.9 Silicate weathering rates in the Deccan Traps and in the Himalaya

River basin	n	Location	Runoff (mm y ⁻¹)	TDS _{sil} (mg l ⁻¹)	SWR (t km ⁻² y ⁻¹)	Reference
<i>Deccan Traps</i>						
Krishna (KRS-2)	2	Alamatti	476	29.8	14	1
West flowing rivers @ Krishna system (east flowing)	10	Western Deccan	1685	31.5	53	1
Narmada-Tapti-Wainganga	33	Deccan	463	28.1	13	1
	19	Northern Deccan	463	80	37 [#]	2
<i>Himalaya</i>						
Yamuna	1	Batamandi	1125	24.7	28	3
Bhagirathi	1	Devprayag	1064	14.3	15	3
Alaknanda	1	Bhagwan	1195	8.53	10	4

[#]Chemical weathering rate @ Sukh, Shashtri, Vashishthi, Gad, Kajli and Arjuna

1 Present study; 2 Dessert et al, 2001; 3 Dalai et al., 2002 and 4 Krishnaswami et al, 1999.

The data in Table 3.9 show that the SWRs of the Krishna system are within a factor of ~2 of the Ganga headwaters (the Yamuna, Bhagirathi and the Alaknanda) in the Himalaya, though these two sets of rivers flow through quite different climatological and lithological basins. The basins of the Yamuna and the Ganga in the Himalaya are multi-lithological, with significant fraction being covered by lithologies other than silicates such as carbonates, whereas the Krishna and the western ghat basins are made almost exclusively of Deccan basalts. Among the silicates of the Yamuna–Ganga basin, granite/gneisses is a significant lithology (Valdiya, 1980). The similarity in SWRs seems to suggest that granites/gneisses of Yamuna–Ganga headwaters in the Himalaya weather roughly at the same rate as the basalts of the Deccan Traps. This inference is also supported by the similarity in Si flux of watersheds of granite terrains of Malaysia (White et al., 1999a) and the Deccan Traps. The granites of Malaysia have been used for comparison as they have temperature range and runoff similar to those of Deccan Traps. Thus under “favourable

conditions”, the silicate weathering rate of granite/granitoid drainage basins can also be as high and/or similar to those of basalts.

In summary, the area-weighted SWR in the Deccan Traps averages $\sim 15 \text{ t km}^{-2} \text{ y}^{-1}$, with significant variation among individual river basins. The SWR derived from the study is a factor of ~ 2 lower than that reported for chemical weathering in the NTW system in the more northern province ($\sim 37 \text{ t km}^{-2} \text{ y}^{-1}$). These results and their comparison with weathering in the Himalaya also suggest that in addition to lithology, other factors such as relief, runoff and associated physical erosion influence silicate weathering (Bluth and Kump, 1994; Berner and Berner, 1996; Kump et al., 2000) and that SWR is a unique characteristic of each basin.

3.3.6 Temperature dependence on weathering

Chemical weathering of silicate rocks, similar to other chemical reactions, is also regulated by temperature (Velbel, 1993; White and Blum, 1995; Berner and Berner, 1997; Kump et al., 2000; Dessert et al., 2001; Dalai et al., 2002). Silicate weathering in nature, however, is a complex function of many parameters, which include lithology of the basin, relief, temperature, vegetation and rainfall. Thus, it is difficult to extract a clear temperature dependence on silicate weathering from river water chemistry, though laboratory studies have established this dependence on mineral weathering. This is because, such laboratory experiments are done by varying the temperature while keeping all other factors constant, which is difficult to attain in natural environments. The role of temperature on weathering rates has been a topic of study both in laboratory and natural systems (White and Blum, 1995 and references therein; White et al., 1999b; Kump et al., 2000; Dalai et al., 2002) mainly to determine activation energy for various minerals based on Arrhenius equation that relates the rate of reaction with temperature.

$$R_t = A \exp(-E_a/RT) \dots \dots \dots (3.20)$$

where R_t is the rate of reaction, A is the frequency or pre exponential factor, E_a is the activation energy, and R and T are universal gas constant and temperature in Kelvin respectively.

The use of relation (3.20) to natural silicate weathering system requires a proxy, such as concentration of major element/ion, for silicate weathering rates. Generally, concentration of Na derived from silicates (Na_{sil}) or Si or HCO_3 serve as proxies (White et. al, 1999a, Kump et al., 2000, Dalai et al., 2002). Recently, Dessert et al. (2001) in their study of basalts used bicarbonate in rivers as an index of silicate

weathering. This relies on the premise that in rivers draining basalts, the only source of bicarbonate is silicate weathering. They used average dissolved concentration of HCO_3^- and temperature from all the basaltic provinces of the world to derive the activation energy for basalt weathering.

To assess the effect of temperature on silicate weathering in the Deccan basin studied, plots of Mg (Si and HCO_3^-) data of a few selected rivers vs. $(1/T)$ were analysed. The temperature used is the water temperature measured during sampling (Table 2.1). Small rivers were selected for investigating the dependence of temperature on weathering to avoid effects of mixing. Plots of Mg (Si and HCO_3^-) vs $1/T$ had considerable scatter, though an inverse trend could be discerned. A reason for the scatter could be the narrow range of temperature in the samples, $292^\circ\text{--}299^\circ\text{K}$ (Table 2.1). For this range and E_a of $\sim 40\text{ kJ mol}^{-1}$ for basalts (Dessert et al., 2001), the silicate weathering flux is expected to vary only by factor of ~ 1.5 . This change may be difficult to resolve in system under study considering that other parameters such as vegetation, soil cover and runoff also affect weathering and contribute to scatter in the Arrhenius plot.

3.3.7 CO_2 consumption rates

Consumption of atmospheric CO_2 during weathering is an important issue in river geochemistry studies, as it has direct coupling to climate. The weathering of silicates consumes CO_2 from the atmosphere, release of one equivalent of cations to river water require one mole of CO_2 . On longer time scales, the weathering of silicates acts as net sink of CO_2 . Weathering of carbonates also consumes CO_2 from the atmosphere, but it is returned to the atmosphere within time scales of $\sim 10^5\text{--}10^6$ years. The release of CO_2 occurs during CaCO_3 precipitation in oceans. The calculation of CO_2 consumption rates requires the knowledge of silicate cations and the runoff of the drainage basins.

The CO_2 consumption rates for the west flowing western ghat rivers with higher runoff and for those belonging to the Krishna river system have been estimated separately. For the rivers draining into the Arabian sea, the CO_2 consumption rates cluster around $\sim 1 \times 10^6$ moles $\text{km}^{-2}\text{ y}^{-1}$ (range being 9.7×10^5 to 11.3×10^5 moles $\text{km}^{-2}\text{ y}^{-1}$; Fig. 3.11 and Table 3.8) whereas for selected rivers of the Krishna system (which are undersaturated in calcite and free of anthropogenic inputs) show much wider range, from 0.05 to 0.76×10^6 moles $\text{km}^{-2}\text{ y}^{-1}$. These translate into area weighted average CO_2 consumption rate for the Krishna basin and the coastal Deccan region to

be 0.36×10^6 moles $\text{km}^{-2} \text{y}^{-1}$. The lower and the upper bounds of the range in CO_2 consumption

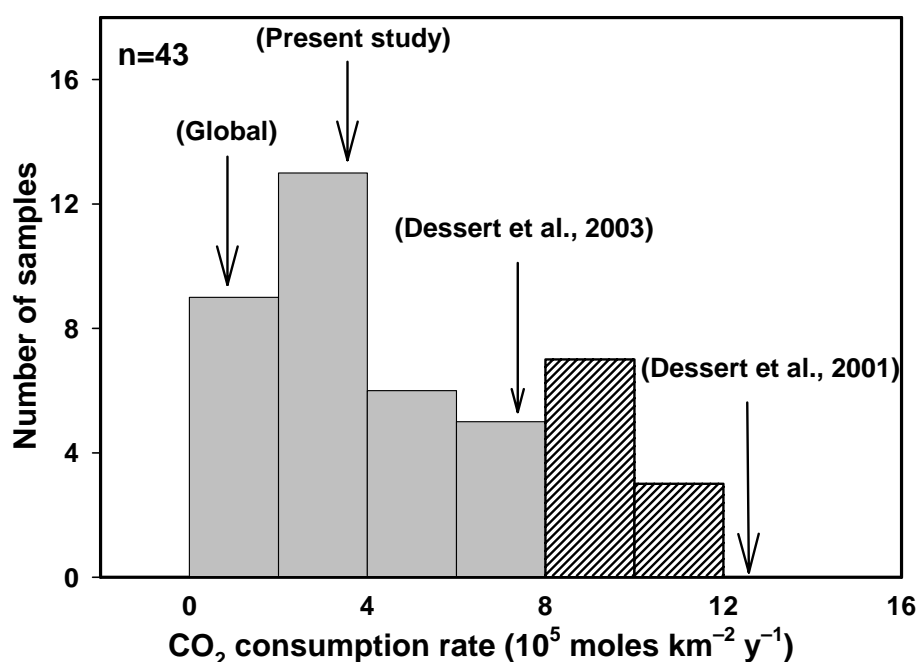


Fig.3.11 CO_2 consumption rates due to silicate weathering in selected basins of the Krishna system and in WFWR (hatched lines). The area-weighted average CO_2 consumption rate for the entire Deccan basin based on these results is $\sim 3.6 \times 10^5$ moles $\text{km}^{-2} \text{y}^{-1}$. The reported CO_2 consumption rates based on results of northern Deccan (Dessert et al., 2001, 2003) and the global CO_2 consumption rate due to silicate weathering (Gaillardet et al., 1999) are also shown for comparison.

rates observed in this study is significantly lower than that reported by Dessert et al. (2001) for the NTW river systems based on HCO_3 data, $0.63\text{--}2.54 \times 10^6$ moles $\text{km}^{-2} \text{y}^{-1}$ (mean: 1.26×10^6 moles $\text{km}^{-2} \text{y}^{-1}$, $n=19$; Fig. 3.11). In a more recent publication (Dessert et al., 2003), this value has been brought down to 0.74×10^6 moles $\text{km}^{-2} \text{y}^{-1}$. Further, many streams analysed in this work have CO_2 consumption rate $< 0.1 \times 10^6$ moles $\text{km}^{-2} \text{y}^{-1}$, factor of ~ 5 or more less than the lowest values reported for the NTW basin. This is an indication that there are areas in the Deccan where silicate weathering is quite low, similar to some of the lowest values reported for Hawaiian basalts (Bluth and Kump; 1994). It may also be possible that silicate weathering and CO_2 consumption rates in parts of the Krishna basin became lower with time due to soil cover and other environmental factors. This difference in the contemporary weathering rates can either be because of natural variations among various regions of Deccan Traps or because of approaches used for estimating CO_2 consumption rates;

sample selection in this work and use of HCO_3 as a “surrogate” for CO_2 consumption (Dessert et al., 2001). Further studies are needed to resolve the cause for this variability. Based on average CO_2 consumption determined in this study and the area of the Deccan Traps ($5 \times 10^5 \text{ km}^2$), the annual CO_2 drawdown for the whole region amounts to 0.18×10^{12} moles (c.f. 0.39×10^{12} moles y^{-1} , Dessert et al., 2003), $\sim 1.5\%$ of the annual global CO_2 consumption (11.7×10^{12} moles y^{-1}) by silicate weathering (Gaillardet et al., 1999a). The proportion of CO_2 consumption by Deccan basalts is a factor of ~ 4 more than its fractional area of continental silicate drainage. This reinforces the earlier findings (Dessert et al., 2001, Amiotte-Suchet et al., 2003) that Deccan Traps (and basalt in general) during their chemical weathering are consuming CO_2 disproportionately more than their aerial coverage.

3.4 SUMMARY AND CONCLUSIONS

A detailed and systematic major ion study of the headwaters of the Krishna and the Bhima and a number of medium and small sized rivers draining the southwest Deccan Traps (India), has been carried out to determine rates of chemical and silicate weathering, and associated CO_2 consumption. The significant differences in characteristics (rainfall, soil cover, altitude) among the basins provide an opportunity to evaluate their role in influencing weathering processes. The important findings borne out of the study are:

- (i) the waters are neutral to mildly alkaline, with TDS in the range of ~ 27 to $640 \text{ mg } \ell^{-1}$, however, nearly half of the samples have TDS $< 100 \text{ mg } \ell^{-1}$. The high TDS are in the Bhima and its tributaries and is a result of abundant Cl , SO_4 and Na concentrations.
- (ii) $(\text{Ca}+\text{Mg})$ and HCO_3 are the most abundant cations and anion in majority of the rivers. Fourteen (out of sixty three) samples are supersaturated with respect to calcite, many of these samples also have high Cl , SO_4 and TDS. Rivers with high Cl also have high SO_4 ; in general, there is a strong correlation between them and also with Na. If these observations are interpreted in terms of supply from saline soils and anthropogenic sources, their average contribution to the tributaries of the Krishna and the Bhima and the Krishna and Bhima mainstream would be $\sim 70\%$ to and $\sim 90\%$ of Cl , and $\sim 40\%$ to $\sim 60\%$ of Na respectively.
- (iii) chemical weathering rates (CWR) of rivers (with $\text{CSI} < 0$, $\text{Cl} < 300 \mu\text{M}$ and $\text{SO}_4 < 100 \mu\text{M}$) range from ~ 3 to $\sim 60 \text{ t km}^{-2} \text{ y}^{-1}$. Silicate weathering rates (SWR) in these rivers, calculated using Mg as an index varies from ~ 3 to $\sim 60 \text{ t km}^{-2} \text{ y}^{-1}$ making up

~95% of CWR. This suggests that major ion abundance in these “selected” rivers is almost entirely of silicate origin. The Ca^*/Mg^* and Na^*/Mg^* in these rivers closely match their ratios in basalts suggesting their near stoichiometric release from basalts to rivers. Estimates of contribution of Ca from carbonates in basalts and in the basin show that it can be ~13% on average; though in some rivers it can be up to ~30% of the Ca budget. The CWR and SWR of west flowing western ghats rivers are ~4 times those of the east flowing rivers. This difference is in proportion to their runoff and attests to the major role of runoff in determining chemical and silicate weathering rates.

(iv) the area weighted average CO_2 consumption rate from silicate weathering in the Deccan Traps is 3.6×10^5 moles $\text{km}^{-2} \text{y}^{-1}$. The CO_2 drawdown by Deccan basalts is estimated to be 1.8×10^{11} moles y^{-1} . This is ~1.5% of CO_2 consumed by continental silicate weathering, ~4 times higher than its fractional area of continental silicate exposures and reaffirms the earlier observation that basalts weather more rapidly and thus contribute to higher CO_2 drawdown.

(v) the CWR, SWR and CO_2 consumption of rivers analysed in this study from the southwest Deccan Traps are 2–4 times lower than those reported for the Narmada–Tapti–Wainganga (NTW) systems from the more northern region of Deccan. Spatial variations in weathering rates, calculation of CWR and SWR in this study based on “selected” rivers and possible supply of major ions to NTW system from sources other than basalts, all are potential causes for the observed differences. The SWR for the Deccan Traps derived in this study is comparable to that reported for the Ganga–Yamuna headwaters in the Himalaya. This suggests that weathering of granites/gneisses can be similar to those of basalts under “favourable” conditions of higher physical weathering and higher runoff.

Chapter Four
Carbon isotopes of DIC

4.1 INTRODUCTION

Chemical weathering of rocks on continents affects the global carbon cycle on long time scales. Chemical weathering of silicate and carbonate rocks sequester atmospheric CO₂ and converts it to dissolved inorganic carbon (DIC) that is transported mainly as bicarbonate to oceans via rivers (Garrels and Mckenzie, 1971; Meybeck, 1987; Berner and Berner, 1996). Weathering of silicates involves the conversion of one mole of CO₂ to one mole of HCO₃⁻ whereas in carbonate weathering, sequestration of one mole of CO₂ produces two moles of alkalinity.



However, on geologic time scales, weathering of silicates (and not carbonates) acts as net sink for atmospheric CO₂. This is because during weathering of a mole of calcium carbonate mineral one mole of CO₂ is consumed (Equation 1.2), and during the precipitation of CaCO₃ in oceans, the same amount of CO₂ is released to the atmosphere. In comparison, silicate weathering involves consumption of two moles of CO₂ (Equation 4.1) and precipitation of CaCO₃ returns only one mole (Equation 1.3), thereby, making this process a net sink for atmospheric CO₂. Thus, the study of this part of carbon cycle helps geochemists to understand better, the coupling between chemical weathering— atmospheric CO₂ concentration—global temperature—climate change.

The CO₂ consumption during chemical weathering occurs through two pathways. One is the conversion of atmospheric CO₂ to soil CO₂. This is accomplished by fixation of atmospheric CO₂ by plants as organic matter and its subsequent release as soil CO₂ by root respiration. The soil CO₂ dissolves in soil/groundwater to yield carbonic acid, which provides proton for chemical weathering. The second sequestration route of atmospheric CO₂ is through its dissolution in rain and surface waters to form carbonic acid and its subsequent reaction with rock forming minerals to generate HCO₃⁻. This reaction, dominates in “bare” mountains (i.e. without or sparse vegetation) with steep slopes as found in some parts of the Indus basin (Karim and Veizer, 2000). However, on a global scale, the first process is significantly more effective for atmospheric CO₂ sequestration as pCO₂ of soil gas can be one to two orders of magnitude higher than pCO₂ of atmosphere (Dever et al., 1983; Salomons and Mook, 1986). These chemical weathering reactions supply DIC to rivers through the dissolution of carbonates, soil

CO₂ and atmospheric CO₂. These sources and their mixing proportions govern the carbon isotopic composition ($\delta^{13}\text{C}$) of DIC in rivers. The $\delta^{13}\text{C}$ of these “carbon reservoirs” are distinctly different and therefore hold potential to trace the sources of carbon in rivers and quantify their contributions. The ranges of $\delta^{13}\text{C}$ values of these reservoirs are: carbonates $0\pm 2\%$, soil CO₂ ($-26\pm 3\%$ or $-13\pm 3\%$, depending on plant type as discussed later) and atmospheric CO₂ (-8.1%) respectively. However, ‘unambiguous’ interpretation of the $\delta^{13}\text{C}$ data of riverine DIC may be difficult in some cases due to multiple end member mixing with sparse knowledge of end member values and processes such as riverine respiration, exchange of CO₂ with atmosphere in non-equilibrium environment and precipitation of calcium carbonate from rivers, all of which can modify the DIC concentration and its $\delta^{13}\text{C}$ (Longinelli and Edmond, 1983; Yang et al., 1996; Amiotte-Suchet et al., 1999).

Determination of CO₂ consumption by silicate weathering is an important goal of geochemical studies, as this is believed to influence significantly the long-term atmospheric CO₂ balance (Berner and Berner, 1996). Silicate weathering rates of river basins are generally derived using major ion abundances in rivers or based on their Sr isotope composition. These approaches, however, have met with only mixed success (Singh et al., 1998; Galy and France-Lanord, 1999; Oliver et al., 2003). In this context, studies of $\delta^{13}\text{C}$ of DIC to trace the sources of carbon in watersheds draining mixed lithologies and relate them to weathering process seem to hold potential (Kendal et al., 1992, 1995; Telmer and Veizer, 1999; Karim and Veizer, 2000).

In this chapter the use of $\delta^{13}\text{C}\text{-HCO}_3$ and $\delta^{13}\text{C}\text{-Si/HCO}_3$ as proxies to determine the contributions from silicate and carbonate weathering to DIC in rivers draining the Deccan Traps are discussed. Major ion chemistry of these rivers (Das et al., 2005; see Chapter 3) and their ratios indicate that many of these river basins are dominated by silicate weathering and that on average up to ~15% of Ca in these rivers can be from non-silicate sources. The additional sources of Ca can be carbonates in basalts and sediments, and calcareous tufas, which are all dispersed in some of these river basins (Jeffery et al., 1988; Pawar et al., 1988). The major ion data also show that, in a few rivers contribution from alkaline/ saline soils and anthropogenic sources could be important (Bhargava and Bhattacharjee, 1982; Pawar and Shaikh, 1995). Knowledge of the proportion of carbonate weathering contribution to Ca and

alkalinity is essential to use HCO_3 as a surrogate of silicate weathering and to calculate CO_2 consumption rates (Dessert et al., 2001).

The carbon isotope study in this work is based on twenty rivers that include the Krishna, two of its large tributaries, the Bhima and the Ghod, and a number of smaller streams or sub-tributaries of the Krishna that flow east of the western ghats (Koyna, Varna, Bhogwati, Dudhganga, Vedganga, Hiranyakeshi, Tamrapani and Ghataprabha). In addition, samples of four rivers draining west of the western ghats (Sukh, Kajli, Shastri and Vashishthi) into the Arabian sea were also analysed (Fig. 4.1). In addition to water samples, two samples each of carbonates contained in basalts and sediments were also analysed for their $\delta^{13}\text{C}$.

4.2 RESULTS

The $\delta^{13}\text{C}$ of the DIC, concentrations of Si, HCO_3 in rivers, and the calcite saturation index are given in Table 4.1. Also included in the Table are $\delta^{13}\text{C}$ of carbonates in bed sediments and basalts. The $\delta^{13}\text{C}$ of the water samples show a wide range, from -8.5‰ to -20.7‰ , with majority falling within -15‰ to -20‰ (Table 4.1 and Fig. 4.2). The samples most depleted in ^{13}C values ($-18.7\pm 2\text{‰}$) belong to the four west flowing western ghat rivers (Sukh, Kajli, Shashtri and Vashishti) and some of the smaller streams of the east flowing western ghat rivers (Ghataprabha and its tributaries, Koyna, Vedganga and the Bhogwati). All these rivers are quite undersaturated in calcite (Table 4.1). The large rivers, the Bhima (BHM-5) and the Ghod (GHOD-1) are enriched in ^{13}C values, -8.5‰ and -13.4‰ , respectively. The Ghod sample is nearly saturated in calcite whereas the Bhima is supersaturated. The mainstream samples of the river Krishna have $\delta^{13}\text{C}$ in the range of -12.5‰ to -16.1‰ with an average of -13.9‰ (Table 4.1). The sample from the Bhima river, BHM-5, has high concentrations of Cl (2183 μM) and SO_4 (1054 μM). These high concentrations have been interpreted (Das et. al, 2005) in terms of supply from saline soils and anthropogenic sources. These saline soils, as mentioned earlier, are mainly Na-salts of Cl and SO_4 with minor amounts of carbonates/bicarbonates (Bhargava and Bhattacharjee, 1982). Among the Krishna samples, KRS-6 is collected close to Wai town; it has high concentrations of HCO_3 (3995 μM), Ca (1162 μM) and NO_3 (92 μM), probably indicating anthropogenic supply and/or from carbonates (Das et al., 2005). Carbonates from basalts and bed sediments of the Bhima and Krishna have

average $\delta^{13}\text{C}$ values of $\sim -14\text{‰}$ and -4.5‰ respectively (Table 4.1). The sediments analysed contain ~ 3 wt% of CaCO_3 (Chapter five).

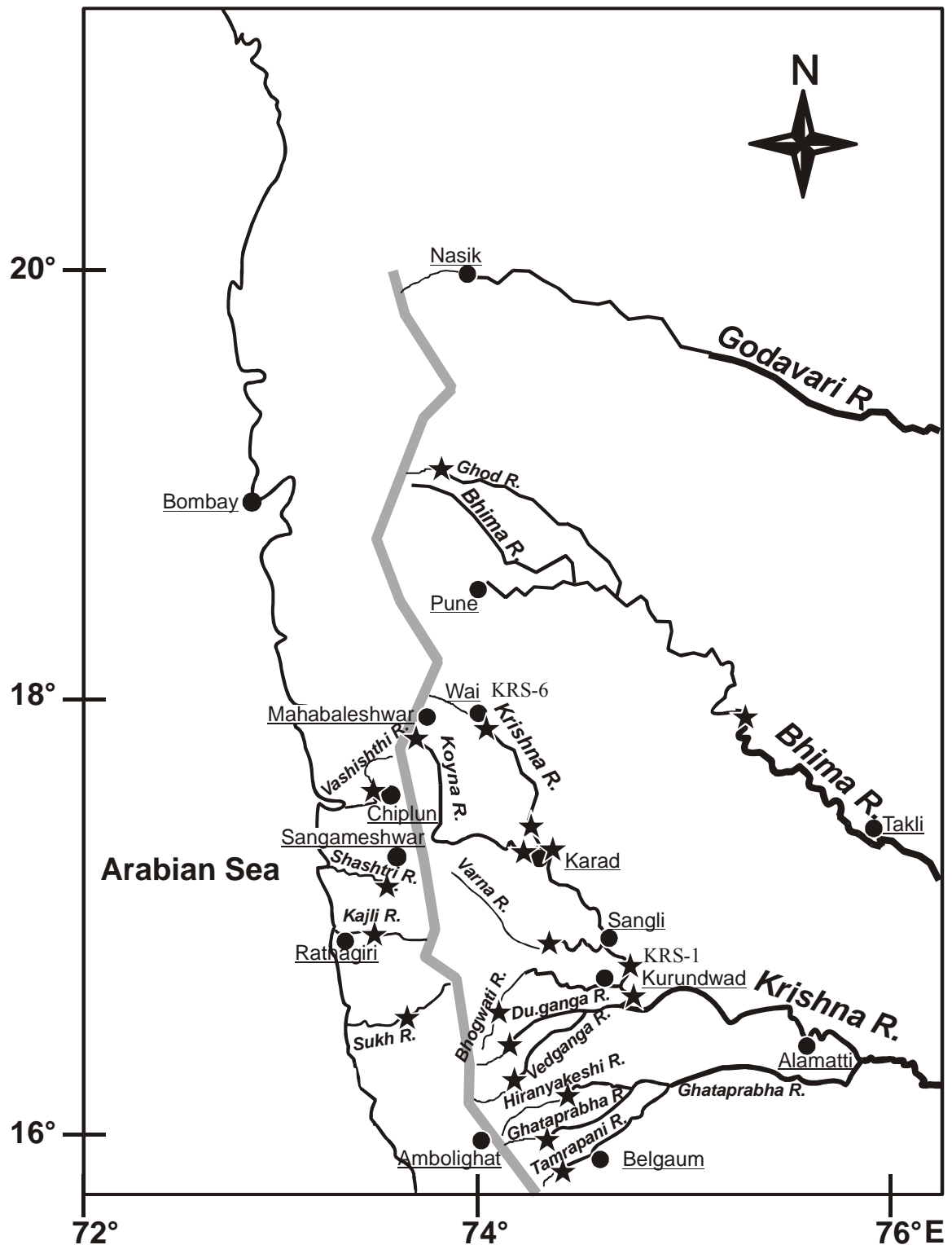


Figure 4.1. Sampling locations (★) for river water analysed for $\delta^{13}\text{C}$. Sampling was done during August, 2001. Some of the major cities are also shown (●) Western ghat is shown by a band almost parallel to west coast.

Table 4.1. $\delta^{13}\text{C}$, Si, HCO_3 and calcite saturation index (CSI) of the Deccan Trap rivers, and $\delta^{13}\text{C}$ of carbonates in bed sediments and basalts.

Sample Code	River name	Si (μM)	HCO_3 (μM)	$\delta^{13}\text{C}$ (‰)	CSI
<u>Krishna mainstream</u>					
KRS-1	Krishna	313	1418	-13.4	-0.55
KRS-2	”	228	776	-15.0	-1.17
KRS-3	”	274	802	-16.1	-1.09
KRS-4	”	341	1672	-12.6	-0.08
KRS-6	”	639	3995	-12.5	0.75
BHM-5	Bhima	323	2934	-8.5	0.78
GHOD-1	Ghod	390	1644	-13.4	-0.06
<u>Western Ghat rivers</u>					
<u>Tributaries of Krishna (East flowing rivers)</u>					
VDG-1	Vedganga	241	530	-18.3	-0.91
TPN-1	Tamrapani	117	234	-19.6	-2.56
GTP-1	Ghataprabha	91	170	-20.7	-2.15
KYN-2	Koyna	165	301	-17.9	-2.22
HRN-1	Hiranyakeshi	129	337	-20.6	-2.22
KYN-1	Koyna	272	713	-16.6	-1.39
BGW-1	Bhogwati	176	395	-18.5	-2.13
VRN-1	Varna	313	1045	-15.0	-0.91
DDG-1	Dudhganga	344	1226	-15.1	-0.95
<u>West flowing rivers</u>					
VAT-1	Vashishthi	364	716	-17.5	-1.68
SHT-1	Shashtri	344	623	-19.1	-1.70
KJL-1	Kajli	396	755	-18.0	-1.58
SUKH-1	Sukh	341	656	-18.1	-1.52
<u>$\delta^{13}\text{C}$ of carbonates</u>					
Sample	Location	$\delta^{13}\text{C}$ (‰)			
Sediment-1	BHM-5	-3.8			
Sediment-2	KRS-4	-5.1			
Basalt-1	Mahabaleshwar	-13.9			
Basalt-2	”	-14.0			

4.3 DISCUSSION

4.3.1 Sources of DIC and their $\delta^{13}\text{C}$

The DIC in rivers comprises of three principal “carbonate” species: H_2CO_3 , HCO_3 and CO_3 . The relative abundances of these species are a function of pH and can

be expressed by the equilibrium reactions 4.1–4.4 (Drever, 1997). The fraction of these species as a function of pH is shown in Fig. 4.3.

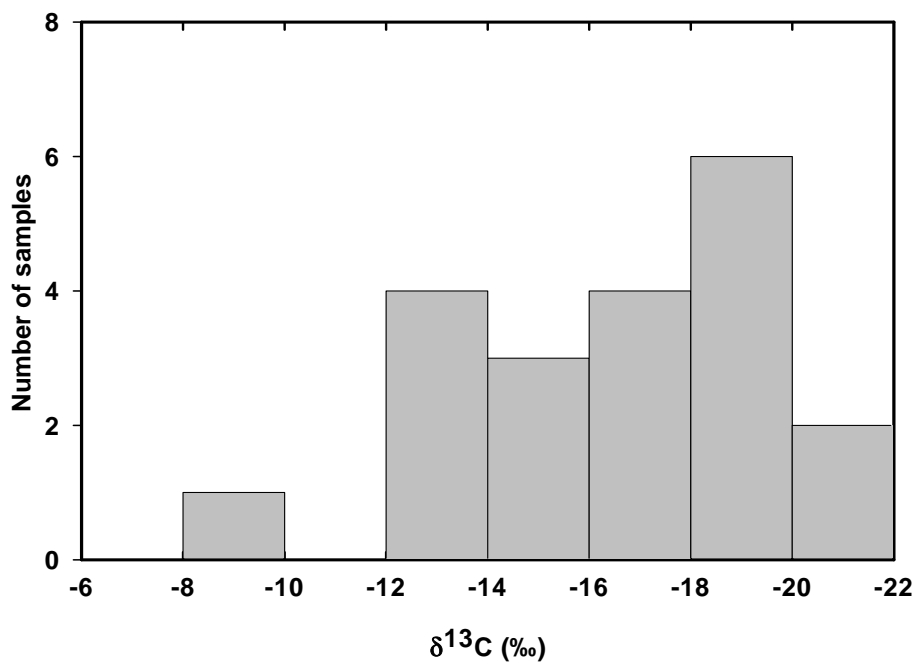


Figure 4.2. Frequency distribution of $\delta^{13}\text{C}$ values of DIC. Half the number of samples analysed have $\delta^{13}\text{C}$ in the range of $-19 \pm 2\%$, indicating exclusive silicate weathering.

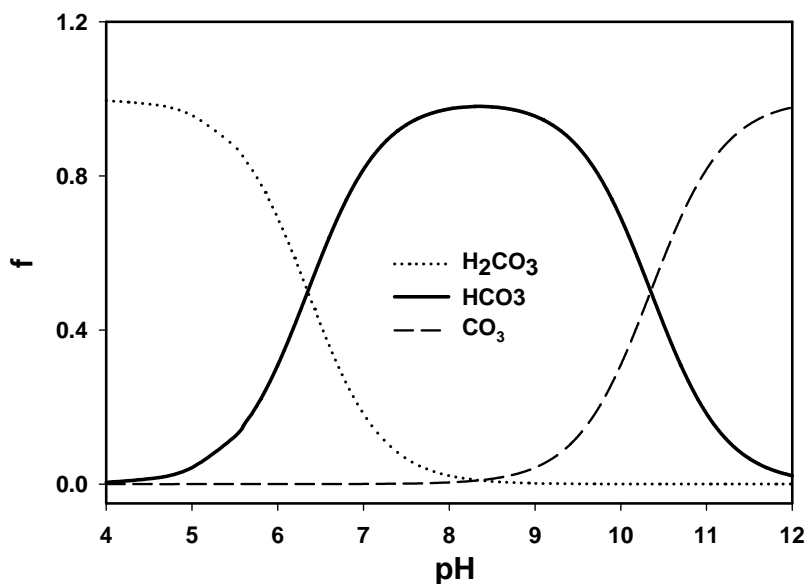
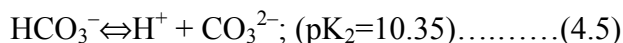
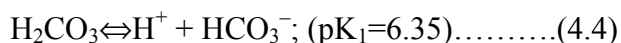
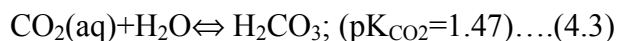


Figure 4.3. Fraction (f) of carbon species (H_2CO_3 , HCO_3^- and CO_3^{2-}) as a function of pH. It is seen that in the pH range of 7.5–9.5 (typical of natural waters) HCO_3^- is the dominant species.

The equilibrium constants for the following reactions are temperature dependent; the pK values reported in brackets are at 25 °C.





Most of the natural surface waters have pH typically in the range of 7–8, in which the major dissolved species is HCO_3^- (Fig. 4.3). For example, at pH 7 and 25°C, the unionized H_2CO_3 can be calculated to be ~18% of DIC, which decrease to ~2.2% at pH 8. DIC in rivers, as mentioned earlier, is mainly derived from two sources; soil CO_2 and dissolution of carbonate minerals. The alkalinity contribution from chemical reactions of atmospheric CO_2 with silicates and carbonates is not very significant for most of the rivers and it generally accounts for <10% of the total alkalinity (see later discussion). The various possible pathways of alkalinity production in rivers and the $\delta^{13}\text{C}$ values that accrue are discussed below.

4.3.1.1 Dissolution of atmospheric CO_2 :

The DIC concentration (\approx activity) in rain depends on atmospheric pCO_2 , surface air temperature and the rainwater pH. In the pH range, 4–6, that are typical of rainwater, the major species is un-dissociated H_2CO_3 (Fig. 4.3). The DIC concentration in rainwater resulting from solution of atmospheric CO_2 is

$$a(\text{H}_2\text{CO}_3) = K(\text{CO}_2) \cdot \text{pCO}_2 \dots (4.6)$$

where $a(\text{H}_2\text{CO}_3)$, $K(\text{CO}_2)$ and pCO_2 , respectively, are activity of carbonic acid, equilibrium constant for dissolution of CO_2 gas and partial pressure of CO_2 . Assuming surface air temperature of 25°C, average pH of 5.5 for rainwater, the amount of DIC (mainly as H_2CO_3) produced in rainwater is calculated to be ~10 $\mu\text{moles } \ell^{-1}$.

The $\delta^{13}\text{C}$ of atmospheric CO_2 show measurable temporal variations. $\delta^{13}\text{C}$ of atmospheric CO_2 is getting lighter from -7.8‰ (in 1990) to a present value of -8.1‰ based on continuous measurements from a number of global stations (<http://www.cmdl.noaa.gov/ccgg/iadv/>). The depletion in ^{13}C is due to the addition of CO_2 lighter in $\delta^{13}\text{C}$ from fossil fuel burning to the atmosphere. Using the present day $\delta^{13}\text{C}$ value of -8.1‰ for atmospheric CO_2 , and an equilibrium fractionation of -1.2‰ during conversion of CO_2 to H_2CO_3 (or $\text{CO}_2(\text{aq})$), the $\delta^{13}\text{C}$ of rainwater DIC is

expected to be -9.3‰ (since at pH range of rainwater, $\text{DIC} \approx \text{H}_2\text{CO}_3$). The fractionation associated among different “carbonate” species is given in Table 4.2. In the present study, the river DIC concentrations vary between $170 \mu\text{M}$ to $3995 \mu\text{M}$, hence, rainwater DIC concentration resulting from atmospheric CO_2 solution is typically factors of ~ 17 to ~ 400 lower than river water DIC. Therefore, in the present case, the atmospheric contribution (due to solution of atmospheric CO_2) to riverine DIC $\delta^{13}\text{C}$ can be neglected.

Table 4.2. Fractionation* during conversion of CO_2 to carbonate species.

Carbonate pairs	Fractionation (‰)
CO_2 (g)– CO_2 (aq)	-1.2
CO_2 (g)– HCO_3 (aq)	$+7.9$
CO_2 (g)– CaCO_3 (solid)	$+10.0$

*(Faure, 1986)

4.3.1.2 Weathering of silicates: Weathering of silicates involves the conversion of one mole CO_2 (soil or atmospheric) to DIC (equation 4.1). It is estimated that on a global scale about two-thirds of the CO_2 consumed by silicate weathering is of soil (i.e. biogenic) origin (Meybeck, 1987; Berner and Berner, 1996). In case of barren hills, with steep slopes and poor soil cover, (such as Indus river system mentioned above) weathering with atmospheric CO_2 can be more dominant (Karim and Veizer, 2000). In these cases, the $\delta^{13}\text{C}$ of DIC of rivers is expected to have a value of -0.2‰ based on $\delta^{13}\text{C}$ of -8.1‰ for atmospheric CO_2 and fractionation of $+7.9\text{‰}$ (at 25°C ; Table 4.3) for conversion of CO_2 (gas) to river HCO_3 (Table 4.2).

In regions with well-developed soil horizons with abundant vegetation, such as those found in the western ghats in the present study, biogenic (soil) CO_2 is the dominant weathering agent and, therefore, contributes to the primary source of DIC in rivers. The $\delta^{13}\text{C}$ of biogenic CO_2 depends on the type of vegetation, i.e., C_3 or C_4 . Vegetation that follows C_3 type photosynthetic pathway is common in temperate land and in high latitudes. These plants have $\delta^{13}\text{C}$ values ranging from -24‰ to -30‰ (average: -27‰ , Karim and Veizer, 2000). Faure (1986) reports an average value of -28‰ for C_3 plants with a range of -24‰ to -32‰ . At present, there are no reports on the $\delta^{13}\text{C}$ of vegetation or soil organic matter in the study area of the Deccan Trap

region. However, Sukumar et al. (1993) reported $\delta^{13}\text{C}$ of vegetation in the Nilgiri hills in the western ghats, slightly south of the present area of study. The average $\delta^{13}\text{C}$ values for C_3 grasses and herbs are $-27.8 \pm 2.3\text{‰}$ ($n=7$) and $-28.7 \pm 1.3\text{‰}$ ($n=8$) respectively. Another study (Rajagopalan et al., 1999) from the same region reports values that center around -27‰ and -13‰ for C_3 and C_4 plants respectively. The oxidation of these plant-remains liberate CO_2 with $\delta^{13}\text{C}$ same as that of parent organic matter.

Therefore, bicarbonate derived from dissolution soil CO_2 from C_3 vegetation during silicate weathering will have $\delta^{13}\text{C}$ values ranging from -16.1‰ to -22.1‰ with an average of -19.1‰ . Similarly, weathering of silicates with CO_2 derived from C_4 type of vegetation would result in DIC with $\delta^{13}\text{C}$ in the range of -2.1‰ to -8.1‰ with average $\delta^{13}\text{C}$ of -5.1‰ (Table 4.3).

The plant species that are found in the Deccan Trap region (listed in chapter 2) are mostly C_3 type, however, species that follow C_4 type of pathway such as bamboo and sugarcane are also present in some regions. Their total contribution to the biota (and hence soil CO_2), however, is small and is neglected from considerations. The assumption is validated from observations and interpretations as discussed later.

In addition, another source of carbon isotope fractionation is during the escape of soil CO_2 to atmosphere (Cerling, 1991). This results in a “fractionation loss of 4.4‰”. This fractionation is not considered in this work as the samples were collected during monsoon when the pore spaces are filled with water, and hence, preferential escape of $^{12}\text{CO}_2$ is expected to be low.

Table 4.3 Expected $\delta^{13}\text{C}$ of DIC in rivers for weathering with different CO_2 sources.

CO ₂ source	$\delta^{13}\text{C}^{\#}$ (‰) of DIC generated from		
	SW	CW I*	CW II*
Atmosphere ($\delta^{13}\text{C} = -8.1\text{‰}$)	-0.2	-0.1	-2.6
C_3 type ($\delta^{13}\text{C} = -27\text{‰}$)	-19.1	-9.6	-12.1
C_4 type ($\delta^{13}\text{C} = -13\text{‰}$)	-5.1	-2.6	-5.1
1:1 C_3 and C_4 $\delta^{13}\text{C} = -20\text{‰}$	-12.1	-6.1	-8.6

SW and CW silicate and carbonate weathering. I*, II* based on carbonate $\delta^{13}\text{C}$ of 0‰ and -5‰.

4.3.1.3 Carbonate weathering: Weathering of one mole of carbonate minerals with CO_2 produces two moles of DIC, one from atmospheric (soil) CO_2 and the other from carbonate minerals (eqn. 1.2). The $\delta^{13}\text{C}$ of DIC formed from carbonate weathering, thus, would depend on the $\delta^{13}\text{C}$ of carbonate mineral, CO_2 (soil or atmospheric) and the isotope fractionation involved in the formation of DIC. Dissolution of carbonate minerals to form DIC involves no carbon isotope fractionation.

Continental crustal carbonate reservoirs are usually derived from marine system and, therefore, have $\delta^{13}\text{C}$ close to zero (Keith and Weber, 1964). Weathering of such carbonate minerals with atmospheric CO_2 ($\delta^{13}\text{C} -8.1\text{‰}$) would produce DIC with $\delta^{13}\text{C} -0.1\text{‰}$. Similarly, weathering with CO_2 derived from C_3 plants (average $\delta^{13}\text{C} -27\text{‰}$) would result in $\delta^{13}\text{C}$ of DIC of about -9.6‰ . If, however, the carbonate weathering occurs with C_4 plant CO_2 (average $\delta^{13}\text{C} -13\text{‰}$), the $\delta^{13}\text{C}$ of DIC in rivers is expected to be -2.6‰ . The source of carbonates in the Krishna basin is uncertain. There are reports of carbonates in the form of calcareous tufas in the upland of Bhima basin (Pawar et al., 1988), the $\delta^{13}\text{C}$ of these are not known at present. The sediments of many of these rivers contain appreciable amount of carbonates and the $\delta^{13}\text{C}$ of two samples measured in this study is $\sim -4.5\text{‰}$ (Table 4.1). Karim and Veizer (2000) have used $\delta^{13}\text{C}$ values of -5 to -4‰ for soil carbonates based on values of siwalik soil carbonates ($+3\text{‰}$ to -13‰) and detrital carbonates (-2.5‰ to -6‰) (Quade and Cerling, 1995).

The expected $\delta^{13}\text{C}$ in DIC of rivers for carbonate and silicate weathering with atmospheric and soil CO_2 are given in Table 4.3. The range, as seen in Table 4.3 is quite wide.

4.3.2 $\delta^{13}\text{C}$ in DIC of Deccan rivers: silicate/carbonate weathering

From the preceding discussions, it is evident that $\delta^{13}\text{C}$ of DIC would depend on the source of CO_2 and the type of lithology being weathered (Table 4.3). Therefore, $\delta^{13}\text{C}$ of DIC has the potential to provide information on the role of carbonates and silicates in contributing to DIC budget of rivers (Kendal et al., 1995). As mentioned above, if silicate weathering by C_3 -soil CO_2 is the primary source of DIC to rivers, then $\delta^{13}\text{C}$ of DIC is expected to be in the range of -16.1‰ to -22.1‰ . More than half of the samples analysed in this study have $\delta^{13}\text{C}$ in this range (Table

4.1), suggesting that most of DIC in these samples can be from silicate weathering with CO_2 from C_3 vegetation. The remaining rivers have $\delta^{13}\text{C}$ heavier than -16‰ (Table 4.1) indicating that DIC in these rivers is derived from multiple sources.

Fig.4.4 presents the variation of $\delta^{13}\text{C}$ in the rivers as a function of inverse HCO_3^- concentration. The results show two trends, a linear decrease in $\delta^{13}\text{C}$ for samples with $\text{HCO}_3^- > 500 \mu\text{M}$ (Fig. 4.4). For samples with HCO_3^- in the range of $\sim 150\text{--}500 \mu\text{M}$ (shown in the box), $\delta^{13}\text{C}$ does not show any systematic trend, but scatter between $\sim -18\text{‰}$ to -20.7‰ . These results in Fig. 4.4 can be interpreted in terms of mixing of three end members, with approximate HCO_3^- and $\delta^{13}\text{C}$ values of: ($\sim 2000 \mu\text{M}$ and -10‰), ($\sim 500 \mu\text{M}$ and -20‰) and ($\sim 150 \mu\text{M}$ and -20‰). Among these, the highly depleted $\delta^{13}\text{C}$ end member ($\sim -20\text{‰}$) is a result of DIC generated from silicate weathering with CO_2 from C_3 vegetation. The observed dispersion around $\delta^{13}\text{C}$ of -19‰ in samples in the box, (Fig. 4.4) most likely results from variability in $\delta^{13}\text{C}$ generated from C_3 plants. The variation in HCO_3^- in these five samples can be ascribed to differences in intensity of chemical weathering, with more HCO_3^- suggesting enhanced silicate weathering. This is attested by the observation

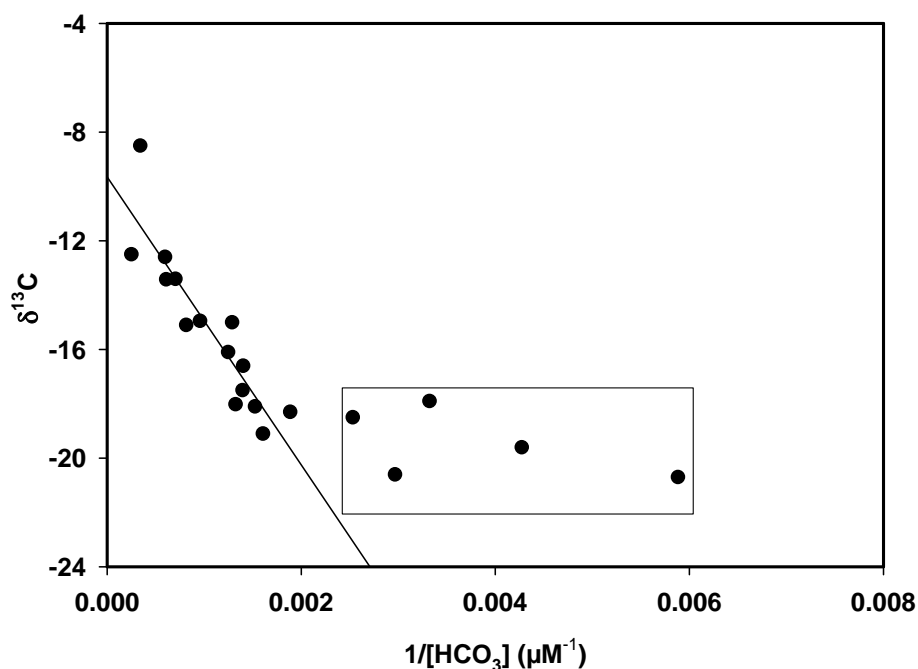


Figure 4.4. Plot of $\delta^{13}\text{C}$ of DIC vs. inverse of HCO_3^- concentration. The data show a strong co-variation between the two in the $\delta^{13}\text{C}$ range of $\sim -8\text{‰}$ and $\sim -18\text{‰}$. The line is the best-fit excluding those in the box. The data points in the box ($\sim -18\text{‰}$ to -20‰) indicate large variations in HCO_3^- corresponding to small $\delta^{13}\text{C}$ change. This could be due intensity of weathering and range in $\delta^{13}\text{C}$ of soil CO_2 .

that HCO_3^- in these five samples shows a strong correlation with Mg ($r^2=0.98$; Fig. 4.5), Mg being used as a proxy for silicate weathering in basalts (Das et al., 2005; Chapter three). The samples with $\delta^{13}\text{C} -18.7\pm 2\text{‰}$ are from the four west flowing rivers (Sukh, Kajli, Shashtri and Vashishthi, Table 4.1) and the smaller east flowing tributaries and sub-tributaries of the Krishna (Table 4.1). Therefore, in all these rivers, basalt weathering accounts for most of the DIC and cation budget. This is consistent with the major ion data that most of the Ca in these rivers, after rainwater correction, is of silicate origin (Das et al., 2005). Only two of the sub-tributaries, the Varna and the Dudhganga, are marginally enriched in ^{13}C ($\delta^{13}\text{C} \sim 15.1\text{‰}$; Table 4.1), compared to that expected from silicate weathering. In contrast, the samples KRS-1, 2, 4 and 6, GHOD-1 and BHM-5 have significantly higher $\delta^{13}\text{C}$ values (-8‰ to -15‰ ; Table 4.1). This enriched ^{13}C values can arise if part of DIC is from (i) carbonate weathering, (ii) silicate weathering with CO_2 from C_4 vegetation and (iii) weathering with atmospheric CO_2 and gaseous exchange with atmospheric CO_2 ($\delta^{13}\text{C}$ of -8.1‰). In addition, the supply of HCO_3^- from alkaline/ saline soils and anthropogenic sources could play some role in a few cases, such as BHM-5 and KRS-6.

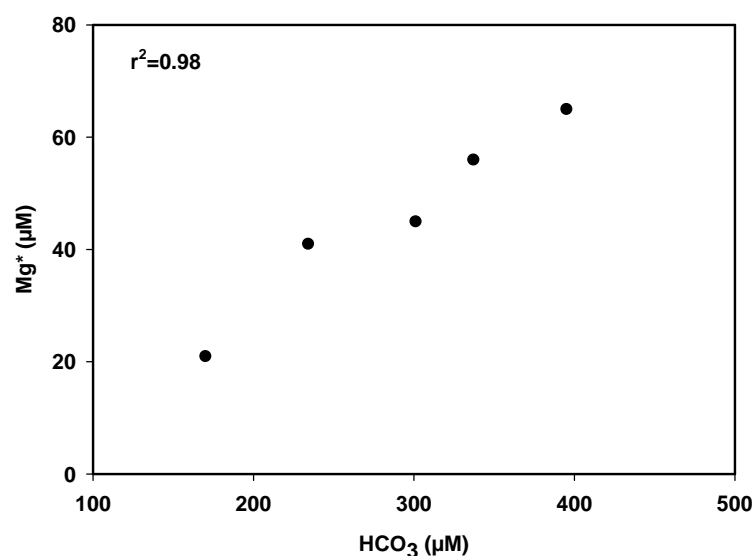


Figure 4.5. *Mg* versus HCO_3^- for the samples in box of Fig. 4.4. The strong linear trend indicates that variation in HCO_3^- is largely accounted for by the intensity of silicate weathering (Mg* is used as an index of silicate weathering).*

To obtain a better insight into the role of these alternatives in contributing to DIC, the dependence of $\delta^{13}\text{C}$ on Si/HCO_3^- was analysed (Fig. 4.6). The weathering of basalts would supply both Si and HCO_3^- to solution with a Si/HCO_3^- ratio that would

depend on the silicate minerals undergoing weathering, and on the reaction pathway. In contrast, the weathering of carbonates would supply HCO_3^- almost without Si, thus accounting for low Si/ HCO_3^- in waters draining them. Therefore, the Si/ HCO_3^- ratios in rivers should be an index to estimate relative contributions of basalts (silicates) and carbonates to their HCO_3^- budget. Further, the $\delta^{13}\text{C}$ of DIC generated from these two sources would also be quite different. This would make the $\delta^{13}\text{C}$ –Si/ HCO_3^- covariation a very useful proxy to determine the magnitude of contribution from basalts and carbonate weathering to DIC budget of rivers draining them. The application of this couple, however, can be limited if the DIC and $\delta^{13}\text{C}$ budgets of the rivers are influenced by other processes such as calcite precipitation and supply of alkalinity through alkaline soils and anthropogenic inputs.

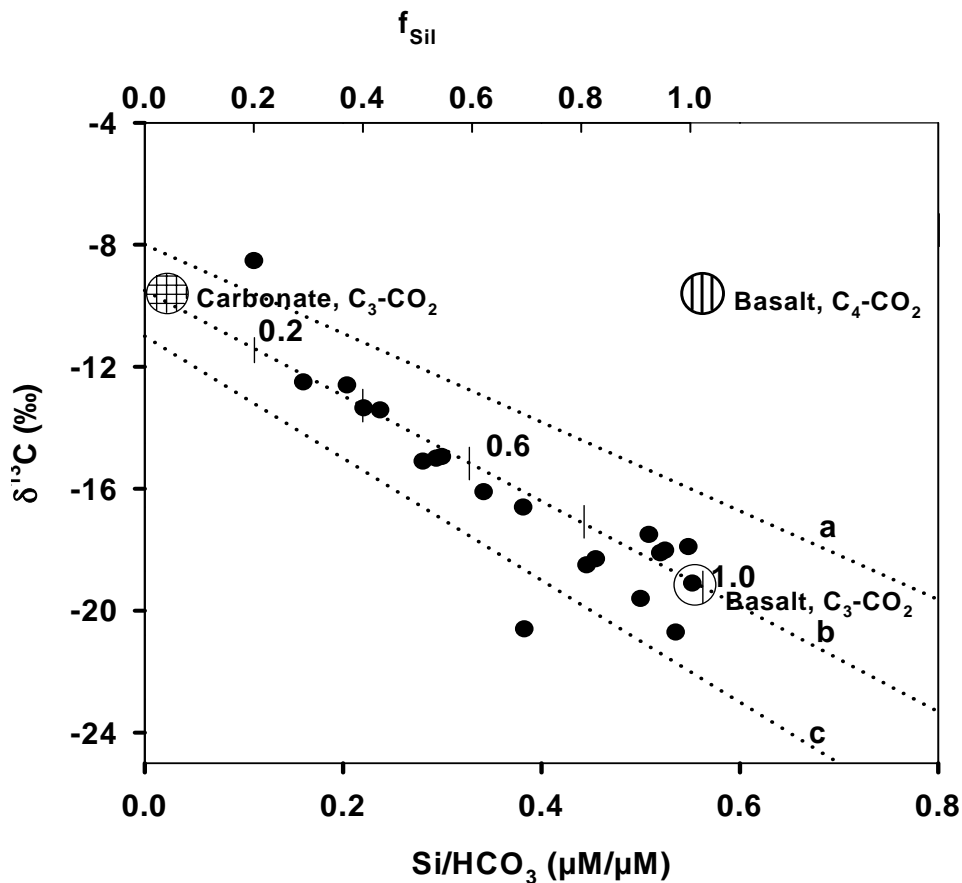
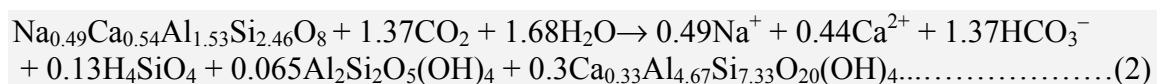
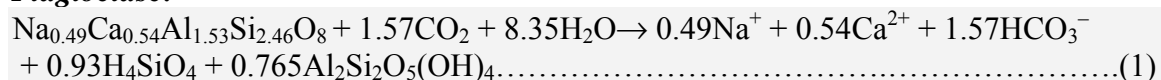


Figure 4.6. Plot of $\delta^{13}\text{C}$ vs. Si/ HCO_3^- ratio in samples. The data show a strong linear trend ($r^2=0.80$) consistent with two-end member mixing. The dashed lines, a, b and c are calculated mixing lines (equation 4.9) for $\delta^{13}\text{C}$ of -24‰ , -27‰ and -30‰ (for soil CO_2) respectively. Most of the data points fall close to the line of $\delta^{13}\text{C}$ of -27‰ . The $\delta^{13}\text{C}$ and Si/ HCO_3^- values for the three end members, basalt weathering with CO_2 from C_3 or C_4 vegetation and carbonate weathering with C_3 CO_2 are also given. The f_{sil} values from 0.2 to 1.0 are marked on line b.

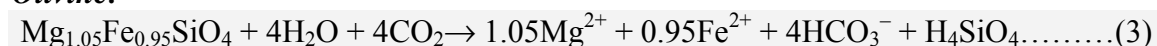
In the samples analysed, the $\delta^{13}\text{C}\text{-Si/HCO}_3$ scatter diagram (Fig. 4.6) shows a strong linear trend ($r^2 = 0.80$) consistent with mixing of two end members. Typical weathering reactions involving silicate minerals of the Deccan Traps, and the molar ratio of various ions released to waters are discussed in Chapter 3 (see Table 3.5). Table 4.4 summarizes the weathering of plagioclase, olivine and pyroxenes group of minerals. The reactions in Table 4.4 have to be multiplied by 0.3, 0.02, and 0.3 respectively to obtain Si and HCO_3 released to rivers in proportion to their molar abundances in basalts; these factors arise from normalisation of mineral formulae. This exercise would yield average Si/HCO_3 of ~ 0.52 in waters. The calculated Si/HCO_3 of ~ 0.52 is quite consistent with the highest ratios measured in this study for many of the east and west flowing western ghat rivers which form a cluster of points around this value (0.5 ± 0.05). These samples also have highly depleted ^{13}C values (Table 4.1, Fig. 4.6).

Table 4.4. Weathering reactions of silicate minerals of the Deccan basalts.

Plagioclase:



Olivine:



Pyroxene:



The $\delta^{13}\text{C}$ of the second end member (Fig. 4.6) is derived to be $-8.9 \pm 0.9\text{‰}$ from the intercept of the best-fit line (Fig. 4.6). The intercepts of Figs. 4.3 and 4.6 overlap within errors and are close to that calculated for $\delta^{13}\text{C}\text{-DIC}$ (-9.6‰ , Table 4.3) from carbonate ($\delta^{13}\text{C} \approx 0$) weathering with CO_2 from C_3 vegetation. This would suggest that DIC derived from this source is very likely to be the second end member. The $\delta^{13}\text{C}$ of carbonates in basalts (Table 4.1) also brings out the importance of CO_2 from C_3 vegetation on weathering in this region (see later discussion). Two of the samples, BHM-5 and KRS-6, are supersaturated in calcite (Table 4.1; Das et al.,

2005) may be receiving major ions from alkaline/saline soils and anthropogenic sources. The effect of these on the budgets of $\delta^{13}\text{C}$ and alkalinity are not well understood. Because of this, if these two data are excluded from regression analysis in Figs. 4.4 and 4.6, the intercepts of the best-fit lines decreases marginally ($-10.4\pm 0.8\text{‰}$ and $-10.1\pm 1.1\text{‰}$ respectively) without any significant change in correlation coefficients. These intercept also overlap with that expected for carbonate weathering with CO_2 for C_3 vegetation.

Another source of DIC enriched in ^{13}C is silicate weathering with CO_2 from C_4 vegetation. The DIC from this source will have $\delta^{13}\text{C}$ of -5.1‰ (Table 4.3). This alternative, however, is unlikely to be the source of the end member in Figs. 4.4 and 4.6, as in such a case; only enrichment in ^{13}C would be expected without change in Si/HCO_3 ratio. The resulting mixing trend would be a line parallel to y- axis, unlike the observed trend, which shows coupled variations in both $\delta^{13}\text{C}$ and Si/HCO_3 . The supply of Si and HCO_3 to water (hence its Si/HCO_3 ratio) is determined by the lithology of the basin, its mineral composition and their chemical weathering and not by the source of CO_2 .

Calcite precipitation is another process, which can alter $\delta^{13}\text{C}$ and Si/HCO_3 of waters. The effect of this process would be to deplete ^{13}C of waters and enhance their Si/HCO_3 ratios. In the samples analysed, only two of them (BHM-5 and KRS-6) are supersaturated in calcite and in another two (GHOD-1 and KRS-4) it is close to saturation. All other samples are undersaturated in calcite by 1–2 orders of magnitude. Therefore, calcite precipitation can be expected only in BHM-5 and KRS-6, and hence this process should not be a cause for the observed trend in Fig. 4.6. Thus, it is difficult to envisage a process other than mixing of DIC generated from silicate and carbonate weathering with CO_2 from C_3 vegetation to explain the strong linear trend in Figs. 4.4 and 4.6.

The $\delta^{13}\text{C}$ of DIC and Si/HCO_3 in river waters can be expressed in terms of the following mixing equations.

$$\delta^{13}\text{C}_{\text{riv}} = \delta^{13}\text{C}_{\text{car}} + f_{\text{sil}} \times (\delta^{13}\text{C}_{\text{sil}} - \delta^{13}\text{C}_{\text{car}}) \dots\dots\dots(4.7)$$

$$\text{R}_{\text{riv}} = \text{R}_{\text{car}} + f_{\text{sil}} \times (\text{R}_{\text{sil}} - \text{R}_{\text{car}}) \dots\dots\dots(4.8)$$

where $\delta^{13}\text{C}_{\text{riv}}$ is $\delta^{13}\text{C}$ of DIC in rivers, $\delta^{13}\text{C}_{\text{sil}}$ and $\delta^{13}\text{C}_{\text{car}}$ refer to $\delta^{13}\text{C}$ of DICs derived from silicate and carbonate weathering respectively, f_{sil} is fraction of HCO_3 derived

from silicate weathering and R is the Si/HCO₃ ratio. Combining equations (4.7) and (4.8),

$$\delta^{13}\text{C}_{\text{riv}} = \delta^{13}\text{C}_{\text{car}} + (\text{R}_{\text{riv}} - \text{R}_{\text{car}}) \times (\delta^{13}\text{C}_{\text{sil}} - \delta^{13}\text{C}_{\text{car}}) / (\text{R}_{\text{sil}} - \text{R}_{\text{car}}) \dots \dots \dots (4.9)$$

Following equation (4.9), the expected $\delta^{13}\text{C}_{\text{riv}}$ is plotted as a function of R_{riv} with $\text{R}_{\text{sil}} \approx 0.55$ and $\text{R}_{\text{car}} \approx 0.00$. The $\delta^{13}\text{C}_{\text{riv}}$ is calculated for three soil CO₂ values of -24‰ , -27‰ and -30‰ . The results (Fig. 4.6) show that the samples analysed in the study fall along the line of $\delta^{13}\text{C}_{\text{riv}}$ derived from soil CO₂ with $\delta^{13}\text{C} -27\text{‰}$ and a number of samples have $f_{\text{sil}} \approx 1$. The $\delta^{13}\text{C}$ value of -27‰ for soil CO₂ is consistent with the abundant C₃ vegetation in the region. The samples with $f_{\text{sil}} \approx 1$ ($\delta^{13}\text{C} = -18.7 \pm 2\text{‰}$, Si/HCO₃ = 0.5 ± 0.05) are the four west flowing rivers and the four east flowing tributaries of the Krishna (VDG-1, GTP-1, KYN-2, BGW-1; Table 4.1). The major ion chemistry of these rivers is consistent with this interpretation, it shows that the major ion abundances in these rivers corrected for rainwater contributions, can be entirely accounted for, by silicate weathering (Das et al., 2005; Chapter three). Samples KRS-1, 2, 4 and 6, GHOD-1 and BHM-5 have ¹³C heavier than -16‰ and Si/HCO₃ from 0.11 to 0.29, implying contributions from both silicate and carbonate weathering. Of these, KRS-6 and BHM-5 are supersaturated in calcite and hence their $\delta^{13}\text{C}$ and HCO₃ may have been affected by calcite precipitation. These two samples also have high concentrations of Cl (335 μM and 2183 μM) and SO₄ (1054 μM in BHM-5); these are interpreted in terms of inputs from anthropogenic sources and saline soils (Das et al., 2005). In KRS-1, KRS-4 and GHOD-1, based on $\delta^{13}\text{C}$ –Si/HCO₃ it can be inferred that in samples roughly half of the HCO₃ can be from carbonate weathering (Fig. 4.6). If carbonates are such a major contributor to DIC then their weathering should also be reflected in the dissolved Ca budget of these rivers. Das et al. (2005) based on weathering reactions (Table 4.4), major ion chemistry of rivers and using Mg as an index of silicate weathering concluded that on average up to $\sim 15\%$ (maximum $\sim 30\%$) of Ca in the Deccan rivers can be from non-silicate sources. Following this approach, the non-silicate contribution to Ca in KRS-1, KRS-4 and GHOD-1 can be calculated to be 15%, 16% and 29%. Even if all the non-silicate Ca is attributed to Ca from carbonates, it is seen that these estimates are lower than that is required to balance the $\delta^{13}\text{C}$ and Si/HCO₃ in some of these samples. An approach to reconcile these requirements is to propose that some of the parent minerals in basalts weather to solid products such as smectite, which can retain part of

their Ca thereby decreasing the Ca contribution from silicates to rivers. Such a decrease in Ca input from basalts to rivers would require enhanced Ca contribution from non-silicate sources (carbonates) to balance its budget. Available data on clay minerals in sediments from Deccan Trap rivers show that smectite is a common clay mineral (Kessarkar et al., 2003). If plagioclase weather to kaolinite and smectite as listed in Table 4.4 (reaction 2), the total Ca supply from basalts to rivers would decrease by ~15%, compared to that if the weathering results in kaolinite (reaction 1, Table 4.4). Further, weathering to kaolinite and smectite would also bring down (~25%) the Si/HCO₃ ratio. This may be a contributing factor to the scatter in the Si/HCO₃ ratio observed in the western ghat rivers with $\delta^{13}\text{C}$ ($-18.7 \pm 2\%$). A combined study of $\delta^{13}\text{C}$, major ion chemistry of rivers and clay mineral abundances and their composition should throw further light on the sources of DIC and their magnitudes.

The effect of carbonate weathering on $\delta^{13}\text{C}$ in waters can be checked through a coupled study of ^{13}C – ^{14}C analysis in these waters. Present day soil CO₂ from C₃ and C₄ vegetation would be characterized by modern or bomb produced radiocarbon. The DIC produced by chemical weathering of silicates with such CO₂ would also have modern/bomb radiocarbon. In contrast, if part of DIC is from carbonate weathering, it will be depleted in radiocarbon because of carbonates, which are generally “aged”, or “dead” in terms of ^{14}C (Trumbore, 2000). Thus, if the DIC has $\delta^{13}\text{C}$ in the range of -19% to -5% (for C₃ and C₄ vegetation respectively) and modern (or bomb) radiocarbon, then the dominant source of DIC is likely to be silicate weathering.

Relation (4.9) provides a means to infer the values of $\delta^{13}\text{C}_{\text{riv}}$ based on measured values of Si and HCO₃, and assumed values of R_{sil} and R_{car} . $\delta^{13}\text{C}_{\text{riv}}$ also depend on $\delta^{13}\text{C}_{\text{sil}}$ and $\delta^{13}\text{C}_{\text{car}}$ resulting from silicate and carbonate weathering (Table 4.3). Based on these parameters, the $\delta^{13}\text{C}_{\text{riv}}$ are calculated, and compared with the measured ones (Fig. 4.7). The plot between the expected and measured $\delta^{13}\text{C}$ gives a straight line with slope of 1.14 ± 0.13 and an intercept of 2 ± 2 (Fig. 4.7). The slope indicates a slight overestimation of the predicted values over the measured numbers, though they overlap within errors. If the predicted slope is indeed higher, the reasons could possibly be uncertainties in the estimation of R_{sil} , $\delta^{13}\text{C}_{\text{car}}$ and $\delta^{13}\text{C}_{\text{sil}}$ values. The close agreement between calculated and measured $\delta^{13}\text{C}$ as indicated by the slope of near unity attests to the validity of various parameters used in the calculation.

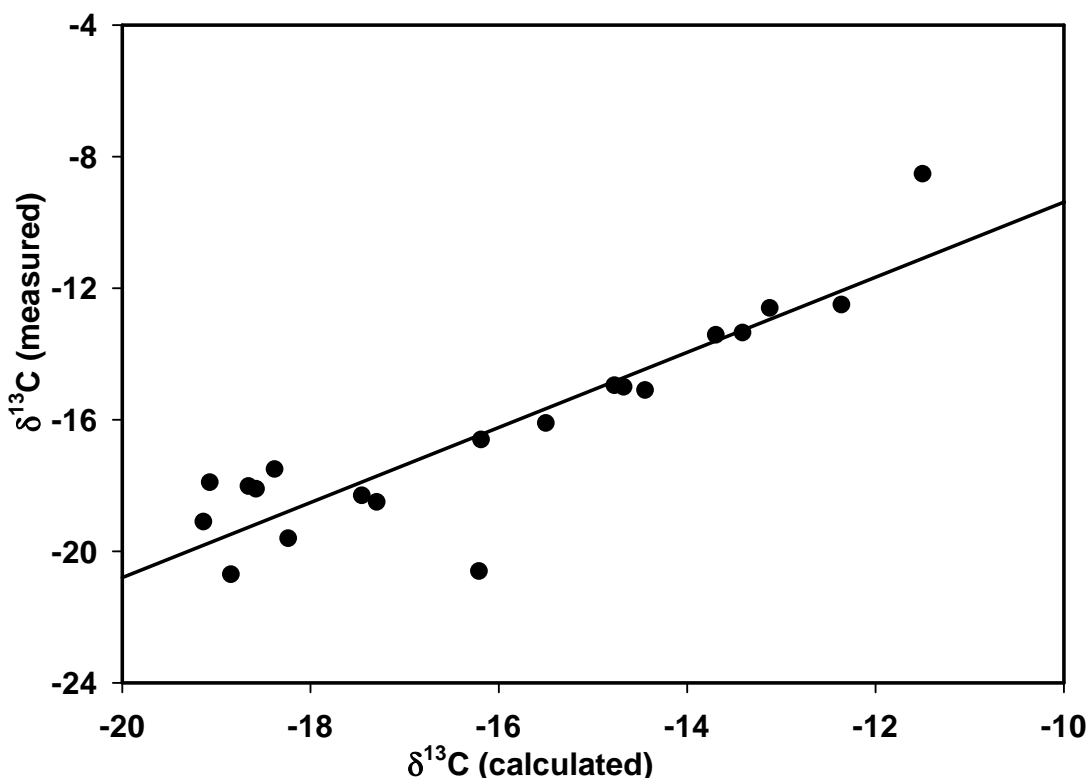


Fig. 4.7 Comparison of measured and calculated $\delta^{13}\text{C}$ in rivers (based on equation 4.9; see text). The data show a good correlation with a slope of near unity.

4.3.3 $\delta^{13}\text{C}$ of carbonates in basalt and bed sediments

Minor amount of carbonates occur in Deccan basalts, which are present as secondary minerals (Sukeshwala et al., 1972; Jeffery et al., 1988). The carbonates from the Mahabaleshwar formation have average $\delta^{13}\text{C}$ value of -14‰ (Table 4.1). The fractionation associated with the conversion of CO_2 (g) to CaCO_3 is $\sim +10\text{‰}$ at 25°C (Zhang et al., 1995; Table 4.2). Therefore, the CO_2 (g) from which these carbonates presumably formed might have $\delta^{13}\text{C}$ of $\sim -24\text{‰}$, which is close to that of C_3 type vegetation. These carbonates, therefore, could have formed from percolation of CO_2 (from C_3 type biotic source) rich water through vesicles of basalts releasing Ca and HCO_3 to solution during their interaction, which subsequently precipitated as CaCO_3 . CO_2 released from mantle degassing or an igneous melt source is unlikely to be the source since $\delta^{13}\text{C}$ of such CO_2 varies typically from $\sim 0\text{‰}$ to $\sim -4\text{‰}$ (Irwin and Barnes, 1980; Ray and Ramesh, 2000; Federico et. al., 2002). These results, further

attests the validity of earlier assumption that the source of CO₂ for weathering in the basin is from C₃ type vegetation.

Two bed sediment carbonates were also analysed for their δ¹³C; they have values of -3.8‰ and -5.1‰ (Table 4.1). Interpretation of these values requires information on their genesis. Considering that river waters in the region from where the bed sediments were collected are supersaturated in calcite (Table 4.1), it is tempting to infer that these carbonates are precipitated from river water. Based on the δ¹³C of HCO₃ in BHM-5 (-8.5‰) and KRS-6 (-12.6‰) and the isotope fractionation for HCO₃-CaCO₃ (~ +2‰ at 25°C), CaCO₃ precipitated from these waters should have δ¹³C of -6.5‰ and -10.6‰ respectively. These are about 2.7‰ and 5.5‰ less than the measured values. The difference could be due to many reasons: these waters may not be the only source of carbonates in the sediments or that the CaCO₃ precipitation may not be an equilibrium process. There could be seasonal variations in δ¹³C of DIC, particularly in summer when groundwater inputs could change river DIC and supersaturation in calcite may be more pronounced, their role in determining δ¹³C of CaCO₃ need to be evaluated. Other sources of sediment carbonate include (i) soil carbonates precipitated from evaporating groundwater, (ii) mechanical transfer of carbonates from upstream, and (iii) carbonates present in the basin. Pawar et al. (1988) have reported presence of calc tufas in the upland of the Deccan Traps, especially, in areas around Pune, near the drainage basin of Bhima. The δ¹³C of the sediment carbonate, therefore, would depend on mixing proportion of carbonates from various sources.

4.3.4 pCO₂ of Deccan rivers

The data on HCO₃, pH and temperature in rivers allow calculating the partial pressure of CO₂ in rivers (Table 4.5). This hypothetically represents the pCO₂ of the soil gas, which dissolves in water to yield its alkalinity. The equation relating pCO₂ and the HCO₃ concentration can be deduced from equations (4.2) and (4.3).

$$\log(p\text{CO}_2) = \log[\text{HCO}_3] + pK_1 + pK_2 - \text{pH} \dots \dots \dots (4.10)$$

Calculations show that all samples (except one) have pCO₂ higher than the atmospheric pCO₂ (Fig. 4.8), with majority of them lying between 1000–2000 ppm and the maximum pCO₂ being ~3500 ppm. The higher pCO₂ values are result of organic matter oxidation taking place in the soil zone through which the rivers drain.

Table 4.5 Calculated values of pCO₂ and F (flux of CO₂ out of river).

Sample Code	T	pH	HCO ₃ ⁻ (μM)	δ ¹³ C (‰)	pCO ₂ (ppm)	F μmol cm ⁻² d ⁻¹
KRS-6	24.3	8.11	3995	-12.5	2030	6.85
KRS-4	24	8.01	1672	-12.6	1065	2.89
KRS-3			802	-16.1	-	-
KRS-1	24.8	7.64	1418	-13.4	2141	7.29
KRS-2	23.8	7.52	776	-15.0	1523	4.78
BHM-5	27.2	8.36	2934	-8.5	873	2.08
GHOD-1	24.2	8	1644	-13.4	1075	2.93
VDG-1	23.1	7.05	530	-18.3	3040	11.03
TPN-1	22	7.1	234	-19.6	1177	3.38
GTP-1	22	7.76	170	-20.7	187	-0.71
KYN-2	20.2	7.25	301	-17.9	1045	2.85
HRN-1	22.8	7.14	337	-20.6	1564	4.96
KYN-1	23.7	7.38	713	-16.6	1929	6.45
BGW-1	22.8	7.1	395	-18.5	2010	6.8
VRN-1	23.4	7.56	1045	-15.0	1860	6.17
DDG-1	23.4	7.35	1226	-15.1	3539	13.07
VAT-1	7.16	7.16	716	-17.5	3298	11.99
SHT-1	7.22	7.22	623	-19.1	2489	8.7
KJL-1	7.18	7.18	755	-18.0	3368	12.24
SUKH-1	7.39	7.39	656	-18.1	1797	5.85

These high pCO₂ values in rivers makes them potential sources of CO₂ to the atmosphere (Telmer and Veizer, 1999)

The diffusion model of Broecker (1974) is used to calculate flux of CO₂ escaping from rivers to the atmosphere.

$$F = D(C_{\text{air}} - C_{\text{riv}})/Z \dots\dots\dots(4.11)$$

where (C_{air} - C_{riv}) is the concentration difference in CO₂ between the overlying air and water, D is the gas and temperature-specific diffusion coefficient (m² d⁻¹) and Z is the thickness of the boundary layer at the air-water interface through which diffusion occurs. The value of Z depends largely on the wind speed and water turbulence (Holley, 1977). Typical values are ~3×10⁻⁵ m for world oceans and ~20×10⁻⁵ m for fresh water lakes (Kempe, 1982). D/Z gives the thickness of the

water column that will equilibrate with the atmosphere per unit time, has typical values of $\sim 1 \text{ m d}^{-1}$.

For the Krishna system rivers, there are no data on D and Z . Therefore, for calculation of $p\text{CO}_2$ fluxes, D and Z values are taken to be the same of those reported for Lawrence rivers (Kempe, 1982; Yang et al., 1996), i.e., $D/Z \approx 1 \text{ m d}^{-1}$. Using this and C_{air} of 360 ppm, the F values calculated for the twenty rivers draining the Deccan Traps are reported in Table 4.5. The flux of CO_2 out from river to the atmosphere varies from 2–13 $\mu\text{mol cm}^{-2} \text{ d}^{-1}$ with an average of $\sim 7 \mu\text{mol cm}^{-2} \text{ d}^{-1}$. This compares with CO_2 drawdown of $\sim 0.1 \mu\text{mol cm}^{-2} \text{ d}^{-1}$, by silicate weathering.

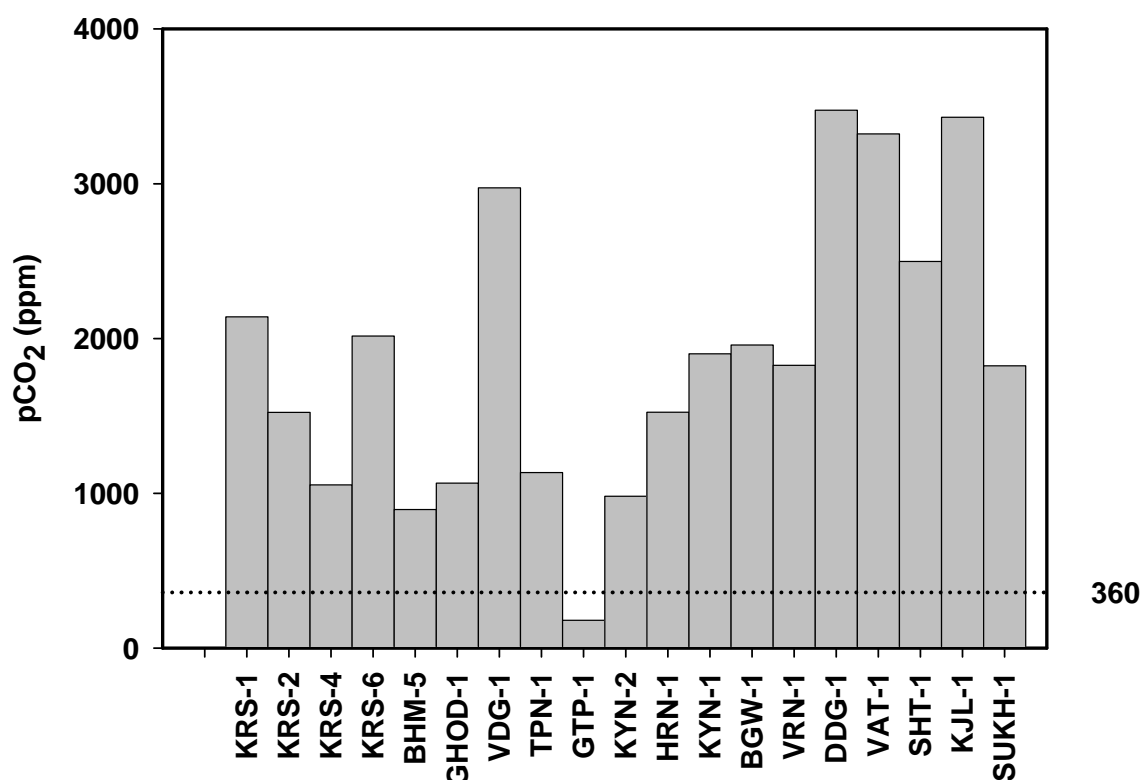


Figure 4.8 Histogram showing $p\text{CO}_2$ of the rivers sampled. The smaller rivers show higher $p\text{CO}_2$ (DDG-1, VAT-1, SHT-1, KJL-1 and SUKH-1). The dotted line is the atmospheric $p\text{CO}_2$ value.

4.4 CONCLUSIONS

The study on carbon isotopes measured in dissolved inorganic carbon from twenty rivers draining the Deccan Traps brings out the following important conclusions:

(i) The potential of using $\delta^{13}\text{C}$ as a tracer to quantify the sources of DIC in Deccan rivers has been established. This helps to understand better the weathering contributions of the silicate and carbonate lithologies to the DIC budget of individual rivers.

(ii) The $\delta^{13}\text{C}$ values in the rivers range from -8.5‰ to -20.7‰ , with most of these falling in the range of $-18.7\pm 2\text{‰}$. These values suggest that DIC in them is derived primarily from products of silicate weathering carried out by CO_2 from C_3 plants. The $\delta^{13}\text{C}$ shows a strong co-variation with $[\text{HCO}_3^-]$, this has been interpreted in terms of mixing between two-end members: DIC generated from weathering of silicates and carbonates. The intercept of the best-fit line, which represents the $\delta^{13}\text{C}$ of the carbonate end member, is -9.6 ± 0.8 ($r^2=0.82$), similar to the value calculated from carbonate weathering reactions.

(iii) The $\delta^{13}\text{C}$ values also show a strong linear trend with Si/HCO_3 ($r^2=0.80$). This also has been interpreted in terms of DIC from the mixing of the silicate and carbonate end members. The intercept of -8.9 ± 0.9 is similar to that calculated from the weathering of carbonate minerals. The cluster of data depleted in ^{13}C values and with Si/HCO_3 ratio close to 0.55 suggests silicate weathering with CO_2 from C_3 type of vegetation. The Si/HCO_3 ratio of 0.55 is consistent with that calculated based on the abundances of minerals in Deccan basalts and their weathering.

(iv) Coulometric analyses of basalts show the presence of measurable quantities carbonates in basalts, in the range of 0–0.9 wt%. The $\delta^{13}\text{C}$ analyses of two of these basalt samples seem to suggest that these carbonates are of secondary origin precipitated from DIC generated by weathering of basalt with CO_2 from C_3 plant.

(v) The pCO_2 of rivers of the Krishna system are factors of 2–8 higher than that of the atmosphere. These high pCO_2 are results of organic matter oxidation in the soil zone and are source of CO_2 escaping to the atmosphere. The calculated fluxes range from $2\text{--}13 \mu\text{mol cm}^{-2} \text{d}^{-1}$; nearly two orders of magnitude higher than that consumed by silicate weathering.

Chapter Five

Geochemistry of river sediments

5.1 INTRODUCTION

Rivers are the major pathways for the transport of continental materials to the oceans. This transport occurs in the form of both particulate and dissolved loads (Martin and Meybeck, 1979), the former being a measure of physical erosion, whereas chemical weathering determines the dissolved load and its composition. Studies on weathering of rocks are important as it regulates continental erosion and consumption of CO₂, which contributes to global climate change (Walker et al., 1981; Raymo and Ruddiman 1992; Berner 1995).

Studies based on “dissolved load” of rivers provide information on contemporary chemical weathering and erosion and the factors influencing them. Such studies on a number of large and small rivers from several parts of the globe have been reported over the years. These have been motivated primarily by the quest to learn about the chemical weathering process in natural settings, the various mineral sources contributing to the chemical composition of rivers and the rate of atmospheric CO₂ drawdown (Berner and Berner, 1996). Chemistry of river particulates, on the other hand, provides information on “longer term” chemical weathering of the basin, the ‘term’ being dependent on the residence time of the particulates in the river basin. In addition, the chemical and isotopic composition of sediments serves as “tags” to identify them after their deposition. Studies on chemical weathering based on riverine particulate loads are less common compared to those based on the dissolved load approach (Martin and Meybeck, 1979; McLennan, 1993; Gaillardet et al., 1995; Canfield, 1997; Picouet et al., 2002). Canfield (1997), from studies of chemistry of particulates from several US rivers related the degree of chemical weathering to parameters such as runoff and temperature, rivers with high runoff generally have less altered sediments. In recent years, simultaneous studies of dissolved and particulate chemistry have provided more quantitative understanding of weathering (Gaillardet et al., 1997; Picouet et al, 2002).

Among the Indian rivers, studies have been reported on sediments from the Ganga and Brahmaputra (Subramanian et al., 1985, 1987; Sarin et al., 1989; Singh and France-Lanord, 2002; Singh et al., 2003), the Yamuna and the Chambal (Jha et al., 1990; Dalai et al., 2004; Rengarajan, 2004) and Indus (Ahmad et al., 1998). Dekov et al. (1998) have summarized the chemistry of suspended matter and sediments from

rivers of the Indian sub-continent. Recently, Singh and France-Lanord (2002) based on Sr and Nd isotope studies, inferred mixing proportions of sediments from various sub-basins of the Brahmaputra drainage to the bed sediments of the Brahmaputra mainstream. Subramanian et al. (1987) studied the trace element geochemistry of particulate and bed sediments of rivers draining the Krishna basin. Their results showed that the concentrations of trace elements in suspended sediments are generally higher than those in the bed sediments, and that trace metal abundances are modified by pollution inputs. Singh and Rajamani (2001), based on their work on the floodplain sediments of the Kavery river (draining Archean gneissic and charnockitic rocks), inferred the dependence of REE concentrations on sediment size, mineral sorting, and presence of Fe-hydroxide phases. Ahmad et al. (1998) inferred that physical weathering and erosion controls the grain size and hence the chemical nature of the Indus sediments.

The present study focuses on the major and minor element geochemistry of bed sediments from rivers draining the Deccan traps, specifically those belonging to the Krishna river system and several smaller rivers draining the western ghats and flowing into the Arabian sea. These studies complement the work on the dissolved major ion chemistry of the same rivers and thus provide wholesome information on chemical weathering and erosion of the Deccan traps.

The work is based on the chemistry of twenty-eight bed sediments collected from seventeen different rivers draining the Deccan Traps. The objectives of the present study are to: (i) obtain baseline data on the major and minor element composition of sediments, and use the data to infer the relative mobility of elements with respect to the parent basalts, (ii) compare results on chemical weathering derived from dissolved (Das et al., 2005) and sediment data, and (iii) estimate physical erosion from the data on dissolved and sediment load.

5.1 RESULTS AND DISCUSSION

The river sediments were collected during the campaign of 2001. The details of sampling locations are listed in Appendix 2.1 (Chapter two). The concentration of major and minor elements of sediments and their carbonate contents are given in Table 5.1. The concentrations are in wt (%) or $\mu\text{g g}^{-1}$ in oven dried ($\sim 90^\circ\text{C}$) samples.

Table 5.1 Major and trace element concentration in sediments from rivers draining the Deccan Traps. Concentration of Na to Mn are in wt %; Sr to P are reported in $\mu\text{g g}^{-1}$.

Samples	Na	K	Mg	Al	Ca	CaCO ₃	Fe	Ti	Mn	Sr	Ba	Ni	Cr	V	Cu	Zn	P
Kishna mainstream																	
KRS-1	0.75	0.21	2.38	6.35	5.02	2.28	17.35	5.45	0.22	240	168	100	176	990	291	223	535
KRS-2	0.52	0.36	1.38	8.85	2.21	0.23	13.58	2.28	0.20	104	186	97	138	512	287	164	1006
KRS-3	0.63	0.26	1.86	7.13	3.59	0.12	13.57	2.65	0.17	210	164	95	151	560	263	170	728
KRS-3R	0.72	0.28	2.13	7.95	3.83	0.13	13.32	2.49	0.17	234	185	99	144	524	253	172	720
KRS-4	1.20	0.27	2.84	6.35	8.93	9.13	13.04	2.73	0.21	260	163	88	206	695	206	191	736
KRS-5	0.71	0.26	1.99	7.78	4.16	2.48	14.01	3.51	0.22	248	209	93	138	617	271	173	666
Bhima mainstream																	
BHM-1	0.47	0.58	1.68	8.81	1.89	0.10	13.04	1.46	0.17	146	273	112	195	425	211	156	917
BHM-2	0.91	0.55	2.31	6.81	5.72	5.70	9.89	1.99	0.15	238	230	88	188	431	169	129	649
BHM-3	0.90	0.60	2.39	7.12	5.00	5.93	8.12	1.41	0.11	219	228	81	161	322	142	113	762
BHM-4	0.86	0.55	2.15	6.93	5.73	6.65	8.86	1.53	0.15	251	252	81	171	343	161	137	913
BHM-4R	0.83	0.58	2.24	7.21	5.80	nd	8.88	1.56	0.16	241	245	80	171	349	158	131	887
BHM-5	0.95	0.57	2.62	6.42	6.56	10.28	7.88	1.35	0.27	287	254	80	105	299	188	188	907
Tributaries of Bhima																	
GHOD-1	1.03	0.57	2.81	7.46	4.69	0.38	11.59	1.83	0.19	235	245	106	306	441	167	146	722
GHOD-2	0.61	0.54	2.03	6.08	8.11	16.88	5.85	0.94	0.16	248	188	68	100	242	126	101	952
MTH-1	0.85	0.53	2.30	6.97	4.61	2.55	9.41	1.77	0.15	220	241	91	248	422	221	214	1804
NIRA-1	1.07	0.23	3.10	5.92	9.39	12.85	10.20	2.11	0.15	340	140	80	165	513	202	144	470
NIRA-2	1.05	0.27	2.74	5.84	8.78	11.85	10.93	2.54	0.19	298	175	82	154	540	219	155	482
Tributaries of Krishna																	
KYN-1	0.69	0.32	1.89	7.87	3.58	1.03	14.64	2.75	0.20	160	168	97	156	592	299	192	879
KYN-2	0.54	0.30	1.64	9.78	2.57	0.10	16.41	2.42	0.22	132	205	126	295	651	297	186	1014
KYN-2R	0.56	0.30	1.72	10.06	2.70	0.10	16.91	2.48	0.23	138	215	128	303	651	299	190	1030
VRN-1	0.59	0.30	1.22	7.76	2.10	0.04	13.85	2.95	0.23	122	183	90	119	531	303	161	845
PGN-1	0.59	0.25	1.24	7.61	2.15	0.10	17.73	5.18	0.23	131	172	96	148	927	324	205	773
GTP-1	0.10	0.55	0.60	10.38	0.34	0.15	14.64	2.66	0.21	40	198	141	246	540	204	147	759
HRN-1	0.22	0.51	0.89	9.12	0.89	0.20	13.21	2.40	0.21	57	199	110	174	503	247	143	1036
HRN-1R	0.22	0.53	0.95	9.65	0.95	nd	14.00	2.39	0.23	62	210	122	188	568	260	151	957
TPN-1	0.13	0.41	0.52	9.78	0.37	0.10	16.30	3.51	0.17	46	194	127	212	620	268	164	998
DDG-1	0.37	0.21	1.13	7.09	1.67	0.35	18.87	6.55	0.23	74	138	92	171	1059	334	238	672
VDG-1	0.18	0.36	0.75	9.35	0.74	0.13	16.01	3.12	0.18	54	193	123	185	616	316	166	855
BGW-1	0.29	0.28	0.87	8.88	1.12	0.13	16.58	3.16	0.21	64	181	99	151	627	327	187	1005
BGW-1R	0.27	0.30	0.90	9.18	1.10	nd	16.98	2.65	0.23	64	175	103	156	657	332	192	902
West flowing western ghat rivers																	
SUKH-1	0.35	0.18	1.04	8.57	1.52	0.11	16.45	2.46	0.20	73	135	119	146	662	329	161	816
KJL-1	0.36	0.15	2.08	6.80	2.20	0.00	30.21	7.62	0.30	61	79	162	235	2165	568	398	503
VAT-1	0.50	0.23	1.95	8.19	2.98	0.05	16.89	3.40	0.21	103	144	113	199	760	328	212	738

The precision of measurements based on repeat analyses is generally better than 5% (see appendix 2.2, Chapter two) for all major and trace elements analysed.

The major element composition of the sediments are presented in two ternary diagrams (Figs. 5.1 a,b). On the ternary diagram of molecular proportions of Al_2O_3 , $(\text{CaO} + \text{Na}_2\text{O})$ and K_2O (A-CN-K), the points lie evenly spread along a mixing line between A-CN apices (Fig. 5.1a) bound by two end members characterizing average basalt and average laterites. The spread of the data seem to suggest that the bed sediments have been weathered to different degrees, some quite extensively such that their composition is close to laterites. A similar ternary plot (Fig. 5.1b) between Al_2O_3 , $(\text{CaO} + \text{Na}_2\text{O} + \text{K}_2\text{O})$ and $(\text{Fe}_2\text{O}_3 + \text{MgO})$ [A-CN-K-FM] indicates that the sediment composition is dominated by contributions from the A and FM apices. Comparison of the composition of the sediments with those of un-altered basalts and laterites (plotted in Figs.5.1a,b) show that many of the sample points cluster around the line connecting basalts and lateritic soils. However, some samples plot away from the mixing line, towards the FM apex, indicating that either the basalts contributing to these samples had a composition different from average and/or that in these sediments there is contribution of Fe from weathering resistant minerals or from precipitation of oxides, (oxy)-hydroxides of Fe.

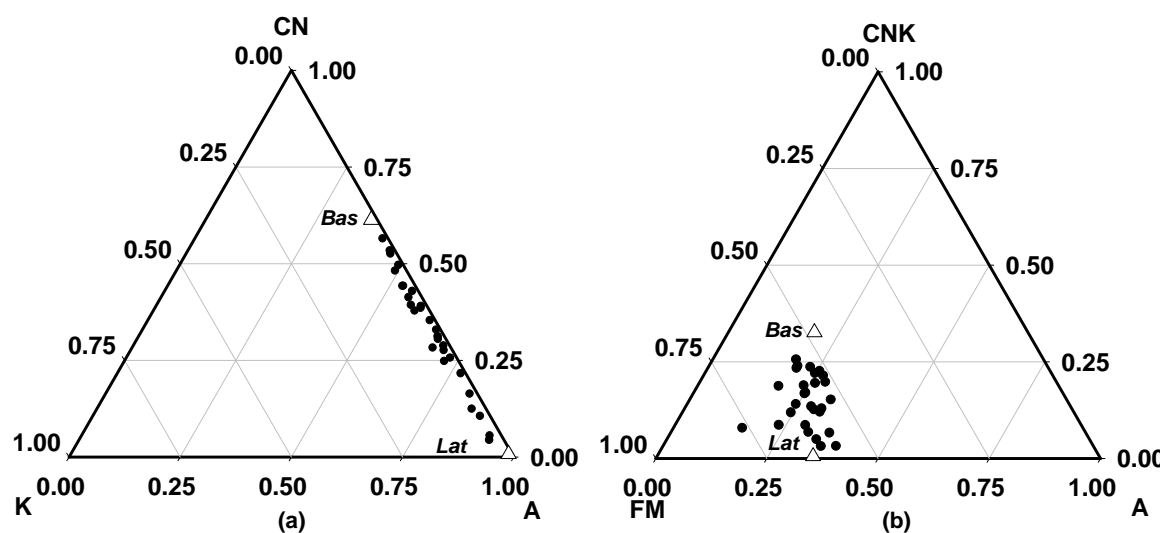


Fig. 5.1 (a) Ternary plot of Al_2O_3 (A), $\text{Ca}^*\text{O} + \text{Na}_2\text{O}$ (CN) and K_2O (K). The sample data lie along the CN—A axes between the basalt and laterite end members, indicating weathering of aluminosilicate minerals in basalts to laterites (b) Ternary plot of Al_2O_3 (A), $\text{Ca}^*\text{O} + \text{Na}_2\text{O} + \text{K}_2\text{O}$ (CNK), and $\text{FeO} + \text{MgO}$ (FM). Most of the data cluster around the mixing line of basalts and laterites (open triangles). A few data points lean towards the FM axis indicating contribution from either Fe rich minerals (ferromagnesium/ilmenite) or the precipitation of Fe-oxides/hydroxide.

A closer look at the elemental abundances show that compared to average basalts, some of the major alkali and alkaline earth elements (e.g., Na, Mg, Ca and Sr) are significantly depleted in the sediments whereas a few others (e.g., Al, Fe and Ti) are enriched. This depletion/enrichment of elemental abundance is a measure of the intensity of alteration of Deccan basalts by chemical weathering and subsequent removal of various elements by rivers. These are discussed in some detail in the following sections. In these discussions, it is, however, recognized that river sediments are often subject to size sorting during transportation and deposition caused by water flow. This sorting can cause local variability in mineralogical and chemical composition of sediments (Pettijohn, 1975), which in turn can contribute to uncertainties in inferences based on elemental concentration/abundance data. This, however, is less likely to influence the interpretations of relative behaviour of elements with similar geochemical characteristics.

5.2.1 Sodium, Magnesium, Calcium and Strontium

These four elements are grouped together, as all of them are depleted in sediments relative to basalts (Tables 5.1 and 5.2). The frequency distribution of Na, Mg, Ca_{sil} and Sr in sediments are shown in Figs. 5.2 a, b, c and d. The concentration of Na in the sediments varies from ~ 0.1 to 1.2 wt.% with an average of 0.61 wt.%, significantly lower than its abundance of 1.95 wt.% in Deccan basalts (Table 5.1). The Na content of all samples analysed are less than average in basalts. This, as expected, shows that Na is quite mobile during chemical weathering and erosion of basalts. Mg in sediments vary from ~ 0.5 to 3.1 wt.%. The average Mg in sediments (1.77 wt.%) is a factor of ~ 2 lower than its abundance of 3.75 wt.% in basalts (Table 5.1). Many of the sediments analysed contain measurable concentration of $CaCO_3$, the role of which in contributing to measured Mg abundance is unclear. To avoid this ambiguity, if average Mg concentration is calculated for sediments with $<0.5\%$ $CaCO_3$, it marginally decreases to 1.33 wt.% from 1.77 wt.%. Analogous to Na, the Mg concentration in all samples analysed are also less than the average basalt value (Fig. 5.2b), suggesting its mobile nature during chemical weathering of basalts. Ca_{sil} concentrations in sediments vary from 0.28 to 5.28 wt.%, with a mean of ~ 2.3 wt.%, a factor of ~ 3 lower than the average Ca in basalts, ~ 7.3 wt.% (Tables 5.1, 5.2). Ca_{sil} represents Ca associated with silicates. Ca_{sil} is calculated by subtracting from the total

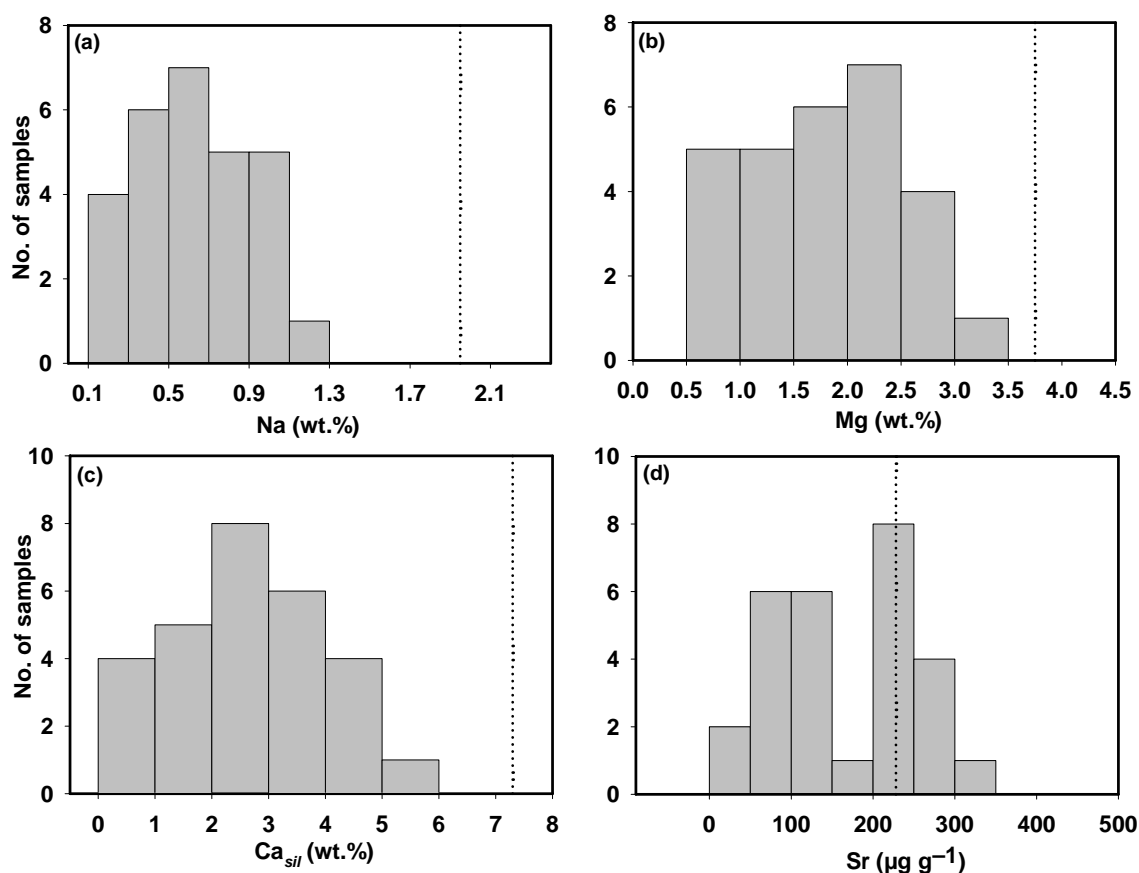


Figure 5.2 a,b,c and d. Frequency distributions of Na, Mg, Ca_{sil} (all in wt. %) and Sr (μg g⁻¹). The dotted lines are the average abundances of these elements in Deccan basalts. These histograms show that the concentrations of elements in sediments are significantly less than that in basalts, suggesting their loss of these during weathering.

Ca, the Ca contribution from carbonates. Towards this, the carbonate measured in sediments is taken to be made entirely of CaCO₃. The source of CaCO₃ in these sediments is not known. From calcite saturation index (CSI) calculations (Chapter three), it is observed that many of the rivers sampled are supersaturated w.r.t. calcite indicating that CaCO₃ in sediments can be of river water origin (Das et al., 2005). The depletion of Ca in sediments again indicates its significant mobility from Deccan basalts during their chemical weathering. Sr in sediments varies from 40 to 340 μg g⁻¹ (average 164 μg g⁻¹). In samples with CaCO₃ < 0.5%, the range narrows down (40 to 235 μg g⁻¹) with a mean of 103 μg g⁻¹.

Table 5.2 Average abundances of major (Na, K, Mg, Ca, Al, Fe and Ti; all in wt.%) and minor elements (Sr and Ba in $\mu\text{g g}^{-1}$) in sediments from groups of rivers.

Sample		Na	K	Mg	Ca	Al	Fe	Ti	Sr	Ba
Krishna mainstream (n=5)	Av.	0.76	0.27	2.09	4.78	7.29	14.31	3.32	212	178
	SD	0.26	0.05	0.55	2.53	1.06	1.73	1.27	63	19
Bhima mainstream (n=5)	Av.	0.82	0.57	2.23	4.98	7.22	9.56	1.55	228	247
	SD	0.20	0.02	0.35	1.81	0.93	2.10	0.26	52	19
Tributaries of Bhima (n=5)	Av.	0.92	0.43	2.60	7.12	6.45	9.60	1.84	268	198
	SD	0.20	0.16	0.43	2.30	0.72	2.24	0.59	50	45
Tributaries of Krishna (n=10)	Av.	0.37	0.35	1.07	1.55	8.76	15.82	3.47	88	183
	SD	0.22	0.11	0.44	1.05	1.11	1.75	1.35	43	20
West flowing western ghat rivers (n=3)	Av.	0.40	0.19	1.69	2.24	7.85	21.18	4.49	79	119
	SD	0.08	0.04	0.57	0.73	0.93	7.82	2.75	22	35

Sr concentration in basalts varies within a narrow range of $228 \pm 32 \mu\text{g g}^{-1}$ (Subbarao et al., 2000). Of the 28 sediment samples analysed, all but three samples have Sr less than average basalt ($+1\sigma$) value. These three samples, (NIRA-1 & 2 and BHM-5) have concentrations of 298, 340 and $287 \mu\text{g g}^{-1}$ respectively (Table 5.1). These samples also have high CaCO_3 indicating the latter's possible role in sequestering Sr to sediments (see later discussions).

The mobility of all these elements during weathering and transportation is borne out clearly from Figs. 5.3 a, b, c and d which are scatter diagrams of Na, Mg, Ca_{sil} and Sr vs. Al. All these plots show anti-correlation suggesting the contrasting geochemical behaviour of Na, Mg, Ca and Sr relative to Al during weathering and transport. As weathering progresses, the more labile elements of rocks (e.g., Na, Mg, Ca, Sr) are released to solution, thereby continuously depleting the residual solid phases in them. In contrast, the more weathering resistant elements (Al, Ti, Fe) get enriched in the residue. This generates an anti-correlation in the abundances of these two groups of elements in the residual solids (sediments), as observed in Figs. 5.3 a,b,c,d. The slope of the best-fit line of these plots is a measure of the degree of depletion of these

elements.

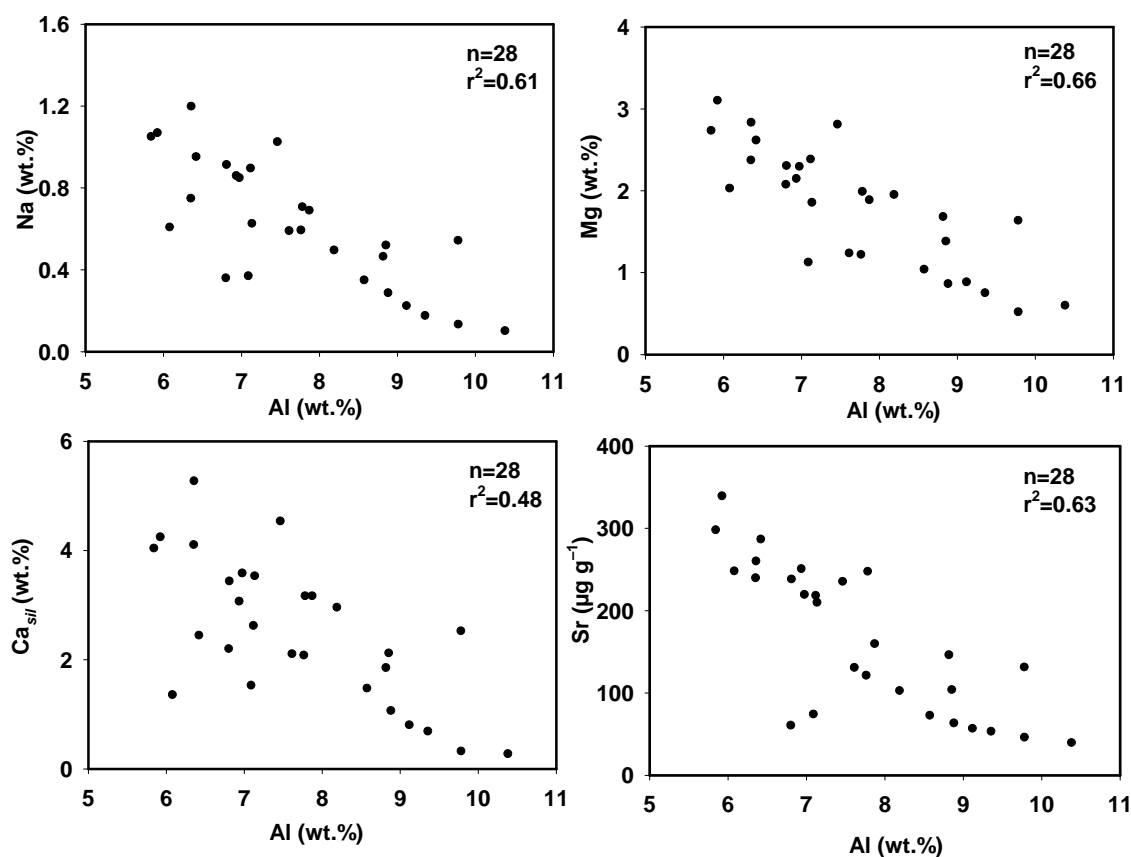


Figure 5.3 (a,b,c and d) Plots of Na, Ca_{sif} , Mg and Sr vs. Al. The figures show inverse correlation indicating their mobile nature relative to Al.

Al is generally used as a normalizing element as it is known to behave conservatively during weathering. Its concentration in sediments shows large variation from a low value of 5.2 wt.% to a high of 10.4 wt.% (Table 5.1). These are on either side of its average concentration in basalts ($7.30\% \pm 0.46$). Al, in basalts, is mainly associated with minerals such as plagioclase, and in sediments it is a major constituent of all clay minerals. The Al content of lateritic soils from Deccan basalts can be quite high, ~ 23.5 wt.% (Widdowson and Gunnell, 2004).

Lower Al concentrations in sediments, as compared to the mean basalt value, can be interpreted in terms of particle sorting and/or dilution with Al poor phases such as carbonates. The enrichment of Al in sediments can result from: (i) the loss of more mobile major elements such as Ca, Mg, Na and Si from rocks, thereby enriching concentration of Al in residual sediment, and/or (ii) particle sorting, contributing to higher abundance of plagioclase in sediments.

The abundances ratios of Na, Mg, Ca and Sr in sediments and in waters relative to that in Deccan basalts reflect their relative mobility. The composition of river water represents recent and short time weathering dictated by residence time of river waters whereas the residence time of sediments in the drainage basin being longer, they provide an integrated weathering-signal. The residence time of sediments in the basin studied in this work is not known. Benninger et al (1975) estimated based on ^{210}Pb inventory and flux that particulate matter residence time in the Susquehanna river basin to be about 5000 years. If such time scales are applicable to the basin sampled in this work, it would lead to infer that sediment composition would yield average elemental mobility over millenia time scales. Fig.5.4a is a plot of Ca_{sil} vs. Mg (wt. %), which shows a strong positive correlation ($r^2=0.78$) with a slope of 1.58 ± 0.16 and intercept of -3.3 ± 3.1 . The arithmetic mean of $\text{Ca}_{\text{sil}}/\text{Mg}$ in sediments is 1.33 ± 0.38 . These compare well with the average Ca/Mg (wt. ratio) of 1.95 ± 0.41 in basalts. All these ratios though overlap within $\pm 2\sigma$ indicating near congruent release of Ca and Mg from Deccan basalts, they also hint at the possibility that on an average Ca may be slightly more mobile ($\sim 20\%$) relative to Mg. The role of carbonates in sediments in sequestering Mg needs to be understood to resolve between the two alternatives. If carbonates contain Mg, appropriate correction need to be made to obtain Mg in silicate phases. The effect of such a correction would be to enhance the $\text{Ca}_{\text{sil}}/\text{Mg}$ in sediments from those derived above (Fig. 5.4a) making it closer to the basalt ratio. The concentrations of Ca and Mg in river waters also suggest that they are released from basalts to water roughly in the same proportion as their abundance in basalts, consistent with the above inference. The Ca/Mg (molar ratio; after rainwater correction) observed in the two groups of rivers; (i) the Krishna and its east flowing tributaries, and (ii) the rivers flowing west into the Arabian sea, have values of 1.27 ± 0.08 and 1.38 ± 0.21 respectively, compared to average Ca/Mg (molar ratio) value of 1.19 ± 0.17 in basalts. The ratios in water though seem marginally higher than that in basalts, they overlap within errors. This has been interpreted in terms of similar mobility of Ca and Mg and/or to a slight preferential mobility of Ca relative to Mg, and/or the supply of Ca from carbonates and/or apatites (Das et al., 2005). Similar to Ca, Na also shows a strong positive correlation ($r^2=0.86$; Fig. 5.4b) with Mg with a slope of 0.39 ± 0.03 as compared to a Na/Mg (wt. ratio) of 0.49 ± 0.11 in basalts. The similarity in these ratios within errors again suggests that these two elements are

released from basalts to water nearly congruently, consistent with inferences drawn from their dissolved concentrations in river waters (Das et al., 2005).

Figs. 5.5 a,b are plots of Sr with Ca_{sil} and Mg, both of which show strong positive correlation. The Sr/Mg ratio ($\mu\text{g g}^{-1}/\text{wt. \%}$) of best-fit line in Fig. 5.5b is 110 ± 10 , compared to the value of 62 ± 13 in basalts. If samples with $>0.5\%$ $CaCO_3$ are excluded from regression analysis (to avoid uncertainties resulting from incorporation

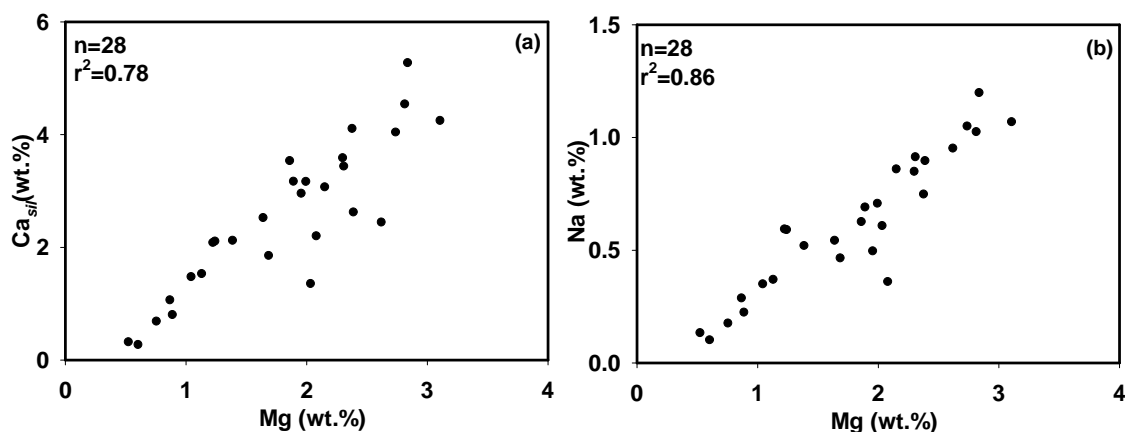


Figure 5.4. a,b. Scatter plots of Ca_{sil} and Na vs. Mg. The plots show a good correlation. The slopes of the lines, when compared to the respective basalt ratios indicate that all these elements are released to rivers nearly congruently.

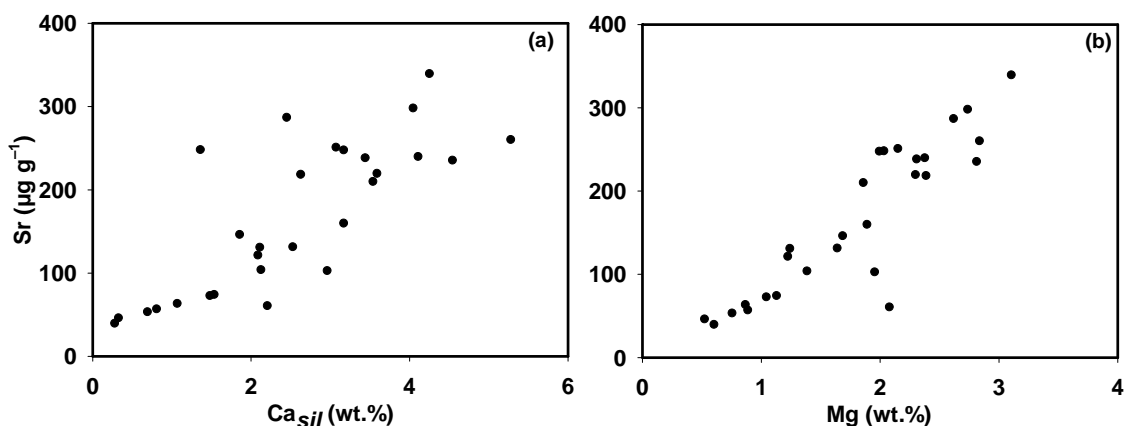


Figure 5.5. Plots of Sr with Ca_{sil} (a) and Mg (b). The linear trend indicate their similar geochemical behaviour during weathering and transport.

of Sr and Mg in $CaCO_3$) the Sr/Mg slope in the sediments becomes 73 ± 16 , overlapping with ratio in basalts. Two inferences can be drawn from the similarity in these two ratios: (i) Sr and Mg are released to waters from basalts nearly congruently

consistent with conclusion drawn from dissolved phase data and (ii) carbonates seem to a carrier phase for both Mg and Sr.

The statistical parameter of concentration data discussed in the preceding section is summarized in Table 5.3.

Table 5.3 Regression analysis of Ca_{sil} , Na and Sr with Mg.

Pair (Y-X)	r^2	Intercept	Slope	*Av. ratio
Ca_{sil} -Mg (n=28)	0.78	-3.3±3.1	1.58±0.16	1.33±0.39
(n=16)	0.87	-0.5±0.3	1.76±0.17	1.29±0.41
Na-Mg (n=28)	0.86	-0.07±0.06	0.39±0.03	0.34±0.08
(n=16)	0.71	-0.0003±0.08	0.32±0.05	0.31±0.09
Sr-Mg (n=28)	0.80	-32±20	110±11 ^s	89±22 ^s
(n=16)	0.60	5±23	73±16	77±20

[#] Samples with $CaCO_3 < 0.5$ wt.%. ^sSr/Mg in $\mu g\ g^{-1}$ /wt.%. *Arithmetic mean of individual ratios

Thus, the strong inter-element correlation among Na, Mg, Ca and Sr in sediments suggests that all these elements are released from basalts to rivers in roughly the same proportion ($\pm 20\%$) as their abundances in basalts. The Deccan Trap basalts, therefore, are weathering nearly congruently with respect to these four elements, a conclusion consistent with that reached based on major ion chemistry of the Krishna river and its tributaries (Das et al., 2005; Chapter three). Further, the sediment and water data lead to the infer that on average the ratios of release of these four elements during the residence time of bank sediments in the various basins have been nearly the same as their contemporary supply ratios, both of which are roughly the same as in Deccan basalts.

5.2.2 Potassium and Barium

K being an alkali element is expected to be mobile during weathering and transport. However, it is often enriched in the residual solid phase after weathering (Nesbitt et al., 1980). The abundance of K in the residue is regulated by two factors; the abundance of weathering resistant K-rich minerals such as biotite, muscovite and

K-felspar in sediments and exchange of dissolved K with clay minerals. K gets associated with clay minerals by exchange and/or adsorption processes during weathering and transport (Nesbitt et al., 1980), a result of interaction between dissolved K with the residual solid phase. K concentration in sediments vary from ~0.15 to 0.6 wt% with an average of (0.37 ± 0.15) wt.% (Table 5.1), overlapping with its abundance in basalts $\sim 0.39 \pm 0.26$ wt.%. The similarity in average K abundance and its wide range both in basalts and sediments make it difficult to quantitatively assess its mobility during weathering and transport, similar to the observations in weathering profiles (Wilkins et al., 1994). The results, however, indicate that K is not mobilized to any significant extent from Deccan basalts. Further, K also does not show any strong correlation with other major elements, possibly because of its exchange/adsorption from solution phase and the variable abundance of K rich minerals.

Ba, though is a member of the alkaline earth group, its relation with Ca shows a significant scatter, indicative of their different geochemical behavior during weathering and transport. Ba concentrations in the sediments analysed range from 79 to 273 $\mu\text{g g}^{-1}$ (average: 189 ± 43 $\mu\text{g g}^{-1}$). This compares with the range of 48–285 $\mu\text{g g}^{-1}$ in Deccan basalts (average: 133 ± 60 $\mu\text{g g}^{-1}$; Subbarao et al., 2000). The average and range of Ba in sediments and basalts overlap within errors, leading to infer that during weathering and transport Ba is by and large retained in residual phase analogous to K. Ba/Al ($\mu\text{g g}^{-1}$ / wt.%) in sediments vary from 11.6 to 39.6 (average 25 ± 7) as compared to the basalt ratio of 18 ± 8 further strengthening the inference of resistance of Ba-minerals to weathering. Indeed, Ba seems to be more closely associated with K as evident from its strong correlation with it ($r^2=0.8$; Fig. 5.6). Dalai et al. (2004) also reported strong coupling between Ba and K in sediments of the Yamuna river system in the Himalaya. Due to similar ionic radius, Ba can substitute for K in many K-bearing minerals (Wedepohl, 1972), as a result, Ba is usually more abundant in the weathering resistant K minerals such as K-felspar, micas, biotite and muscovite. It is also known that Ba is retained in clays and Fe-oxides/hydroxides during weathering and transport (Wedepohl, 1972).

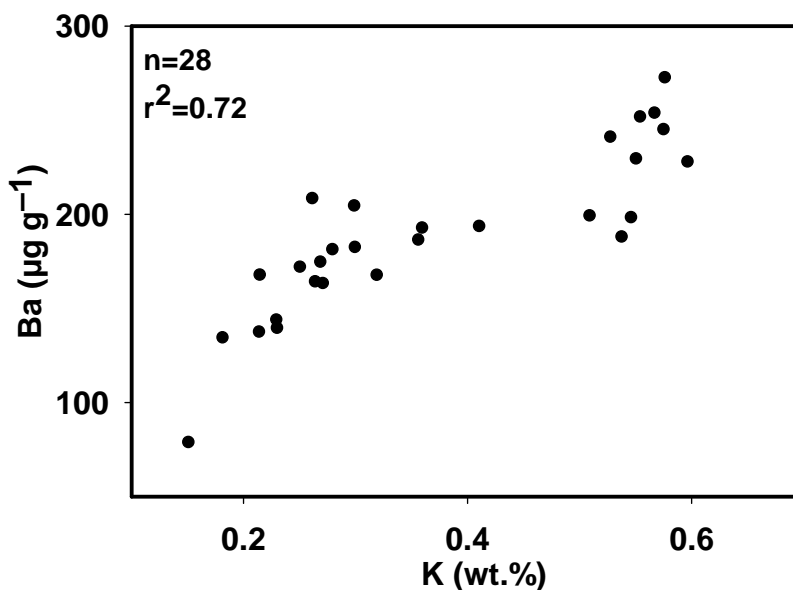


Fig. 5.6. Scatter plot of Ba vs. K. The high correlation between the two elements is evident from the linear trend of the plot.

5.2.3 Iron and Titanium

Iron and Titanium, analogous to Al, are two other elements, which because of their geochemical properties in natural waters are expected to be retained in the solid phase during weathering and erosion.

In basalts, Fe and Mg co-occur in ferromagnesium minerals, which also contain Ti. In sediments, minerals of Fe are generally more abundant in the sand fraction, whereas Fe occurs with clays in the form of oxy-hydroxides. Ti is a typical lithophile element, mainly tetravalent, and associated with silicates and oxides. The dominant minerals of Ti are titanomagnetite, ilmenite (FeTiO_3) and rutile (TiO_2). These are some of the highly weathering resistant minerals and hence Ti is more likely to be enriched in sediments relative to parent basalts. These minerals are known to be present in Deccan (De, 1974).

Fe abundances in sediments vary widely, from a low 5.85 wt% to a high of 30.2 wt% (Table 5.1). In general, Fe is enriched over Al, probably due to size sorting and mineral differentiation in sediments. Fe (or Ti) is known to be generally associated with all size fractions of solid phases whereas Al is more concentrated in the finer fraction, i.e., clay minerals. As a result, Al and Fe (Ti) can be fractionated in solid phases of rivers depending on the energy carried by the stream. In a turbulent,

energetic river, more fine particles are likely to be transported with water, depleting the sediments in Al. In contrast, in quiescent rivers, clays also will be deposited in the sediments. Thus, size sorting can contribute to abundances of Fe and Al and their variability in sediments. Many samples, such as the KJL-1 and DDG-1 show higher Fe/Al ratios; these samples also show higher concentration of Ti, probably because of presence of Fe-Ti minerals such as ilmenite and titanomagnetite.

Ti in sediments varies from 1.4% to 7.6 wt% (Table 5.1) compared to an average of 1.2 wt% in basalts (Subbarao et al, 2000). In general, Ti shows an enrichment w.r.t. Al in these sediments. The highest abundance of Ti is observed KJL-1 (Table 5.1), which also has a very high concentration of Fe (30.2%). This probably results from higher abundance of ilmenite and titanomagnetite in the river sediment. In general, Ti shows a tight correlation ($r^2=0.76$; Fig. 5.7) with Fe, indicating a strong association between them in sediments, attributable to presence of ilmenite.

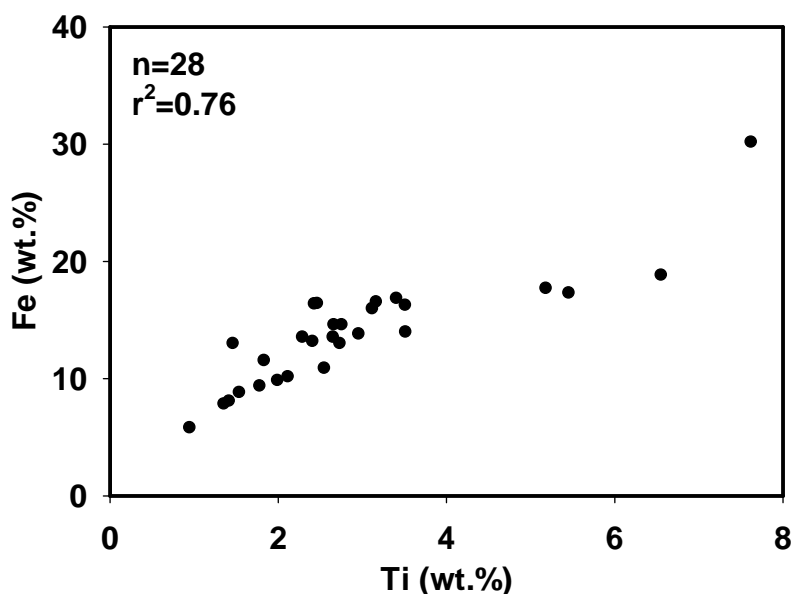


Figure 5.7 Ti correlation with Fe. These two elements are strongly coupled most likely through their presence of common minerals such as ilmenite and titanomagnetite.

Another parameter that provides information on the fractionation between Ti and Al during weathering is “titanium coefficient”, defined as $\text{Al}_2\text{O}_3/\text{TiO}_2$ (wt. ratio). The $\text{Al}_2\text{O}_3/\text{TiO}_2$ in basalts is ~ 6.2 . In general, all sediments analysed in this study have a much lower Ti coefficient than the mean basalt value, largely reflecting either a

greater weatherability of Al compared to Ti or because of size sorting leaving the bed sediments enriched in Ti minerals. The average Ti coefficient in Bhima and Krishna rivers are 5.4 and 2.8 respectively. In contrast, the west flowing WG rivers having more stream energy, show an average Ti coefficient of ~2. A quantitative relationship between Ti coefficient and weathering intensity is difficult to arrive at because of multiple processes governing the abundance of Ti and Al in sediments, which include the variable Ti/Al ratios in Deccan basalts and preferential settling of titanium rich minerals.

5.3 Measure of Depletion/Enrichment of elements in sediments

The percentage depletion or enrichment (PD or PE respectively) of an element in sediment is calculated using the following equation (Canfield, 1997).

$$(\text{PD or PE}) = \left[\frac{(X/\text{Al})_{\text{sed}} - (X/\text{Al})_{\text{bas}}}{(X/\text{Al})_{\text{bas}}} \right] \times 100 \dots\dots\dots(5.1)$$

where X=Na, Mg, Ca, Sr etc.

In this calculation it is assumed that Al behaves conservatively, i.e., it is not mobilized into the solution phase (Garrels and Mckenzie, 1971). The percentage depletion (enrichment) is a measure of the extent of mobilization (or enrichment) of an element from basalts to river water. For example, a percentage depletion (or enrichment) of 90% means that the Al normalized ratio of the element in sediment is one-tenth (or ten times) of that of that in basalts. The percentage depletion or enrichment of various elements in sediments analysed in this study is reported in Table 5.4.

Na is depleted in the sediments from 25 to 96% with an average of $\sim 65 \pm 20\%$. This implies that on average about two-thirds of Na is lost (relative to Al) from basalts to dissolved phase in rivers over the residence time of sediments. The average depletion of Mg and Ca_{sil} are also similar to that of Na within errors, $51 \pm 26\%$ and $65 \pm 22\%$ respectively. Sr shows both depletion and enrichment. The depletion varies from 9 to 89% (average: $24\% \pm 50\%$). If these calculations are made by excluding samples with $\text{CaCO}_3 > 0.5$ wt.% in sediments to avoid any uncertainty because of the incorporation of Mg and Sr in carbonates, the average percent depletion of Mg and Sr are 67 ± 16 and 59 ± 16 respectively (n=16). The similarity in these depletion factors, further attest to the conclusions arrived earlier that all these four elements are mobilized from Deccan basalts to river waters nearly congruently.

With a view to assess spatial variability in the mobilization of various elements, the percentage depletions are compared for the various sub-basins. These

results given in Table 5.4, show that in the large river systems such as the Bhima and the Krishna, on average, Na is mobilized from basalts roughly to the same extent (55%). Relative to the Bhima and the Krishna sediments, those from the east flowing tributaries of the Krishna, and the west flowing rivers show a higher depletion ranging from 65% to 96%. This higher depletion of Na in the WG rivers signifies more intense chemical weathering in these rivers.

In general, all elements show higher depletion in the tributaries of Krishna and WFWG. This can be interpreted in terms of more intense weathering in these regions.

Analogous to Na and Ca, Sr also shows maximum depletion in sediments of Krishna tributaries and WFWG rivers. In the Krishna, Bhima and the Bhima tributaries, Sr behaviour is inconsistent. In sediments of the Bhima tributaries, for example, there is an enrichment of Sr. This behaviour can result if part of Sr is associated with CaCO_3 , which is abundant in the Bhima system samples. Indeed, Sr-enrichment shows a positive correlation ($r^2 = 0.5$, $n=11$) with the CaCO_3 content in sediments (with $\text{CaCO}_3 > 2\%$) indicating that CaCO_3 may be sequestering part of Sr in sediments.

Weathering profile (from basalts to a bole) studies by Wilkins et al. (1994) also suggest the depletion of Ca (~60%) and Na (~75%) and Mg (~35%) from basalts. K behaviour is highly variable and shows little apparent change within the profile. Fe and Al abundances though varying, they show very little change (loss/gain) within the profile. All these attest to the findings that are borne out of the present study from the chemistry of river sediments.

5.4 Chemical Index of Alteration (CIA)

One approach to quantify the extent of chemical weathering is through the calculation of chemical index of alteration, CIA, (Nesbitt and Young, 1982) defined as

$$\text{CIA} = [\text{Al}_2\text{O}_3 / (\text{Al}_2\text{O}_3 + \text{Na}_2\text{O} + \text{K}_2\text{O} + \text{CaO}^*)] \times 100 \dots\dots\dots(5.2)$$

The CIA values are calculated using the molar concentrations of the oxides, CaO^* being the concentration of CaO derived only from silicates. In this study, Ca derived from carbonates has been corrected by assuming that all carbonates to be CaCO_3 . Further, it is also assumed that there is no contribution of Ca from apatites. As weathering progresses, the more labile cations such as Na, Ca and Mg would be released from the source rocks, thereby depleting their concentrations in the residual material. In contrast, the less mobile elements such as Al, Fe and Ti concentrations

would increase in the residue. Thus, with increase in silicate weathering, the ratio would increase, ultimately reaching the limiting value of 100. Typical CIA values for

Table 5.4 Percentage depletion/enrichment of elements in the Deccan Trap sediments.

	Na	K	Mg	Ca _{sil}	Fe	Ti	Sr	Ba
Krishna mainstream								
KRS-1	-54	-36	-27	-35	97	372	22	45
KRS-2	-77	-24	-69	-76	10	42	-62	16
KRS-3	-65	-30	-49	-50	37	104	-5	27
KRS-4	-26	-20	-13	-17	48	136	32	41
KRS-5	-64	-37	-50	-59	30	148	2	47
Average	-57	-29	-42	-47	44	160	-2	35
SD (1σ)	19	7	22	23	32	125	37	14
Bhima mainstream								
BHM-1	-79	23	-63	-79	6	-9	-47	70
BHM-2	-47	53	-34	-49	5	60	13	85
BHM-3	-50	58	-34	-63	-18	9	-1	76
BHM-4	-51	51	-39	-56	-8	21	17	100
BHM-5	-42	67	-20	-62	-12	16	44	117
Average	-54	50	-38	-62	-5	19	5	90
SD (1σ)	15	16	15	11	11	26	33	19
Bhima Tributaries								
GHOD-1	-46	45	-26	-39	12	35	2	80
GHOD-2	-61	67	-35	-78	-31	-15	31	70
MTH-1	-52	43	-36	-48	-3	40	1	90
NIRA-1	-29	-27	3	-28	24	96	85	30
NIRA-2	-29	-13	-8	-31	35	139	64	64
Average	-43	23	-20	-45	7	59	37	67
SD (1σ)	14	41	17	20	25	60	37	23
Krishna Tributaries								
KYN-1	-65	-24	-53	-60	34	92	-35	17
KYN-2	-78	-42	-67	-74	21	36	-57	15
VRN-1	-70	-27	-69	-73	28	109	-50	29
PGN-1	-69	-38	-68	-72	68	274	-45	24
GTP-1	-96	-1	-89	-97	2	41	-88	5
HRN-1	-90	5	-81	-91	4	45	-80	20
TPN-1	-95	-21	-90	-97	20	97	-85	9
DDG-1	-79	-43	-69	-78	92	408	-66	7
VDG-1	-93	-28	-84	-93	23	83	-82	13
BGW-1	-87	-41	-81	-88	34	96	-77	12
Average	-82	-26	-75	-82	33	128	-66	15
SD (1σ)	11	17	12	13	28	119	19	8
WFWG rivers								
SUKH-1	-84	-60	-76	-83	38	58	-73	-14
KJL-1	-79	-58	-40	-68	220	515	-71	-36
VAT-1	-76	-47	-53	-64	49	128	-59	-3
Average	-80	-55	-57	-71	102	234	-68	-18
SD (1σ)	4	7	18	10	102	247	7	17

some common rocks and rock forming minerals are (Nesbitt and Young, 1982): unweathered albite, anorthite and K-felspar ~50, diopside has 0; fresh basalts have in the range of 30–45, granites 45–55. Clays minerals such as illite and montmorillonite have 70 to 85, the CIA values for kaolinite and chlorite are ~100 whereas the average shale has values within 70-75 (Nesbitt and Young, 1982). From the composition of laterites (Widdowson and Gunnell, 2004), the CIA values of laterites—common end product of the basalt weathering, can be calculated to be ~100.

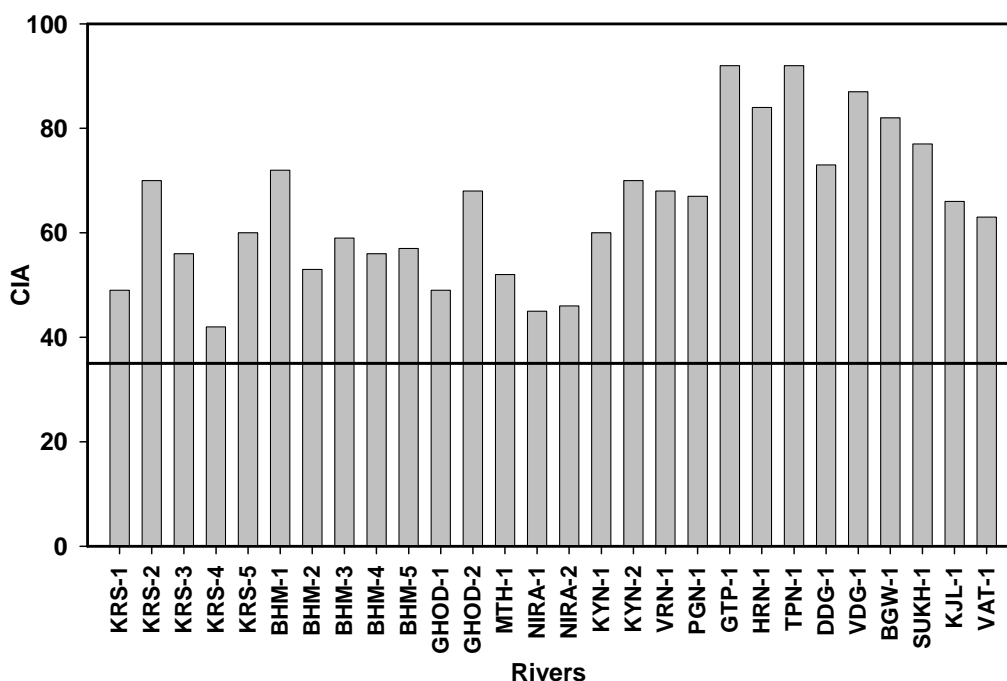


Figure 5.8. CIA values of individual river sediments analysed. The line parallel to X-axis is the CIA for un-altered Deccan basalts. The height of the bars above the reference basalt line indicates the extent of alteration of sediments w.r.t. basalts.

The average CIA value of Deccan basalts, based on the reported composition (Subbarao et al., 2000) is ~35. Fig. 5.8 is a bar diagram of CIA value of sediments analysed in this study with the reference line that of the un-weathered basalt. The height of the bars above the “basalt line” indicates the extent of chemical alteration of the sediments. It shows that the least altered sediment is KRS-4 (CIA=42) and the most altered is TPN-1 (92). The frequency distribution of CIA (Fig. 5.9) shows that it is fairly evenly distributed in the range of 40–80 indicating varying degrees of alteration. This is consistent with the observations made earlier from the distribution of sample data in ternary plots. Average CIA of the two large river systems, the Krishna and the Bhima, are roughly the same with CIA values of 55 ± 11 and 59 ± 7

respectively. In contrast, the smaller tributaries of the Krishna and the west flowing western ghat river sediments have higher CIA values of 75 ± 11 . The higher CIA values for the smaller WG rivers can result from more intense weathering, and/or higher abundances of laterites in these sediments, lateritic soils being brought into rivers by higher amount of rainfall.

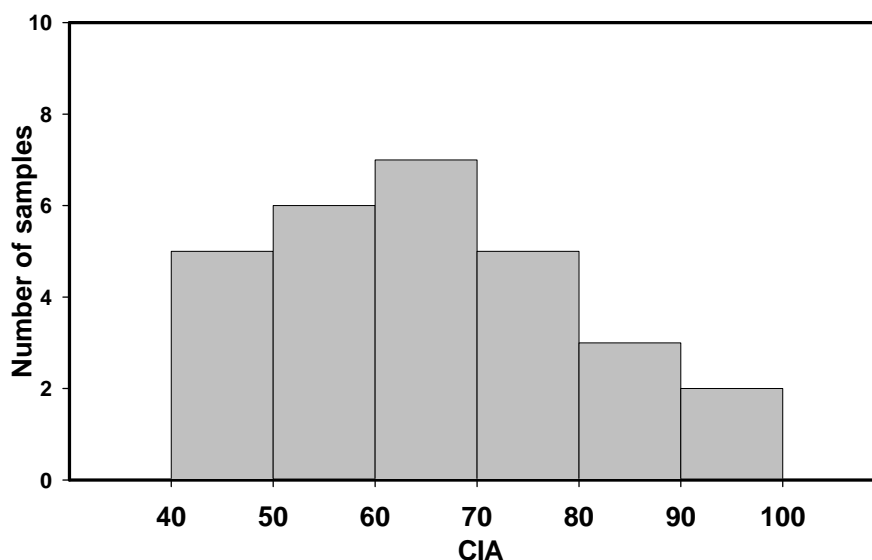


Figure 5.9. Frequency distribution of CIA. The nearly uniform spread between values of 40 to 80 in the distribution suggests the widely varying extent of alteration within the basin.

5.5 Sediment composition and physical erosion

The concentration of elements in particulate and dissolved phases, coupled with that of bedrock composition, can be used to derive particulate matter abundances. This is based on a steady state erosion model for fluvial transport, which hypothesizes that the amount of sediment produced in a drainage basin is equal to the amount exported by the rivers (Stallard, 1995; Gaillardet, 1999b). The model is a material balance between the amount of eroded bedrock and the amounts of solutes and sediment in rivers. Essentially, it is an interplay between chemical weathering, releasing solutes to the rivers and, physical weathering, which transports the solid residues (soils/sediments) of chemical weathering. If $C_{bas}(i)$, $C_{sed}(i)$ and $C_r^{sil}(i)$ denote the concentration of an element (i) in basalt, sediment and rivers (derived from silicates) respectively, then the steady state material balance equation can be written as:

$$M_{bas}C_{bas}(i) = M_{sed} \cdot C_{sed}(i) + C_r^{sil}(i) \dots \dots \dots (5.3)$$

Where M_{bas} and M_{sed} ($M_{bas} > M_{sed}$) are the mass of basalt eroded and suspended load per unit volume of river water (g l^{-1}). For a weathering resistant mineral (e.g. Al),

with almost no contribution from the dissolved phase to its budget, equation (5.3) reduces to

$$M_{bas}C_{bas}(Al) \approx M_{sed} \cdot C_{sed}(Al) \dots\dots\dots(5.4)$$

Combining these two equations, will yield (5.5), which relates the weathering index of an element to its concentration in rivers and sediments, and sediment yield.

$$WI(i) = 1 + C_r^{sil}(i)/M_{sed} \cdot C_{sed}(i) \dots\dots\dots(5.5) \text{ where } i = \text{Na, Ca and Mg.}$$

The sediment yield can be calculated from the slope of $C_r^{sil}(i)/C_{sed}(i)$ vs. $WI(i)$. Cations derived from silicate weathering in river waters, $C_r^{sil}(i)$, are discussed in Das et al. (2005; Chapter three). Using dissolved Mg as a proxy of silicate weathering; Ca and Na derived from basalts are calculated from their abundance ratio in basalts (Chapter three).

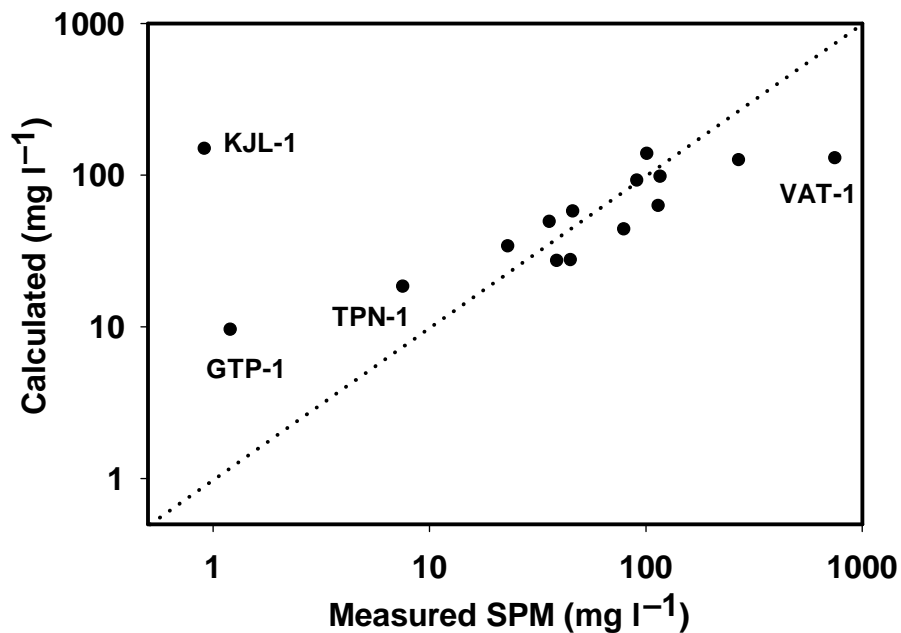


Figure 5.10. Scatter plot of estimated and the observed sediment yield, assuming steady state model of erosion. Except four samples, the data show a good agreement within factors of 2-3. The dotted line is the 1:1 line.

Fig. 5.10 is a plot of the predicted and the measured sediment yield (in mg/l). Of the 15 samples, 3 samples (GTP-1, VAT-1 and KJL-1) plot far away from the equiline; whereas others are generally within a factor of ~2-3 indicating that in a majority of the samples, there is an overall agreement between the predicted and the measured sediment yields. Factors, which can contribute to discrepancy, include trapping of sediments along the course of rivers by check dams, flash flooding causing transient

physical erosion and enhancing sediment fluxes, snap snot single time sampling, the impact of bed load in contributing to removal of eroded parent material and heterogeneity in sediment composition.

Therefore, a more detailed study involving long term monitoring of sediment yield (to obtain a time average data) and more representative sampling of river sediment (suspended and bedload) may help in obtaining better estimates of physical weathering. Further, Sr and Nd isotope studies may also help in sediment budget studies.

5.6 Minor elements

In addition to the major elements discussed in the preceding sections, the abundances of several minor and trace elements were also measured in the sediments to characterize their behaviour during weathering and transport.

5.6.1 Manganese and Phosphorous

The average Mn concentration in basalts is ~0.15 wt%. Mn in sediments vary from ~0.11 wt% to 0.27 wt%. Mn/Al in basalts is $\sim 0.021 \pm 0.03$ as compared to the range of values of 0.016–0.043 in sediments. These numbers indicate that Mn behaviour during weathering and transportation is variable. One of the cause for Mn enrichment is particle sorting, another from its removal onto particulate and hydroxides along with Fe. The positive correlation between Mn/Al and Fe/Al (Fig. 5.11) is suggestive of the association of Fe and Mn during weathering and transport in the Deccan Traps. Enrichment of Mn can also occur if Mn rich solids are discharged to these rivers from industrial sources. Heavy metal pollution from industrial sources, and discharge of domestic sewage and municipal wastes are reported for the Koyna and the Krishna rivers (Trivedy, 2000). Industries that engage in ferromanganese alloys could be a source of Mn to rivers. The depletion of Mn can arise, if it is released to solution and transported out. Sub-oxic and reducing conditions favour such release of Mn; physical process, such as particle sorting may also contribute to Mn depletion.

Phosphorus in basalts occurs mainly as apatites (Best, 1986). The average concentration of P in basalt is $\sim 830 \mu\text{g g}^{-1}$, based on the reported abundance of 0.19% of P_2O_5 (Subbarao et al., 2000). The P concentration in sediment samples range between 470 and $\sim 1800 \mu\text{g g}^{-1}$. However, in a majority of the samples it is less than that in basalts, indicating its loss to rivers during weathering. Sediments with P in excess of basalt concentration require additional inputs or precipitation of P from dissolved phase to the sediments. Co-precipitation of P along with hydroxides and oxides of Fe are reported by Berner and Rao (1994). In addition, P in sediments can have contribution from land derived organic matter (Jha et al., 1990) and fertilizers.

5.6.2 V, Cr, Ni, Cu and Zn

The trace element abundances in basalts are highly variable, and therefore, the quantification of their relative mobility/enrichment during weathering is difficult to

assess critically. The abundances ($\mu\text{g g}^{-1}$) of these five trace elements in basalts are summarized in Table 5.5.

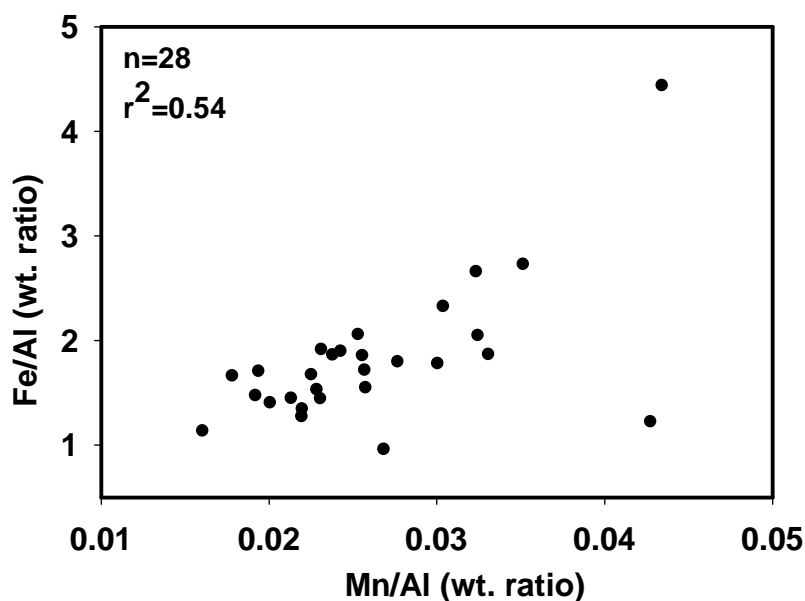


Figure 5.11 Plot of Mn/Al with Fe/Al showing close association of Mn and Fe, mostly Mn associated with Fe-hydroxides (oxides)

Table 5.5 Abundances of trace elements in Deccan basalts

Element	¹ Ambenali (n=60)	¹ Poladpur (n=5)	² Deccan
V	411±44	417±13	-
Cr	-	-	[§] 200±103
Ni	73±14	44±5	[*] 102±44
Cu	237±40	288±77	-
Zn	114±10	159±24	-

¹Peng et al., 1998; ²Subbarao et al., 2000; [§] n=16 and ^{*} n=23 (errors are 1σ)

Vanadium is usually associated with minerals such as pyroxenes, amphiboles, ferromagnetites and magnetites. In sediments, it is known to be associated with organic carbon (Breit and Wanty, 1991; Arthur and Sagemann, 1994). The average V abundance in basalts is $\sim 411 \pm 44 \mu\text{g g}^{-1}$ (Peng et al., 1998), resulting in V/Al ($\mu\text{g g}^{-1}/\text{wt.}\%$, hereafter Al normalized ratios of all trace elements are in $\mu\text{g g}^{-1} / \text{wt.}\%$) ratios of $\sim 56 \pm 7$. In contrast, V/Al in sediments shows much larger range, it varies from ~ 40 to ~ 320 (average 84 ± 54), the higher values indicating large enrichments. These enrichments are probably due to its association with Fe and Ti minerals such as magnetite and titanomagnetite. In general, V shows tight correlation with both Fe and Ti ($r^2 = 0.84, 0.82$ respectively).

Cr shows large variability in basalts, ranging from ~ 80 to $400 \mu\text{g g}^{-1}$ (average: 203 ± 100 ; Subbarao et al., 2000). Cr/Al ratio in sediments vary from 15 to 41 overlapping with the range of ~ 11 to ~ 55 in basalts indicating that Cr is not mobilized significantly during weathering and erosion. The role of industrial pollutants in modifying Cr abundances in sediments needs to be assessed, as it is known to be used in selected industries.

Similar to Cr, Ni also varies significantly in basalts, its concentration ranges between $\sim 35 \mu\text{g g}^{-1}$ to $\sim 220 \mu\text{g g}^{-1}$ (av: 102 ± 44 ; Subbaro et al., 2000). Ni/Al ratios in sediments generally vary with in a narrow range of ~ 11 to 14 (except in KJL-1, Ni/Al ~ 24). This compares to an average Ni/Al of $\sim 14 \pm 6$ in basalts, assuming an average Ni concentration of $102 \pm 44 \mu\text{g g}^{-1}$ in basalts. The data of Peng et al. (1998) for the Ambenali Formation, however yield, a lower Ni/Al ratio of $\sim 10 \pm 2$. All these numbers overlap with each other, suggesting comparable mobility of Ni relative to Al. Ni shows good correlation with Fe ($r=0.77$), probably resulting from its association with Fe in ferro-magnesium minerals.

Cu is mainly associated with sulfide mineral, and chalcopyrites are reported in basalts (Sen, 2001). Cu/Al ratios in sediments range from ~ 20 – 84 (average 34 ± 12) as compared to average basalt value of $\sim 32 \pm 6$ (Peng et al., 1998). This indicates contrasting geochemical behavior of Cu in sediments, and overall indication of similar mobility relative to Al. Average Zn/Al ratio in basalts is $\sim 16 \pm 2$ whereas the Zn/Al ratios in sediments vary from ~ 14 to ~ 60 (Average 24 ± 9). Therefore, overall Zn shows an indication of enrichment in these sediments. In addition, inputs of Zn in the Krishna and the Koyna from anthropogenic sources are also reported (Trivedy, 2000).

5.7 CONCLUSIONS

The abundances of Ca, Mg, Na and Sr in sediments relative to parent basalts confirm that they are quite mobile during chemical weathering. The inter-element ratios relative to that in basalts suggest that all these elements are released to the waters nearly congruently ($\pm 20\%$), however, there is a hint that Ca may be released marginally more than others. Sr in some of the sediments is enriched relative to basalts possibly because of its incorporation in carbonates. The conclusions derived from the sediment data are consistent with the findings that are obtained from major ion data in dissolved phases. The major loss of these elements from basalts is also attested from the reported weathering profile study (Wilkins et al., 1994) from this

region. Fe and Ti are retained in the solid phases, and they show similar behaviour during weathering and transport, possibly due to their close association in heavy mineral (titanomagnetite, ilmenite) phases. Their abundances in sediments are also governed by particle and size sorting of minerals. K abundances in sediments overlap with that of basalts indicating its overall poor mobility during weathering and transport. Ba shows similar behaviour with K and correlates well with it.

Based on steady state models, sediment yield estimates have been made. These estimates are in general in agreement within factors of ~2-3 with measured values. It is, however, recognized that snap-shot, single event sampling may not be representative of the chemistry and abundance of particulates matter. Further, factors such as damming, flash flood and particle sorting all would contribute to discrepancy between the estimates and observation.

The abundances of several minor and trace elements measured in sediments are highly variable and their ratios w.r.t. Al often overlap with those in basalts. This indicates that the elements analysed by and large are retained in solid phase during chemical weathering and transport. Mn correlates well with Fe, suggestive of its association with Fe phases, most likely in the hydroxides (oxides). P in many of the sediments shows depletion relative to basalts indicating its loss from the apatite phases. In a few sediment samples, however, P is enriched probably because of its sequestration with Fe-hydroxides.

Vanadium behaviour in sediments is highly variable with signatures of both depletion/enrichment relative to parent basalts and shows good correlation with Fe and Ti indicating its association with Fe-Ti phases. Abundances of Cr and Ni are also highly variable and their ratios relative to Al overlap with those in basalts. Ni correlates with Fe suggestive of its association with ferro-magnesium minerals. More data, especially those in various size fractions, may help in understanding better the weathering geochemistry of these elements.

Chapter Six

Sr concentrations and $^{87}\text{Sr}/^{86}\text{Sr}$ in rivers

6.1 INTRODUCTION

Chemical weathering and erosion of rocks on continents determines their geomorphologic evolution, controls the geochemical cycles of elements, and acts as a sink for atmospheric CO₂ on Ma time scales. Rivers transport the weathering products, both dissolved and particulates to the oceans. In recent years there has been a surge of interest to determine silicate weathering rates on continents as it is a process drawing down atmospheric CO₂. Among the various chemical elements and isotopes that are transported to the oceans by rivers, dissolved Sr isotopes are often considered as a proxy of silicate weathering (Raymo et al., 1988; Singh et al., 1998; Oliver et al., 2003). The relative proportions of silicates and carbonates contributing Sr to rivers determine their Sr isotope composition; therefore, variations in this proportion can affect the Sr isotope composition of oceans. To assess the evolution of Sr isotope ratio in oceans through geologic past, it is necessary to know with a fair degree of accuracy the various sources contributing Sr to the oceans, and their relative magnitudes. River water discharge, mantle inputs through hydrothermal activity, and sediment diagenesis are the major sources of Sr to the oceans (Peterman et al., 1970; Brass, 1976; Elderfield and Gieskes, 1982; Palmer and Edmond, 1989; Richter et al., 1992). The ⁸⁷Sr/⁸⁶Sr ratio of oceans depends on the fluxes and the isotope ratio of Sr supplied by these sources. Measurements of Sr concentration and ⁸⁷Sr/⁸⁶Sr of major world rivers yield an average contemporary riverine Sr flux of 3.3 × 10¹⁰ moles y⁻¹ with ⁸⁷Sr/⁸⁶Sr of 0.7119 (Palmer and Edmond, 1989). In comparison, hydrothermal input (⁸⁷Sr/⁸⁶Sr ~0.7035, Palmer and Edmond, 1989) and pore water source (⁸⁷Sr/⁸⁶Sr 0.706-0.709; Elderfield and Gieskes, 1982) tend to buffer the more radiogenic Sr from rivers to yield a contemporary seawater ratio of ~ 0.7092. The ⁸⁷Sr/⁸⁶Sr of seawater has undergone significant excursions in the past (Palmer and Elderfield, 1985; Hess et al., 1986; Veizer J, 1989; Richter et al., 1992).

The ⁸⁷Sr/⁸⁶Sr evolution of seawater (Fig. 3; Hess et al., 1986; Richter et al., 1992) over the last ~ 100 Ma show that (i) it has been steadily increasing from a value of 0.7078 about 40 Ma ago to the present day value of 0.7092 (ii) there is an overall marginal decrease in ⁸⁷Sr/⁸⁶Sr during 67 Ma to ~ 55 Ma with a maximum around 66 Ma, around K/T boundary. The steady increase in ⁸⁷Sr/⁸⁶Sr during the past ~ 40 Ma has been attributed primarily to the weathering of the Himalaya, Andean and Alpine orogenies supplying more radiogenic Sr to the oceans via rivers (Palmer and

Elderfield, 1985; Raymo et al., 1988; Hodell et al., 1989; Krishnaswami et al., 1992; Richter et al., 1992). The uplift of the Himalaya and the weathering and erosion of silicic rocks rich in radiogenic Sr by the Ganga-Brahmaputra and the Himalayan rivers has been suggested as an important source of radiogenic Sr to the oceans during this period (Edmond, 1992; Krishnaswami et al., 1992; Richter et al., 1992).

The Sr concentration and its $^{87}\text{Sr}/^{86}\text{Sr}$ ratio in rivers are, in general, derived from two major sources; the silicates (more radiogenic in $^{87}\text{Sr}/^{86}\text{Sr}$) and carbonates (with lower $^{87}\text{Sr}/^{86}\text{Sr}$). Carbonates rocks, which generally are of marine origin, supplies Sr with $^{87}\text{Sr}/^{86}\text{Sr} \sim 0.707$ to ~ 0.709 . Exceptions to this general trend are some very radiogenic carbonates reported in the Himalaya (Blum et al., 1998; Singh et al., 1998; Bickle et al. 2001). The $^{87}\text{Sr}/^{86}\text{Sr}$ of silicate rocks depends on their age and Rb content. For example, granites, gneisses and shales of the Himalaya have $^{87}\text{Sr}/^{86}\text{Sr}$ ratios ranging from ~ 0.71 -1.0 (Krishnaswami et al., 1999; Jacobsen et al., 2002). In comparison, uncontaminated basalts which are of mantle origin and recently emplaced, such as the Deccan Traps, have $^{87}\text{Sr}/^{86}\text{Sr}$ of ~ 0.704 (Mahoney et al., 1988). Their weathering, therefore, will tend to buffer the $^{87}\text{Sr}/^{86}\text{Sr}$ of rivers, analogous to input from carbonates. Considering rapid weatherability and global coverage of basalts (Dessert et al., 2001; Das et al., 2005) it becomes important to study their role in influencing the Sr isotope budgets of rivers.

Deccan Traps are a major basaltic region of the world. Rivers draining these basalts have been studied for their major ion chemistry and Sr isotopes (Ramesh and Subramanian, 1988; Trivedi et al., 1995; Dessert et al., 2001; Das et al., 2005). Sr isotope study by Dessert et al. (2001) in the Narmada and the Tapti river systems showed $^{87}\text{Sr}/^{86}\text{Sr}$ variations from 0.707-0.714. The more radiogenic Sr isotope composition of the Narmada and Tapti can be a result of crustal contamination of Deccan basalts (Mahoney, 1988) and the presence of lithologies other than basalts in the drainage basin. The Sr concentration of these rivers yield an average Sr flux of $3.75 \times 10^8 \text{ mol y}^{-1}$ from Deccan. This flux represents $\sim 3.5\%$ of the annual dissolved *silicate* riverine Sr flux and $\sim 1.15\%$ of global supply of Sr to oceans via rivers (Dessert et al., 2001). These are, however, disproportionately higher than the exposed area of the Deccan ($\sim 0.4\%$ of the continental area).

The role of Deccan in contributing to Sr isotope excursions in oceans around ~ 66 Ma ago with the major pulse of its eruption coinciding with K/T boundary has been a topic of interest among geochemists.

Model calculations (Dessert et al., 2001) predict a rise in temperature by $\sim 4^{\circ}\text{C}$ due to the Deccan Trap emplacement and associated CO_2 release ~ 66 Ma ago. It is argued that the higher temperature and the higher CO_2 partial pressure could have caused enhanced weathering of the continents resulting in an increase in the $^{87}\text{Sr}/^{86}\text{Sr}$ ratios of oceans around ~ 66 Ma, coinciding with the K/T boundary (Officer and Drake 1983; Dessert et al., 2001). This suggestion is consistent with the reported high-resolution $^{87}\text{Sr}/^{86}\text{Sr}$ data of foraminifera during this time period, which show a spike (Martin and Macdougall, 1991; Vonhof and Smit, 1997). An alternative hypothesis for the minor peak in $^{87}\text{Sr}/^{86}\text{Sr}$ at KTB ~ 66 Ma ago is that it is a result of enhanced continental weathering brought about by impact of extraterrestrial bolides on the earth (Mcdougall, 1988; Martin and Mcdougall, 1991; Vonhof and Smit, 1997; Ravizza and Peucker-Ehrenbrink, 2003). These authors also reported a minor dip in $^{87}\text{Sr}/^{86}\text{Sr}$ ~ 150 ka before KTB, which they attribute to non-radiogenic Sr released from Deccan basalts.

A key set of data needed to assess the role of Deccan Traps in contributing to $^{87}\text{Sr}/^{86}\text{Sr}$ excursion in ocean is Sr flux and $^{87}\text{Sr}/^{86}\text{Sr}$ transported by rivers draining them. In light of this, the present study was initiated (i) to obtain Sr flux and the $^{87}\text{Sr}/^{86}\text{Sr}$ ratio of rivers draining the Deccan basalts, (ii) to identify and characterize the sources of Sr in these waters, and (iii) to establish the role of Deccan basalt weathering in defining the marine $^{87}\text{Sr}/^{86}\text{Sr}$ record around the K/T boundary period (~ 66 Ma ago).

6.2 RESULTS AND DISCUSSION

Sr concentrations and the $^{87}\text{Sr}/^{86}\text{Sr}$ isotope ratios of rivers analysed are reported in Table 6.1. Also presented in this Table are Si, HCO_3 , Ca and Mg concentrations in the dissolved phase. Detailed discussions on the geochemistry of the major elements were presented in chapter three. In this chapter, the discussion is focused on the Sr geochemistry and its relation to major elements. Sr in the water samples vary from ~ 130 nM to ~ 1390 nM (average ~ 490 nM) with $^{87}\text{Sr}/^{86}\text{Sr}$ ratio of 0.70614 to 0.70986, about two thirds of the samples have ratios of 0.706-0.708. Samples with the higher $^{87}\text{Sr}/^{86}\text{Sr}$ of 0.708-0.710, mainly belong to the Bhima, Ghod and the Mutha rivers.

Table 6.1 Ca, Mg, Na, HCO₃ and Si (μM), Sr (nM), and ⁸⁷Sr/⁸⁶Sr in rivers.

Code	River	Ca	Mg	Na	HCO ₃	Si	⁸⁷ Sr/ ⁸⁶ Sr	Sr
<u>Krishna</u>								
<u>mainstream</u>								
KRS-1	Krishna	454	270	484	1468	334	0.70686	592
KRS-2	”	329	206	363	862	291	0.70706	567
KRS-3	”	490	295	410	1653	350	0.70690	705
KRS-4	”	645	375	503	2226	419	0.70682	798
KRS-5	”	390	247	468	1326	327	0.70683	679
KRS-6	”	903	578	587	3252	520	0.70690	1394
<u>Bhima sytem</u>								
BHM-1	Bhima	182	110	174	585	309	0.70822	378
BHM-3	”	768	479	1229	2464	396	0.70977	1029
BHM-4	”	822	547	1494	2499	390	0.70969	1240
<u>Tributaries of Bhima</u>								
GHOD-1	Ghod	610	340	327	1999	418	0.70858	907
MTH-1	Mutha	771	464	1137	2501	398	0.70986	930
<u>Tributaries of Krishna</u>								
KYN-1	Koyna	309	201	276	1111	353	0.70692	499
KYN-2	Koyna	81	59	103	300	179	0.70698	164
VRN-1	Varna	297	185	273	990	292	0.70695	352
PGN-1	Panchganga	208	125	239	611	238	0.70718	368
PGN-2	Panchganga	212	138	210	680	257	0.70713	346
GTP-1	Ghataprabha	74	52	127	212	126	0.70842	149
HRN-1	Hiranyakeshi	71	54	131	216	128	0.70819	134
TPN-1	Tambrapani	107	74	150	319	166	0.70842	194
DDG-1	Doodhganga	289	168	223	835	268	0.70733	322
VDG-1	Vedganga	172	110	178	562	247	0.70751	301
BGW-1	Bhogwati	193	128	192	603	271	0.70717	360
<u>West flowing Rivers</u>								
ARJ-1	Arjuna	167	131	181	633	366	0.70683	206
GAD-1	Gad	153	114	179	604	323	0.70984	210
SUKH-1	Sukh	163	130	165	624	332	0.70687	204
KJL-1	Kajli	162	128	168	633	353	0.70614	251
SHT-1	Shastri	181	127	178	678	386	0.70652	281
VAT-1	Vashisthi	197	142	176	725	391	0.70711	225
<u>Others</u>								
AMB-1	Ambika	539	349	265	1876	685	0.70786	493

Typical errors ($\pm 2\sigma$) in ⁸⁷Sr/⁸⁶Sr are 0.00004

The Krishna river was sampled at six locations. The Sr concentrations in the samples show a decrease from the value of ~ 1390 nM (KRS-6) to values of $\sim 650 \pm 100$ nM in the remaining samples. The cause for such a high concentration in KRS-6 is unclear, however, all the major ions also show high concentration in this sample (Table 6.1). The $^{87}\text{Sr}/^{86}\text{Sr}$ ratios of the samples are largely invariant with values in the range of 0.7068-0.7070 (Table 6.1). This near constancy in $^{87}\text{Sr}/^{86}\text{Sr}$ is not unexpected considering that the drainage is made almost entirely of Deccan basalts and the tributaries Koyna, Varna and Panchganga merging with the main stream all have ratios in the range of 0.7069-0.7072.

The Bhima river was sampled at three locations, the $^{87}\text{Sr}/^{86}\text{Sr}$ in these samples, 0.70822 to 0.70977, is marginally higher than those in Krishna. The concentration of Sr in these samples is also high, 1029 and 1240 nM respectively. Two of Bhima's tributaries, the Mutha and the Ghod, also have $^{87}\text{Sr}/^{86}\text{Sr}$ ratios similar to that of the Bhima (0.70986 and 0.70858). The east flowing tributaries and sub-tributaries of the Krishna have Sr ranging from ~ 134 nM to ~ 500 nM (average of ~ 290 nM) with $^{87}\text{Sr}/^{86}\text{Sr}$ of 0.70692 to 0.70842 (Table 6.1). In contrast, the small rivers flowing west into the Arabian sea have Sr within a narrow range of about 240 ± 40 nM and $^{87}\text{Sr}/^{86}\text{Sr}$ from 0.70614 to 0.70984.

In contrast to the rivers draining the Krishna basin, the Narmada-Tapti rivers flowing through the northern Deccan Traps carry more radiogenic Sr (Trivedi et al., 1995; Dessert et al., 2001) with a range of 0.70758–0.71493, with majority of samples having ratios ≥ 0.709 . The more radiogenic Sr isotope composition in the Narmada-Tapti waters can arise from basalts with crustal contamination (Mahoney, 1988) and/or because of contribution of Sr from lithologies in addition to Deccan basalts. Widespread crustal contamination of Deccan basalts contribute to enhancement of the $^{87}\text{Sr}/^{86}\text{Sr}$ though has been reported among the various Formations (Table 6.2). It must be mentioned that the Jabalpur section which forms a part of the Narmada basin has a present day $^{87}\text{Sr}/^{86}\text{Sr}$ in the range of 0.70416-0.70719.

6.2.1 Sources of dissolved Sr:

Chemical weathering of rocks is the main source of dissolved elements to rivers, though; atmospheric deposition and anthropogenic inputs can also be important suppliers. Sr concentrations of rivers draining a single lithology will be governed by the extent of water-rock interaction, and the $^{87}\text{Sr}/^{86}\text{Sr}$ ratio in these rivers will be and

large be that of the rocks. Small differences in $^{87}\text{Sr}/^{86}\text{Sr}$ between rocks and river waters, however, can arise because of differences in weatherability of various minerals in the rock and their $^{87}\text{Sr}/^{86}\text{Sr}$. In case of larger rivers, in addition to water-rock interactions, the contribution from tributaries can also modify their Sr abundance and $^{87}\text{Sr}/^{86}\text{Sr}$. The samples analysed in this study are from rivers which drain the Deccan basalts. Therefore, the Sr concentration in the water would depend on the extent of basalt weathering and the $^{87}\text{Sr}/^{86}\text{Sr}$ of water is expected to be same as or close to that of basalts.

6.2.2 Sr in Deccan basalts:

As already discussed earlier (Chapter two) the Deccan basalts have been subdivided into different Formations. The rivers draining these Formations acquire their Sr and $^{87}\text{Sr}/^{86}\text{Sr}$ from the basalts of these Formations. The Sr abundance and $^{87}\text{Sr}/^{86}\text{Sr}$ of basalts reported for the different Formations are presented in Table 6.2.

The data in Table 6.2 show that the $^{87}\text{Sr}/^{86}\text{Sr}$ of the Ambenali basalts, less than 0.705, is close to pristine mantle values. The Podalpur Formation has values ranging from 0.705 to 0.713, the higher values resulting from the crustal contamination of these basalts (Mahoney, 1988). Among others, the Bushe formation is the most contaminated with $^{87}\text{Sr}/^{86}\text{Sr}$ as high as ~ 0.719 . In summary, the basalts of the western Deccan Traps have $^{87}\text{Sr}/^{86}\text{Sr}$ ranging from 0.704-0.719, indicating that many of them

Table 6.2 Mg, Ca, Sr abundances[§] and $^{87}\text{Sr}/^{86}\text{Sr}$ ratios in different Formations of the western Deccan Traps.

Formation	n	Mg (wt.%)	Ca (wt.%)	Sr ($\mu\text{g g}^{-1}$)	$^{87}\text{Sr}/^{86}\text{Sr}$
Poladpur	4	3.71 \pm 0.49	7.65 \pm 0.36	224 \pm 13	0.705-0.713
Ambenali	3	3.67 \pm 0.43	7.93 \pm 0.43	227 \pm 3	<0.705
Mahabaleshwar	3	3.35 \pm 0.13	7.65 \pm 0.79	227 \pm 14	>0.705
Bushe	3	3.82 \pm 0.95	7.15 \pm 0.43	171 \pm 55	0.713-0.719
Thakurwadi	7	3.91 \pm 0.86	6.93 \pm 1.14	249 \pm 10	-
Bhimashanker	3	3.59 \pm 0.05	7.00 \pm 0.29	254 \pm 3	-
<i>Overall</i>	23	3.74 \pm 0.66	7.29 \pm 0.86	228 \pm 32	

[#] Devey and Lightfoot, 1986; Lightfoot et al., 1990. [§] Subbarao et al., 2000.

have acquired “excess” radiogenic component (in excess of 0.704) due to crustal contamination (Mahoney, 1988). In addition to basalts, other minor phases of the drainage basins include carbonates in basalts, sediments and calcareous tufa. The $^{87}\text{Sr}/^{86}\text{Sr}$ values of these trace carbonate phases are not known. If they have $^{87}\text{Sr}/^{86}\text{Sr}$ ratios overlapping with that of the range in basalts (0.704-0.713), then the use of

$^{87}\text{Sr}/^{86}\text{Sr}$ as a proxy of silicate (basalt) weathering would be limited as the $^{87}\text{Sr}/^{86}\text{Sr}$ of the various components overlap.

In order to constrain the relative significance of different sources to dissolved Sr in Deccan rivers (e.g. silicates, trace carbonates), it is necessary to determine the Sr released from them to solution. For silicates, this is generally done using a proxy of silicate weathering, commonly Na_{sil} ($= \text{Na}_r - \text{Cl}_r$). The silicate component of dissolved Sr is calculated as $[\text{Sr}_{sil} = (\text{Sr}/\text{Na})_{sol} \times \text{Na}_{sil}]$ where $(\text{Sr}/\text{Na})_{sol}$ is the ratio of (Sr/Na) released to solution from basin lithology (Krishnaswami et al., 1999). The use of Na_{sil} as a proxy, can however be compromised if the basin has saline/alkaline soils, which are Cl , SO_4 and carbonate salts of Na. In this work, therefore, Mg is used as an index of silicate weathering (Chapter three; Das et al., 2005). Sr derived from silicate weathering (Sr_{sil}) has been calculated from the relation:

$$\text{Sr}_{sil} = \text{Mg}_r \times (\text{Sr}/\text{Mg})_{sol}$$

where *sil*, *r* refers to silicate, rivers and $(\text{Sr}/\text{Mg})_{sol}$ is the ratio released to solution from basalt weathering. The Mg and Sr data of the west flowing western ghat (WFWG) rivers have been used to calculate the $(\text{Sr}/\text{Mg})_{sol}$, as they are a group of small rivers which receive inputs by and large only from chemical weathering and atmospheric deposition (Chapter three). These rivers (n=6) have an average Mg^* (corrected for rainwater) and Sr of $\sim 114 \pm 9 \mu\text{M}$ and $\sim 230 \pm 31 \text{ nM}$ respectively. This yields Sr/Mg^* ($\text{nM}/\mu\text{M}$) ratio of 2.02 ± 0.31 . Average Sr in different Formations of Deccan basalts varies from $171\text{-}249 \mu\text{g g}^{-1}$ with an average of $228 \pm 32 \mu\text{g g}^{-1}$. Average Mg in Deccan basalts is of $3.74 \pm 0.66 \text{ wt.}\%$ (Table 6.2; Das et al., 2005). This would yield an average of Sr/Mg ($\text{nmole } \mu\text{mol}^{-1}$) of 1.69 ± 0.38 . The Sr/Mg ratios in basalt and waters overlap within errors, indicating that they are released to waters in roughly the same proportion as their abundances in basalts. There, however, seems to be a hint that Sr may be released to waters slightly more preferentially than Mg.

6.2.3 Sr co-variation with other elements:

Figs. 6.1 a,b,c and d are scatter plots of Sr with major ions (Ca^* , Mg^* , Na^* and HCO_3) where * indicates concentration after correction for atmospheric inputs. Only samples which have $\text{Cl} < 300 \mu\text{M}$ and $\text{SO}_4 < 100 \mu\text{M}$ (to minimize anthropogenic and saline/alkaline salt contributions) and having $\text{CSI} < 0$ (Das et al., 2005) are plotted in these figures. It is seen that in all these plots Sr shows strong positive correlation with major ions (Table 6.3). For example, $\text{Ca}^*\text{-Sr}$ plot has r^2 of 0.77 with an intercept of

113 nM and a slope $[\text{Sr (nM)}/\text{Ca } (\mu\text{M})]$ of 1.14 ± 0.13 . This slope compares with the

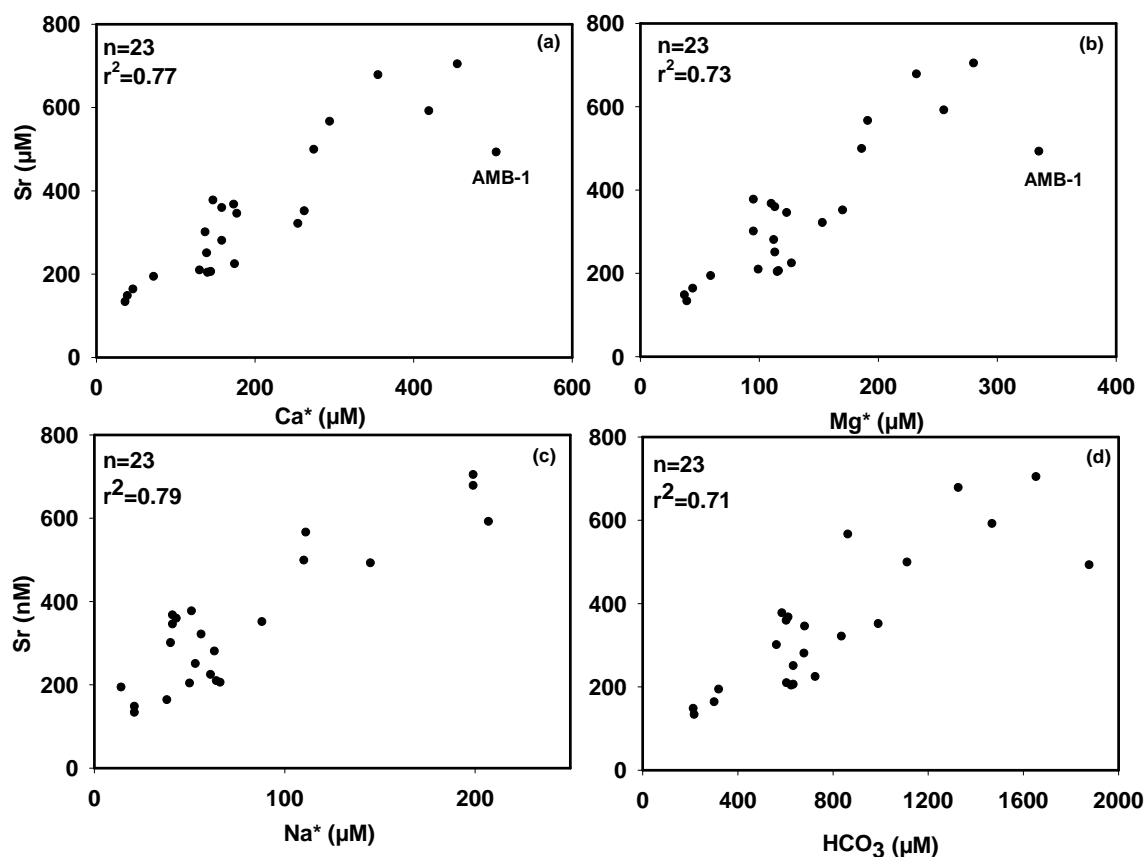


Figure 6.1 (a,b,c,d) Variation of Sr with Ca^* , Mg^* , Na^* and HCO_3^- . A strong correlation between Sr and these major ions is evident. The slope of the respective plots is a measure of relative mobility of these elements w.r.t. Sr.

value of 1.43 ± 0.26 in basalts. This comparison though seems to indicate that Ca may be preferentially mobilized over Sr from basalts, considering that slope of the line overlaps with the ratio in basalts within errors, it can also be argued that both Sr and Ca are mobilized from basalts to rivers to the same extent. The latter inference seems to draw further support from the observation that if the Ambika river data is excluded from the regression analysis (Fig. 6.1a), the slope (1.36 ± 0.12) approaches closer to the basalt ratio with a higher r^2 (Table 6.3).

Similarly, Sr also varies with Mg^* (Fig. 6.1b) and Na^* (Fig. 6.1c) with slopes of 1.86 ± 0.24 and 2.59 ± 0.29 respectively (Table 6.3). These compare with ratios (nM/ μM) of 1.69 ± 0.38 (Sr/Mg) and 3.23 ± 0.68 (Sr/Na) in basalts indicating that Sr and all these major ions are released to rivers in roughly the same proportion as their abundances in basalts. Sr varies positively with HCO_3^- ($r^2 = 0.71$; Fig. 6.1d),

suggesting that these are released to solution in roughly same proportion during weathering, the proportion being governed by the ratio of release of Sr to major cations from basalts. The plot of Sr with Si (Fig. 6.2) however shows significant scatter, the data seem to show two trends. The trend with the lower slope (Sr/Si) corresponds to the WFWG rivers (and Ambika). Cation deficient lateritic soils form a significant part of the drainage basins of these rivers, which may be contributing to lower Sr/Si ratios. Fig. 6.3 is a plot of Sr vs. Si/HCO₃. The trend shows a two end member mixing between a high Sr concentration and low Si/HCO₃, and low Sr and high Si/HCO₃. Weathering of silicates will release both Si and HCO₃ to waters; the Si/HCO₃ in them will depend on the mineralogical and chemical composition of basalts. In contrast, carbonate and apatite weathering will supply Si/HCO₃ with a low ratio close to zero. Based on this criterion, it would require that the high Sr concentration end member to be carbonates and apatites. Analyses of these minor phases are needed to validate this inference. Similar inferences indicating mixing of silicate and carbonate components are drawn from Si/HCO₃ vs. $\delta^{13}\text{C}$ co-variation (Chapter four).

In summary, the ⁸⁷Sr/⁸⁶Sr ratio in Krishna system waters are consistent with the range of ⁸⁷Sr/⁸⁶Sr values reported for Deccan basalts, however, significantly lower than those reported for the rivers draining the northern Deccan Traps (Dessert et al., 2001). Dissolved Sr shows good correlation with all major dissolved cations and HCO₃ indicating that Sr is released to rivers in roughly the same proportions as their abundances in basalts. Co-variation of Sr with Si shows two distinct trends, possibly related to availability of Sr in the lithologies being weathered.

Table 6.3 Statistical analyses of Sr-major ion data.

Pair (Y-X)	n	r ²	Slope	Intercept	Ratio in basalts
Sr-Mg*	23	0.73	1.86±0.24	89±39	1.69±0.38
	22 [#]	0.86	2.34±0.22	35±33	-
Sr-Ca*	23	0.77	1.14±0.13	113±32	1.43±0.26
	22 [#]	0.86	1.36±0.12	80±27	
Sr-Na*	23	0.79	2.59±0.29	146±27	3.23±0.68
	22 [#]	0.78	2.62±0.30	145±28	
Sr-HCO ₃	23	0.71	0.32±0.04	0.40±0.04	-
	22 [#]	0.8	0.40±0.04	0.32±0.04	

[#] (excludes Ambika)

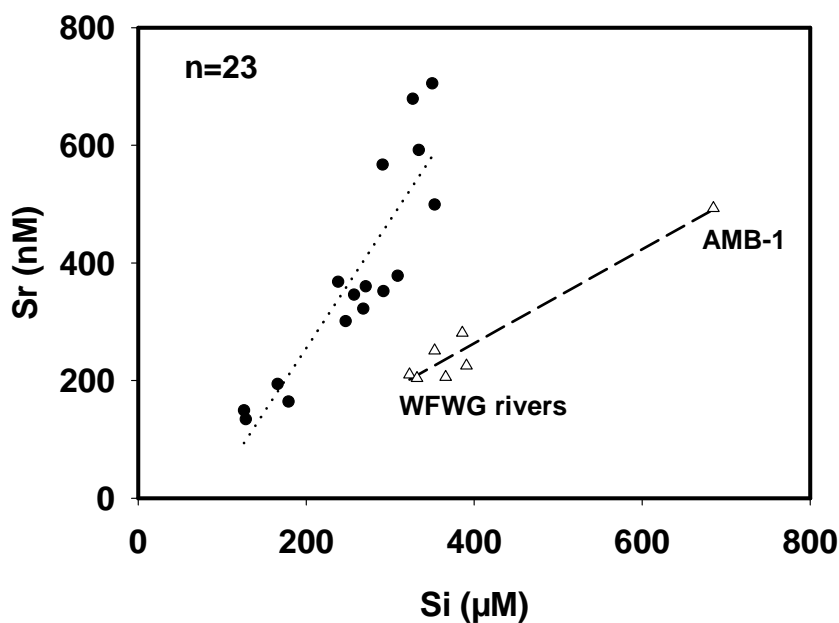


Figure 6.2 Scatter plot of Sr with Si. The data seem to show two trends—the one with a lower slope (dashed line) are from the western ghat rivers and Ambika which drain through cation deficient lateritic soils.

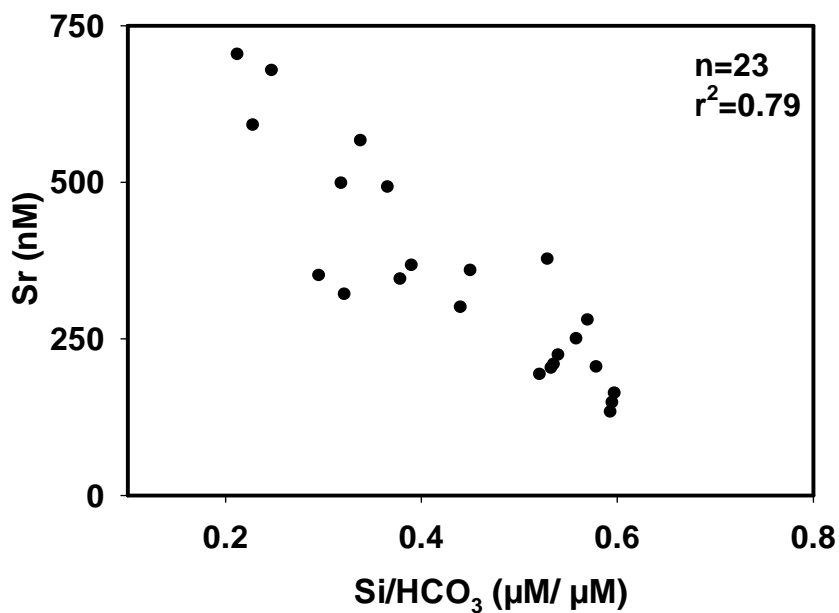


Figure 6.3 Sr shows an inverse correlation with Si/HCO₃, indicating a mixing between silicate and carbonate end members.

6.2.4 Role of Deccan in Sr isotopic excursions of oceans at ~66 Ma:

One of the aims of this study is to assess the effect of Deccan Trap emplacement and their weathering on the marine $^{87}\text{Sr}/^{86}\text{Sr}$ record during the Cretaceous-Tertiary (K/T)

transition. A short-term Sr isotope ratio enrichment around K/T was reported by Hess et al. (1986) though the follow up investigations led to contrasting results. (see, for example, Jones et al., 1987; Koepnick et al., 1988; Macdougall, 1988; Martin and Macdougall, 1991; Nelson et al., 1991; McArthur et al., 1994). This enrichment has been attributed to enhanced continental weathering during the transition, however, the driver contributing to the enhanced weathering is debated, some attribute it to impact of extraterrestrial bolide (Martin and Macdougall, 1991) whereas others, to Deccan Trap emplacement (Officer and Drake, 1983; Dessert et al., 2001.).

Martin and Macdougall (1991) reported high-resolution $^{87}\text{Sr}/^{86}\text{Sr}$ isotope data on foraminifera sampled from DSDP cores. Their data shows general increase in $^{87}\text{Sr}/^{86}\text{Sr}$ from ~ 70 Ma to ~ 66.4 Ma, with the maximum $^{87}\text{Sr}/^{86}\text{Sr}$ of 0.70789 around ~ 66.4 Ma. The data near the K/T boundary show (i) a marked increase from ~ 0.70780 to ~ 0.70789 . This spike in $^{87}\text{Sr}/^{86}\text{Sr}$ has been attributed to increased continental weathering following the Deccan emplacement (Dessert et al., 2001). It is estimated that Deccan volcanism introduced $\sim 10^{18}$ moles of CO_2 to the atmosphere, which contributed to enhanced continental weathering by increasing the surface temperature on earth and also by providing more CO_2 for weathering (Dessert et al., 2001) and (ii) gradual decrease in $^{87}\text{Sr}/^{86}\text{Sr}$ ratio from ~ 0.70789 between 66.4 Ma and 63 Ma attributed to a decrease in continental weathering following the consumption of CO_2 released to atmosphere within few hundreds of kilo years. An alternative hypothesis to the enhanced chemical weathering is the impact of extraterrestrial bolide and associated acid rain (Martin and Macdougall, 1991). The choice between these two hypotheses depends on the timing of major Deccan eruption and K/T boundary, a topic of significant debate. Courtillot et al. (1986, 1999) and others claim K/T boundary to coincide with Deccan eruption, whereas Venkatesan et al. (1993) and Pande (2002) suggest that the main pulse of Deccan eruption predate K/T (or the meteoroid impact at Chixculub, Mexico) by more than ~ 1 Ma.

In addition to these two gross trends, higher resolution (shorter time scales, ~ 100 ka) studies show measurable excursions in $^{87}\text{Sr}/^{86}\text{Sr}$ (Vonhof and Smit, 1997) near K/T boundary. $^{87}\text{Sr}/^{86}\text{Sr}$ records from KTB sections of Bidart (France) and El Kef (Tunisia) show a decrease in $^{87}\text{Sr}/^{86}\text{Sr}$ around ~ 150 ka prior to KTB (Fig. 6.4).

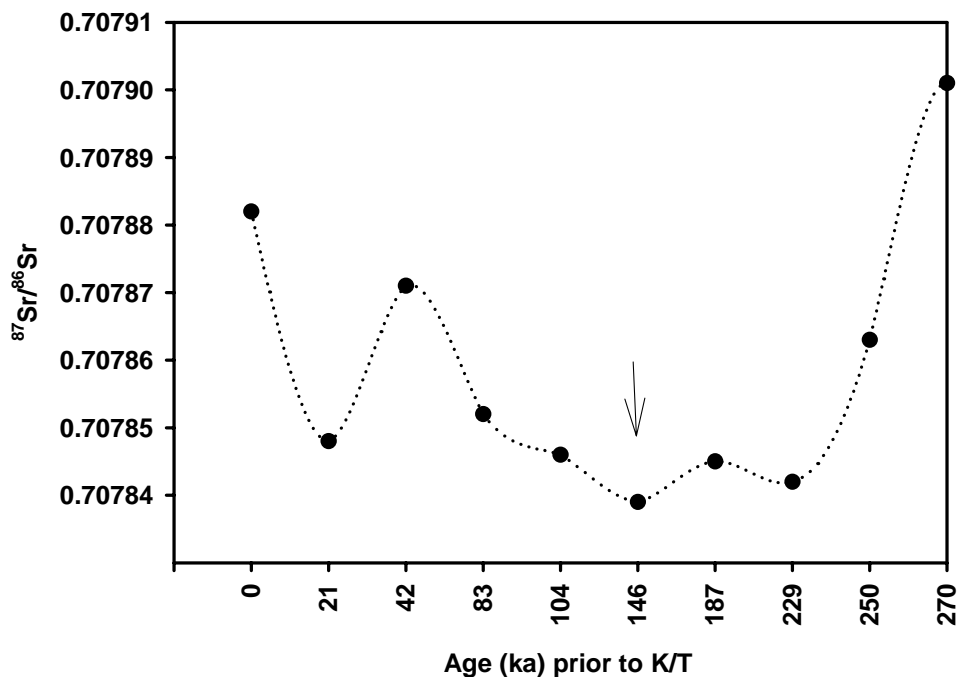


Figure 6.4 Sr isotope excursions observed at K/T site (Bidart, in France). The decrease in ⁸⁷Sr/⁸⁶Sr during ~270-146 Ka is evident, with a dip shown by an arrow at ~146 ka.

This decrease has been attributed to supply of non-radiogenic Sr from weathering of Deccan basalts (Vonhof and Smit, 1997). Implicit in this suggestion is that Deccan erupted prior to K/T. The significance of Deccan in contributing to the decrease can be estimated from commonly used Sr isotope budget models (Brass, 1976; Richter et al., 1992). The pertinent equations for Sr and the ⁸⁷Sr/⁸⁶Sr are:

$$dN/dt = \sum J_n - J_{out} \dots \dots \dots (6.1)$$

$$d(NR_{sw})/dt = \sum J_n R_n - J_{out} R_{sw} \dots \dots \dots (6.2)$$

$$R_{sw} (dN/dt) + N (dR_{sw}/dt) = \sum J_n R_n - J_{out} R_{sw} \dots \dots (6.3)$$

where N is the total moles of Sr in oceans, J_n the fluxes of Sr and R_n the corresponding ⁸⁷Sr/⁸⁶Sr ratio (e.g., rivers, hydrothermal inputs and sediment diagenesis), J_{out} is the total Sr flux out of the oceans (precipitation in the form of carbonates) and R_{sw} is the ⁸⁷Sr/⁸⁶Sr ratio of seawater. In equation (2), the concentration of Sr has been assumed to be proportional to ⁸⁶Sr. From (1) and (3), one can derive

$$N d(R_{sw})/dt = \sum J_n (R_n - R_{sw}) \dots \dots \dots (6.4)$$

Equation (4) can be written in terms of inputs from rivers (riv), hydrothermal alteration (h) and diagenesis (d) as:

$$N d(R_{sw})/dt = J_{riv} (R_{riv} - R_{sw}) + J_h (R_h - R_{sw}) + J_d (R_d - R_{sw}) \dots \dots (6.5)$$

It has been shown by Kump (1989) that diagenetic flux is small relative to J_{riv} and J_h and therefore, can be ignored. Further, the riverine component can be divided into Deccan Trap rivers (dtr) and other world rivers (owr).

$$N d(R_{sw})/dt = J_{dtr}(R_{dtr} - R_{sw}) + J_{owr}(R_{owr} - R_{sw}) + J_h(R_h - R_{sw}) \dots(6.6)$$

The role of Deccan Trap rivers in contributing to either decrease or increase (in the past) the rate of change of seawater ratio (dR_{sw}/dt) is dependent on R_{dtr} . The magnitude of $d(R_{sw})/dt$ will depend on magnitudes of J and $(R_{dtr/owr/d} - R_{sw})$ values in past. If $R_{dtr} > R_{sw}$, then it would enhance the rate of change and if $R_{dtr} < R_{sw}$, it would decrease the rate of change. The present day $^{87}Sr/^{86}Sr$ of most of rivers measured in the study are less than contemporary R_{sw} . The results of Dessert et al. (2001) on Narmada and Tapi, however, show the opposite trend. Considering that the rivers analysed in this study drain Deccan Traps almost entirely and that their major ion chemistry are consistent with inputs from basalts, in the following calculations values of 0.705, 0.706 and 0.707 have been used for R_{dtr} . The effect of using such non-radiogenic $^{87}Sr/^{86}Sr$ for Deccan Trap rivers would be that it would tend to lower $^{87}Sr/^{86}Sr$ of oceans, analogous to inputs from hydrothermal vents. Thus Sr supply from Deccan basalts and hydrothermal vent would act in tandem to bring down oceanic $^{87}Sr/^{86}Sr$.

Palmer and Edmond (1989) estimated present day dissolved riverine flux of 3.3×10^{10} moles y^{-1} for Sr with average $^{87}Sr/^{86}Sr$ of 0.7119 based on measurements of a large number of rivers. The Sr flux of rivers and its $^{87}Sr/^{86}Sr$ ratio during the K/T has to be derived through modeling. In the following, it is done assuming that the riverine flux during K/T was “f” times ($f=0.75-1.25$) the present day flux. The present day Sr fluxes delivered to oceans from weathering of Deccan Traps can be calculated from water discharge and Sr concentration of rivers draining them. The river discharges, Sr concentrations and Sr flux of large rivers draining the Deccan (Godavari, Tapi, Narmada and the Krishna) are given in Table 6.4.

The data in Table 6.4 show that the dissolved Sr flux from these four major rivers which have significant part of their drainage basin in Deccan basalt is $\sim 5 \times 10^8$ moles y^{-1} , $\sim 1.5\%$ of present day Sr supplied to the oceans. These data though represent their fluxes to the sea, they are not entirely derived from the Deccan. These large rivers also drain other lithologies in addition to Deccan, which can have impact on their Sr concentration and isotope ratios.

Table 6.4. Sr concentration (nM) and water discharge of large rivers draining the Deccan Traps.

Rivers	Sr (nM)	Discharge ($10^{13} \ell \text{ y}^{-1}$)	Sr flux ($10^8 \text{ moles y}^{-1}$)
Godavari	1375*	8.8 [§]	1.21
Krishna	3742*	6.8 [#]	2.54
Tapti	2200 [@]	1.8 [#]	0.40
Narmada	2156*	4.1 [#]	0.88

Data: [#]Rao (1975); *Trivedi et al. (1995); [§]Sarin et al. (2002); [@]Dessert et al. (2001)

This raises doubt on the use of these data as representative flux from Deccan basalts. In this work, the measurements are on rivers draining only the Deccan. Using KRS-2 as representative of the Deccan, and assuming a runoff of 463 mm y^{-1} and area of $\sim 5 \times 10^5 \text{ km}^2$ for the total Deccan, the present day flux out of the Deccan can be calculated to be $1.3 \times 10^8 \text{ moles y}^{-1}$. This compares with the value of $3.75 \times 10^8 \text{ moles y}^{-1}$ for the northern Deccan reported by Dessert et al. (2001). It is also important to mention that Narmada, Tapti and Godavari rivers draining Deccan have $^{87}\text{Sr}/^{86}\text{Sr}$ ratios higher than those measured in this study (Trivedi et al., 1995; Dessert et al., 2001). As mentioned earlier, some Formations of Deccan have acquired higher $^{87}\text{Sr}/^{86}\text{Sr}$ because of the crustal contamination (Mahoney, 1988) contributing to more radiogenic $^{87}\text{Sr}/^{86}\text{Sr}$ in rivers draining them. In addition, the Krishna in its lower reaches flows through Archean crystallines which can contribute to its higher $^{87}\text{Sr}/^{86}\text{Sr}$ at Vijaywada (Trivedi et al., 1995). Similarly, the Godavari receives significant amount of water from rivers such as the Indravati and the Pranhita draining central India, which have granites and gneisses in their lower catchments (Sarin et al., 2002). These are potential sources of more radiogenic $^{87}\text{Sr}/^{86}\text{Sr}$ ratios.

However, in order to estimate the maximum impact of Deccan on the oceanic $^{87}\text{Sr}/^{86}\text{Sr}$ excursions, in the discussions to follow, we have used $5 \times 10^8 \text{ moles y}^{-1}$ as the Sr flux from Deccan.

Assuming ratios of 0.705–0.707 and Sr flux of $5 \times 10^8 \text{ moles}$ derived from Deccan basalt weathering, the present day $^{87}\text{Sr}/^{86}\text{Sr}$ for ‘other world rivers’ (J_{owr}) can be calculated to be in the range of 0.71198–0.71201 using the equations.

$$J_r = J_{\text{dtr}} + J_{\text{owr}} \dots \dots \dots (6.7)$$

$$J_r \times R_r = J_{\text{dtr}} \times R_{\text{dtr}} + J_{\text{owr}} \times R_{\text{owr}} \dots \dots (6.8)$$

Hydrothermal inputs: The present day estimate of Sr flux and $^{87}\text{Sr}/^{86}\text{Sr}$ from hydrothermal inputs are 1×10^{10} moles y^{-1} and 0.7035 respectively (Palmer and Edmond, 1989, Elderfield and Schulz, 1996). The hydrothermal component, as mentioned, will lower the seawater ratio, the magnitude being dependant on its flux relative to rivers. At present the hydrothermal flux is about a third of the dissolved riverine flux and a factor of ~ 20 higher than that supplied by Deccan basalts (5×10^8 moles). Temporal variations in hydrothermal flux have been estimated based on seafloor spreading rates (Richter et al., 1992). There is, however, some controversy on past seafloor spreading rates, contributing to uncertainties in the Sr flux estimates (Richter et al., 1992; Rowley, 2002).

The effect of weathering of Deccan basalts, which supply less radiogenic Sr will be to lower the seawater ratio. To estimate the effect of Deccan Trap weathering on decreasing the seawater ratio, on different timescales (100 ka to 1 Ma) eq. (6.5) can be approximated as:

$$\Delta R_{\text{sw}} = [J_{\text{dtr}}(R_{\text{dtr}} - R_{\text{sw}}) + J_{\text{owr}}(R_{\text{owr}} - R_{\text{sw}}) + J_{\text{h}}(R_{\text{h}} - R_{\text{sw}})] \times \Delta t / N \dots (6.9)$$

Change in seawater $^{87}\text{Sr}/^{86}\text{Sr}$ at ~ 66 Ma was calculated using the above relation for various of R_{dtr} (0.705–0.707) and J_{dtr} . Contemporary Sr flux for Deccan is $\sim 5 \times 10^8$ moles y^{-1} . It is often suggested (Courtilot et al., 1986) that the areal exposure of Deccan Trap at emplacement might have been ~ 2 -3 times than that of today. If the flux derived from basalt weathering is proportional to its surficial exposure, the J_{dtr} could have been (10 to 15) $\times 10^{10}$ moles y^{-1} at its emplacement. The changes in R_{sw} have been calculated for J_{dtr} of 10×10^{10} moles y^{-1} and 15×10^{10} moles y^{-1} for R_{sw} of 0.707943 observed during K/T. The results are presented in Table 6.5.

Table 6.5. Expected changes in seawater ratios (around K/T) due to the supply of Sr by Deccan Traps.

J_{dtr} (10^8 moles y^{-1})	R_{dtr}	ΔR_1	ΔR_2	ΔR_3
5	0.705	-1.18	-5.89	-11.8
	0.706	-0.78	-3.89	-7.8
	0.707	-0.38	-1.89	-3.8
10	0.705	-2.35	-11.77	-23.5
	0.706	-1.55	-7.77	-15.5
	0.707	-0.75	-3.77	-7.5
15	0.705	-3.53	-17.66	-35.3
	0.706	-2.33	-11.66	-23.3
	0.707	-1.13	-5.66	-11.3

$R_{\text{sw}}=0.707943$, $\Delta R_{1,2,3}$ (in units of 10^{-6}) correspond to Δt of 100 ky, 500 ky and 1000 ky respectively.

The calculations show that the maximum change in R_{sw} could be in the 5th significant place, for J_{dtr} value of 15×10^8 moles y^{-1} and $\Delta t = 1$ My. For $\Delta t = 100$ Ky, the change in seawater ratio would be much lower, observed only in the 6 or 7th significant places, less than the errors reported in many earlier studies (Hess et al., 1986; Martin and Macdougall, 1991). Therefore, for time intervals of a few hundred ka, changes in seawater ratio resulting from weathering of Deccan basalts would be difficult to establish unequivocally. The data of Vonhoff and Smit (1995) around the K/T section of Bidart shows a dip in $^{87}\text{Sr}/^{86}\text{Sr}$ (0.000019) during the period of 270 ka to 150 ka before the KTB (Fig. 6.4). The flux of Sr required from Deccan Trap to produce this change can be calculated assuming that: (i) hydrothermal Sr flux and its $^{87}\text{Sr}/^{86}\text{Sr}$ ratio has remained constant at a value of 0.7035 during 270 ka to 150 ka, (ii) the inventory of Sr in the oceans during the period is 1.13×10^{17} moles (Martin and Macdougall, 1991) and (iii) the $^{87}\text{Sr}/^{86}\text{Sr}$ supplied from Deccan basalts is in the range of 0.705 to 0.707.

Fig. 6.5 shows Sr flux required from Deccan Traps to produce the observed $^{87}\text{Sr}/^{86}\text{Sr}$ dip, for (i) 0.75 to 1.25 times the present day riverine Sr flux, (ii) R_{owr} values of 0.7092 and 0.7096, and R_h values of 0.8 and 1.0×10^{10} moles y^{-1} . Assuming R_{dtr} to be 0.705, it is seen from Fig.6.5 that the minimum flux required from Deccan has to be $\sim 1.1 \times 10^{10}$ moles y^{-1} at around KTB.

If we assume values of 0.706 and 0.707 for the $^{87}\text{Sr}/^{86}\text{Sr}$ supplied by Deccan, the Sr fluxes required to explain the dip would be $\sim 1.46 \times 10^{10}$ moles y^{-1} and $\sim 2.1 \times 10^{10}$ moles y^{-1} . The present day Sr flux supplied by Deccan Traps is only $\sim 5 \times 10^8$ moles y^{-1} , factor of ~ 30 to 40 lower than that required to explain the dip. Even though, the area of the Deccan Traps at K/T might have been ~ 3 times that of today, it can't account for the factor of ~ 30 to ~ 40 .

An independent estimate of Sr fluxes supplied by Deccan at around K/T can be made from the model results of Dessert et al. (2001). They modeled the combined effect of $p\text{CO}_2$, temperature, runoff and exposed surface area on the Sr flux supplied by Deccan (see equations 8,9 and 10; Dessert et al., 2001). Assuming an area twice (thrice) that of today and $p\text{CO}_2$ of 1760 ppmv at K/T, the Sr flux supplied by Deccan at around K/T is calculated to be 2.9 (or 4.4) times that of present day flux supplied by Deccan. This would correspond to 14.5×10^8 moles y^{-1} and 22×10^{10} moles y^{-1} of Sr supplied by Deccan. Therefore, it is hard to reconcile that the decrease in the $^{87}\text{Sr}/^{86}\text{Sr}$

observed in the Bidart KTB section during the ~150 ka is only due to Deccan Traps, unless the intensity of weathering was significantly higher.

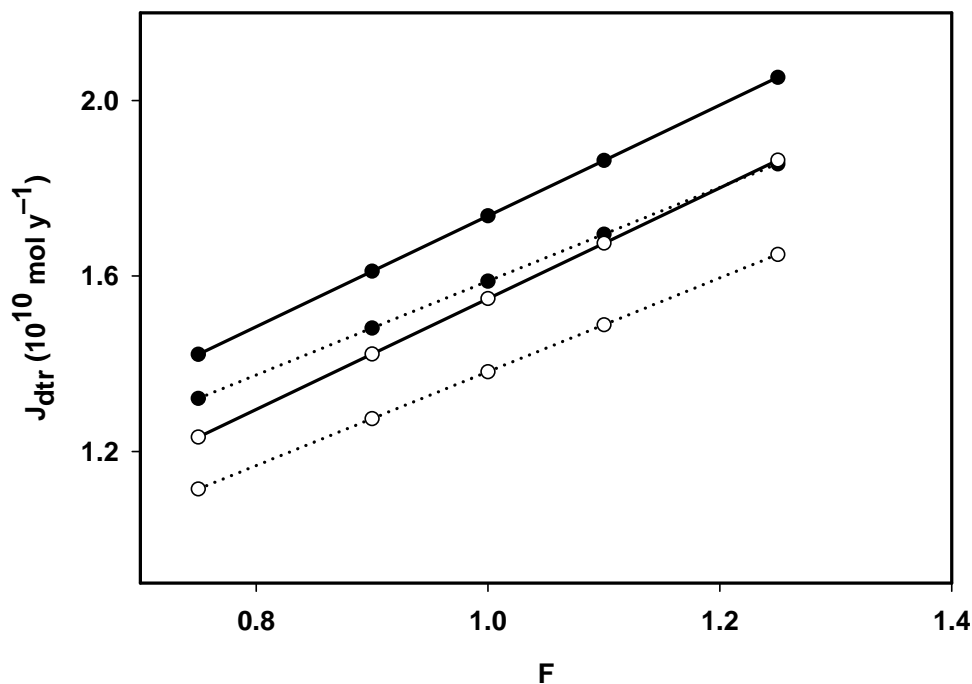


Figure 6.5 Sr fluxes required from Deccan Traps (at around K/T) to explain the ⁸⁷Sr/⁸⁶Sr dip prior to K/T (Fig. 6.4) The dotted line is for $R_{owr}=0.7092$ and the solid line is for $R_{owr}=0.7096$. The solid circle (●) and open circle (○) are for $J_h=0.8 \times 10^{10}$ moles y^{-1} and 1.0×10^{10} moles y^{-1} respectively.

6.3 CONCLUSIONS

The measurement of Sr concentration and ⁸⁷Sr/⁸⁶Sr ratios in the Krishna system and WFWG rivers lead to the following inferences/conclusions regarding Sr flux out of the Deccan and its relation to Sr isotope excursions of oceans during ~66 Ma:

(i) the Sr concentrations in rivers vary from ~130 nM to ~1390 nM with an average of ~490 nM which yield present day Sr flux of $\sim 1.15 \times 10^8$ moles y^{-1} . The ⁸⁷Sr/⁸⁶Sr in them varies from 0.70614–0.70984; with two-thirds of the samples having ratios within 0.706–0.708. These ratios are lower compared to those reported for the Narmada-Tapti-Wainganga draining the northern Deccan Traps. The higher ratios observed in NTW rivers can be a result of interaction of river water with crustally contaminated basalts and/or impact of contribution from lithologies in addition to basalts.

(ii) using simple mass balance equations for Sr and $^{87}\text{Sr}/^{86}\text{Sr}$ in oceans, it has been shown that the maximum change in oceanic $^{87}\text{Sr}/^{86}\text{Sr}$ brought about by weathering of Deccan Traps during K/T is only in the 5th significant place.

(iii) high resolution study by Vonhof and Smit (1997) reported a dip in $^{87}\text{Sr}/^{86}\text{Sr}$ around ~270–150 ka prior to KTB. In order to explain the observed dip, the minimum Sr flux required from Deccan (with $^{87}\text{Sr}/^{86}\text{Sr}$ of 0.705) would be $\sim 1.1 \times 10^{10}$ moles y^{-1} , assuming total riverine Sr flux to be 0.75 times that of the present day. If the $^{87}\text{Sr}/^{86}\text{Sr}$ supplied from Deccan was 0.706 or 0.707, the required Sr fluxes would be 1.46×10^{10} moles y^{-1} and 2.13×10^{10} moles y^{-1} respectively. Even considering that the areal exposure of the Deccan Traps at around K/T to be 2-3 times that of present day, it is hard to reconcile that the dip is due to supply from Deccan Trap unless the weathering intensities and associated Sr fluxes were much higher at that time.

Chapter Seven

Synthesis and scope of future research

Weathering and erosion of continental rocks is an important process that regulates the morphology of earth's surface, the geochemical cycles of elements, and most importantly regulates the CO₂ drawdown from the atmosphere. Among the silicate rocks, whose weathering acts as a net sink for atmospheric CO₂, basalts are known to weather faster than others as demonstrated in this work and some of the earlier investigations. This makes basalt weathering important from CO₂-drawdown considerations. Deccan basalts (India) accounts for ~8% of the total basalts exposures on continents. This coupled with their geographic location and tropical/monsoon climate makes them an important for quantifying global basalt erosion. The present study address to chemical weathering and erosion of Deccan basalts based on chemical and isotopic measurements in the headwaters of the Krishna, the Bhima and their tributaries, and a number of small rivers draining the coastal tracts draining into the Arabian sea.

The present study was carried out to (i) obtain data on major ion composition and selected isotopes (⁸⁷Sr/⁸⁶Sr, ¹³C/¹²C) in dissolved and particulate phases, (ii) apportion the major ions in solution to different sources, (iii) characterize the mobility and behaviour of various elements during weathering and transport, and (iv) determine factors affecting chemical weathering, and erosion of basalt and CO₂ consumption rates, and compare them to those of different weathering regimes.

This study comprises river water and sediment chemistry data from twenty-three rivers, and is based on a multi-tracer approach, which includes the major ion chemistry, Sr isotopic composition of rivers, δ¹³C of dissolved inorganic carbon, and major (Ca, Na, Mg, K, Fe, Al, Ti, Mn, P) and minor elements (Sr, Ba, V, Cu, Zn, Ni, Cr) in sediments. It also integrates the limited amount of data (Dessert et. al, 2001) existing on weathering of Deccan basalts to provide a wholesome picture of basalts weathering and erosion. The summary of the results obtained in this study are:

7.1 Major ion chemistry

The total dissolved solids (TDS) in the samples range from ~27 to 640 mg ℓ⁻¹. The rivers draining the western ghats which flow through patches of cation deficient soils have lower TDS (average: 74 mg ℓ⁻¹) whereas the Bhima (except at origin) and its tributaries which seem to receive Na, Cl and SO₄ from saline soils and anthropogenic inputs have values in excess of 170 mg ℓ⁻¹. The Ca/Mg and Na/Mg in these rivers are similar to those in average basalts of the region, suggesting near congruent release of

Ca, Mg and Na from basalts to rivers. Comparison of calculated and measured silicate–Ca in these rivers indicates that at most ~30% of dissolved Ca can be of non–silicate origin, a likely sources being trace carbonates in basalts, calcareous tufas and/or carbonates in sediments.

The chemical erosion rates (CER) of “selected” basins (excludes rivers supersaturated in calcite and which have high Cl and SO₄) are in range of ~3 to ~34 t km⁻² y⁻¹. This yields an area–weighted average of ~16 t km⁻² y⁻¹ for the Deccan Traps, a factor of ~2 lower than the reported for the Narmada–Tapti–Wainganga (NTW) systems draining the more northern regions of the Deccan (Dessert et. al, 2001). This difference is interpreted as (i) natural variations in CER among the different basins of the Deccan, (ii) “selection” of river data for CER calculation in this study and (iii) possible contribution of major ions from sources (such as carbonates) in addition to basalts to rivers of the northern Deccan Traps.

The chemical and silicate erosion rates (SER) of the west flowing rivers of the Deccan are ~4 times higher than the east flowing rivers. This difference is due to the correspondingly higher rainfall and runoff in the western region and thus re-emphasizes the dominant role of runoff in regulating erosion rates. The SER in the Krishna basin is ~15 t km⁻² y⁻¹, within a factor of ~2 to those in the Yamuna, Bhagirathi and Alaknanda basins of the Himalaya, suggesting that under favourable conditions granites and the other silicates in the Himalaya erode at rates similar to that of Deccan basalts. The CO₂ consumption rate is calculated to be ~3.6×10⁵ moles km⁻² y⁻¹ for the Deccan based on the silicate cations. The rates though are 2 to 3 times lower than reported for the NTW rivers system, they still reinforce the earlier findings that, in general, basalt weather more rapidly than other silicates and that they significantly influence the atmospheric CO₂ budget on long-term scales.

7.2 Carbon isotopes

The work presented in this thesis on stable carbon isotopes provides a new approach to determine silicate weathering contribution to DIC in the Krishna river system based on δ¹³C–Si/HCO₃ systematics of the waters. δ¹³C in the samples range from –8.5‰ to –20.7‰ and shows a strong linear inverse trend with Si/HCO₃ (r²=0.80). The Si/HCO₃ ratios in rivers vary from ~0.55 to ~0.10, the higher value matches the expected ratio for chemical weathering of Deccan basalts (to kaolinite) based on their chemical and mineralogical composition. The δ¹³C–Si/HCO₃ trend suggests mixing of

two end members, a carbonate derived end member with low Si/HCO₃ and enriched in ¹³C, and a silicate derived end member with higher Si/HCO₃ and depleted in ¹³C. Small rivers are characterized by depleted ¹³C (−18.7±2‰) and high Si/HCO₃, interpreted as signatures of basalt weathering with CO₂ from C₃ vegetation. Three samples from the Krishna mainstream and two of its larger tributaries, the Bhima and the Ghod, are enriched in ¹³C (−8.5‰ to −15‰) with higher HCO₃ concentration and lower Si/HCO₃ ratios, indicating that a significant fraction of DIC in these samples is derived from carbonate weathering.

The partial pressure of CO₂ in these waters, on an average, is about ~5 times that of atmosphere. This coupled with, thin film gas diffusion model, yield a CO₂ flux of ~7 μmol cm^{−2} d^{−1} from these rivers to the atmosphere. This flux is orders of magnitude in excess of the reported atmospheric CO₂ drawdown of ~0.1 μmol cm^{−2} d^{−1} due to silicate weathering in this region.

7.3 Sr isotopes

Sr concentrations in the water samples vary from ~130 nM to ~1390 nM with an average of ~490 nM. The ⁸⁷Sr/⁸⁶Sr in these waters vary from 0.70614—0.70987 (±4). These values are between the ⁸⁷Sr/⁸⁶Sr ratios of the pristine non-radiogenic Ambenali basalts (0.7038–0.7044), and those of the more contaminated Mahabaleshwar basalts (0.706–0.719). The range of ⁸⁷Sr/⁸⁶Sr in basalts overlaps with those of marine carbonates (0.709) of various ages, thereby limiting the use of ⁸⁷Sr/⁸⁶Sr to derive contribution of Sr to waters from carbonate and silicates.

The Krishna river shows a major downstream decrease in Sr, from a value of ~1390 nM near its source to a value of ~570 nM downstream. The source of high Sr near the source is unclear; this sample also has high concentration of many major ions. The decrease in the Krishna samples is explained in terms of mixing with tributaries. The ⁸⁷Sr/⁸⁶Sr ratios in the Krishna samples are fairly invariant. The east flowing tributaries and sub-tributaries of the Krishna has Sr from ~134 nM to ~500 nM, (average ~290 nM) with a narrow range in ⁸⁷Sr/⁸⁶Sr from 0.70692 to 0.70842. The rivers flowing into the Arabian sea are more dilute w.r.t to Sr, with an average Sr of ~130 nM, and ⁸⁷Sr/⁸⁶Sr from 0.70614 to 0.70984. The range in ⁸⁷Sr/⁸⁶Sr of the samples analyzed in this study are generally lower than those reported for the Narmada Tapti Wainganga (0.70758 to 0.71493).

Using simple mass balance equations for Sr and $^{87}\text{Sr}/^{86}\text{Sr}$ in oceans, it has been shown that the maximum change brought about by the weathering of Deccan traps during K/T is only in the 5th significant place.

7.4 Major and trace elements in sediments

Na, Mg, Ca and Sr abundances in sediments are significantly depleted compared to those in average basalts. The average depletions (w.r.t. basalts) for Na, Ca, Mg and Sr are ~65%, ~65%, ~50% and ~25% respectively. These depletions are a measure of the intensity of alteration of Deccan basalt by chemical weathering and the relative mobility of various elements during the process. The results show that in general, these elements are released to rivers roughly in the same proportion as their abundances in basalts.

The value of chemical index of alteration (CIA) for sediment samples from the larger river systems, the Krishna and the Bhima, are roughly the same, 55 ± 11 and 59 ± 7 respectively. This compares with the value of ~35 for basalts, indicating significant chemical weathering in the samples analyzed. The smaller tributaries of the Krishna and the west flowing western ghat river have still higher CIA values, indicating higher degree of alteration. The Ca/Mg molar ratio in sediments has a large scatter with an average of 0.81 ± 0.23 . This value though overlaps within errors with that in basalts (1.19 ± 0.17), there is a hint that Ca may be mobilized preferentially over Mg. This is consistent with the observed molar ratio for Ca^*/Mg^* (corrected for atmospheric inputs) in river water, which show marginal excess of Ca over Mg relative to basalts. Trace metal abundances in sediments indicate that are generally immobile; their abundances largely affected by mineral differentiation, and are often associated with the Fe-phases.

7.5 Scope of future work: In spite of the detailed study carried out in the thesis on weathering and erosion of Deccan basalts, there still remain a few issues, which if addressed can help in providing a more wholesome understanding of the chemical weathering and erosion of Deccan basalts and their global significance. A few of these, in terms of future work are presented.

Weathering profile study: Most of the information in this work on the weathering and erosion of Deccan basalts is based on river water chemistry. This can be complemented by study of soil profiles. Weathering profiles preserve longer time, continuous records of rock weathering. Studies on the weathering profiles are made not only to quantify the mobility of elements during weathering but also to assess the

relative weatherability of minerals. Such studies are based on direct measurements, and hence more suited to study relative mobility of elements.

Use of isotopes of Li, Magnesium and Calcium to study their fractionation during weathering and U-Th isotopes to determine time-scale of erosion can also be attempted in soil profiles.

Clay mineral studies: Clays are the end product of aluminosilicate mineral weathering; these minerals make up a major fraction in basalts. Though, smectite/montmorillonite groups are the general end products of basalt weathering, better/precise quantification of their abundances is required to calculate Si/HCO₃ ratios and ratios of major ion (Ca/Mg, Na/Mg) released to the solution phase. This would provide a better characterization of chemical weathering reactions and end products.

C₃/C₄ vegetation and $\delta^{13}\text{C}$ of soil organic matter: In this work, the vegetation in the drainage basin of the rivers is taken to be predominantly C₃ photosynthetic type based on available information on plants. Data on $\delta^{13}\text{C}$ of carbonates in basalts supports this contention. However, to confirm this as well as to understand the range in $\delta^{13}\text{C}$ values of DIC of rivers, data on $\delta^{13}\text{C}$ of soil organic matter would be beneficial. Such a study would place better constraints on the range of $\delta^{13}\text{C}$ and thereby makes it more quantitative.

Calcareous tufas/saline soils and their effect on the water chemistry: One of the observations made in this study is higher abundance of HCO₃, SO₄ and Cl in some samples of the Bhima, its tributaries and some of Krishna waters. The high Cl and SO₄ in these waters have been attributed to supply from saline/alkaline soils whereas most of the HCO₃ is derived from carbonates in basalts, calcareous tufas and alkaline/saline soils. An attempt to better quantify the contributions of these sources requires a detail study on their exposures in the basin and their chemistry. Similarly, many river sediments are found to contain high abundances of carbonates. The sources of these carbonates and their role in contributing to Ca and alkalinity budget of the rivers needs to be assessed. $\delta^{13}\text{C}$ of these carbonates may throw more light on their sources and thereby in the assessment of their role in contributing to the HCO₃ in waters, and carbonates in sediments.

Physical weathering: Though this study is more on issues related to chemical weathering, knowledge of physical weathering in terms of particulate matter

abundances in water would have been helpful to derive total erosion rates and the interrelation between physical and chemical erosion.

References

- Ahmad T., Khanna P. P., Chakrapani G. J., and Balakrishnan S. (1998) Geochemical characteristics of water and sediment of the Indus river, trans-Himalaya, India: Constraints on weathering and erosion. *J. Asian Earth Sci.*, **16**(2-3), 333-346.
- Allegre C. J., Birck J. L., Capmas F., and Courtillot V. (1999) Age of the Deccan Traps using ^{187}Re – ^{187}Os systematics. *Earth Planet. Sci. Lett.* **170**, 197–204.
- Amiotte-Suchet P., and Probst J. L. (1995) A global model for present-day atmospheric/soil CO_2 consumption by chemical erosion of continental rocks (GEN- CO_2). *Tellus* **47B**, 273–280.
- Amiotte-Suchet P., Aubert D., Probst J. L., Gauthier-Lafaye F., Probst A., Andreaux F., and Vivelle D. (1999) $\delta^{13}\text{C}$ pattern of dissolved inorganic carbon in a small granitic catchment: the strengbach case study (Vosges Mountain, France). *Chem. Geol.* **159**, 129–145.
- Amiotte-Suchet P., Probst J. L., and Ludwig W. (2003) Worldwide distribution of continental rock lithology: Implications for the atmospheric/soil CO_2 uptake by continental weathering and alkalinity river transport to the oceans. *Global Biogeochem. Cycles* **17**, 1891–1903.
- Arthur M. A., and Sagemann B. B. (1994) Marine black shales: depositional mechanisms and environmental of ancients deposits. *Annu. Rev. Earth Planet. Sci.* **22**, 499-551.
- Beane J. E. (1988) Flow stratigraphy, chemical variation and petrogenesis of Deccan flood basalts, Western Ghats, India; Ph. D. Dissertation, Washington State University, Pullman, 576p.
- Benninger L. K., Lewis D. M., and Turekian K. K. (1975) The use of natural Pb-210 as a heavy metal tracer in the River-Estuarine system. In: *Marine chemistry in coastal environment* (Ed: T. M. Church), ACS symposium series, **18**, 202-210.
- Berner R. A., Lasaga A. C., and Garrels R. M. (1983) The carbonate–silicate geochemical cycle and its effect on atmospheric carbondioxide over the past 100 million years. *Am. J. Sci.* **284**, 641–683.
- Berner R. A. (1992) Weathering, plants and the long term carbon cycle. *Geochim. Cosmochim. Acta* **56**, 3225–3231.
- Berner R. A., and Rao J. L. (1994) Phosphorus in sediments of the Amazon river and estuary: Implications for global flux of phosphorus to the sea. *Geochim. Cosmochim. Acta* **58**, 2333-2339.

- Berner R. A. (1995) Chemical weathering and its effect on atmospheric CO₂ and climate. *Rev. mineral.* **31**, 565–583.
- Berner E. K. and Berner R. A. (1996) *Global Environment: Water, Air and Geochemical Cycles*. Prentice Hall, New Jersey, pp. 376.
- Berner R. A. and Berner E. K. (1997) Silicate weathering and Climate. In: *Tectonic Uplift and Climate Change* (Ed. W. F. Ruddiman), 354–365.
- Best M. (1986) *Igneous and Metamorphic Petrology*, CBS Publishers, New Delhi, pp. 630.
- Bickle M.J., Harris N.B.W., Bunbury J., Chapman H.J., Fairchild I.J., and Ahmad T. (2001) Controls on the ⁸⁷Sr/⁸⁶Sr of carbonates in the Garwal Himalaya, headwaters of the Ganges. *J. Geol.* **109**, 737–753.
- Bhargava G. P. and Bhattacharjee J. C. (1982) Morphology, genesis and classification of salt-affected soils. In: *Review of Soil Research in India*, Part II, Indian Society of Soil Science, New Delhi, pp. 508–528.
- Biksham B., and Subramanian V (1988) Nature of solute transport in the Godavari river basin, India. *J. Hydrol.* **103**, 375–392.
- Blum J. D., Gazis C. A., Jacobson A. D., and Chamberlin C. P. (1998) Carbonate versus silicate weathering in the Raikhot watershed within the High Himalayan Crystalline Series. *Geology* **26**, 411–414
- Bluth G. J. S., and Kump L. R. (1994) Lithologic and climatic control of river chemistry. *Geochim. Cosmochim. Acta* **58**, 2341–2359.
- Borole D. V., Krishnaswami S., and Somayajulu B. L. K. (1982) Uranium isotopes in rivers, estuaries and adjacent coastal sediments of western India: their weathering, transport and oceanic budget. *Geochim. Cosmochim. Acta* **46**, 125–137.
- Brady P. V. (1991) The effect of silicate weathering on global temperature and atmospheric CO₂. *J. Geophys. Res.* **96**, 18101–18106.
- Brady P. V., Carroll S. A. (1994) Direct effects of CO₂ and T on silicate weathering: Possible implications for climate control. *Geochim. Cosmochim. Acta* **58**, 1853–1856.
- Brass, G. W. (1976) The variation of marine ⁸⁷Sr/⁸⁶Sr during Phanerozoic time: interpretation using a flux model. *Geochim. Cosmochim. Acta* **40**, 721–730.
- Breit G. N., and Wanty R. B. (1991) Vanadium accumulation in carbonaceous rocks: A review of geochemical controls during deposition and diagenesis. *Chem. Geol.* **91**, 83–97.
- Broecker W.S. (1974) *Chemical Oceanography*, Javanovich, Harcourt-Brace, 214 pp.

- Canfield D. E. (1997) The geochemistry of river particulates from the continental USA: Major elements. *Geochim. Cosmochim. Acta* **61**, 3349–3365.
- Cerling C. E. (1984) The stable isotopic composition of modern soil carbonate and its relationship to climate, *Earth Planet. Sci. Lett.* **71**, 229–240.
- Cerling T. E., Solomon D. K., Quade J., Bowman J. R. (1991) On the isotopic composition of carbon in soil carbon dioxide. *Geochim. Cosmochim. Acta* **55**, 3403–3405.
- Chandrasekharam D., and Prasad S. R. (1998) Geothermal waters in Tapti basin, Northern Deccan, India. In: *Proc., 9th Water-Rock Interaction Congress*, Balkema, The Netherlands, pp. 667-670.
- Chandrasekharam D., Vasseli O., Sheth H. C., and Keshav S. (2000) Petrogenetic significance of ferro–enstatite orthopyroxene in basaltic dikes from the Tapti rift, Deccan flood volcanic province, India. *Earth Planet. Sci. Lett.* **179**, 469–476.
- CPCB (90) *Basin sub-basin inventory of water pollution: The Krishna basin* (1990) (Ed. Central Pollution Control Board, Delhi. pp. 145.
- Courtillot V., Besse J., Vadammme D., Montigny R., Jaeger J. J., and Cappetta H. (1986) Deccan flood basalt at Cretaceous/Tertiary boundary? *Earth Planet. Sci. Lett.* **80**, 361–364.
- Courtillot V., Jaupart C., Manegheeti I., Tapponnier P., and Besse J. (1999) On casual links between flood basalts and continental breakup. *Earth Planet. Sci. Lett.* **166**, 177–195.
- Dalai T. K. (2001) Major ions, stable isotopes, $^{87}\text{Sr}/^{86}\text{Sr}$ and Re in the headwaters of the Yamuna: Implications to chemical weathering in the Himalaya. Ph.D. Dissertation, M. S. University of Baroda, Vadodara, India.
- Dalai T. K., Krishnaswami S., and Sarin M. M. (2002) Major ion chemistry in the headwaters of the Yamuna river system: chemical weathering, its temperature dependence and CO_2 consumption rates. *Geochim. Cosmochim. Acta* **66**, 3397–3416.
- Dalai T. K., Rengarajan R., and Patel P. P. (2004) Sediment geochemistry of the Yamuna River System in the Himalaya: Implications to weathering and transport. *Geochem. J.* **38**, 441-453.
- Das A., Krishnaswami S., Sarin M. M., and Pande K. (2005) Chemical weathering in the Krishna basin and the western ghats of the Deccan Traps: Rates of weathering and their control. *Geochim. Cosmochim. Acta* (in press).
- De A. (1974) Silicate liquid immiscibility in Deccan Traps and its petrogenetic significance. *Bull. Geol. Soc. Am.* **85**, 471–474.

- Dekov V. M., Subramanian V., and Van Grieken R. (1998) Chemical composition of suspended matter and sediments from the India sub-continent: a fifteen year research survey, In: *Recent trend in Environmental Biogeochemistry*, ENVIS center, School of Environmental Sciences, Jawaharlal Nehru University, New Delhi, 81–92.
- Deshpande G. C. (1998) Deccan Traps. In: *Geology of Maharashtra* (Ed. Geological Society of India), Bangalore, 129–162.
- Dessert C., Dupre B., Francois L. M., Schott J., Gaillardet J., Chakrapani G., and Bajpai S. (2001) Erosion of Deccan Traps determined by river geochemistry: impact on the global climate and the $^{87}\text{Sr}/^{86}\text{Sr}$ ratio of sea water. *Earth Planet. Sci. Lett.* **188**, 459–474.
- Dessert C., Dupre B., Gaillardet J., Francois L. M., and Allegre C. J. (2003) Basalt weathering laws and the impact of basalt weathering on the global carbon cycle. *Chem. Geol.*, **20**, 1-17.
- Dever L., Durand R., Fontes J. Ch., Vachier P. (1983) Etude pedogenetique et isotopique des neoformations de cacite dans un sol sur craie. Caracteristiques et origins: *Geochim. Cosmochim. Acta* **46**, 1947–1956.
- Devey C. W., and Lightfoot P. C. (1986) Volcanological and techtonic control of stratigraphy and structure in western Deccan traps, *B. Volcanol.* **48**, 195–207.
- Drever J. I. (1994) The effect of land plants on weathering rates of silicate minerals. *Geochim. Cosmochim. Acta* **58**, 2325–2332.
- Drever J. I. (1997) *The geochemistry of natural waters: Surface and groundwater environments*. Prentice Hall, New Jersey, pp. 436.
- Dupre B., Gaillerdet J., Rousseau D., and Allegre C. J. (1996) Major and trace elements of river borne amterial: The Congo Basin. *Geochim. Cosmochim. Acta* **60**, 1301–1321.
- Edmond J. M. (1992) Himalayan tectonics, weathering processes, and the strontium isotope records in marine limestone. *Science* **258**, 1594-1597.
- Edmond J. M., Palmer M. R., Measures C. I., Grant B., and Stallard R. F. (1995) The fluvial geochemistry and denudation rate of the Guayana shield in Venezuela, Colombia, and Brazil. *Geochim. Cosmochim. Acta* **59**, 3301–3325.
- Edmond J. M. and Huh Y. (1997) Chemical weathering yoelds from basement and orogenic terrians in hot and cold climates. In: *Tectonic Uplift and Climate Change*, (Ed.: W. F. Ruddiman), Plenum Press, New York, pp. 330-351.
- Elderfield H, and Gieskes J. M. (1982) Sr isotopes in interstitial waters of marine sediments from Deep Sea Drilling Project Cores, *Nature* **300**, 493-497.

- Elderfield H., and Schultz A. (1996) Mid-ocean ridge hydrothermal fluxes and the chemical composition of the ocean. *Annu. Rev. Earth Planet. Sci.* **24**, 191-224.
- Faure G. (1986) *Principles of Isotope Geology* (2nd Edition), John Wiley and Sons, pp. 589.
- Federico C., Aiuppa A., Allarad P., Bellano S., Jean-Baptiste, Parello F, and Valenza M. (2002) Magma-derived gas influx and water-rock interactions in the volcanic aquifer of Mt. Vesuvius, Italy. *Geochim. Cosmochim. Acta* **66**, 963–981.
- Gaillardet J., Dupre B., and Allegre C. J. (1995) A global geochemical mass budget applied to the Congo basin rivers: Erosion rates and continental crust composition. *Geochim. Cosmochim. Acta* **59**, 3469–3485.
- Gaillardet J., Dupre B., Allegre C. J., and Negrel P. (1997) Chemical and physical denudations in the Amazon river basin. *Chem. Geol.* **142**, 141–173.
- Gaillardet J., Dupre B., and Allegre C. J. (1999a) Global silicate weathering and CO₂ consumption rates deduced from the chemistry of large rivers. *Chem. Geol.* **159**, 3–30.
- Gaillardet J., Dupre B., and Allegre C. J. (1999b) Geochemistry of large river suspended sediments: Silicate weathering or recycled tracer. *Geochim. Cosmochim. Acta* **63**, 4037–4051.
- Galy A. and France-Lanord C. (1999) Weathering processes in the Ganges-Brahmaputra basin and the riverine alkalinity budget. *Chem. Geol.* **159**, 31–60.
- Garrels R. M., and Mackenzie F. (1971) *Evolution of sedimentary rocks*: W. W. Norton, New York, pp. 397.
- Gislason S. R., and Eugster H. P. (1987) Meteoric water-basalt interactions II: A field study in N.E. Iceland. *Geochim. Cosmochim. Acta* **51**, 2841–2855.
- Gislason S. R., Arnorsson S., and Armannsson H. (1996) Chemical weathering of basalt in southwest Iceland: Effects of runoff, age of rocks and vegetative/glacial cover. *Am. J. Sci.* **296**, 837-907.
- Steffansson A., and Gislason S. R. (2001) Chemical weathering of basalts, southwest Iceland: Effect of rock crystallinity and secondary minerals on chemical fluxes to ocean. *Am. J. Sci.* **301**, 513–556.
- Hess J., Bender M. L., K and Schilling J. G. (1986) Evolution of the ratio of strontium 87 to strontium 86 in seawater from the Cretaceous to Present. *Science* **231**, 979-984.
- Hodell D. A., Mueller P.A., Mckenzie J. A., and Mead G. A. (1989) Strontium isotope stratigraphy and geochemistry of the late Neogene ocean, *Earth Planet. Sci. Lett.* **92**, 165-178.

- Holley E. H. (1977) Oxygen transfer at the air-water interface. In: *On Transport Processes in the Ocean*, AICE Symp. Proc., Plenum, 117–150.
- Huh Y., Panteleyev G., Tsoi Mai-Yin, Zaitsev A., and Edmond J. M. (1998a) The fluvial geochemistry of the rivers of Eastern Siberia: I. Tributaries of the Lena draining the sedimentary platform of the Siberian Craton. *Geochim. Cosmochim. Acta* **62**, 1657–1676.
- Huh Y., Panteleyev G., Babich D., Zaitsev A., and Edmond J. M. (1998b) The fluvial geochemistry of the rivers of Eastern Siberia: II. Tributaries of the Lena, Omoloy, Yana, Indigirka, Kolyma and Anandyr draining the collisional/accretionary zone of the Verkhoyansk and Cherskiy ranges. *Geochim. Cosmochim. Acta* **62**, 2053–2075.
- <http://www.cmdl.noaa.gov/ccgg/iadv/>
- <http://www.tropmet.res.in>
- Irwin W. P., and Barnes I. (1980) Tectonic relations of carbon dioxide discharges and earthquakes. *J. Geophys. Res.*, **101**, 3115–3121.
- Jacobson A. D., Blum J. D., and Walter L. M. (2002) Reconciling the elemental and Sr isotope composition of Himalayan weathering fluxes: insights from the carbonate geochemistry of streams waters. *Geochim. Cosmochim. Acta* **66**, 3417–3429.
- Javoy M., and Michard G. (1989) Am. Geophys. Union EOS Trans. **70**, 1421.
- Jeffery K. L., Henderson P., Subbarao K. V., and Walsh J. N. (1988) The Zeolites of the Deccan basalt— A study of their distribution. In: *Deccan Flood Basalts* (Ed. K. V. Subbarao), *Mem. Geol. Soc. India* **10**, 151–162.
- Jha P. K., Subramanian V., Sitaswad R., and van Grieken R. (1990) Heavy metals in sediments of the Yamuna River (A tributary of the Ganges), India. *Sci. Tot. Environ.* **95**, 7-27.
- Jones D.S., Mueller P. A., Bryan J. R., Dobson J. P., Channel J. E. T., Zachos J. C. Arthur M. A. (1987) Biotic, geochemical and paleomagnetic changes across the Cretaceous/Tertiary boundary at Brags, Alabama. *Geology* **15**, 311-315.
- Kaila K. L., Reddy P. R., Dixit M. M., Lazarenko M. A. (1981) Deep crustal structure at Koyna, Maharashtra, indicated by deep seismic sounding. *Jour. Geol. Soc. India* **9**, 97-105.
- Karim A., and Veizer J. (2000) Weathering processes in the Indus River Basin: implications from carbon, sulfur, oxygen and strontium isotopes. *Chem. Geol.*, **170**, 153–177.
- Keith M.L., and Weber J.N. (1964) Isotopic composition and environmental classification of selected limestone and fossils. *Geochim. Cosmochim. Acta* **28**, 1787–1816.

- Kempe S. (1982) Long-term records of CO₂ pressure fluctuations in fresh water. In: *Transport of Carbon and Minerals in Major World Rivers* (Ed. E.T. Degens), Part 1, Mitt. Geol-Palaont. Inst., Univ. Hamburg, Hamburg, **52**, 91–332.
- Kendal C., Mast M. A., and Rice K. C. (1992) Tracing watershed weathering reactions with $\delta^{13}\text{C}$: In: *Proc. 7th Intern. Symp. On Water Rock Interaction*, USA (Ed: Kharaka, Maest), 1, 569–572.
- Kendal C. Sklash M. G., and Bullen T. D. (1995) Isotope tracers of water and solutes sources in catchment: Solute Modeling in Catchment System, 262–303.
- Kessarkar P.M., Rao V.P., Ahmad S.M., and Babu G.A. (2003) Clay minerals and Sr-Nd isotopes of sediments along the western margin of India and their implication for sediment provenance. *Mar. Geol.* **202**, 55-69.
- Koepnick R. B., Dennison R. E., and Dahl D. A. (1988) The Cenozoic seawater $^{87}\text{Sr}/^{86}\text{Sr}$ curve: Data review and implications for correlation of marine strata: *Paleoceanography* **3**, 743-746.
- Krishnan M. S. (1982) The Deccan Traps. In: *Geology of India and Burma*, 6th Edition, CBS Publishers and Distributors, India pp. 405.
- Krishnaswami S., Trivedi J. R., Sarin M. M., Ramesh R., and Sharma K. K. (1992) Strontium isotopes and rubidium in the Ganga-Brahmaputra river system: Weathering in the Himalaya, fluxes to the Bay of Bengal and contributions to the evolution of oceanic $^{87}\text{Sr}/^{86}\text{Sr}$. *Earth Planet. Sci. Lett.* **170**, 197–204.
- Krishnaswami S., Singh S. K., and Dalai T. K. (1999) Silicate weathering in the Himalaya: Role in contributing to major ions and radiogenic Sr to the Bay of Bengal. In: *Ocean Science, Trends and Future Directions* (Ed. B. L. K. Somayajulu), Indian National Science Academy and Akademia International, New Delhi, 23–51.
- Kump L. R. (1989) Alternative modeling approaches to the geochemical cycles of carbon, sulfur, and strontium isotopes. *Am. J. Sci.* **289**, 390-410.
- Kump L.R., Brantley S. L., Arthur M. A. (2000) Chemical weathering, atmospheric CO₂ and climate. *Annu. Rev. Earth Planet. Sci.* **28**, 611-667.
- Langmuir D. (1971) The geochemistry of some carbonate ground waters in central Pennsylvania. *Geochim. Cosmochim. Acta* **35**, 1023–1045.
- Lightfoot P. C., Kwakesworth C. J., Devey C. W., Rogers N. W., and van Calsteren P. W. C. (1990) Source and differentiation of Deccan Trap lavas: implications of geochemical and mineral chemical variations. *J. Petrol.* **31**, 1165-1200.

- Longinelli A., and Edmond J. M. (1983) Isotope geochemistry in the Amazon basin: A reconnaissance. *J. Geophys. Res.* **88**, 3703-3717.
- Louvat P. (1997) Etude geochimique de l'érosion fluviale d'îles volcaniques à l'aide des bilans d'éléments majeurs et traces, Ph.D. Thesis, Université Paris 7.
- Louvat P. and Allegre C. (1997) Present denudation rates on the island of Reunion determined by river geochemistry: Basalt weathering and mass budget between chemical and mechanical erosions. *Geochim. Cosmochim. Acta* **61**, 3645–3669.
- Macdougall J. D. (1988) Seawater strontium isotopes, acid rain and the Cretaceous-Tertiary boundary. *Science* **239**, 485-487.
- Mahoney J. (1988) Deccan Traps, In: *Continental Flood Basalts, Petrology and structural Geology* (Ed. J. D. Macdougall), Kluwer Academic, Dordrecht, 151–194.
- McArthur (1994) Recent trends in strontium isotope stratigraphy. *Terra Nova* **6**, 331-358.
- Martin J. M. and Meybeck M. (1979) Elemental mass-balance of material carried by major world rivers. *Mar. Chem.*, **7**, 173–206.
- Martin E. E., and Macdougall J. D. (1991) Seawater Sr isotopes at the Cretaceous/Tertiary boundary. *Earth Planet. Sci. Lett.* **104**, 166–180.
- McLennan S. M. (1993) Weathering and global denudation. *J. Geol.* **101**, 295-303.
- Meybeck M. (1986) Composition chimique des ruisseaux non pollués de France. *Sci. Geol. Bull. (Strasbourg)* **39**, 3–77.
- Meybeck M. (1987) Global chemical weathering of surficial rocks estimated from river dissolved loads. *Am. J. Sci.* **287**, 401–428.
- Minissale A., Vaselli O., Chandrasekharam D., Magro D., Tassi F., and Casiglia A. (2000) Origin and evolution of 'intracratonic' thermal fluids from central–western region peninsular India. *Earth Planet. Sci. Lett.* **181**, 377–394.
- Naik P. K., Awasthi A. K., Anand A. V. S. S., and Mohan P. C. (2001) Hydrogeologic framework of the Deccan terrain of the Koyna River basin, India. *Hydrogeol. J.* **9**, 243–264.
- Naik P. K., Awasthi A. K., and Mohan P. C. (2002) Springs in a headwater basin in the Deccan Trap country of the western ghats, India. *Hydrogeol. J.* **10**, 553–565.
- Nelson B. K., Macleod G. K., and Ward P. D. (1991) Rapid change in strontium isotopic composition of sea water before the Cretaceous/Tertiary boundary. *Nature* **351**, 644-646.

- Nesbitt H. W., Markovics G., and Price R. C. (1980) Chemical processes affecting alkalis and alkaline earths during continental weathering. *Geochim. Cosmochim. Acta* **44**, 1659–1666.
- Nesbitt G. W., and Young G. M. (1982) Early Proterozoic climates and plate motions inferred from major element chemistry of lutites. *Nature*, **299**, 715–717.
- NRSA (1998) Salt affected soils, Maharashtra, Map 4, 5 and 6. National Remote Sensing Agency, Hyderabad, India.
- Officer C. B., and Drake C. L. (1983) The Cretaceous-Tertiary transition. *Science* **219**, 1383-1390.
- Oliva P., Dupre B., Martin F., and Viers J. (2004) The role of trace minerals in chemical weathering in a high-elevation granitic watershed (Estibere, France): Chemical and mineralogical evidence. *Geochim. Cosmochim. Acta* **68**, 2223–2243.
- Oliver L., Harris N., Bickle M., Chapman H., Dise N., and Horstwood M. (2003) Silicate weathering rates decoupled from the $^{87}\text{Sr}/^{86}\text{Sr}$ ratio of the dissolved load during Himalayan erosion, *Chem. Geol.* **201**, 119-139.
- Palmer M. R., and Elderfield H. (1985) Sr isotope composition of sea water over the past 75 Myr. *Nature* **314**, 526-528.
- Palmer M. R., and Edmond J. M. (1989) The strontium isotope budget of modern ocean. *Earth Planet. Sci. Lett.* **92**, 11–26.
- Pande (2002) Age and duration of Deccan Traps, India: A review of radiometric and paleomagnetic constraints. *Proc. Ind. Acad. Sci. (Earth Planet. Sci.)* **111**, 115–123.
- Parashar D. C., Granat L., Kulshretha U. C., Pillai A. G., Nail M. S., Momin G. A., Rao P. S. P., Safai P. D., Khemani L. T., Naqvi S. W. A., Narverkar P. V., Thapa K. B., and Rhode H. (1996) Chemical composition of precipitation in India and Nepal: A preliminary report on Indo-Swedish project on atmospheric chemistry. **Report CM-90**, Department of Meteorology, Stockholm University, Sweden, pp. 27.
- Pawar, N.J., Kale, V.S., Atkinson, T.C., Rowe, and P. J. (1988) Early Holocene waterfall tufa from semi-arid Maharashtra Plateau (India). *J. Geol. Soc. India* **32**, 513–515.
- Pawar N. J., and Shaikh I. J. (1995) Nitrate pollution of groundwaters from shallow basaltic aquifers, Deccan Trap Hydrologic Province, India. *Environ. Geol.* **25**, 197-204.
- Pawar N. J., Pondhe G. M., and Patil S. F. (1997) Groundwater pollution due to sugar-mill effluent, at Sonai, Maharashtra, India. *Environ. Geol.* **34**, 151-158.
- Peng Z. X., Mahoney J. J., Hooper P. R., Macdougall J. D., and Krishnamurthy P. (1998) Basalts of the northeastern Deccan Traps, India: isotopic and elemental geochemistry

- and relation to southwestern Deccan Trap stratigraphy. *J. Geophys. Res.* **103**, 29843–29865.
- Peterman Z. E., Hedge C. E., and Tourtelot H. A. (1970). Isotopic composition of strontium in seawater throughout Phanerozoic time. *Geochim. Cosmochim. Acta* **34**, 105–120.
- Pettijohn F. J. (1975) *Sedimentary Rocks*, Harper and Row, New York, pp. 628.
- Picouet C., Dupre B., Orange D. and Valladon M. (2002) Major and trace element geochemistry in the upper Niger river (Mali): physical and chemical weathering rates and CO₂ consumption. *Chem. Geol.* **185**, 93–124.
- Probst J. L., Mortatti J., and Tardy Y. (1994) Carbon river fluxes and weathering CO₂ consumption in the Congo and Amazon river basins. *Appl. Geochem.* **9**, 1–13.
- Puri G. S., Meher-Homji V. M., Gupta R. K., and Puri S (1989) *Forest Ecology: Plant form, Diversity, Communities and Succession*. Oxford and IBH Publishing Co. Pvt. LTD., **2**, pp. 582.
- Quade J., and Cerling T. E. (1995) Expansion of C₄ grasses in the late Miocene of Northern Pakistan: evidence from stable isotopes in paleosols. *Palaeogeogr., Palaeoclimatol., Palaeoecol.* **115**, 91–116.
- Rajagopalan G., Ramesh R., and Sukumar R. (1999) Climatic implications of $\delta^{13}\text{C}$ and $\delta^{18}\text{O}$ ratios from C₃ and C₄ plants growing in a tropical montane habitat in southern India. *J. Biosci.* **24** (4), 491–498.
- Ramesh R., and Subramanian V. (1988) Nature of the dissolved load of the Krishna river basin, India. *J. Hydrol.* **103**, 139–155.
- Rao K. L. (1975) *India's Water Wealth*. Orient Longman Ltd., New Delhi pp. 255.
- Ravizza G, and Peucker-Ehrenbrink B. (2003) Chemostratigraphic evidence of Deccan volcanism from the marine osmium isotope record. *Science* **302**, 1392–1395.
- Ray J.S., and Ramesh R. (2000) Rayleigh fractionation of stable isotopes from a multicomponent source. *Geochim. Cosmochim. Acta* **64**, 299–306.
- Raymo M. E., and Ruddiman W. F. (1992) Tectonic forcing of late Cenozoic climate. *Nature* **359**, 117–122.
- Raymo M. E, Ruddiman W. F., Froelich P. N. (1988) Influence of late Cenozoic mountain building on ocean geochemical cycles. *Geology* **16**, 649–653.
- Rengarajan R. (2004) Radium isotopes and rare earth elements in Indian rivers and the Bay of Bengal. Ph.D. Dissertation, Mohan Lal Sukhadia University, Udaipur, India.

- Richter F. M., Rowley D. B., and DePaolo D. J. (1992) Sr isotope evolution of seawaters: the role of tectonics. *Earth Planet. Sci. Lett.* **170**, 197–204.
- Rowley D. B. (2002) Rate of plate creation and destruction: 180 Ma to Present. *GSA Bulletin* **114**, 927–933.
- Salomons W., and Mook W. G. (1986) Isotope geochemistry of carbonates in the weathering zone, In: *Handbook of Environmental Isotope Geochemistry: The terrestrial environment* (Ed: Fritz P., and Fontes J. Ch.) Elsevier Amsterdam, **2**, 239–269.
- Sarin M. M., Krishnaswami S., Dilli K., Somayajulu B. L. K., and Moore W. S. (1989) Major ion chemistry of the Ganga-Brahmaputra river system. Weathering processes and fluxes to the Bay of the Bengal. *Geochim. Cosmochim. Acta* **53**, 997–1009.
- Sarin M. M., Krishnaswami S., Trivedi J. R., and Sharma K. K. (1992) Major ion chemistry of the Ganga source waters. Weathering in the high altitude Himalaya. *Proc. Ind. Acad. Sci. (Earth Planet. Sci.)* **101**, 89–98.
- Sarin M. M., Sudheer A. K., and Balakrishna (2002) Significance of riverine carbon transport: A case study of a tropical river, Godavari (India). *Science in China (series C)* **45**, 97–108.
- Sen G. (1980) Mineralogical variations in Delakhari Sill, Deccan Trap intrusion, Central India. *Contrib. Mineral. Petrol.* **75**, 71–78.
- Sen G. (1986) Mineralogy and petrogenesis of the Deccan Trap lava flows around Mahabaleshwar, India. *J. Petrol.* **27**, 627–663.
- Sen G. (2001) Generation of Deccan Trap Magma. *Proc. Ind. Acad. Sci. (Earth Planet. Sci.)* **110**, 409–431.
- Sequeria R., and Kelkar D. (1978) Chemical composition of monsoonal rain water over India. *J. Appl. Met.* **17**, 7–18.
- Sethna S. F., and Sethna B. S. (1988) Mineralogy and petrogenesis of Deccan Trap basalts from Mahabaleshwar, Igatpuri, Sagar, and Nagpur areas, India. In: *Deccan Flood Basalts* (Ed: K. V. Subbarao), *Mem. Geol. Soc. Ind.* **10**, 69–90.
- Shankar D., Kotamraju V., and Shetye S. R. (2004) A quantitative framework for water resources in India. *Curr. Sci.* **86**, 543–552.
- Sheth H., Pande K., Bhutani R. (2001) ^{40}Ar - ^{39}Ar dating of a national geological monument: the Gilbert Hill basalt, Bombay, Deccan Traps. *Curr. Sci.* **80**, 1437–1440.
- Singh P., and Rajamani V. (2001) REE geochemistry of recent clastic sediments from the Kaveri floodplains, southern India: Implication to source area weathering and sedimentary processes. *Geochim. Cosmochim. Acta* **65**, 3093–3108.

- Singh S. K., Trivedi J. R., Pande K., Ramesh R., and Krishnaswami S. (1998) Chemical and Sr, O, C isotopic composition of carbonates from the Lesser Himalaya: Implications to the Sr isotopic composition of the source waters of Ganga, Ghaghara and Indus Rivers. *Geochim. Cosmochim. Acta* **62**, 743–755.
- Singh S. K., and France-Lanord C. (2002) Tracing the distribution of erosion in the Brahmaputra watershed from isotopic composition of stream sediments. *Earth Planet. Sci. Lett.* **202**, 645-662.
- Singh S.K., Reisberg L., and France-Lanord C. (2003) Re-Os isotope systematics of sediments of the Brahmaputra River system. *Geochim. Cosmochim. Acta* **67**, 4101–4111.
- Stallard R. F. and Edmond J. M. (1983) Geochemistry of the Amazon 2. The influence of geology and the weathering environment on the dissolved load. *J. Geophys. Res.* **88**, 9671–9688.
- Stallard R. F. (1995) Tectonic, environmental and human aspects of weathering and climate: A global review using a steady-state perspective. *Annu. Rev. Earth Planet. Sci.* **23**, 11-39.
- Steffansson A., and Gislason S. R. (2001) Chemical weathering of basalts, southwest Iceland: Effect of rock crystallinity and secondary minerals on chemical fluxes to ocean. *Am. J. Sci.* **301**, 513–556.
- Strickland J. D. H., and Parson T. R. (1972) *A practical handbook of seawater analysis*. Bulletin **167**, Fisheries Research Board of Canada, pp. 310.
- Subramanian V., Dack L. Van't, and Grieken R. Van (1985) Chemical composition of river sediments from the Indian subcontinent. *Chem. Geol.* **48**, 271–279.
- Subramanian V., Dack L. Van't, and Grieken R. Van (1987) Heavy metal distribution in the sediments of Ganges and Brahmaputra rivers. *Environ. Geol. Water Sci.* **9**, 93–103.
- Subbarao K. V., Bodas M. S., Khadri S. R. F., Bean J. E., Kale V., Widdowson M., Hooper P. R., Walsh J. N. (2000) Field excursion guide to the western Deccan Basalt Province, Penrose Decan 2000, pp. 249.
- Subramanian V. (2000) Water: Quantity-Quality perspective in South Asia. Kingston International Publishers, UK, pp. 256.
- Sukeshwala R., Avasia K., and Gangopadhyay M (1972) Observations on the occurrence of secondary minerals in the Deccan Traps of western India. *The Indian Mineralogist* **13**, 50–68.

- Sukumar R., Ramesh R., Pant R. K., and Rajagopalan G. (1993) A $\delta^{13}\text{C}$ record of late Quaternary climate change from tropical peats in southern India. *Nature* **364**, 703–706.
- Telmer K., and Veizer J. (1999) Carbon fluxes, pCO_2 and substrate weathering in a large northern river basin, Canada: Carbon isotope perspectives. *Chem. Geol.* **159**, 61–86.
- Thorat P. K., and Ravi Kumar M. (1987) Geology of parts of Ratnagiri, Raigad and Satara districts of Maharashtra. Geological Survey of India, Maharashtra Circle (West).
- Trivedi J. R., Pande K., Krishnaswami S., and Sarin M. M. (1995) Sr isotopes in rivers of India and Pakistan: A reconnaissance study. *Curr. Sci.* **69** (2), 171-178.
- Trivedy R. K. (2000) *Pollution and biomonitoring of Indian rivers*. ABD Publishers, Jaipur, pp. 344.
- Trumbore S. (2000) Age of soil organic matter and soil respiration: Radiocarbon constraints on belowground dynamics. *Ecological Applications*, **10** (2), pp.399-411.
- UNESCO (1993) Discharge of selected rivers of the world, UNESCO, Paris. pp. 600.
- Valdiya K. S., (1980) *Geology of the Kumaun Lesser Himalaya*. Wadia Institute of Himalayan Geology, Dehradun pp. 291.
- Veizer J. (1989) Strontium Isotopes in Seawater through Time. *Annu. Rev. Earth Planet. Sci.* **17**, 141-167.
- Velbel M. A. (1993) Temperature dependence of silicate weathering in nature: How strong of a negative feedback on long term accumulation of atmospheric CO_2 and global greenhouse warming? *Geology* **21**, 1059–1062.
- Venkatesan T. R. Pande K., and Gopalan G. (1993) Did Deccan volcanism pre-date the Cretaceous/Tertiary transition? *Earth Planet. Sci. Lett.* **119**, 181–189.
- Viers J., Dupre B., Braun J. -J., Deberdt S., Angeletti B., Ngoupayou J. N., and Michard A. (2000) Major and trace element abundances, and strontium isotopes in the Nyong basin rivers (Cameroon): Constraints on chemical weathering processes and elements transport mechanisms in humid tropical environments. *Chem. Geol.* **169**, 211–241.
- Volk T. (1987) Feedbacks between weathering and atmospheric CO_2 during the last 100 million years. *Am. J. Sci.* **287**, 763-779.
- Vonhof H. B., and Smit J. (1997) High-resolution late Maastrichtian-early Danian oceanic $^{87}\text{Sr}/^{86}\text{Sr}$ record: Implications for Cretaceous-Tertiary boundary events. *Geology* **25**, 347-350.

- Walker J. C. G., Hays P. B., and Kasting J. F. (1981) A negative feedback mechanism for the long-term stabilization of the Earth's temperature. *J. Geophys. Res.* **86**, 9776–9782.
- Wedepohl K. H. (1972) *Handbook of Geochemistry*, Vol II-3, Springer Verlag, Berlin, Heidelberg.
- White A. F., and Blum A. E. (1995) Effects of climate on chemical weathering in watersheds. *Geochim. Cosmochim. Acta* **59**, 1729–1747.
- White A. F., Bullen T. D., Vivit D. V., Schultz M. S., and Clow D. W. (1999a) The role of disseminated calcite in the chemical weathering of granitoid rocks. *Geochim. Cosmochim. Acta* **63**, 1939–1953.
- White A. F., Blum A. E., Bullen T. D., Vivit D. V., Schultz M., and Fitzpatrick J. (1999b) The role effect of temperature on experimental and natural chemical weathering rates of granitoid rocks. *Geochim. Cosmochim. Acta* **63**, 3277–3291.
- Widdowson M., Cox K. G. (1996) Uplift and erosional history of the Deccan Traps, India: Evidence from laterites and drainage patterns of the Western Ghats and Konkan Coast. *Earth Planet. Sci. Lett.* **137**, 57–67.
- Widdowson M., and Gunnell Y. (2004) Laterites of the Konkan and Kanara coastal Plateaux as keys to understanding the denudation chronologies of the Western Ghats. In: *Sahyadri: The Great Escarpment of the Indian Sub-continent*, (Ed: Gunnell Y., and Radhakrishna B. P.) Memoir 47 (2), Geological Society of India.
- Wilkins A., Subbarao K. V., Ingram G., and Walsh J. N. (1994) Weathering regimes within the Deccan Basalts. In: *Vocanism*, (Ed: K. V. Subbrao), Wiley Eastern, New Delhi, pp. 217-231.
- Yang C, Telmer K., and Veizer J. (1996) Chemical dynamics of “St. Lawrence” riverine system: δD_{H_2O} , $\delta^{18}O_{H_2O}$, $\delta^{13}C_{DIC}$, and dissolved $^{87}Sr/^{86}Sr$. *Geochim. Cosmochim. Acta* **60**, 851-866.
- Zhang J., Quay P. D., and Wilbour D. O. (1995) Carbon isotope fractionation during gas-water exchange and dissolution of CO₂. *Geochim. Cosmochim. Acta* **59**, 107–114.

List of Publications

1. **Das Anirban**, and Shukla A. D. (1999) A rapid method for determination of platinum group elements using NiS fire assay technique followed by Neutron Activation. In proceedings of Symposium on Nuclear, Analytical and Radiochemistry (NUCAR 1999), Bhabha Atomic Research Centre, Mumbai, pp. 321-322.
2. Shukla P. N., Bhandari N., **Das Anirban**, Shukla A. D., and Ray J. S. (2001) High Iridium concentration of alkaline rocks of Deccan and implications to K/T boundary. *Proc. Indian Acad. Sci. (Earth Planet. Sci.)* **110**, 103-110.
3. **Das Anirban**, Pande Kanchan, Sarin M. M., and Krishnaswami S. (2003) Geochemistry of rivers draining the Deccan basalts, India. 13th V. M. Goldschmidt Conference Abstract, Kurashiki, Japan. *Geochim. Cosmochim. Acta* **67**, No.18, pp. A74.
4. **Das Anirban**, Krishnaswami S., and Bhattacharya S. K. (2004) $\delta^{13}\text{C}$ of dissolved inorganic carbon in rivers draining the Deccan Traps: A proxy of silicate weathering. In: Proceedings of Indian Society of Mass Spectrometry Workshop 2004.
5. **Das Anirban**, Krishnaswami S., Sarin M. M., and Pande K. (2005) Chemical weathering of the Krishna basin and Western ghats of the Deccan Traps, India: Rates of basalt weathering and their controls. *Geochim. Cosmochim. Acta* (in Press).

Communicated

1. **Das Anirban**, Krishnaswami S., and Bhattacharya S. (2005) Carbon isotope ratio of dissolved inorganic carbon (DIC) in rivers draining the Deccan Traps, India: Sources of DIC and their magnitudes. *Earth Planet. Sci. Lett.* (submitted after revision)